PHD

The application of microfiltration as a partial sterilisation technique for the reduction of psychrotrophic spore forming bacteria from viscous dairy feeds

Fitzgerald, Laura

Award date:
2012

Awarding institution:
University of Bath

The application of microfiltration as a partial sterilisation technique for the reduction of psychrotrophic spore forming bacteria from viscous dairy feeds

Laura Emma Fitzgerald (née Head)

A thesis submitted for the degree of Doctor of Philosophy

University of Bath

Department of Chemical Engineering

November 2012

Acknowledgments

First and foremost I would like to thank Dr Mike Bird, my supervisor for all the time and guidance that he has provided me during my time at Bath for which I am extremely grateful and also to Dr Tim Mays who acted as supervisor during the period when Mike was on sabbatical.

In addition I would like to thank all of the technicians of the Chemical Engineering department namely Fernando, Richard, Merv, John, Robert and Suzanne. I am very grateful for the friendly help they provided in the form of poster printing, using and repairing laboratory equipment, and with setting up and maintaining the filtration rig. I would also like to thank my colleges Sarah Jones, Iain Argyle and Peter Bechevaise for their help and advice throughout the project I would to give extra gratitude to Peter Bechevaise who took the lead in the construction of the filtration system used for experimentation.

I am also extremely grateful to Professor Mike Danson, Carolyn Williamson and Chris Davey of Lab 1.33, Department of Biology and Biochemistry, University of Bath for allowing me to use both their lab space, consumables and equipment and for their invaluable time and guidance with regards to the microbiological work carried out within this project.

I would also like to thank Dr John O'Connell, Dr Christer Viebke, David Carr and Eve Manning of *Kerry Ingredients* for their technical advice and input, and *Kerry Group* for supplying the MPI powder used for experimentation. In addition I would like to give extra gratitude to Eve Manning for allowing me to visit and carry out work at the pilot plant in Listowel, Ireland.

I would like to thank Dr Jeanette Lindau of *Tetra Pak, Lund, Sweden* for loaning the 0.8 and 1.4 µm ceramic membranes and the stainless steel module used to house them and Dr Frank Lipnizki of *Alfalaval* for the kind donation of the polymeric flat sheet membranes.

On a more personal note I would like to give a huge amount of thanks to my husband Peter Fitzgerald for the constant love and support he has given me over the past three years. He has encouraged me to carry on even when things were difficult and somehow he is able to pick me up every time I have felt down.

Lastly, I would like to thank the University of Bath for providing financial support in the form of an EPSRC DTA Studentship.

Abstract

The use of microfiltration as an alternative to pasteurisation to reduce the microbial load of raw skimmed milk is a well established technology. However, its application in reducing bacteria from highly viscous dairy based solutions has not due to issues of low flux and high fouling tendency. This study involves the application of microfiltration to remove spores from high solids content Milk Protein Isolate (MPI) solutions. MPI feeds were inoculated with *Bacillus mycoides* spores a safer alternative to *Bacillus cereus*, a psychrotrophic spore forming bacteria found in dairy feeds.

Suitable protocols for MPI resolubilisation, *Bacillus mycoides* cell and spore preparations were established and the membranes, MPI and spores were fully characterised by scanning electron microscopy (SEM), particle size distribution, rheology and pure water flux (PWF) measurements. Feed and permeate samples collected during experiments were analysed for solids content by oven drying, protein content using the Bradford assay and spore content using *Petrifilm*^{TM} Aerobic count plates. To try and determine an optimum protocol for MPI filtration, a variety of filtration rig set-ups, modules and membranes were tested. Experiments were carried out at different MPI concentrations (4 – 16 wt%), cross flow velocities (CFV's) (0.7 – 2.0 m s^{-1}) and transmembrane pressures (TMP's) (1 and 2 bar).

The filtration of 15 wt% MPI proved challenging. The best set of results were obtained using the 12.0 µm membrane at 1.4 m s^{-1}, producing a 27 LMH flux, 96.5% protein transmission and a 2.1 log spore reduction. These results indicate that large pore ceramic microfiltration may be a suitable technology to replace or augment pasteurisation for high solids content dairy feeds. The effect of backwashing using different durations and frequencies was investigated. Backwashing parameters of 10 seconds every 5 minutes at 1 bar were found to be the most effective.

The optimum cleaning regime found for MPI fouled ceramic membranes involved a long rinsing backflush at 1 bar, acid and alkali steps without backwashing, which produced a 99.6% flux recovery.

List of publications, conference and industry visits arising from the project

Referred journal papers

Head, L. E., and Bird. M. R., 2011. The removal of psychrotropic spores from milk protein isolate feeds using tubular ceramic microfilters. *Journal of Food Process Engineering*, DOI: 10.1111/j.1745-4530.2011.00661.x

Head, L. E., and Bird. M. R. Backwashing of tubular ceramic microfilters fouled with Milk Protein Isolate feeds. *Journal of Food Process Engineering*, DOI: 10.111/j.1745-4530.2012.00676.x

Conferences

International Congress on Membranes and Membrane Processes (ICOM), 24 – 29th July 2011 held at the RAI convention centre, Amsterdam, Holland. Abstract and poster entitled "Performance of tubular ceramic microfiltration membranes at removing psychrotrophic spore forming bacteria from high solids content Milk Protein Isolate".

Fouling and Cleaning in Food Processing (FCFP), 22 – 24th March 2010 held at Jesus College Cambridge, UK. Paper and poster entitled "Fouling of microfiltration membranes during the removal of thermophilic spores from high solids content Milk Protein Isolate solutions".

Industry visit

Carried out pilot plant trials using MPI concentrate solutions of 10, 17 and 25 wt% at Kerry Foods, Listowel, Ireland between 16 – 19th November 2009.

Meetings

Presentations given during regular progress meetings with interested industry parties from Kerry Ingredients, namely Eve Manning, Dr John O'Connell, Dr Christer Viebke and David Carr

Contents

Chapter 2. Materials and filtration methods

Chapter 3. Characterisation

Chapter 4. Filtration Results

List of Figures

Page

List of Tables

Page

Nomenclature

Abbreviations	Descriptions
α-LA	α- lactalbumin
ACDP	Advisory Committee on Dangerous pathogens
ACP	Aerobic Count Plates
AFM	Atomic Force Microscopy
AOAC	Association of Analytical Communities
APHA	American Public Health Association
β-LG	β-lactoglobulin
BATH	Bacterial Adherence to Hydrocarbons
BF	Backflushing
BP	Backpulsing
BSA	Bovine Serum Albumin
BW	Backwashing
CFMF	Cross Flow Microfiltration
cfu ml^{-1}	colony forming units per millilitre
CFV	Cross Flow Velocity
CIP	Cleaning In Place
cP	centipoise
CP	Centrifugal pump
DLS	Dynamic Light Scattering
DSS	Danish separation systems
ESL	Extended Shelf Life
EU	European Union
F	Electromagnetic flow meter
FT	Feed tank
FTIR	Fourier Transform Infrared
GC	Nitrogen gas cylinder
GDA	Glutaraldehyde
GP	Gradient of Polarisation
GU	Graticule units
H	Oil circulation pump and heater
HE	Heat exchanger
HMDS	Hexamethyldisilazane
HPLC	High performance liquid chromatography
HTST	High-Temperature Short-Time
IgG	Immunoglobulin
kDa	Kilo Dalton
LMH	Litres $metre^{-2}$ hr^{-1}
M	Molar
M1	Membrane module
MATH	Microorganism Adhesion To Hexadecane
MF	Microfiltration
mmol	millimole
mPa s	millipascal seconds
MPC	Milk Protein Concentrate
MPI	Milk Protein Isolate
NB	Nutrient Broth

NCIMB	National Collection of Industrial, food and Marine Bacteria
NF	Nanofiltration
P	Poise
P1, 2 and 3	Pressure transducers
Pa s	Pascal seconds
PCT	Permeate collection tank
PDP	Positive displacement pump
PE	Polyethylene
PF	Pre-filter
pH	Measure of acidity / alkalinity
PP	Polypropylene
ppm	parts per million
PS	Polysulfone
PTFE	Polytetrafluoroethylene
PT	Pressurised tank
PVDF	Polyvinylidene Fluoride
PWF	Pure water flux
RO	Reverse Osmosis
RP	Reciprocating pump
rpm	revolutions per minute
S1 and 2	Sample collection taps
SCB	Sorbitol citrate buffer
SD	Standard Deviation
SDS-PAGE	Sodium Dodecyl Sulfate Polyacrylamide Gel Electrophoresis
SEM	Scanning Electron Microscopy
S.G	Specific Gravity
Spp	Species
SV	Solenoid valve
T	Thermocouple
TEM	Transmission Electron Microscopy
TMP	Transmembrane Pressure
TS	Tryptone soya
TTC	2, 3, 5-triphenyltetrazolium chloride
UF	Ultrafiltration
UHT	Ultra Heat Treated
UK	United Kingdom
USA	United States of America
UTMP	Uniform Transmembrane Pressure
UV	Ultraviolet
WPC	Whey Protein Concentrate
wt%	weight percentage

Symbols	**Description**	**Units**
A_f	Absorbance of aqueous phase	---
A_i	Absorbance of original sample	---
A_m	Membrane area	m^2
C	Concentration of solute in the stream	g $litre^{-1}$

C_b , C_B	Concentration of solute in the bulk	wt%
C_m	Membrane surface concentration	wt%
C_p	Concentration of solute in the permeate	wt%
C_{pf}	Concentration of protein in the feed	µg ml^{-1}
C_{pp}	Concentration of protein in the permeate	µg ml^{-1}
C_{sf}	Average feed *Petrifilm*™ plate counts	spore ml^{-1}
C_{sp}	Average permeate *Petrifilm*™ plate counts	spore ml^{-1}
D	Diffusion Coefficient	m^2 s^{-1}
DM_F	Dry mass in feed	wt%
DM_P	Dry mass in permeate	wt%
d_s	Mean spore diameter	m^2
G	Shear modulus	---
J_v	Permeate flux	LMH or m s^{-1}
k	Mass transfer coefficient	m s^{-1}
M	Molecular weight of the solute	g mol^{-1}
r	Specific resistance of the cake	---
R	Universal gas constant	litre bar K^{-1} mol^{-1}
R_a	Adsorption resistance	m^{-1}
R_{bl}	Boundary layer resistance	m^{-1}
R_c	Cake layer resistance	m^{-1}
R_{CP}	Concentration polarisation resistance	m^{-1}
R_{coeff}	Observed rejection coefficient	---
R_F	Fouling resistance	m^{-1}
R_g	Gel layer resistance	m^{-1}
R_I	Irreversible fouling resistance	m^{-1}
R_m	Membrane resistance	m^{-1}
R_{max}	Maximum rejection coefficient	---
R_p	Pore blocking resistance	m^{-1}
R_R	Reversible fouling resistance	m^{-1}
R_S	Percentage solids retention	%
R_{TOT} , R_T	Total resistance	m^{-1}
t	time	seconds
T	Temperature	K
V	Volume of fluid	g, kg
V_s	Volume of spores deposited	m^3

Greek Symbols	**Description**	**Units**
σ	Shear stress	Pa
γ	Shear rate	s^{-1}
μ_a	Apparent viscosity	cP, Pa.s
δ	Boundary layer thickness	m^{-1}
μ_P	Viscosity of the permeate	Pa.s
ε	Porosity	---
π	Osmotic pressure	bar
π_m	Osmotic pressure difference across a membrane	bar
η	Feed viscosity	cP, Pa.s
ΔP	Transmembrane pressure	bar or Pa

INTRODUCTION

i. Preface

Man has used milk in his diet for 8000 years and a major industry has developed around the processing of milk of a few species for human foods, especially milk from cattle, buffalo, sheep and goats (Fox, 2009). Milk and other dairy products are highly nutritious media, in which micro-organisms can multiply and cause spoilage. The use of microfiltration as an alternative to using pasteurisation to reduce the microbial load in skimmed milk is a well established technology, being used to produce commercially available products such as Cravendale® milk. However, its application in reducing bacteria from high solids content highly viscous dairy based solutions has not become established due to issues of low flux and poor solids transmission.

The most common spoilage micro-organisms found in milk and other dairy products are Gram-negative rod-shaped bacteria (e.g. *Pseudomonas* spp., and coliforms), gram-positive spore-forming bacteria (e.g. *Bacillus* spp., and *Clostridium* spp.), lactic acid producing bacteria (e.g. *Streptococcus* spp.) and yeasts and moulds, the gram-positive spore forming bacteria are the main focus of this project. Micro-organisms found within milk and dairy products are also to a limited extent associated with foodborne illness. Dairy products were the cause of 90% of the 105 reported cases of foodborne disease outbreaks in the USA between 1993 - 1997 (te Giffel, 2003).

If possible microfiltration a physical (size exclusion) process would be the preferred processing technique over pasteurisation a thermal process, which is currently the main method used to reduce the bacterial load for dairy products. Pasteurisation only destroys heat-sensitive spoilage and pathogenic bacteria present within raw milk whereas microfiltration is capable of removing all types of micro-organisms including thermoduric and spore forming bacteria such as *Bacillus cereus* that survive pasteurisation and regerminate. Also microfiltration can be carried out at lower temperatures than pasteurisation with 50 ºC used during this project as opposed to 71.7 ºC used during pasteurisation. This benefits the manufacturer as production costs would be lowered and also the sensory characteristics i.e. the colour, flavour and texture and nutritional quality of the product as there is less chance of chemical changes happening such as whey protein denaturation if a lower temperature is applied to the milk. Heat processing also results in the release of sulphurous compounds from dairy products and the typical eggy aroma associated with scalded milk (Drake *et al*, 2009).

Changes such as this will have to be made in the future as global environmental issues can be expected to have an impact on future food production. This is starting to happen as currently *Dairy UK* is chairing the dairy supply chain forum's sustainable consumption and production taskforce who are a collaboration of 15 organisations that cover the production, processing and consumption of dairy products. Together they have developed a Milk roadmap (DEFRA [online, accessed 15/09/11]), which is a set of targets aiming at decreasing the environmental impact each area of dairy product production has with deadlines up until 2050.

There are three main areas concerning the dairy industry that are related to climate change these are water consumption that occurs both on the farm and during processing, methane production from the cows directly that account for 28% of methane emissions from human related activities and energy consumption (Boland, 2009). Reducing energy consumption during dairy product manufacture is the area concerning this project as the aim was to try and develop a microfiltration process that could replace or augment pasteurisation. Milk is energetically very expensive to produce, as it requires the cow to eat vegetable material that could be used itself to produce proteins. It has been estimated that production of 50 kg of milk protein in the USA requires 7×10^6 kcal of feed energy i.e. 585 kJ kg^{-1} equating to an energy efficiency of 30 : 1, compared to 58 kJ kg^{-1} for corn or soy protein production (Pimentel and Pimentel, 1979). This means that the whole dairy industry will need to start becoming more energy efficient in regards to production.

Traditionally milk and whey powders were used as animal feed but due to changes in agricultural policies the dairy industry was forced to find alternative uses for dairy surplus and for the by-products of cheese (whey) produced from milk and buttermilk produced from cream (Schuck, 2009). As a result over the past 25 years the dairy industry has developed new processes for extracting and purifying proteins producing a large variety of products as can be seen in Figure 3. These are marketed in dehydrated spray-dried form and are used as either nutritional or functional ingredients within food products.

There are ~200 million dairy cattle worldwide with 1.9 million within the UK (DEFRA 2010), Holstein-Fresian is the main breed representing ~35% (~70 million cows) but

there are other breeds such Brown Swiss (~4 million), Jersey (~2 million), Ayrshire, Guernsey and Red Dane. Currently about 600 x 10^6 tonnes of milk is produced worldwide per annum. 85% of which is bovine, 11% buffalo, 2% sheep, 2% goat with small amounts produced from horses, donkeys, camels, yaks and reindeers (Fox, 2009). Within the UK 12,858 million litres of milk were produced in 2008 / 2009 with 6690 million litres (51%) being made into liquid milk and the remainder making other dairy products such as cheese, yoghurt and butter (DEFRA, 2009). According to Barker (2003) in the UK milk and other dairy products supplied ~30% of dietery protein consumed by children ~27% of dietary lipids and ~65% of calcium, so it is a very valuable food source.

Cravendale® milk is a commercially available product produced using microfiltration in addition to UHT treatment and sales show that the demand for such extended shelf life products is increasing. Sales in the UK for Cravendale® were recorded at over 165 million litres in 2009 and the brand was ranked 43 in a poll of the UK's top 100 brands (figures taken from Cravendale® semi-skimmed [online, accessed 15/09/11]).

ii. Project aims and objectives

The aim of this project was to try and develop an experimental protocol in which microfiltration could be used to reduce the bacterial content of high solids content highly viscous milk protein isolate (MPI) feed solutions containing up to 15 wt% solids. The feed used during the project was a reconstituted *Ultranor*™ 9075 Milk Protein Isolate spray dried powder supplied by *Kerry Ingredients*, Ireland. This powder was resolubilised and inoculated with spores of *Bacillus mycoides* before experimentation. *Bacillus mycoides* was selected to act as a suitable analogue to *Bacillus cereus*, which is the main type of gram-positive spore forming psychrotrophic bacteria found within dairy products (Andersson *et al.*, 1995).

During experiments a high rejection of spores was required whilst maintaining a high permeate flux and a high transmission of solids through the membrane. If achieved this process could potentially be used commercially within industry to augment or replace pasteurisation. Suitable targets were set at the start of the project for spore rejection, permeate flux and solid transmission during the filtration of a 15 wt% MPI feed, by consideration of values achieved within industry and those reported within the

literature. Spore rejections of 2.08 ± 0.12 and 2.15 ± 0.10 $\log_{10}$ cfu ml^{-1} have been reported by Fritsch and Moraru, (2008), 3.79 $\log_{10}$ cfu ml^{-1} by Elwell and Barbano (2006), 4.5 – 5.91 $\log_{10}$ cfu ml^{-1} by Tomasula *et al.*, (2011) and 2.28 ± 0.17 $\log_{10}$ units by Madec *et al.*, (1992). All of these rejections were found using a feed of raw skimmed milk and a 1.4 µm membrane. A similar minimum reduction target of ~2 $\log_{10}$ orders cfu ml^{-1} was set for 15 wt% MPI filtration during this project. With regards to permeate flux and solids transmission in industry steady state permeate fluxes of 500 litres m^{-2} hr^{-1} (LMH) and solids transmissions of > 99% are typically obtained during the filtration of skimmed milk over a 10 hour period (Saboya and Maubois, 2000). Considering the difference in solids content between skimmed milk (3 - 4 wt%) and the MPI (up to 15 wt%) a realistic target of 50 LMH or higher for steady state permeate flux and > 80% for solids transmission were set.

iii. Approach

In order to try and develop an effective microfiltration protocol the following steps were carried out during the project.

1. Protocols were developed for MPI resolubilisation (section 2.4), sample protein content determination (section 2.10.4), total solids measurement (2.10.5), *Bacillus mycoides* cell and spore preparation and spore harvesting (section 2.2.1) and lastly, sample spore enumeration (section 2.3).

Ideally liquid milk prior to being both pasteurised and spray-dried would have been used during this project but due to issues of safety and practicality in terms of storage, a spray dried milk powder prepared using pasteurised skim milk was used for experimentation. This meant that an effective resolubilisation protocol for the MPI powder had to be developed and a suitable bacteria type selected to inoculate the resolubilised MPI with that was representative of the spoilage bacteria typically found within dairy products. Lastly, a suitable spore enumeration method was required to enumerate the bacterial content of samples taken during experiments of the feed and permeate streams to establish spore rejection. *Petrifilm*™ aerobic count plates produced by 3M™ were selected for use during this project after the traditionally used counting chambers and haemocytometers enumeration techniques were tested and found to be unsuitable (discussed in more detail in section 2.3).

2. A suitable filtration system and membrane type was established, involving the construction of a new filtration system and sourcing of membranes.

This step involved firstly testing the Danish separation systems (DSS) LabUnit M10 filtration rig (historically used within the research group for food processing) this was found to be unsuitable as only low CFV's (up to 0.8 m s^{-1}) were able to be reached producing low permeate fluxes when filtering only low solids content MPI feeds of 3.5 wt% (section 4.2). As a result a new suitable filtration system was constructed, this process was led by Peter Bechervaise (a fellow PhD student within our research group) (section 2.9). This was initially tested with a stainless steel flat sheet module which was also unsuitable as only low fluxes were produced, resulting in tubular ceramic *Membralox*™ membranes with GP modification of 0.8 and 1.4 µm pore diameters able to withstand backwashing being sourced and tested.

3. Preliminary testing of the 0.8 and 1.4 µm pore size ceramic membranes was carried out using 'sterile' MPI (section 4.5.3 and 4.5.5), inoculated RO water (section 4.5.1 and 4.5.2) and MPI feeds (section 4.5.3, 4.5.4 and 4.5.5) at different MPI concentrations, cross flow velocities (CFV's) (0.7 and 1.4 m s^{-1}) and transmembrane pressures (TMP's) (1 and 2 bar) (section 4.6.1).

These experiments were carried out to establish the spore rejections and the permeate flux and solid and protein transmissions possible for MPI feeds of different concentrations using different process conditions. Experiments were carried out using inoculated RO water feeds to find the separation provided solely by the membranes and then within MPI solutions to see if the presence of MPI particles affected the separation. These experiments showed that the separation was possible with spore rejections of 99% measured and that increasing MPI concentration increased the spore rejection produced. Unfortunately, the steady state permeate fluxes and solids transmissions produced during experiments were low but suggested that increasing CFV could increase these values.

4. The filtration rig was modified several times in order to increase the CFV able to be reached during experiments (section 2.9.1 and 2.9.2). Tubular ceramic *Membralox*™ membranes of larger pore sizes 2.0, 5.0 and 12.0 µm were sourced and tested using the

modified system at different CFV's (0.7 – 2.0 m s^{-1}) and using feeds of different MPI concentrations (5 – 15 wt%) to try and establish an optimum membrane pore size to use, in terms of steady state spore rejection, permeate flux and solid and protein transmission (section 4.6.2, 4.6.3, 4.6.4, 4.6.5 and 4.6.6).

5. Optimisation of high solids content (15 wt%) MPI filtration using optimum membrane pore sizes. This involved testing different water backwashing durations and frequencies during the filtration of 15 wt% MPI feed through the 0.8, 2.0 and 12.0 µm membranes using the optimum process conditions established during previous experimentation (section 4.7.3, 4.7.4, 4.7.5 and 4.7.6).

6. Characterisation of the *Bacillus mycoides* spores, MPI and tubular ceramic membranes. The size of the *Bacillus mycoides* spores and determining whether the developed harvesting protocol was damaging the spores was investigated using a combination of particle size distribution (section 3.1.2) and optical microscope (section 2.2.1) and scanning electron microscopy (SEM) imaging (section 3.1.1 and 2.2.1) and the hydrophobicity of the spore surface using the microorganism adhesion to hexadecane (MATH) assay (section 3.1.3). The MPI was characterised by viscosity measurements, SEM and particle size distribution and the tubular ceramic membranes were characterised using pure water flux (PWF) measurements (section 4.3).

7. Lastly, the efficiency of the selected disinfection procedure carried out both before and after filtration experiments using inoculated feeds was established (section 4.1) and optimum rinsing and cleaning regimes for MPI fouled ceramic membranes were developed through experimentation (section 4.7.7).

iv. Outline of the thesis

This thesis is composed of five different chapters. Chapter 1 provides a literature review covering background information on membrane separation, the composition of milk, the processing of dairy products, the types of bacteria found within dairy products including *Bacillus mycoides*, bacteria counts typically found within dairy products, microfiltration, membrane fouling and cleaning, techniques for bacteria removal and microfiltration improvement, analysis techniques as well as similar studies that have involved the processing of low solids content dairy streams.

Chapter 2 describes all of the raw materials, analytical techniques and physical equipment used in this study, including the microfiltration modules, membranes and the various filtration systems.

Chapter 3 presents all of the characterisation results including *Bacillus mycoides* spore size, hydrophobicity, *Petrifilm*^{TM} aerobic count plate testing and MPI viscosity measurements.

Chapter 4 presents all of the filtration experiment results including all the steady state permeate flux, solid transmission and spore rejection data found for all the filtration systems, membranes and process conditions tested during normal crossflow experiments as well as the backwashing experiments results, comparisons between normal crossflow, backflushing and backpulsing experiments and determination of an optimum cleaning regime for MPI fouled tubular ceramic membranes.

Chapter 5 concludes all of the findings of the study and discusses the potential recommendations for future work. This is followed by a list of references and the appendices.

LITERATURE REVIEW

1.1 INTRODUCTION TO MEMBRANE SEPARATION

Membrane separation processes were introduced in the 1960's with cross flow microfiltration (CFMF) introduced in the 1980's. CFMF is a technology experiencing rapid growth particularly in the field of food processing, with interest in their use to aid or to replace exiting technologies increasing (James *et al.,* 2003). This is because these processes unlike ones used traditionally within industry such as pasteurisation for bacterial removal can often be operated at low or even ambient temperature making them ideal for handling sensitive components such as food and pharmaceuticals. Membrane processes also tend to have relatively low capital and energy costs, do not use additives, have a compact design and can be easily scaled-up all factors that increase the appeal for their use (Kuberkar and Davis, 2001). More specifically the use of CFMF in dairy processing applications such as milk component separation and the removal of bacterial species from low viscosity feeds to extend shelf life are now well established technologies but this is not the case for high viscosity feeds.

1.2 COMPOSITION OF MILK

Milk is a complex fluid, the main constituents of which are water, lipids, sugar (lactose), and proteins. There are also other minor constituents such as minerals, vitamins, hormones and enzymes found at trace levels. In nature the main purpose of milk is to provide nutrition and colostrum to newborn mammals. The concentration of the main components of milk varies between species: lipids 2 - 55%, proteins 1 - 20%, lactose 0 - 10%, this is a result of the different energy requirements (lipids and lactose) and growth rates (mainly proteins) of the newborn species (Fox, 2009).

There are two types of protein found within milk, whey and casein, the proportions of each vary widely, as does the total protein content between milk samples as stated before, but bovine milk typical consists of 80% casein and 20% whey protein. Casein proteins have primarily nutritional functions by providing a source of amino acids whereas whey proteins are used as carriers for ligands and trace elements and for other biological functions for example bovine serum albumin (BSA) is used to bind insoluble

fatty acids for transportation in the blood (De Wit, 1998). Molecular size data for the major components of milk are shown in Table 1.

1.2.1 Casein proteins

Casein proteins within milk are unusual in that they are neither globular nor fibrous and do not have defined secondary or tertiary structures being present instead in the form of flexible micelles. This is the case for casein proteins within the milk of all species. The detailed structure of micelles is not defined but there is agreement on their general structure and properties (Fox, 2009). A typical micelle contains about 2 x 10^4 casein molecules (Coultrate, 1989) and there are 10^{14}-10^{16} micelles ml^{-1} of milk. Electron microscopy has shown that micelles are generally spherical in shape having diameters between 50 – 500 nm (average 120 nm) and masses ranging between 10^6 – 10^9 Da (average 10^8 Da) (Fox and McSweeney, 1998). Also about half of the phosphate and a third of the calcium within raw milk is bound onto casein micelles (Muir and Banks, 2003). Lastly, casein micelles scatter light and the white colour of milk is due largely to this light scattering (Thompson *et al.,* 2009).

There are various theories that claim to describe the structure of a micelle one such theory states that α-casein makes up the interior of the micelle which is held together by hydrophobic interactions and calcium mediated phosphoserine crosslinks and the surface of the micelle is covered by κ-casein (Tuinier and Kruif, 2002). A second theory known as the nanocluster theory proposes that calcium-linked phosphoserine residues act as nuclei for the association of casein nanoclusters. These clusters associate until the aggregate surface is predominantly covered with κ-casein (Tuinier and Kruif, 2002). Lastly, the submicelle theory proposed by Slattery and Evard (Coultrate, 1989) describes a micelle as an aggregate of submicelles, each of which are made up of α, β and χ (also known as κ) -casein polypeptide chains of about 25 - 30 molecules in length, which are present in proportions similar to those found within milk as a whole. These polypeptide chains fold themselves into elongated shapes where one end is made up of predominantly hydrophobic amino acids with the other mainly hydrophilic. These hydrophobic ends group together forming a submicelle, a schematic of which is shown in Figure 1a. The polar hydrophilic end of α-Casein contains eight serine residues to which phosphates can be esterified making a phosphoserine residue with β-Casein containing four of these residues. χ-Casein differs in that one or more of its threonine amino acid residues on the hydrophilic end carries a trisaccharide unit. The micelle

structure is held together by calcium phosphate bridges with the Ca^{2+} ions reacting with the phosphate groups attached to both α and β-Casein. This linkage between submicelles may be either direct or in chains involving additional Ca^{2+} ions and citrate. A schematic of a micelle is shown in Figure 1b. The size of a micelle is restricted by the fact that as further submicelles are added the proportion of the surface occupied by the non-linking hydrophobic χ-Casein areas is increased until eventually they dominate the surface and prevent any further increase in size.

Casein micelles are known to have good emulsifying properties being able to stabilise fat droplets in solution. This is because the acidic amino groups (carboxyl and ester phosphate) are unevenly distributed along their polypeptide chains. As a result caseins have highly charged polar regions and contrasting hydrophobic domains, these polar regions are able to associate with the aqueous phase while the hydrophobic regions bind to the lipids (Muir and Banks, 2003).

Table 1. Molecular sizes of milk components (Taken from Cheryan and Alvarez, 1995).

Component	Molecular weight	Diameter (nm)
Water	18	0.3
Chloride ions (Cl^-)	35	0.4
Calcium ions (Ca^{2+})	40	0.4
Lactose	342	0.8
α-lactalbumin	14500	3
β-lactalbumin	36000	4
Blood serum albumin	69000	5
Casein micelles (milk protein in solution)	107 – 109	25 - 130
Fat	---	2000 - 10000

Glover and Brooker (1974) found through the use of electron micrographs that casein micelles were the dominant species involved in the formation of a gel layer resistance during RO membrane applications used in the dairy industry. Kulozik (1998) investigated the effect calcium has on the formation of a fouling layer in more detail, by removing bound and unbound (soluble) calcium from micelles in turn using diafiltration and ion exchange respectively. Kulozik found that when unbound calcium was removed the resulting deposit had a loose open structure with a low resistance to flux. Contrastingly, when both types of calcium are removed this resulted in a breakdown of

the micelle structure into submicelles causing the fouling layer to be dense and have a high flux resistance.

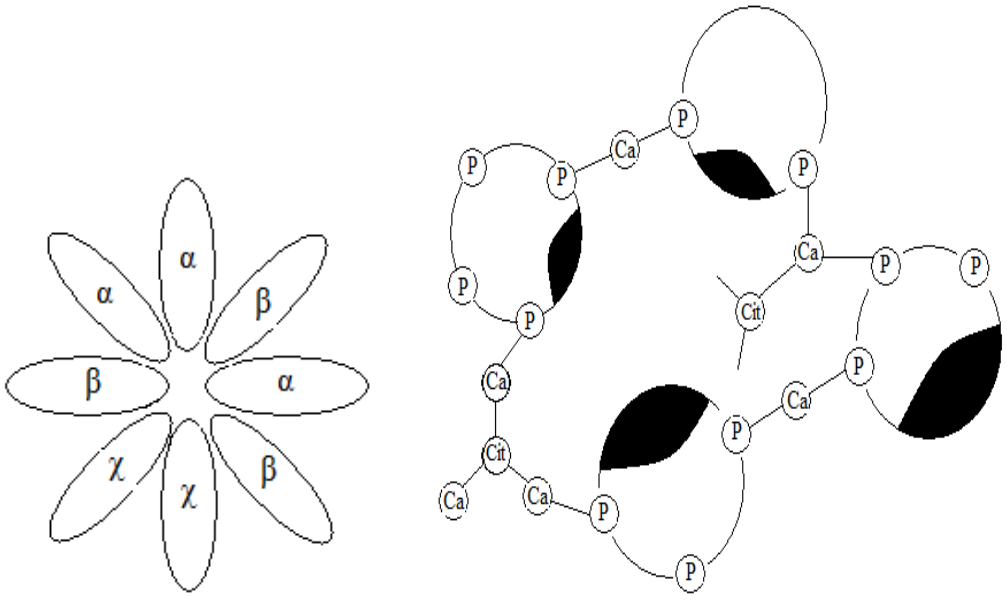

(a) *(b)*

Figure 1(a) Schematic of a submicelle, (b) Schematic of a micelle where P is phosphate, Ca is calcium, Cit is citrate and the black shaded areas are the non-linking χ-casein regions (Taken from Coultate, 1989).

1.2.2 Whey proteins

Whey proteins are highly structured and much smaller when compared to casein micelles with the major whey proteins α- lactalbumin (α-LA), β-lactoglobulin (β-LG), bovine serum albumin (BSA) and immunoglobulins (IgG) having radiuses of 1.8, 3.5, 4 and 6 nm respectively (De Wit, 1998). This difference in size is reflected in the numerical contribution of whey proteins compared to casein micelles in milk with the numbers of distinct whey protein molecules per average casein micelle in milk being 325, 335, 22 and 8 for α-LA, β-LG, BSA and IgG respectively (De Wit, 1998).

β-Lactoglobulin is the most abundant whey protein accounting for 50% of whey protein and 12% of the total milk protein in bovine milk. Because of this high abundance its properties largely influence the properties of whey protein as a whole. β-LG contains one mole of cysteine per monomer. When the protein is thermally denatured the cysteine reacts with the disulfide in k-casein which significantly affects the heat stability of milk as a whole. β-LG also causes the cooked flavour in heated milks (Thompson *et al.*, 2009). The biological role of β-LG is thought to be either as a binding site for retinal (vitamin A) and/or to stimulate lipase activity because of its ability to bind fatty acids (Fox, 2009). α-LA accounts for 20% of whey protein and 3.5% of milk protein as a

whole in bovine milk, in human milk it is the main whey protein. It acts as a carrier for Ca^{2+} ions and is the most thermally stable whey protein being able to renature when carrying an ion after relatively low heat denaturation (Fox, 2009). β-LG and α-LA are the smallest milk proteins and consist of a single globular domain that is stabilised by the presence of either disulfide bridges or metal clusters. BSA and IgG that typically account for 0.1 - 0.4g L^{-1} and 0.6 – 1 g L^{-1} of bovine milk have longer polypeptide chains. With BSA normally folded into two or more domains, useful for its role as a ligand and drug binder within the body. IgG is folded into a Y-shaped structure which is necessary as its role is to provide ligand binding sites that can be used as carriers of passive immunity in newborns (Goodsell and Olson, 1993). Recently the biological properties of individual whey proteins has drawn attention due to their potential as ingredients of functional and health related foods (Akpinar-Bayizit *et al.*, 2009). Whey proteins are known for their antioxidant activity, anticarcinogenic effects, anti-microbial effects, binding of toxins, promotion of cell growth, anti-inflammatory and anti-hypertensive actions (McClements *et al.*, 2009).

1.2.3 Comparison of casein and whey milk protein properties

Fox (2009) made a series of comparisons between casein and whey milk proteins based on their solubility, heat stability, amino acid composition and their physical state in milk. Solubility; at pH 4.6 caseins are insoluble whereas whey proteins are soluble, this difference is used during the production of casein and caseinate powders, fermented milk products and coagulated cheeses. Heat stability; caseins are very stable in regards to heat with sodium caseinate able to withstand being heated to 140 °C for several hours without any visible change. Whereas the heat stability of whey is similar to that of other globular proteins being irreversibly denatured when heated at 90 °C for 10 minutes. Amino acid composition; caseins contain high levels of proline which makes them more susceptible to proteolysis; this facilitates their natural function as a source of amino acids. Whey proteins are more resilient to proteolysis, which is important as they generally have non-nutritional roles acting as either carriers or binding sites. Caseins are low in sulfur (0.8%) compared to whey proteins (1.7%), which is because whey is relatively rich in cysteine and/or cystine residues. Lastly, in regards to their physical state in milk as stated previously caseins are present in the form of large aggregates known as micelles whereas whey proteins exist as monomers or as small quaternary structures.

1.3 MILK SALES

The demand for milk and in particular filtered milk is increasing in the UK, shown when sales from May 2008 - May 2009 are compared to the previous years (figures taken from DairyCo Datum [online, accessed 17/07/09]) as the total milk sales increased by 0.9% to 4935.7 million litres. Filtered milk showed the largest relative growth with its sales increasing by 11.4% (29.3 million litres) to 286.3 million litres. The only other type of milk that showed an increase in sales within this period was UHT by 1.3% (4.8 million litres) to 366.0 million litres, this may due to consumers looking to reduce waste because of climate change or to find the most cost effective type of milk because of the present state of the financial market. The drop in sales in specialised types of milk such as organic, Channel Islands and soya milks by 2.6%, 2.6% and 7.4% respectively also reflects this trend.

1.4 MILK PROCESSING

1.4.1 Pasteurised milk

Milk can be processed using various methods, which result in products that differ in their microbiological status, and therefore keeping ability. Processed milk products are categorised as either pasteurised or ultra heat treated (UHT) milk. Legislation for the treatment and distribution of milk and other dairy products varies depending on which part of the world you live (Rysstad and Kolstad, 2006). Milk production in the UK is governed by EU legislation, this states that pasteurised milk must have undergone a heat treatment involving a high temperature for a short time, of at least 71.7 °C for 15 seconds or any equivalent combination. Following this treatment the milk must show a negative reaction to the phosphatase test and a positive reaction to the peroxidase test. Also immediately after pasteurisation the milk must be cooled to 6 °C or below. If packaged hygienically and kept under refrigerated conditions it should have a shelf life of over 10 days or 48 hours without refrigeration (Lewis, 2003). But due to the survival and growth of thermoduric spore forming bacteria and / or the result of any post-pasteurisation contamination milk products will eventually spoil.

When it is known that raw milk may be held for some time under chilled conditions before being processed, thermisation is often used to increase its keeping quality. This involves heating at 57 - 68 ºC for 15 seconds followed by refrigeration and aims to

reduce the growth of psychrotrophic bacteria (Lewis, 2003) Psychrotrophic bacteria are those that have an optimum growth temperature between 20 - 30 ºC but are also able to grow albeit slower at refrigerated temperatures (Muir and Banks, 2003). This is the reason why it is so important for shelf life to keep milk stored at refrigerated temperatures of 4 ºC or lower throughout its lifetime.

1.4.2 UHT (Ultra-High Temperature) milk

UHT processing is intended to destroy all the micro-organisms present in milk both vegetative forms and spores, or at least make them incapable of growth so that long keeping quality is obtained without refrigerated storage being necessary (te Giffel, 2003). In contrast to pasteurisation in order to comply with EU legislation must have been obtained by applying a continuous flow of heat to raw milk at a high temperature of at least 135 °C for a short time, no less than one second. There also must be no sign of deterioration after it has been stored in a closed container either at 30 °C for fifteen days or at 55 °C for 7 days (Rysstad and Kolstad, 2006).

UHT milk is popular and widely used in many parts of the world where problems with refrigeration limits widespread distribution or home use of fresh milk. But in other countries such as the UK it is not generally used and is often disliked due to the perceived ‘cooked’ taste of the product (Rysstad and Kolstad, 2006). In addition to this other factors such as the increased competition between dairy companies, less frequent shopping trips and the increasing distribution times and distances dairy products have to travel, have resulted in the need to develop a milk product with an increased shelf life compared to that of pasteurised milk but without the change in flavour associated with UHT (Rysstad and Kolstad, 2006). In the UK before the introduction of UHT processing milk products were sterilised this was first used commercially in 1894 (Lewis, 2009). This involved heating dairy products in a sealed container at 114 - 120 ºC for 20 - 30 minutes. This results in considerable changes to the nutritional value and sensory characteristics, such as a cooked or caramelised flavour and brown colour (Fox, 2003). These changes occurred to a much greater extent compared to that associated now with UHT processed milks. Many dairy products are still produced by in-container sterilisation worldwide including sterilised milk, evaporated milk, custards and canned puddings and desserts (Lewis, 2009). Sterilised milks are now processed by steam injection or infusion involving a combination of rapid heating and cooling before being

aseptically packaged that result in a reduced amount of sensory and nutritional product changes (Lewis, 2009).

Applying heat treatments such as pasteurisation and UHT to milk products to destroy potentially harmful bacteria has been carried out for many years. But after these types of treatment, dead bacterial cells remain in the milk along with their potentially active enzymes. This enzyme activity along with the metabolic activity created by growth of remaining thermoduric bacteria defined as bacteria that can survive the pasteurisation process, causes alterations to liquid milks during storage leading to a reduction in shelf life. Specifically the shelf life of pasteurised milk and dairy products is determined by the regermination of thermoduric spore forming bacteria. But the shelf life of UHT dairy products is largely determined by enzymatic activity as psychrotrophic spore forming bacteria are destroyed when temperatures in excess of 110 ºC are used during processing (Muir and Banks, 2003).

1.4.3 Extended Shelf Life (ESL) milk

Extended shelf life (ESL) milk is thought to be the solution to this problem. It is a relatively recent addition to the dairy industry and fills the gap in shelf life between High-Temperature Short-Time (HTST) pasteurised milk which has a shelf life of about seven days when kept refrigerated and ultra-high temperature (UHT) milk, which is able to be stored at ambient temperature for a few months (Hoffmann *et al.,* 2006). ESL milks are favoured as they have a longer shelf-life than pasteurised milk but do not have the negative sensory characteristics and decrease in nutritional quality associated with UHT milks.

The production of ESL products dates back to the early 1960's with dairies within North America and Canada using this technology for slow turnover products such as whipping cream and coffee creamers. Traditional ESL technology within North America involved carrying out conventional pasteurisation along with ultraclean packaging, which involves using a controlled filling environment and sterilising containers before use (Henyon, 1999).

ESL products do not at present have a legal definition but can be described as "products that have been treated in a manner to reduce the microbial count beyond normal pasteurisation, packaged under extreme hygienic conditions, and which have a defined

prolonged shelf life under hygienic conditions" (Rysstad and Kolstad, 2006). This definition shows that production of ESL milk products involves a combination of both processing and packaging methods.

One type of ESL commercially available is Cravendale® milk which is produced by using a combination of microfiltration and pasteurisation, a schematic of the process is shown in Figure 2. The MF step involves filtration using a ceramic membrane of 1.4 µm, but as native milk fat globules are similar in size to bacteria the milk must be skimmed before the MF step. The cream is then UHT treated separately (Muir and Banks, 2003). This process is claimed to produce a product with a shelf life in excess of 21 days but the added production cost and complexity of the process have cast doubt over its viability.

There are various processing methods that can be used to increase the shelf life of milk in addition to or ideally as an alternative to conventional pasteurisation. The methods currently in use commercially are microfiltration (which is the main focus of this project), direct heat sterilisation treatments such as steam injection or infusion known in the USA as ultrapasteurised milk and also indirect heat treatments (UHT milk). Using steam injection or infusion leads to an improvement in the degree of cooked flavour produced and reduces other chemical changes compared to that produced during indirect heat treatments (UHT processing). But these changes are still apparent when using these processes; this is not the case when using microfiltration.

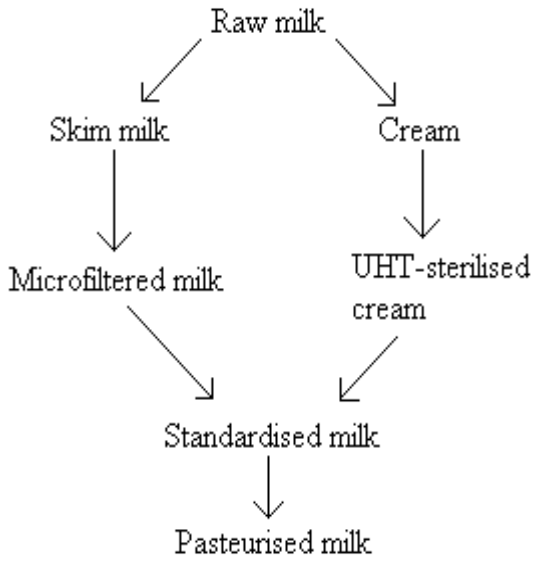

Figure 2. Manufacturing process of ESL milk

1.4.4 Factors affecting the shelf life of dairy products

Lewis (2009) stated that the main control points for ensuring good quality dairy products are; raw milk quality (discussed in detail in section 1.8), processing conditions: temperature and time (discussed in section 1.4), post-processing contamination (PPC) and storage temperature. PPC is a term that refers to recontamination that occurs anywhere downstream of the end of the holding tube (where pasteurisation takes place). Ensuring that all internal plant surfaces in contact with the product are heated at 95 ºC for 30 minutes reduces contamination, but it can only be completely eliminated by employing aseptic techniques. Most problems are thought to arise in the filling line where open containers permit access for contaminants, this can be reduced by filling the line when not in use with sterile air (Muir and Banks, 2003). It has been shown that when PPC is completely eliminated by carrying out pasteurisation inside a closed aseptic container in laboratory conditions that the produced milk if stored at <7 ºC has a shelf life of 3 – 5 weeks as opposed to 8 - 12 days typical of commercially pasteurised milk (Sorhaug and Stepaniak, 1997). In regards to storage temperature the lower the temperature the longer the keeping quality of dairy products. This is shown by the fact that before domestic refrigeration the keeping time of pasteurised milk was only 24 hours.

In order to effectively reduce the number of bacteria and bacterial enzymes within pasteurised dairy products and as such extend their shelf life all aspects from milking at the farm to storage of the product by the consumer have to be considered. Hygiene in all aspects of milk handling is a must both at the farm, in the tanker used to transport the milk and within the dairy itself. It is important to cool the milk as quickly as possible and keep it refrigerated at 4 ºC for no longer than necessary. All this should be carried out to ensure that raw milk with a bacterial load as low as possible is processed. Once processed aseptic filling techniques should be employed and the product kept refrigerated when transported to the retailers, within the stores themselves and by the consumer.

1.5 DEHYDRATED DAIRY PRODUCTS

Dairy proteins are valuable ingredients that have a variety of functional and nutritional properties. They are usually marketed in dehydrate form to increase their shelf life with spray drying being the principle dehydration method used. Pisecky (1997) described

spray drying as an industrial process used for the dehydration of a liquid containing dissolved and / or dispersed solids (e.g. dairy products), by transforming the liquid into a spray of small droplets and exposing these droplets to a flow of hot air. As the droplets have a large surface area this causes water evaporation to occur very quickly converting the droplets into dry powder particles. The essential feature of spray drying is that it reduces the moisture content of the powder to a level at which no bacterial growth can occur and causes little damage to the functionality of the milk components themselves (Muir and Banks, 2003). There are a large variety of dehydrated dairy products available the products produced from solely whey are shown in Figure 3. The shelf life of spray dried milk powders is determined by three factors; the quality of the raw material, the drying process and the storage conditions once spray dried (Muir and Banks, 2003).

1.6 WHAT ARE MILK PROTEIN ISOLATE (MPI) POWDERS?

Milk protein concentrate (MPC) and isolate (MPI) powders are a newer category of dried dairy ingredients that are rapidly gaining in popularity (Drake *et al.*, 2009). Both are manufactured from skimmed milk, which is ultrafiltrated to remove lactose and any soluble salts and to concentrate the milk proteins and then spray dried into a powder. MPC and MPI powders differ in their protein contents. MPC's are powders in which 55 - 85% of the dry matter is protein and the ratio of casein to whey proteins is between 98 : 2 and 50 : 50. MPC's are often described by placing the % of dry matter that is protein after MPC, for example MPC70 is an MPC powder with 70% of its dry matter consisting of protein. In contrast MPI's have a greater protein content with greater than 85% of their dry matter being protein. They also differ in that they contain casein to whey proteins in the same 80 : 20 ratio as they are found in milk (Bhaskar *et al.*, 2006).

The MPI powder used during this project was *Ultranor*™ MPI. *Ultranor*™ milk proteins are used in a variety of different applications such as in infant formulas and foods, in fresh dairy and ice cream products, in nutritional beverages and bars, and in enteral feeds. *Ultranor*™ milk protein isolate powders maintain casein to whey protein ratios in their native state in bovine milk of 80 : 20 and contain a minimum of 86% protein (*Kerry Ingredients* [online, accessed 15/09/11]).

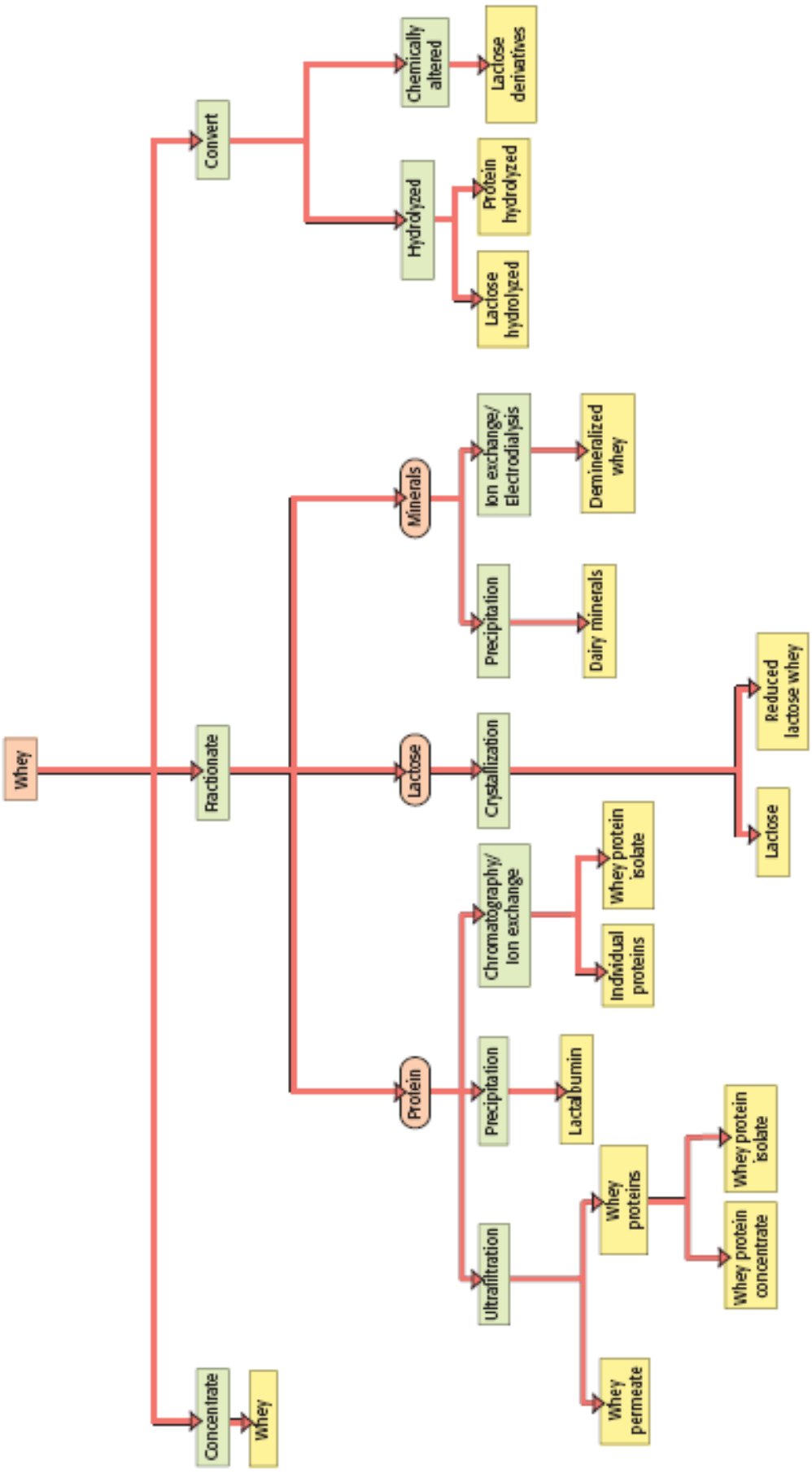

Figure 3. Showing the variety of dehydrated dairy products currently produced and marketed from whey (Taken from Smith, 2008)

1.7 RESOLUBILISATION OF MILK PROTEIN ISOLATE (MPI) POWDERS

Heat treatment of milk above 70 ºC is known to cause denaturation of whey proteins, some of which complexes with casein micelles (Oldfield *et al.*, 1998) it is also generally known that resolubilisation of MPC and MPI powders at ambient temperature results in a fraction of solid remaining undissolved that settles at the bottom of the container. The amount of insoluble material produced varies between products and has been found to increase with storage time at high temperatures. As a result applications that use MPC's within industry such as cheese manufacture reconstitute MPC at 50 ºC, as at this temperature this fraction of material is readily dissolved (Havea, 2006).

Caseins are known to be stable when moderately heated under normal pH and ionic concentrations. However, if they are heated at elevated temperatures for a significant length of time hydrolytic cleavage of pepetide and phospate bonds can occur. This affects the stability of the micelle and can result in milk coagulation (Hui, 2007).

Bernal and Jelen (1985) used differential scanning calorimetry to find the denaturation temperatures of an ultrafiltration WPC and of some individual whey proteins within the pH range 2.5 - 6.5. The denaturation temperatures found can be seen below in Table 2. WPC denaturation as with most WPC properties appeared to be controlled mainly by the β-lactoglobulin protein component. This denaturation can be observed using differential scanning calorimetry because unfolding of globular proteins such as whey proteins is associated with an endothermal heat effect.

Table 2. Denaturation temperatures found for an ultrafiltrated WPC and the individual whey proteins at different pH's using differential scanning calorimetry (Taken from Bernal and Jelen, 1985).

	Denaturation temperatures (± 5ºC)			
pH	β-lactoglobulin	α-lactalbumin	Serum Albumin	WPC
6.5	75.9	61.0	71.9	**76.9**
5.5	77.8	61.2	72.6	78.8
4.5	81.2	61.5	74.0	82.1
3.5	81.9	58.6	73.5	88.0
2.5	78.7	--	--	80.6

It is important not to thermally denature milk proteins as it has been found that at near pH 7 proteins denatured by heat tend to interact by thiol-disulphide reactions forming

protein aggregates, which further group themselves into large sediment particles resulting eventually in precipitation from solution (Morr and Josephson, 1968). Specifically whey protein denaturation has been found to occur in a two stage process, the first involves the unfolding of the polypeptide chain this may be either reversibly or irreversible. If the unfolding is irreversible then this is followed by aggregation (De Wit and Klarenbeek, 1984).

1.8 TYPES OF BACTERIA FOUND WITHIN MILK

Milk collected within dairy plants always contains microbiological flora, this contamination comes from a number of potential sources such as cow's udders, the milking machine, the local farm atmosphere, the bulk tank and the transportation equipment (Saboya and Maubois, 2000).

The quality and shelf life of dairy products depends greatly on the microbiological quality of raw milk. Gram-negative psychrotrophic bacteria such as *Pseudomonas spp.* are the predominant type of microflora found in refrigerated raw milk but it does not survive pasteurisation (Sorhaug and Stepaniak, 1997). However, it produces heat-resistant extracellular proteases and lipases, which as well as spores and somatic cells are not affected by pasteurisation (Fritsch and Moraru, 2008). Spoilage of milk can be caused by these proteases and lipases, spore germination, recontamination after pasteurisation or a combination of all three. Proteolysis by *Pseudomonas* spp. proteases for example can lead to bitterness in milk and rancidity can be caused by lipase activity (Sorhaug and Stepaniak, 1991).

Psychrotrophic bacteria such as *Pseudomonas spp.* became a problem within the dairy industry after the introduction of refrigerated storage of raw milk, a reduction in frequency of raw milk collection from dairy farms to just two or three times a week and further refrigerated storage of raw milk in dairy plants over weekends (Sorhaug and Stepaniak, 1991).

Thermoduric and spore forming bacteria are also a problem in the dairy industry. Thermoduric bacteria are defined as those that can survive 63 ºC for 30 minutes and spore forming bacteria are defined as those which survive 80 ºC for 10 minutes, both types of bacteria survive pasteurisation. Bacteria that survive pasteurisation and are psychrotrophic belong to one of these genera *Bacillus, Clostridium, Arthrobacter,*

Microbacterium, Streptococcus, Micrococcus or *Corynebacterium* (McKellar, 1989). Spore forming *Bacillus cereus* is the main type of spore forming psychrotrophic bacteria, which often causes food spoilage but rarely food poisoning as infected foods are so unacceptable (Lewis, 2003).

Bacterial spores are dormant cells that can endure a wide range of extreme environmental stresses while retaining the ability to germinate and return to vegetative growth. This can occur almost immediately once the stress is removed. The formation of a spore occurs in stages, the first stage involves the creation of a double bound membrane compartment inside the vegetative cell, and this is known as a forespore. A forespore is made up of a core that is surrounded by an inner membrane and a thick layer of peptidoglycan called the cortex (Carrera *et al.,* 2006). Once formed a series of protective layers termed the 'coat' comprising of protein surround the forespore. Once the coat is formed lysis of the surrounding cell occurs and the spore is complete. The dormacy and resistance of a spore depends on the partial dehydration of the core maintained by the peptidoglycan layer. The 'coat' contributes to the protection and germination of the spore. When germination is triggered water enters the spore core causing it to swell and convert into a vegetative cell (Chada *et al.,* 2003).

All *Bacillus* spores have the same 'coat' structure consisting of a series of concentric protein shells but some *Bacillus* species spores including *cereus* and *mycoides* have an additional external structure on top of the coat called the exosporium (Carrera *et al.,* 2006).

Bacillus spp. are known to secrete heat-resistant extracellular proteases, lipases and phospholipase (lecithinase) that have a similar heat resistance to those secreted by *Pseudomonas* spp. These enzymes when secreted into the raw milk before heat treatment along with enzymes and metabolites produced during bacterial growth in the cold chain leads to spoilage of dairy products (Sorhaug and Stepaniak, 1997). Phospholipases, proteinases and lipases secreted by *Bacillus* spp have been found to be associated with defects such as off-flavours, sweet curdling and 'bitty cream' (te Giffel, 2003).

The generation times and lag periods of *Pseudomonas* spp are much shorter compared to psychrotrophic *Bacilli* when stored at temperatures between 2 - 9 ºC. With

Pseudomonas spp having a generation time of 3.5 - 4 hours compared to 7 hours for *Bacillus* at 7 - 9 ºC (McKellar, 1989). But if milk is stored above this temperature *Bacillus* and other psychrotrophic spore formers will start to become the dominant species having shorter generation times. This means that recontamination of milk after pasteurisation by *Pseudomonas* spp. is more detrimental to the keeping quality of pasteurised milk when stored at 4 - 8 ºC than thermoduric and spore forming bacteria that survive pasteurisation usually at a level of ~1000 cfu ml^{-1} (Sorhaug and Stepaniak, 1997).

1.8.1 *Bacillus cereus*

Bacillus cereus is a gram-positive endospore forming pathogenic bacterium that is frequently detected within dairy products as well as other foods such as rice, meat, spices and eggs (Andersson *et al.,* 1995). *Bacillus cereus* as stated before causes food spoilage in the form of 'bitty cream', off flavours and sweet curdling (Hassan *et al.,* 2010) but is also potentially a source of two types of food poisoning namely vomiting and diarrheal. The diarrheal type is caused by enterotoxins produced during vegetative growth of the bacteria in the small intestine. The vomiting type produces the more severe and acute symptoms and in contrast is caused by emetic toxins that are already present within food products (Granum and Lund, 1997). Enterotoxins are heat labile and inactivated during digestions by trypsin and pronase enzymes, whereas the emetic toxin is stable to heat, pH 2 - 11 and enzymatic digestion by trypsin and pronase (Hassan *et al.,* 2010). Certain strains of *Bacillus cereus* have been found to cause food poisoning with an infective dose as low as 10^3 - 10^4 cells ml^{-1} (Andersson *et al.,* 1995). But as stated before food poisoning caused by *Bacillus cereus* is rare as the infected products are so unacceptable (Lewis, 2003).

Bacillus cereus is a major concern in the dairy industry as its spores are commonly found within soil, air, water, animal feed, agricultural products, and dung and from these sources it can easily spread to cows udders and then into raw milk (Zhou *et al.,* 2008). *Bacillus* spores in general have a high resistance to both heat and chemicals, which allows them to survive disinfection as well as pasteurisation; this makes it hard for the food industry to completely exclude it from their products (Bowen *et al.,* 2002a). As a result it has frequently been detected in dairy products such as dried, fermented and pasteurised milk and is considered to be an important factor in determining the shelf life of milk and other dairy products. Griffiths (1992) stated that *Bacillus cereus* was the

most common spoilage bacterium found in liquid milk at temperatures above 6 °C, although other *Bacillus* sp. may also be found occasionally.

In addition to the spores ability to survive pasteurisation they also easily attach onto hydrophobic surfaces such as stainless steel (which is commonly used in the dairy processing equipment) due to the presence of appendages (also known as fimbria) and the hydrophobic nature of the spores surface (Husmark and Ronner, 1992). Once attached it can then multiply and then resporulate. As stated before a final problem is that several strains of *Bacillus cereus* have become psychrotrophic (Andersson *et al.*, 1995) meaning that they are now able to grow at temperatures as low as 4 - 6 °C so are able to continue to growing even when placed into the cold chain. In the absence of post-pasteurisation contamination growth of psychrotrophic spore-forming bacteria will limit the bacteriological keeping quality of pasteurised milk (Christiansson *et al.*, 1997).

1.8.2 *Bacillus mycoides*

Bacillus cereus is not an ideal bacterium to choose to work with during this project as it is considered to belong to hazard group 2, defined by the Advisory Committee on Dangerous pathogens (ACDP) as 'A biological agent that can cause human disease and may be a hazard to employees' (ACDP Classification of Pathogens [online, accessed 15/09/12]). As a result another member of the *Bacillus* family, *Bacillus mycoides,* was selected for experimentation; specifically strain 13305 (NCIMB, Aberdeen UK) as it has been previously used within the literature (Husmark and Ronner, 1992, Bowen *et al.,* 2002 a). *Bacillus mycoides* is considered as a safer analogue than *Bacillus cereus* belonging instead to Hazard Group 1, defined by ACDP as 'A biological agent unlikely to cause human disease' (ACDP Classification of Pathogens [online, accessed 15/09/12]). *Bacillus cereus* and *Bacillus mycoides* spores have many similarities in regards to their size and structure. Both types of spore have appendages (also known as fimbria) and an outer exosporium layer on top of their coat layer both of which help promote their adhesion onto surfaces (Husmark and Ronner, 1992). The surfaces of *Bacillus cereus* and *mycoides* spores are also more hydrophobic when compared to those of the other *Bacillus* species (Bowen *et al.,* 2002 a). Carrera *et al.,* (2007) found that the average length and diameter of 100 *Bacillus cereus* spores to be 1.55 µm ± 0.16 µm and 0.90 µm ± 0.07 µm using transmission electron microscopy (TEM) images. Chada *et al.*, (2003) report similar values of 1.60 µm for length and 0.90 µm for diameter these values were an average of 1000 spores using AFM images. Similar

values have been reported for *Bacillus mycoides* spores Bowen *et al.,* (2002 a) used AFM images to estimate their size by taking an average of 30 measurements, they found the diameter to be 1.56 ± 0.25 µm. Zandomeni *et al.,* (2005) used TEM pictures to measure their size and from an average of 100 measurements found them to be 1.85 ± 0.21 µm. A third studied conducted by Bradley and Franklin (1958) measured the spore size to be 0.9 - 2.0 µm from electron microscope pictures.

When carrying out filtration experiments it is important to consider the size of the species that is wanted to be retained by the membrane and what is wanted to be transmitted through in order to select a suitable membrane pore size. The aim of this project was to retain spores of *Bacillus mycoides* and to transmit through MPI so it was very important that the size of the selected analogue was similar to *Bacillus cereus*, *Bacillus mycoides* was of a similar size. But as stated by Mukhopadhyay *et al.,* (2010) there are various other factors in addition to spore size that may contribute to determining the effectiveness of spore separation by MF, these include the affinity between the membrane and spore, fluid hydrodynamic force and the intensity of shear forces on the spore.

1.8.3 Raw milk total bacteria, total spore and *Bacillus cereus* spore counts

The bacterial content of raw milk is highly dependent upon the cleanliness of milking conditions. There are various figures quoted within the literature for total bacteria, spore and specifically *Bacillus cereus* spore counts within raw milk. Desmasures *et al.,* (1997) quote a total bacterial count of 2×10^4 cfu ml^{-1} within raw milk. Whereas Elwell and Barbano (2006) tested raw milk that had a bacteria count between $1.5 - 3.6 \times 10^3$ cfu ml^{-1}. Sorhaug and Stepaniak (1997) state that 'poor quality raw milk' contains $\geq 6 \times 10^6$ cfu ml^{-1} bacteria.

In regards to spore counts Bramley and McKinnon (1990) found that spore counts in raw milk were 3×10^5 ml^{-1} and in particular Hassan *et al.,* (2010) examined 50 samples of raw milk from different localities in Beni-Suef governorate, Egypt and found that 30% of the samples contained spores of *Bacillus cereus* having an average count of $9.11 \times 10^2 \pm 4.87 \times 10^2$ cfu ml^{-1}. Taking into consideration these values it was decided during this project that RO water and MPI would be inoculated to produce feeds having spore

contents of between 10^4 - 10^5 ml^{-1} so that feeds are at least as contaminated as raw milk and to allow the maximum log reduction possible during experiments to be measured.

1.9 MEMBRANE FILTRATION

1.9.1 Introduction

Membrane filtration processes involve the use of a selective barrier i.e. a membrane between two phases in solution or suspension. All membrane processes divide the feed stream into two different streams, the material that passes through the membrane is known as the permeate or filtrate stream and the retained material is known as the retentate or concentrate stream. A membrane has the ability to transport one component more readily compared to others because of differences in physical and / or chemical properties between the membrane and the permeating components (Mulder, 2000).

Membrane separation occurs when a driving force is applied to the feed, this can be a pressure, concentration, electric field or temperature gradient. This project is concerned with microfiltration, which is a pressure driven process where a pressure gradient is created between the retentate and permeate in order to create flux. Membrane processes are classified according to the size range of the materials that can be separated and the driving force used in order to accomplish this separation. An overview of some of the different membrane processes, the driving forces used and the components that make up the retentate and permeate streams for each can be found in Table 3.

The membrane pore sizes used within the pressure driven processes MF, UF, NF and RO decreases from MF down to RO as the size of molecules wanting to be retained becomes smaller. This implies that the membrane resistance to mass transfer also decreases with decreasing pore size and in order to obtain the same flux the applied transmembrane pressures has to increase. A schematic showing the separation characteristics of the different pressure driven membrane processes can be seen in Figure 4.

Pressure driven membrane processes are widely used in the dairy industry, Modern processes typically employ one of two major system configurations either a spiral wound cartridge with a polysulfone or polyethersulfione membrane or a tubular ceramic membrane based on zirconium or aluminium oxide (Popović *et al.,* 2009).

The performance of a membrane can be described in terms of two factors, flux and selectivity. Flux can be defined as the volumetric (mass or molar) flow rate of fluid passing through the membrane per unit area, per unit time. This is usually expressed in litres m^{-2} hr^{-1}, but can alternatively be expressed as a velocity in m s^{-1}.

The selectivity of a membrane is a measure of its ability to separate different components. For particulates in liquids and gases selectivity is expressed in terms of retention. Whereas for mixtures of miscible liquids and gases selectivity is expressed as a separation factor, defined as the ratio of the concentration in the permeate divided by that in the feed for two components (Scott and Hughes, 1996).

Percentage solids retention can be calculated using equation 1, where DM_P and DM_F are the wt% dry masses of permeate and feed samples respectively

$$R_S = \left(1 - \frac{DM_P}{DM_F}\right) \times 100 \qquad (1)$$

If the membrane completely rejects the particulate, in other words there is a perfect separation, then R_S = 100%. But if the membrane does nothing and all the particulate passes through, then R_S = 0%.

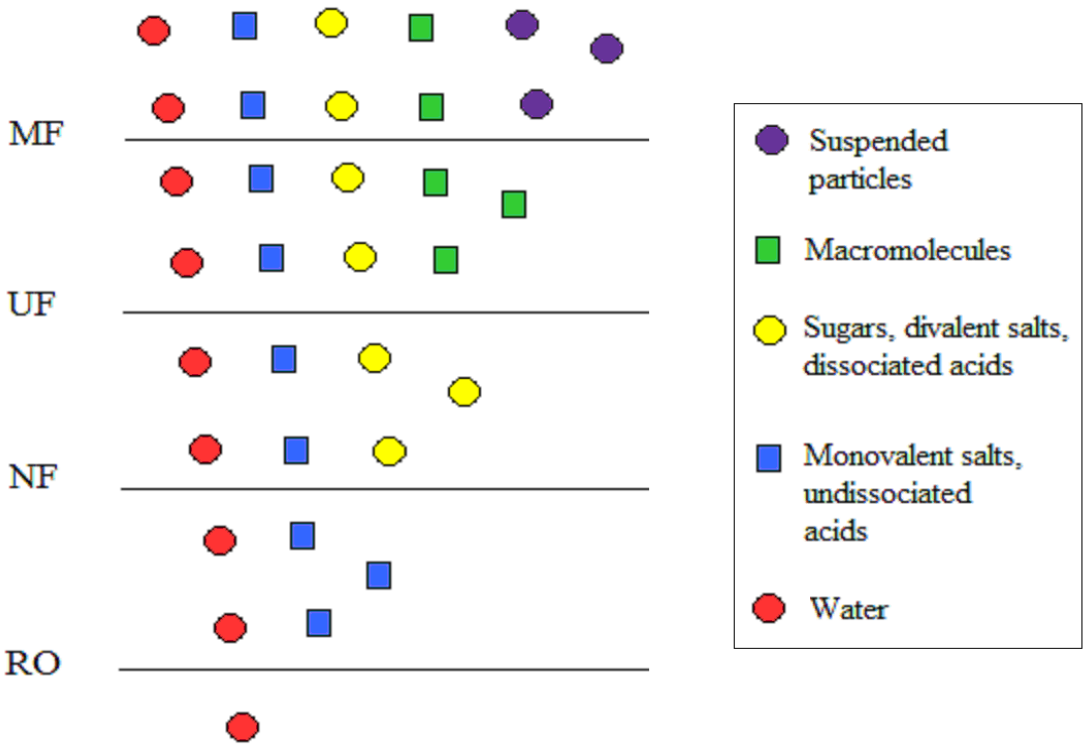

Figure 4. Simple schematic showing the separation characteristics of the different pressure driven membrane processes; MF, UF, NF and RO (Taken from Cheryan, 1998).

Table 3. Overview of various types of membrane separation processes, their driving force and the material found in permeate and retentate streams (Taken from Cheryan, 1998).

Process	Driving Force	Retentate	Permeate
Osmosis	Chemical	Solutes, water	Water
Dialysis	Concentration	Large molecules, water	Small molecules, water
Microfiltration	Pressure	Suspended particles, water	Dissolved solutes, water
Ultrafiltration	Pressure	Large molecules, water	Small molecules, water
Nanofiltration	Pressure	Small molecules, divalent salts, dissociated acids, water	Monovalent ions, undissociated acids, water
Reverse Osmosis	Pressure	All solutes, water	Water
Electrodialysis	Voltage / current	Non-ionic solutes, water	Ionised solutes, water
Pervaporation	Pressure	Non-volatile molecules, water	Volatile small molecules, water

According to Akpinar-Bayizit *et al.*, (2009) commercial membrane applications used within the dairy industry can be classified into four main areas, i) alternatives to a unit operation (centrifugation, evaporation, debacterization, and demineralisation), ii) resolving separation issues (defatting of whey, protein recovery and separation, milk fat globule fractionation and spore removal), iii) creating new dairy products (i.e. UF chesses, whey-based beverages and textured milk products), and iv) improvement of cheese yield and product consistency. This project is concerned with using microfiltration for debacterization and spore removal.

1.9.2 Microfiltration membranes

Microfiltration (MF) is the membrane process that most closely resembles conventional coarse filtration. The pore diameter of MF membranes ranges from 10 - 0.1 μm (Saboya and Maubois, 2000), which makes the process suitable for the concentration of colloid suspensions, bacteria, fat droplets and yeast cells (Cheryan, 1998). The thickness of microfiltration membranes ranges between 10 - 150 μm and the driving force used as stated before is a pressure gradient.

Microfiltration membranes are currently used for a number of applications within the food industry such as fruit juice clarification (Madaeni *et al.*, 2011). In particular the dairy industry uses microfiltration for bacterial removal, milk tailoring prior to cheese

production, selective separation of micellar casein and milk fat, fat removal from whey and cheese brine purification (Mourouzidis-Mourouzis and Karabelas, 2008). When used as an alternative to pasteurisation for bacterial removal, the retentate stream usually contains the bacteria this is heat sterilized and then either recombined with the sterile permeate stream or discarded.

1.9.3 Membrane structure

There are a large variety of materials that can be used for membrane production these materials can be classified as one of three types: Synthetic polymers such as perfluoropolymer, silicone rubbers, polyamides and polysulfones. Modified natural products such as cellulose based membranes or as miscellaneous these include inorganic, ceramic, metals, dynamic and liquid membranes (Scott and Hughes, 1996). Commercial membranes consist mainly of polymers and some ceramics.

Membranes are also categorised according to their wettability, in other words whether they are hydrophilic ("water-liking") or hydrophobic ("water-hating"). Hydrophobic membranes (e.g. polysulfone, polypropylene, polyvinyldienefluoride and polytetrafluorethylene) absorb more proteins than hydrophilic membranes (e.g. cellulose acetate, poly-acrylonitrile). This is one of the reasons for choosing a hydrophilic membrane for a separation process involving proteins (Makardij *et al.*, 1999).

There are two different types of membrane structure namely symmetric and asymmetric. Symmetric membranes have a uniform structure with a uniform pore size distribution throughout the whole of the membrane whereas asymmetric membranes consist of a very thin dense top layer (< 0.5 μm), known as the active layer supported by a porous sublayer (50 - 200 μm). The top or barrier layer performs the separation whereas the porous sublayer acts only as a support. The permeation rate is inversely proportional to the thickness of the barrier layer, and this is the reason why asymmetric membranes are preferred as they show a higher flux than symmetric membranes of comparative thickness (Bird *pers comm.*, 2009).

Microfiltration membranes can be prepared from a range of different organic materials such as polysulfone or cellulose acetate (polymers) and inorganic materials such as alumina, zirconia, titania or silicium carbide (ceramics), glass, metals and carbon. These

materials have vastly different chemical and physical properties and the membrane they are used to produce express these characteristics.

1.9.4 Ceramic membranes

Ceramic membranes have an asymmetric structure; the active layer is usually composed of alumina, titanium or zirconia oxide or a mixture of oxides and the support layer of alumina, carbon, stainless steel or silicon carbide. The active layer is formed by coating the support with a colloidal suspension of highly divided powder, which is sintered onto the support by firing (Saboya and Maubois, 2000).

Ceramic membranes are largely used in the dairy industry as they satisfy all the requirements necessary for use as they have a high mechanical resistance which allows the use of high recirculation velocities of viscous MF retentates and they have a wide temperature and pH tolerance being able to withstand temperatures over 100 °C and pH values between 0.5 - 13.5. This allows CIP regimes involving the use of NaOH up to 3 wt%, nitric acid up to 2 wt% to be carried out and for sodium hypochlorite to be used for sanitation (Saboya and Maubois, 2000).

Since their introduction to the dairy industry ceramic membranes have been widely used due to their increased hydrophilicity compared to flat sheet polymeric membrane materials such as polypropylene and polysulfone. This results in lower protein adhesion during filtration when compared to using hydrophobic polymeric membranes. Ceramic membranes also tend to have narrower pore size distributions than polymeric membranes but they are about an order of magnitude more expensive (Baruah *et al.*, 2006).

1.9.5 Module Designs

Membranes are packaged into modules for convenient operation; modules that have been connected together are called a stage. Important properties for a module to possess include good mechanical and chemical robustness, good flow distribution ensured by having low pressure drops, high shear near the membrane surface, low dead volumes and low sensitivity to feed channel plugging. They must also be easily cleaned, low in cost, easy to assemble, have a high product recovery and be consistent (Scott and Hughes, 1996).

There are many different cross flow module designs possible but they are all based on two types of membrane configuration flat sheet and tubular. There are two types of flat sheet module configuration these are plate and frame and spiral wound modules. In a plate and frame module sets of two membranes are packed together separated by a spacer material with their active top layers facing outwards so that they are in contact with the feed streams, or instead a single membrane sheet is used inserted into the module so that its active layer is facing the feed stream. Their packing density is relatively low ranging from 100 – 400 $m^2 m^{-3}$.

A spiral wound module is very similar to a plate and frame module having the same design of two membranes packed together separated by a permeate channel spacer but is instead wrapped around a central collection pipe. The feed flows parallel to the central pipe through the cylindrical module. The advantage of using this design over a plate and frame module in that it is more compact having a much larger packing density between 300 – 1000 $m^2 m^{-3}$. But these systems are prone to fouling and are difficult to clean due to their design.

There are three types of tubular modules namely tubular, capillary and hollow fibre. Tubular modules consist of a number of tubes mounted into a porous support. The feed is passed down the tubes and the permeate travels through the porous support into the module housing which surrounds the outside of the module. Tubular membranes are usually ceramic. Their packing density is relatively low < 300 $m^2 m^{-3}$, as a result of their large tube diameter of > 5 mm this is the largest of the three tubular modules designs; they are very brittle and often expensive. However as stated before they are highly resistant to both chemical cleaning and heat treatment so much so in that they can be autoclaved in order to remove bacteria. As a result their lifetimes are often much longer compared to flat sheet membranes.

Capillary modules consist of a number of capillaries that have a diameter between 0.5 – 5 mm assembled together. The free ends of the fibres are ‘potted’ with compounds such as epoxy resins, polyurethanes or silicone rubber. As this type of module is strong enough to resist filtration pressures it can be set up in one of two different arrangements (Lennetech tubular-shaped membranes [online, accessed 15/09/12]). Within the first the feed solution is passed through the inside of the capillary and the permeate is collected on the outside. In the other the feed solution is passed along the outside of the capillary

known as the ‘shell’ side and the permeate is collected on the inside of the capillary. If the feed is thought to contain a large amount of fouling material it is advised to use the module in the second arrangement because the capillaries have a smaller diameter compared to those in a tubular membrane meaning there is a greater chance that deposits will plug them. But deposits can potentially be removed from the inside of the capillaries by passing either a liquid or gas down the tube.

Lastly, the hollow fibre module this operates in the same fashion as the capillary module. The difference being that the module is made up of a number of fibres assembled together as opposed to capillaries. The fibres are much smaller compared to the capillaries having a diameter < 0.5 mm this causes the packing density of this module to be much larger having a value normally close to 30,000 m^2 m^{-3}, but also means there is a higher risk of tube plugging by foulants (Lennetech tubular-shaped membranes [online, accessed 15/09/12]).

A comparison of the characteristics of the different types of module design described above can be found within Table 4. During this study the use of both a flat sheet plate and frame module and a tubular ceramic module will be investigated.

Table 4. Comparison of the characteristics of the different types of module design (Taken from Bird *pers comm.*, 2009).

Characteristic	Tubular	Plate and frame	Spiral wound	Capillary	Hollow fibre
Packing density	Low	→	→	→	Very high
Cost	High	→	→	→	Low
Fouling tendency	Low	→	→	→	Very high
Ease of cleaning	Good	→	→	→	Poor
Ability to replace membrane	Yes / No	Yes	No	No	No

1.9.6 Membrane preparation

Membrane preparation can be carried out using various techniques such as sintering, stretching, track etching and phase inversion. The method employed determines the characteristics displayed by the membrane such as the porosity and the pore size distribution. The characteristics of membranes produced by the different techniques are

shown in Table 5. In order to optimise MF membranes it is necessary to make the porosity as high as possible and the pore size distribution as narrow as possible, so that a high flux as well as a suitable separation of components is achieved.

Sintering can be used to prepare microfiltration membranes with pore sizes between 0.1 – 10 μm and of low porosity between 10 – 20%. It is a relatively simple technique that can use either organic or inorganic materials. It involves compressing a powder made up of particles of a particular size and sintering at a specific temperature, which depends on the material used. During sintering the interfaces between the particles disappear producing a pore, this is shown by the simple schematic in Figure 5. A large range of materials can be used during sintering including polymer powders such as polyethylene (PE), polytetrafluoroethylene (PTFE) and polypropylene (PP). The structures of which are shown within Figures 6 (a), (b) and (c) respectively. Ceramics, glass and carbon powders can also be used.

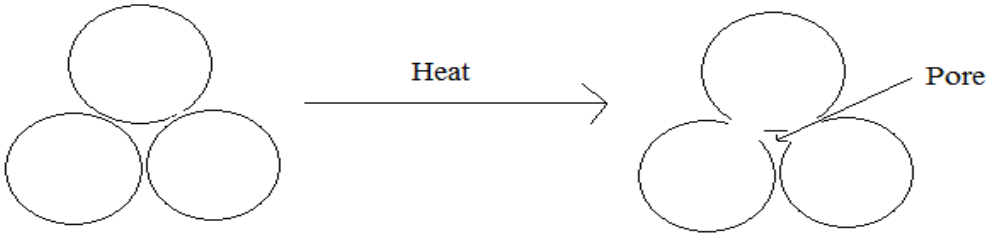

Figure 5. Simple schematic showing sintering method of membrane production (Taken from Mulder, 2000)

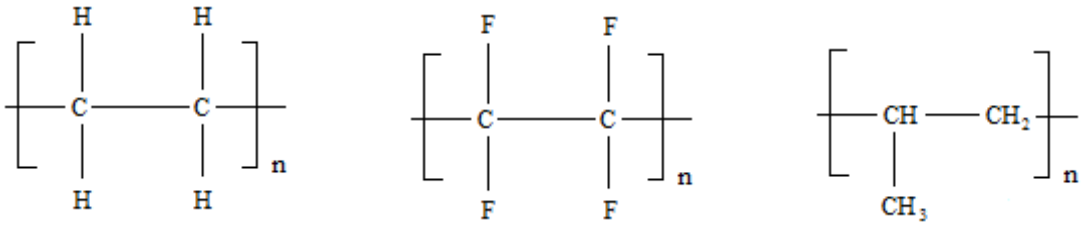

(a) *(b)* *(c)*

Figure 6. Structures of the polymers a) polyethylene, b) polytetrafluoroethylene and c) polypropylene.

Stretching is a second technique that can be used to produce MF membranes from semi crystalline polymers. Membranes produced using this technique can have a much higher porosity with values up to 90% possible but the range of pore sizes able to be formed is slightly smaller ranging between 0.1 – 3 μm. During this technique an extruded film or foil made from the polymer is stretched perpendicular to the direction of extrusion, so that the crystalline regions are parallel to the direction of extrusion. Lastly a mechanical stress is applied that results in membrane pore formation (Mulder, 2000).

Track etching is used to produce membranes that have the simplest pore geometry containing a series of parallel cylindrically shaped pores of uniform dimension. During this technique a film or foil normally made of polycarbonate is subjected to high-energy particle radiation, which damages the polymer matrix and creates tracks. The film is then immersed in either acid or alkali, which breaks down (etches) the polymeric material along the tracks producing pores. This method produces membranes of low porosity that have pore sizes ranging from 0.02 – 10 μm. The radiation time determines the membrane porosity and the pore diameter by the time the membrane material is left to etch.

Immersion precipitation is a type of phase inversion preparation from which most commercially used membranes are produced. Phase inversion involves conversion of a polymer from a liquid to a solid state. Transforming the polymer from one liquid state into two liquids often induces this solidification. At a certain stage during demixing the phase containing the larger amount of polymer solidifies producing a solid matrix. This process involves firstly casting a polymer solution of between 5 - 25 wt% solids onto a support such as non-woven polyester. This is then immersed into a coagulation bath filled with a nonsolvent (normally water). Precipitation occurs as the nonsolvent replaces the solvent. Other methods can be used to induce precipitation such as solvent evaporation, precipitation from the vapour phase, by controlled evaporation and thermal precipitation. Phase inversion membranes can be prepared from a wide range of polymers; the only requirement being that the polymer must be soluble in either a solvent or solvent mixture. The structure of the membrane can be manipulated by varying one of many parameters such as the polymer concentration in solution, the evaporation time, humidity, temperature and the composition of the polymer (casting) solution (Mulder, 2000).

Table 5. Porosities and pore size distributions achieved by various membrane preparation methods (Taken from Bird *pers comm.*, 2009).

Preparation technique	Porosity achieved	Pore size distribution achieved
Sintering	Low / medium	Narrow / wide
Stretching	Medium / high	Narrow / wide
Track etching	Low	Narrow
Phase inversion	High	Narrow / wide

Inorganic membranes can be manufactured with more control leading to a narrower pore size distribution compared to polymeric based membranes. Because of this and their higher resistance to both chemical and thermal degradation they have a longer lifetime and are usually much more expensive than polymeric membranes. Ceramic membranes are also very fragile and if dropped often become irreparable damaged and must be replaced.

Once prepared or during preparation membrane surfaces can be modified in order to reduce fouling or improve its chemical resistance. This can involve adding surface-modifying agents directly to the polymer (casting) solution or modifying the cast membrane through chemical or physical treatment (Mulder, 2000). Liu *et al.,* (2008) found through surface modification of flat sheet polysulfone UF membranes to increase hydrophilicity, achieved through grafting hydrophilic polymers onto an UV / ozone pretreated membrane surface that protein fouling through adsorption was reduced by 20 - 60% compared to an unmodified virgin membrane.

1.10 FILTRATION MODES

1.10.1 Dead-end operation

This is the traditional and simplest mode of operation used during membrane separation, in which the feed flows perpendicular to the membrane, as shown in Figure 7. Retained particles form a cake on the membrane surface, the thickness of which increases with filtration time and leads to a reduction in flux. As filtration time increases not only does the permeate flux decline so does the quality of the permeate, as with time the concentration of retained solutes in the feed solution increases. To help reduce cake build up when asymmetric membranes are used they can be inserted so that their open porous side is facing the feed so that retained particles can penetrate the membrane and be dispersed without blinding off the membrane surface and plugging pores as quickly. But even when this technique is adopted the membrane filter will eventually reach an impractical or uneconomical low filtration rate and has to be either cleaned or replaced. Due to these issues dead-end filtration is now used only for applications in which the feed stream has a very low solid content of < 0.5% solids content (Scott and Hughes, 1996). In order to help prevent this problem cross flow filtration was developed.

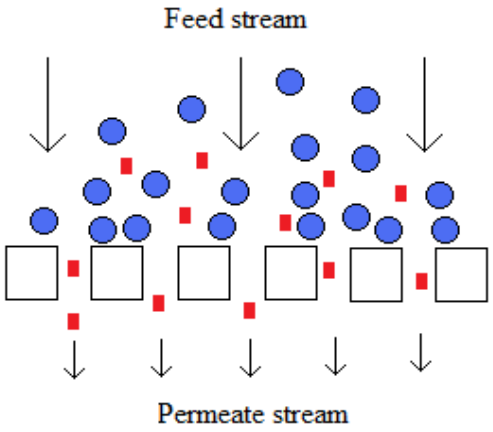

Figure 7. Schematic showing dead-end filtration (Adapted from Mulder, 2000).

1.10.2 Cross-flow operation

This mode of operation is more commonly used at present and is generally utilised within the dairy industry. It differs from dead-end filtration as the feed stream is swept across the membrane tangentially as opposed to perpendicularly, as shown in Figure 8. Inside the module the composition of the feed changes as a function of distance being separated into a retentate and permeate stream. The permeate is collected and the retentate recirculates through the system (Mulder, 2000). The philosophy behind this set-up is that as the feed is swept over the membrane if a high enough cross flow velocity is used any rejected material that has become loosely bound onto the surface can be removed and transported back to the bulk flow. When an asymmetric membrane is used it must be inserted into the module with the active top layer facing the feed so that any retained particles can be acted upon by the tangential flow.

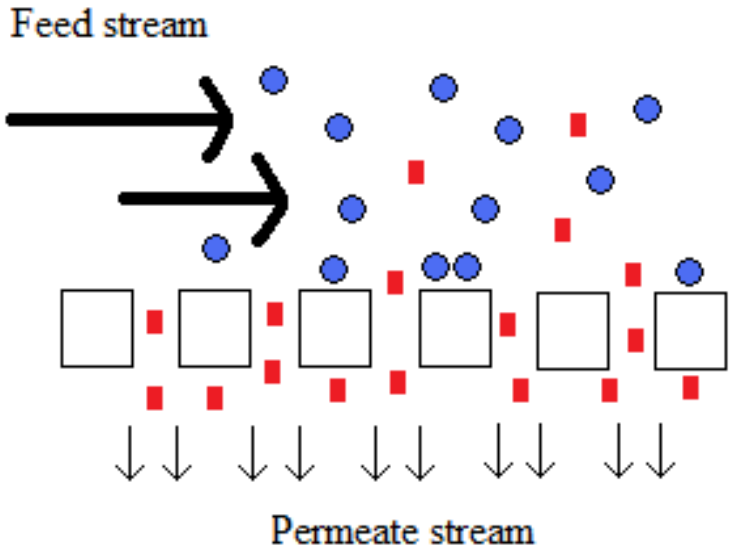

Figure 8. Schematic showing cross-flow filtration (Adapted from Mulder, 2000).

1.11 MEMBRANE FOULING

This project was concerned with minimising fouling due potentially to proteinaceous deposits from the highly viscous MPI feed solutions and biofouling due to spores of *Bacillus mycoides* used to inoculate the MPI feed streams.

Fouling is one of the major factors that influence the economical feasibility of a membrane separation technique (Mulder, 2000). Fouling is a general term used to describe any mechanism that has a negative effect on permeate flux and / or membrane selectivity. Fouling can either be reversible or irreversible, reversible fouling has been defined as "being rinsable at zero transmembrane pressure" (Shorrock and Bird, 1998), this includes concentration polarisation layers and loosely bound deposits. Accumulation of rejected particles on the top surface of the membrane occurs as external fouling or cake formation and is usually reversible (Wakeman and Williams, 2002). In contrast irreversible fouling has been described as "not being removed by rinsing such as adhesion and pore blinding" (Shorrock and Bird, 1998). Deposition and adsorption of small particles within the internal pore structure of the membrane known as internal fouling is usually irreversible fouling (Wakeman and Williams, 2002). The presence of reversible fouling such as concentration polarisation and cake formation increase the likelihood of irreversible fouling formation.

In theory all components except the solvent present in the feed stream can potentially foul the membrane. The specific physical and chemical characteristics of the individual components, the membrane and the permeate flux level determines the nature and extent of fouling. It is often the case that the species causing the dominant fouling effects are present only in trace amounts. For example the fouling seen in many biological separations is often caused by trace amounts of aggregated and / or denatured protein (Makardij *et al.*, 1999).

Defining when fouling is occurring is not straight forward, in the past it has often been concluded that any flux decline that occurs at the start of a filtration process is the result of concentration polarisation followed by gel formation and that any long term flux decline is the result of fouling. However fouling can also develop very quickly, for example the characteristic time for protein adsorption to solid surfaces can often be as short as several seconds. Also long term flux decline can also reflect an alteration in the

feed stream (e.g. slow increase in fluid viscosity due to ageing or an accumulation of retained solutes) or a slow physical or chemical alteration of the membrane structure or composition (Makardij *et al.*, 1999).

Membrane properties such as surface roughness, pore size distribution, hydrophobicity and charge can all affect the fouling characteristics of a membrane. The extent to which each of these properties affects the fouling tendency of the membrane depends upon the experimental set up. Riedl *et al.,* (1998) found that surface roughness was the dominant factor determining fouling behaviour during the clarification of apple juice using MF. As PES and PVDF membranes that had a relatively rough surface produced a higher flux compared to the smoother nylon and PS membrane surfaces. They concluded this was because only a loose fouling layer with a low resistance could be formed on the rough membrane surface compared to a dense fouling layer that were able to be formed on the smooth membrane surface.

1.11.1 Proteinaceous fouling

Protein adsorption onto membrane surfaces as stated before often occurs very rapidly and has even been found to occur in the absence of permeation (James *et al.,* 2003).

According to Vétier *et al.,* (1988) the loss of flux during skim milk microfiltration is initially caused by protein adsorption and then to micelle deposit into which soluble proteins are entrapped, with time this leads to a decrease in the porosity of the fouling layer. At a certain point under specific conditions termed the Critical Hydrodynamic Conditions (CHC) an irreversible fouling layer is created. Jimenez- Lopez *et al.,* (2007) established that micelles were the major milk component responsible for the set up of CHC and that soluble protein just participated in its development.

Makardji *et al.,* (1999) investigated the fouling of a flat sheet PVDF MF membrane and a PS UF membrane with reconstituted skim milk. They found through AFM images that pore blockage was the main cause of fouling as only the large pores remained free of deposits and so membrane morphology and pore size distribution were found to be the dominant factors in membrane fouling.

It has been stated that pore blocking can be attributed to interactions between protein molecules or clusters and the membrane polymer along with protein-protein

interactions. James *et al.,* (2003) during the MF and UF of reconstituted skim milk found evidence to support this theory using SEM images which showed that protein particles interacted with both the pore walls of the membrane through protein-polymer reactions and also that they formed agglomerates through protein-protein reactions leading to pore narrowing and eventually pore blocking.

There appears to be some contrast of opinion within the literature because as stated before Vétier *et al.,* (1988) and Jimenez- Lopez *et al.,* (2007) believe that casein micelles are responsible for milk protein membrane fouling but Tong *et al.,* (1988) during whole milk filtration report that fouling resulted from whey protein fractions and not casein micelles. Through SDS-PAGE characterisation 95% of the foulant material was found to consist of α-lactalbumin and β-lactalbumin.

1.11.2 Biofouling

The unwanted accumulation of microorganisms and cell debris on membrane surfaces is generally referred to as biofouling. More specifically biofouling can be defined as "the deleterious attachment of a mat of cells and extracellular polymeric substances (EPS) to a solid surface" (Blanpain-Avet *et al.,* 2009).

There are various stages that occur during biofouling, firstly viable cells attach irreversibly onto the surface of the membrane as a result of both electrokinetic and hydrophobic interactions. Once attached the bacteria then synthesis and excrete EPS mainly consisting of polysaccharides and protein. Finally, a biofilm is developed through cell growth and multiplication. The formation of a biofilm is a type of gel layer and as such if formed its presence will cause a gel layer resistance.

A number of techniques have been developed to enumerate microorganisms that have become attached onto a membrane surfaces. Blanpain-Avet *et al.,* (2009) outlines some of these techniques which include microscopic cell counts involving staining the bacteria with a particular fluorochrome or using crystal violet and then viewing the membrane by bright field microscopy. Plate counts, which involve using a nutrient medium involving incubating small sections of the membrane or the surface of both the membrane and module can be swabbed, this is then diluted down in a suitable buffer and incubated. Radioactive labelled bacteria that can be counted using a liquid scintillation counter and lastly scanning electron microscopy (SEM) can be used.

1.12 FILTRATION FLUX

The flux J, through a membrane can be described simply as the volume of fluid V, permeating through the membrane in a given time t, over a known membrane area A_M, shown by equation 2.

$$J = \frac{\Delta V}{\Delta t \times A_M} \tag{2}$$

Membrane performance often changes as a function of filtration time with the flux decreasing when a constant pressure is applied. Flux decline can be caused by concentration polarisation and various types of fouling, which are summarised in Figure 9. These phenomena introduce additional resistances on the feed side to transport across the membrane. The flux in a pressure driven process such as microfiltration when additional resistances are present can be calculated using equation 3, where ΔP is the driving force, η is the feed viscosity and R_{TOT} is the total resistance.

$$J = \frac{\Delta P}{\eta \times R_{TOT}} \tag{3}$$

In an ideal system the resistance of the membrane itself is the only resistance acting on the filtration process. This is found from experiments and is shown as R_m (the procedure for how to calculate R_m and permeate flux and the equations used can be found in Appendix 1). But during filtration if the membrane is working correctly permeate flux typically decreases as a function of time with a rapid initial decline followed by a more gradual long-term decline. The initial decline is due to a build up of solute on the membrane surface, known as concentration polarisation, which is described in more detail in section 1.15 and the more gradual decline to membrane fouling. The resistance produced by trying to overcome this increase in concentration is R_{cp}.

The accumulation of solute molecules may become so high that either a gel or cake layer forms, a gel layer creates an additional layer of resistance known as the gel layer resistance, R_g. Blanpain-Avet *et al.*, (2009) have outlined the detrimental effects that the formation of a gel layer can have on membrane performance. These include a reduced permeate flux, reduced membrane lifetime, selectivity and an increased module differential pressure resulting in higher energy consumption.

A porous cake layer may instead be formed due to an accumulation of solute molecules near the membrane surface causing a second type of additional layer resistance, R_c. The formation of a cake layer can be considered as the formation of a pre-filter that has greater retention capabilities than the membrane itself. A cake layer is usually very dense at the membrane surface and becomes more porous as the cake layer transforms into the concentration polarisation region (Tarabara *et al.*, 2004).

Solutes may also foul the membrane itself causing an increase in membrane resistance either by adsorbing onto the membrane surface or they may even penetrate into the membrane pores and absorb onto the surface, this results in the effective pore diameter to be reduced creating the resistance R_a. This may lead to complete pore blocking producing the resistance R_p.

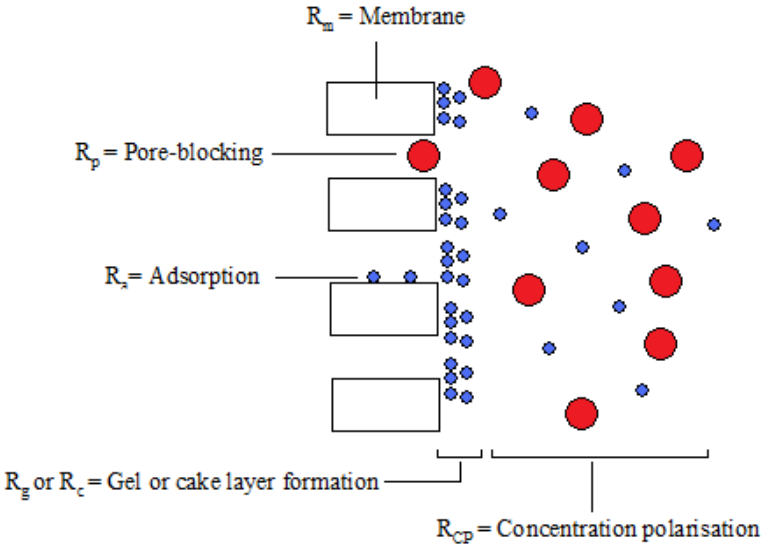

Figure 9. Schematic showing the various types of resistance towards mass transport across a membrane (Adapted from Mulder, 2000).

These resistances can be combined producing a total fouling resistance R_{TOT} and summarised as a resistance in series model as shown below in equations 4, 5 and 6.

$$R_{TOT} = R_m + R_p + R_a + R_{cp} + R_g + R_c \quad (4)$$

A fouling resistance R_F, can be shown as:

$$R_F = R_p + R_a + R_g + R_c \quad (5)$$

And the total hydraulic resistance can be summarised as:

$$R_{TOT} = R_m + R_F + R_{CP} \quad (6)$$

The procedure for how to calculate R_{TOT} using experimental flux data and the equations used can be found in Appendix 1.

1.13 BLOCKING FILTRATION LAWS

Blocking filtration laws are used to describe the four mechanisms of membrane fouling; complete pore blocking, standard pore blocking, intermediate blocking and cake filtration, a schematic of each is shown in Figure 10. Wang and Tarabara (2008) and Vela *et al.*, (2009) have described each of these models. According to the complete blocking model it is assumed that each solute molecule arriving at the membrane surface blocks a pore and that a molecule never settles on another molecule that has previously been deposited on the membrane surface. The permeate flux through the unblocked pores is unaffected so the reduction in flux is equal to the reduction in membrane surface area corresponding to unblocked pores. This type of fouling occurs when the solute molecules are greater in size than the membrane pores.

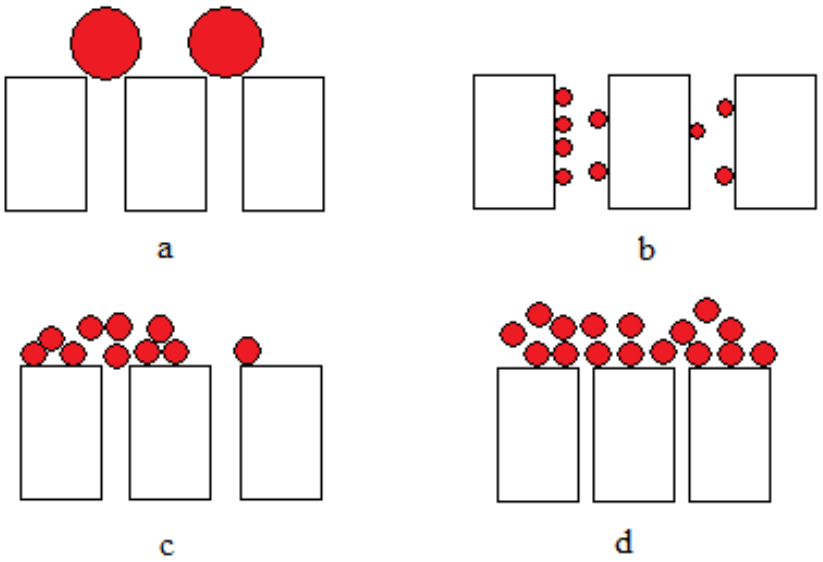

Figure 10. Schematic illustration of the four fouling mechanisms; a) complete blocking, b) standard blocking, c) intermediate blocking and d) cake filtration.

According to the standard blocking model it is assumed that particles enter pores and deposit onto pore walls meaning that pore volume decreases proportionally to the volume of deposited particles, this type of fouling is caused by solute molecules that are smaller that the membrane pore size. According to the cake filtration model it is assumed that depositing particles do not block pores either because the membrane is

dense and there are no pores to block or because the pores are already covered by other particles. Lastly, the intermediate blocking model is a combination of the cake filtration and complete blocking laws and assumes that some particles deposit onto other particles and that others block membrane pores. The probability of a molecule blocking a pore decreases continuously with time. This type of fouling occurs when solutes have a similar size to that of the membranes pores.

1.14 CRITICAL FLUX THEORY

The critical flux theory proposed by Field *et al.,* (1995) for microfiltration states "on start-up there exists a flux below which a decline in flux with time does not occur; above it fouling is observed. This flux is the critical flux and its value depends on the hydrodynamics and possibly other variables".

According to this theory three different regimes can be distinguished each of which has a different TMP to flux relationship as can be seen in diagrammatic form in Figure 11. In regime 1 the TMP is lower than the critical pressure and filtration occurs with no fouling. Filtration in this regime is termed sub-critical flux operation and is advised to obtain optimal selectivity. However, as flux is low a large membrane area is needed but can be increased by increasing CFV (Brans *et al.,* 2004). In regime 2 TMP is above the critical pressure and flux is equal to the limiting flux, as the transport of material towards the membrane is in equilibrium with the back transport to the bulk solution. In this regime flux is independent of TMP and pore size but increasing CFV will increase flux and may shift the process back into regime 1. In regime 3 TMP is much higher than the critical pressure and causes a time dependent flux mainly due to cake compaction. For long-term stable operation in regime 3 fouling must be removed after short intervals using e.g. backpulsing. Microfiltration processes used for spore and bacteria reduction and concentration of casein micelles are usually operated just above the critical pressure in the lower part of region 2 (Brans *et al.,* 2004).

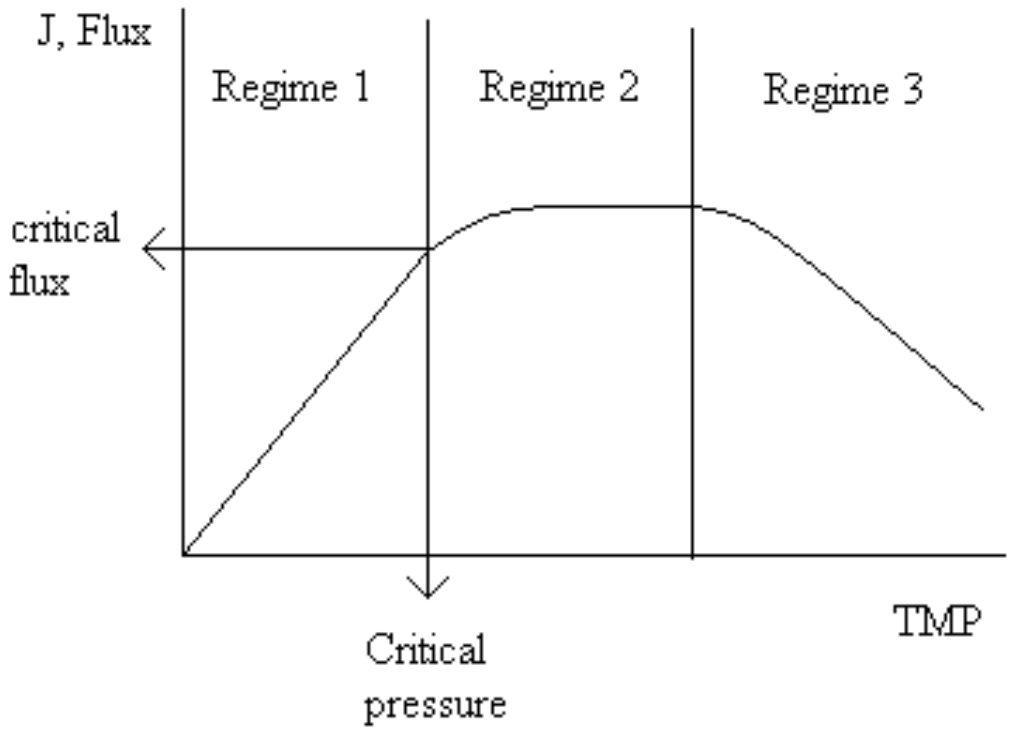

Figure 11. Schematic showing the TMP to flux relationship of the three different filtration regimes distinguished by critical flux theory (Taken from Brans et al., *2004).*

1.15 CONCENTRATION POLARISATION

During membrane filtration when a driving force is applied to a feed solution the solute is partly retained by the membrane whereas the solvent permeates through. This results in the concentration of solute in the permeate (c_P) being lower than in the bulk solution (c_b). The retained solutes accumulate at the surface of the membrane, causing the concentration to be greater at the membrane surface than in the bulk feed solution, this results in the development of a decreasing concentration gradient from the membrane surface to the bulk feed solution. This causes a diffusive backflow of solute from the membrane surface to the bulk solution. After a given time steady state conditions are reached where the movement of solute towards the membrane will be balanced by solute flux through the membrane plus the diffusive flow away from the membrane. This phenomenon is known as concentration polarisation as is shown by the schematic in Figure 12 and equation 7.

$$J.c = D\frac{dc}{dx} + J.c_p \qquad (7)$$

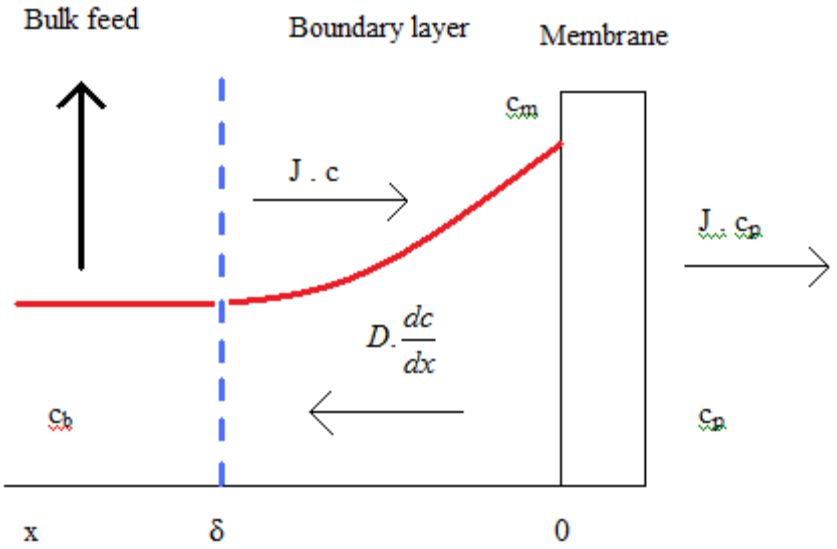

Figure 12. Concentration polarisation; concentration profile under steady-state conditions (Adapted from Mulder 2000)

Where the boundary conditions are:

$$x = 0 \longrightarrow c = c_m$$
$$x = \delta \longrightarrow c = c_b$$

and integrating equation 7 within these boundary conditions results in equation 8.

$$In\left[\frac{c_m - c_p}{c_b - c_p}\right] = \left(\frac{J_v \delta}{D}\right) \tag{8}$$

The ratio of the diffusion coefficient D, and the thickness of the boundary layer δ, is termed the mass transfer coefficient, shown in equation 9.

$$k = \frac{D}{\delta} \tag{9}$$

The effect of concentration polarisation can be very severe in microfiltration and ultrafiltration because the fluxes J, are high and the mass transfer coefficients *k*, are low, as a result of the low diffusion coefficients of the retained material. Manipulating either of these parameters J_v or *k* can reduce the effect of concentration polarisation. As can be seen in equation 9 the diffusion coefficient and the boundary layer thickness determine the mass transfer coefficient. As a solutes diffusion coefficient can only be increased by raising the temperature (which would lead to an increase in flux as the feed viscosity is decreased that would oppose the effect of improved mass transfer) mass transfer can only be increased by altering the boundary layer thickness. This layer can be reduced by

either using a higher flow velocity, using turbulence promoters, or by using a pulsatile flow.

1.16 OSMOTIC PRESSURE MODEL

This model assumes that any deviation away from a membranes pure water flux occurs solely due to the osmotic pressure at the membrane surface and is shown in equation 10. During filtration at the membrane surface solutes within the permeate diffuse back across the membrane into the more concentrated feed stream by osmosis. The osmotic pressure for permeate and feed streams can be calculated using equation 11. Where C is the concentration of solute in the stream (g litre^{-1}), R is the universal gas constant (litre bar K^{-1} mol^{-1}), T the temperature (K) and M the molecular weight of the solute (g mol^{-1}). The difference across a membrane (π_m) can be calculated by subtracting the permeate pressure from that calculated for the feed. In RO and NF this osmotic effect is quite large when solutes molecular weights are small. Whereas in UF and MF this term is often ignored as it is assumed that the osmotic pressure for macromolecules is negligible compared to the applied hydraulic pressure $\Delta P - \pi_M \approx \Delta P$. It was initially thought that osmotic pressure may have had an effect on filtration during this project as the feed concentrations being used were so high but the osmotic pressure was calculated as shown in Appendix 7 and was found to be negligible compared to the TMP used. This is explained in more detail in section 4.4.

$$J = \frac{\Delta P - \pi_m}{R_m} \tag{10}$$

$$\pi = \frac{CRT}{M} \tag{11}$$

1.17 MEMBRANE CLEANING

Membrane cleaning is one of the most important steps for maintaining membrane performance, such as permeability and selectivity. It has been defined as “a process where the membrane is relieved of materials, which are not an integral part of the membrane” (Tragardh, 1989). Ideally cleaning should be efficient, easy and fast, with no damage to the membrane or installation, and must meet sanitary requirements.

In practice all membranes eventually need to be cleaned in one way or another, the various methods of cleaning are hydraulic, mechanical, electrical and chemical cleaning. Hydraulic cleaning can only be applied to tubular membranes as polymeric

membranes are not able to withstand the high pressures that are used. A common hydraulic cleaning technique is backwashing the use of which during this work is discussed in more detail in section 2.10 and 4.7.3, 4.7.4, 4.7.5 and 4.7.6.

Mechanical cleaning as with hydraulic cleaning can only be applied to tubular membranes and involves scouring the fouled surface with a solid abrasive material sponge balls are commonly used.

Electrical cleaning involves the application of a voltage across the surface of the membrane, which results in the formation of micro bubbles which pushes deposited material off and into the feed stream. This type of cleaning is not widely used, as it requires a module capable of applying a voltage to the membrane and for the membrane itself to be conductive.

Lastly, chemical cleaning this is the most important method of removing foulant from a membrane and is usually performed as cleaning in place (CIP). Cleaning in place can be defined as "the cleaning of complete items of plant or pipeline circuits without dismantling or opening of the equipment and with little or no manual involvement on the part of the operator" (Romney, 1990). These processes are fully automated and the type of chemical used depends on the type of deposit to be removed and the surface of the membrane, some of the choices available and what they are effective in removing can be seen in Table 6.

During cleaning energy is applied to foulants in three basic forms kinetic energy creating solution turbulence, thermal energy by increasing solution temperature and lastly, chemical energy as chemical reactions between the foulant and components of the detergent (Shorrock and Bird, 1998). While a deficiency in one of these can be compensated for by an increase in the other two, all three are vital to the total operation (Romney, 1990).

Three levels of membrane cleanliness have been defined in order to assess different cleaning and disinfection procedures, namely hydraulic, chemical and microbiological cleanliness (Blampain-Avet *et al.,* 2009). Hydraulic cleanliness is achieved when membrane permeability or initial pure water flux is restored; chemical cleanliness when all foulants and impurities including those from any cleaning agent used have been

removed and lastly microbiological cleanliness is achieved when the membrane surface is free from living organisms. The international standard for microbiological cleanliness within the dairy industry is the presence of up to 2 microorganisms cm^{-2} on any equipment surface (Plett, 1992).

Table 6. Common detergents and the materials they remove (Adapted from Shorrock and Bird, 1998).

Detergent	Effective in removing
Acids	Inorganic salts and oxide films
Alkalis	Hydroxides, fats and proteins
Enzymes	Used on sensitive membranes
Sequestrants (or chelating agents)	Prevention of re-deposition and / or removal of mineral deposits
Disinfectants	Pathogenic micro-organisms
Surfactants	Increases wettability promoting contact between detergent and membrane surface

Romney (1990) states that a dairy detergent should ideally exhibit the following characteristics.

1. Organic dissolving power so that it can solubilise proteins, fats and other dairy components.
2. Dispersing and suspending power, so that it can bring insoluble deposits into suspension and prevent their redeposition on clean surfaces
3. Emulsifying power, to hold oils and fats dispersed within the cleaning solution
4. Sequestering power, so that it can combine with calcium and magnesium salts found in hard water to form water-soluble compounds and to aid detergency.
5. Wetting power, to decrease surface tension and therefore aid deposit penetration.
6. Lastly, rinsing power the ability to rinse away clearly and completely without leaving any trace of foulant or detergent on the cleaned surface.

1.17.1 Removal of dairy foulants from membrane surfaces

Bird and Bartlett (1995) report optimal conditions found when cleaning a sintered stainless steel MF membrane fouled with a 3.5 wt% reconstituted whey protein concentrate powder. These optima were a NaOH concentration of 0.2 wt% when cleaning with an applied TMP of 0.5 bar, at a CFV of 1.6 m s^{-1} and 50 °C producing a

flux recovery of > 94% and of 0.5 wt% when cleaning with no TMP using a CFV of 1.6 m s^{-1} at 50 °C, producing a flux recovery of > 97%. Bartlett *et al.,* (1995) reports an optimal NaOH concentration of 0.2 wt% for the removal of whey protein fouling from a sintered stainless steel membrane and 0.4 wt% from a ceramic membrane. Popović *et al.,* (2009) tested a range of NaOH concentrations for cleaning tubular ceramic membranes of 50 and 200 nm pore sizes fouled with a reconstituted whey solution and reported the highest flux recovery of 78% when using a 0.6 wt% solution at 50 ºC, 1.73 m s^{-1} CFV and 0.3 bar TMP.

Various studies report the presence of a maximum flux recovery time such as James *et al.,* (2003) who report a maximum flux recovery of 75% after five minutes of flushing a fouled MF membrane with RO water. This could be explained by a mechanism proposed by Bird (1997) and explored further in Bird and Bartlett (2002). Which states that after cleaning begins the cake layer or large surface foulant particulates are removed resulting in an initial sharp increase in flux. But this may lead to the formation of smaller particles due to the dissolution of the soluble parts of the large particles. These small particles may then fit into the pores themselves causing a decrease in flux. It may also be the case as suggested by Makardij *et al.,* (1999) and Bird and Bartlett (2002) that after a certain cleaning time due to additional hydration that any in-pore fouling may start to swell causing more of the pore to become blocked leading to a decrease in flux recovery.

1.17.2 Disinfection of biofouled membranes

It is well known that spores are more resistant to disinfectants than vegetative cells. Young and Setlow (2003) summarised various factors that have been identified as important in spore resistance. These include 1) the thick proteinaceous coats that are resistant to many chemicals 2) the low water content in the spores core that is important in heat resistance 3) the saturation of spores DNA by a group of small acid soluble proteins that protect spore DNA from damage by UV radiation, heat and some chemicals 4) the low permeability of the inner spore membrane to hydrophilic molecules and lastly, 5) the repair of DNA damage when spores germinate.

But spores can be killed using some chemicals; hydrogen peroxide and sodium hypochlorite are two well-known spore decontaminants. Both chemicals cause disruption and extraction of coat material that allows further penetration of the

chemicals to the cortex and protoplast of bacterial spores (DeQueiroz and Day, 2008). Hypochlorous acid is the active component in sodium hypochlorite the disinfectant selected for use during this project, which is known to react rapidly with proteins, DNA, lipids, thiols and disulfides (Noguchi *et al.*, 2002).

Young and Setlow (2003) treated spores of *Bacillus subtilis* with sodium hypochlorite at concentrations of 2500 ppm (at pH 11) and 50 ppm (pH 7) at ambient temperature (23 - 25 ºC) after decoating them using 100 mmol litre^{-1} NaOH. They found that both treatments produced a near 100% spore reduction. This took ~60 minutes when using 2500 ppm as opposed to 10 minutes using 50 ppm NaOCl. This provides evidence that the NaOCl disinfection protocol selected for use during this project was sufficient. As described in section 4.1 this involved using a concentration of 200 ppm, at ambient temperature for a disinfection time of 10 minutes.

Bloomfield and Arthur (1992) tested the efficiency of three different chlorine-releasing agents sodium hypochlorite, sodium dichloroisocyanurate and chloramine-T at killing spores of *Bacillus subtilis* at a concentration of 3 x 10^8 cfu ml^{-1} both in the presence and absence of NaOH. Sodium hypochlorite was found to be the most effective chlorine-releasing agent producing a 3.7 log > 99.9% spore reduction at 200ppm after 5 minutes. Treatment of spores in the presence of 0.4 wt% NaOH increased the spores sensitivity to NaOCl producing a 4.0 log > 99.9% spore reduction. This was found to be because treatment with NaOH causes spore coat extraction, which allows greater penetration of NaOCl. This study provides further evidence that the disinfection protocol used during this project to remove spores of *Bacillus mycoides* was sufficient. As the concentrations of bacterial spores used during experiments was much lower than that tested during this study and also a greater concentration of both NaOH and NaOCl were used during experiments.

The antimicrobial activity of sodium hypochlorite is a function of pH and storage time. Sagripanti and Bonifacino (1996) showed that storing a 0.05 wt% sodium hypochlorite solution for 0.8 days resulted in a 50% reduction in efficiency; this is because when stored, degradation of its antimicrobial components occurs. Sagripanti and Bonifacino also showed that the disinfecting efficiency of sodium hypochlorite decreases as pH increases. They found that a 0.05 wt% hypochlorite solution was inactive at alkaline pH and most effective at neutral pH. As a result during this project sodium hypochlorite

solutions once prepared were used as soon as possible and it was ensured that after cleaning the NaOH solution was completely flushed out of the filtration system before the membrane was sanitised with sodium hypochlorite.

Blanpain-Avet *et al.,* (2009) investigated the cleanability of a 0.45 μm ceramic membrane that had been biofouled with spores of *Bacillus cereus.* They report that hydraulic but not microbiological cleanliness was achieved using 0.5 wt% sodium hydroxide as the cleaning agent at a temperature of 55 °C, a CFV of 4.0 m s^{-1} and a TMP between 0.3 – 0.4 bar for a period close to 10 minutes. Microbiological cleanliness was not achieved as between 2.7 – 5.2 log cfu cm^{-2} spores remained after cleaning, this is over the 2 log cfu cm^{-2} dairy industry threshold required for this level of cleanliness.

Shorrock and Bird (1998) describe two effective cleaning strategies they found for the removal of microorganisms in the form of yeast cells from a polyethersulfone MF membrane with a pore size of 0.1 μm. The first involves the use of dilute NaOH at a concentration of 0.01 wt% for two minutes followed by HNO_3 at a concentration of 0.064 M at 40 ºC for 8 minutes. The second involves treating the surface with *P3 Ultrasil 11* with a temperature of 60 °C and a concentration of at least 0.002 wt% with complete flux recovery achieved after 10 - 20 minutes.

It is important for industry to develop optimal cleaning conditions as the associated costs can be significant with chemicals having to be purchased, effluent disposed of, liquids pumped and solution temperatures increased, as well as the loss of production costs due to cleaning related downtime. Cleaning procedures are also of environmental concern due to the generation of large quantities of effluent that are produced which are usually highly alkaline. In the near future it may be necessary not only in terms of costs but by law to show that these processes are being optimised meaning energy consumption and effluent disposal are being minimised.

1.18 TECHNIQUES AVAILABLE FOR THE REMOVAL OF BACTERIA FROM MILK

Bactofugation is the traditional method used for reducing the bacterial content within milk. It is a centrifugation technique based on the difference in density between bacteria and milk components, with bacteria having a higher density. This process is both energy demanding and the spore reducing effect is limited with just 90 - 95% of the spores

being removed during a single step. As a result alternative techniques for spore removal have been investigated, the use of microfiltration membranes is one such technique.

The use of microfiltration membranes to produce ESL milk and cheese milk was introduced more than 20 years ago (Hoffmann *et al.*, 2006) According to Madaeni *et al.*, (2011), Holm and Malmberg (1988) were the first to report pilot plant work on the application of microfiltration for milk sterilisation.

The main problem in using MF for microorganism removal from milk is that most of the fat globules (diameters 0.2 - 15 µm) present are as large as the bacteria present in milk (sizes 0.2 - 6 µm). This results in very rapid fouling of the membrane and as a result this process can only be performed on skim milk (Fritsch and Moraru, 2008). This was not an issue during this project as the MPI powder was produced from skim milk and particle size data for the MPI along with spore size measurements (results of which can be found within sections 2.4 and 3.1.1 respectively) show that the separation is physically possible.

Fouling caused by milk feeds can be minimised by using either high cross-flow velocities (4 - 8 m s^{-1}) and / or backwashing. Both techniques create a high shear stress at the membrane surface and reduce the deposition of particles as any rejected particles are removed from the surface and recycled back into the bulk solution. The problem with operating at a high CFV is that it requires a large amount of energy and a large pressure drop is formed as a function of distance along the membrane, with a higher TMP found at the inlet compared to the outlet. This leads to uneven fouling along the length of the membrane, being more severe at the inlet compared to the outlet. This leads to an uneven flux and separation performance along the length of the membrane. These problems can be largely solved by employing the concept of uniform transmembrane pressure (UTMP) involving permeate recirculation, developed and first patented by Sandblom in 1974 (Baruah *et al.*, 2006). Using this concept Holm *et al.*, (1986) developed the *Bactocatch system* at *Alfa-Laval* to remove bacteria from skim milk. Where a 1.4 µm membrane and a high cross flow velocity of 6 - 8 m s^{-1} are used. Bacteria are retained by the membrane and the permeate stream is recirculated in order to create a UTMP of around 0.5 bar along the length of the membrane. This is achieved by flowing the filtrate cocurrently using a permeate recycle loop simultaneously with a retentate recycle loop as shown in Figure 13. Using a ceramic *Membralox*™ 1.4 µm

membrane and the *Bactocatch* process a spore reduction of 3 $\log_{10}$ steps can be achieved; this is associated with the loss of only 0.02 % protein (Hoffmann *et al.*, 2006). But when a modern *Sterilox*™ membrane of the same pore size with a narrower pore size distribution is used a reduction of 4 -5 $\log_{10}$ steps has been reported. However this process still has a high-energy demand, which reduces its application in the dairy industry (Guerra *et al.*, 1997). Narrower pore size distributions are achieved by accurately controlling the size of sintered colloidal particles and by sintering two or three layers on top of one another (Saboya and Maubois, 2000).

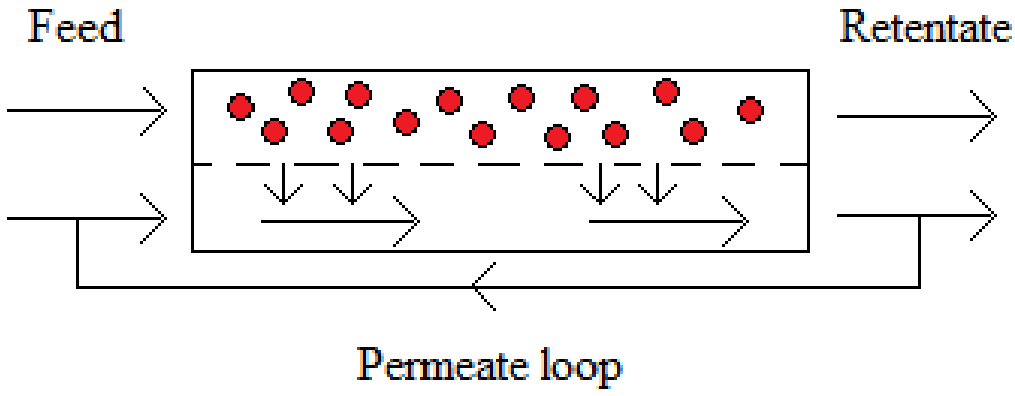

Figure 13. Schematic showing the operation of the permeate recirculation technique developed by Sandblom 1974 to create a UTMP (Taken from Baruah et al.*, 2006).*

Recently, as permeate recirculation can lead to high pumping costs and temperature rise within a system possible alternatives have been developed to create UTMP. *Membralox*™ GP modules have been created by US Filter (Warrendale, PA) and *Isoflux* modules by Tami (Nyons, France) (Baruah *et al.*, 2006). *Membralox*™ GP modules create a UTMP by having a longitudinal permeability gradient built into the support structure without modification of the filtration layer. Isoflux modules instead create a UTMP by having a decreasing active layer thickness along the length of the module. Such membranes result in an improved performance in terms of long-term flux rates and allow better separation homogeneity over the length of the element. Also the fouling layer is similar over the entire membrane area, which makes it easier to remove during chemical cleaning. Skrzypek and Burger (2010) monitored the performance of two 1.4 µm Isoflux® membranes installed in dairy microfiltration plants and found that after 5 years of service the number of microorganisms in the feed stream was still able to be reduced from 60,000 – 160,000 ml^{-1} to fewer than 10 ml^{-1} in the permeate. In regards to aerobic spore reduction out of the 35 samples tested that had initially counts of 40 – 210 ml^{-1} 32 samples had no spores present and 3 had only 1 spore remaining.

Backwashing is an alternative method that can be used to remove foulant and increase flux. It is a cyclic process of forward filtration followed by reverse filtration. Reverse filtration involves periodically reversing the direction of permeate flow through the membrane by changing the sign of the TMP. When permeate is forced back across the membrane it dislodges and lifts loosely bound deposits blocking membrane pores and particles forming a cake on the membrane surface as it passes back into the feed stream, these foulants are then swept away by the cross flow. There are several parameters that can be adjusted during backwashing, backwash duration, amplitude and interval. Backwash duration is defined as the amount of time the filtration system operates under negative TMP, wash amplitude is the absolute value of maximum TMP during washing and backwash interval is the duration of time in between two consecutive washes (Sondhi and Bhave, 2001). Backwashing 2 – 10 times an hour for a period of 5 – 30 seconds is termed backflushing and has been found to increase the average flux even though it decreases the effective operation time and results in a loss of permeate to the feed (Cakl *et al.,* 2000). Alternatively, forcing permeate back across the membrane more frequently 1 – 10 times every minute for less than a second termed backpulsing has been reported to also increase flux and is thought as well as removing loosely bound deposits that this also disturbs the concentration polarisation layer (Fadael *et al.,* 2007). A third technique that optimises this technique further is backshocking where permeate is forced backwards for an even shorter period of time of less than 0.2 seconds and even more frequently around every 0.2 - 1 seconds (Guerra *et al.,* 1997).

The advantage of using backshocking is that it means low cross-flow velocities (1 m s^{-1}) can be used making this technique more cost effective. Jonsson and Wenton (1994) report the advantages of using a reverse asymmetric membrane where the porous support layer instead of the active layer faces the feed stream with the backshock technique. Using this type of membrane structure means that the fouling layer forms inside the porous support layer making it less compact and as a result has a lower resistance making it easier to remove than if it were formed on the surface of the active layer. Guerra *et al.,* (1997) researched this and found high fluxes when using a low cross flow velocity of 0.5 – 1.0 m s^{-1} through reverse asymmetric membranes with pore sizes 0.87 µm up until the permeate flux reaches 600 litres m^{-2} h^{-1}. Beyond this value a gel layer formed inside the porous support layer, but at permeate fluxes of 100 litres m^{-2} h^{-1} flux was stable through the reverse asymmetric membrane for 4 hours with 100% protein transmission and a high spore reduction of 4 – 5 $\log_{10}$ steps. Elwell and Barbano

(2006) suggest that using a combination of MF followed by HTST pasteurisation could result in a significant increase in the shelf life of dairy products. Reporting a 3.79 $\log_{10}$ reduction in bacteria using MF and a further 1.84 $\log_{10}$ following pasteurisation. Tomasula *et al.,* (2011) filtered inoculated raw skim milk with spores of *Bacillus anthracis* (BA) through both a 0.8 and 1.4 µm tubular ceramic *Membralox*^{TM} membranes at 6.2 m s^{-1} CFV and 1.27 bar TMP and report spore removals of 5.91 ± 0.05 and 4.50 ± 0.35 $\log_{10}$ BA spores ml^{-1} respectively. Pafylias *et al.,* (1996) reported a similar spore reduction of 4 – 5 log cycles equating to 99.84 – 99.9% when filtering 8.25 wt% raw whole and skim milk feed solutions through a 1.4 µm membrane at 5.0 m s^{-1} CFV, 1 bar TMP and 50 °C.

Fritsch and Moraru (2008) developed a cold MF process involving the use of a CO_2 backpulsing technique in order to remove vegetative bacteria, spores and somatic cells from skim milk. They report an effective removal of bacterial species at a temperature of 6 °C using a ceramic 1.4 µm pore size membrane at a CFV of 7 m s^{-1}, a TMP of 0.6 - 0.85 bar and backpulsing with CO_2 once a minute for an average of 10 seconds at a pressure of 1.38 bar, whilst still maintaining a protein composition close to that found in skim milk. These fluxes are lower than the fluxes achieved by Saboya and Maubois (2000) at 53 °C of 350 litres m^{-2} h^{-1}, which is within the 50 – 55 °C temperature range used within industry, this is due to the increase in viscosity at the lower temperature.

There are various studies within the literature regarding the processing of skim milk and other dairy products of low solids content using microfiltration to remove microorganisms (typically vegetative cells, not spores), some of which have been described within this literature review. The novelty of this present study is that it involves the processing of a high solids content dairy stream up to 15 wt% in order to remove bacterial spores typically found within dairy products. The difference in these MPI streams compared to skim milk is highlighted in the viscosities of MPI (5 – 15 wt%) measured within this work (section 3.4).

1.19 TECHNIQUES TO IMPROVE MICROFILTRATION

Various techniques have been suggested to improve the performance of microfiltration systems some of which are; feed pre-treatment, changing the membrane material, backwashing using both gas, permeate or water, crossflushing, manipulating flow by

using turbulence promoters, rotating membranes or introducing pulsations into feed or filtrate channels.

Feed pre-treatment can be either a physical or chemical process that aims to remove particulates that may either clog the module or foul the surface of the membrane. Physical pre-treatment involves prefiltration or centrifugation to remove suspended solids. Whereas chemical methods include feed pH adjustment so that molecular or colloidal foulants are further from their isoelectric points which reduces their tendency to form gel layers (Wakeman and Williams, 2002).

The choice of membrane material is important but it only affects the initial rates of particulate adsorption or deposition as once a fouling layer is formed any effect the membrane material has beneficial or otherwise to filtration is made negligible until this layer is removed. Selecting an appropriate choice of membrane material can lead to looser binding of solutes to the membrane surface making fouling less severe and easier to remove during cleaning.

The various methods of flow manipulation used to reduce concentration polarisation and fouling are summarised in Figure 14. Within steady flow systems these methods include increasing CFV or by using turbulence promoters such as static mixer, inserts or rods to increase shear at the surface of the membrane and remove foulant. Kristic *et al.,* (2002) report a 300% increase in permeate flux when using a *Kenics* static mixer as a turbulence promoter when filtering skim milk through *Membralox*^{TM} membranes of 50, 100 and 200 nm pore diameters. A high shear stress can also be developed at the membrane surface by rotating the surface at high speed rather than pumping the feed across the surface at high CFV's. This is achieved in dynamic filters, which have a rotating disk or cylinder element (Wakeman and Williams, 2002).

In unsteady flow systems fluid instabilities such as Taylor and Dean vortices in the feed are created near the membranes surface to disturb formed cake or gel layers and induce mixing at the surface of the membrane. These fluid instabilities can be caused by use of pulsatile flow or rough channel surfaces or use of inserts. The use of inserts may be problematic though in terms of cleaning as there use creates dead areas within the system that cannot be reached by cleaning solutions; therefore there use is not optimal when filtering milk (Brans *et al.,* 2004).

Backwashing is an in-situ foulant removal technique involving the periodic reversal of permeate flow, but it can alternatively be carried out by periodically forcing gas such as nitrogen from the permeate side across the membrane, this is termed gas backwashing.

Crossflushing is another type of in-situ cleaning method, accomplished by maintaining flow over the membrane while periodically stopping the permeate flow, this eliminates the pressure drop across the membrane and allows the shear exerted by the cross flow to erode the foulant layer (Kuruzovich and Piergiovanni, 1996). Crossflushing is relatively simple compared to permeate or gas backwashing as it does not require a pressurized tank or pump. But is a weaker technique as the shear force exerted by crossflushing is not as effective as backwashing at removing foulant especially when internal fouling is present (Ma *et al.,* 2001). It is thought to be effective at removing very mobile/loose cake but ineffective for an adhesive/compact cake (Kuberkar and Davis, 2001). It has been found that neither very long or short backwashes nor crossflushes are desirable as no permeate is collected during this time and using short washes are insufficient to remove foulants effectively.

Redkar and Davis (1995) studied the effect of crossflushing when filtering washed yeast suspensions. They report nearly a 10-fold increase in flux when crossflushing for 2 seconds every 9 seconds. This increase in flux is smaller compared to the 30-fold increase in flux observed when backpulsing for 2 seconds every 9 seconds. Kuberkar and Davis (2001) found the effect of crossflushing and backflushing during the filtration of yeast suspensions, BSA solutions and mixtures of yeast and BSA. Backflushing for 5 seconds every 5 minutes was found to be highly effective and crossflushing for 5 seconds every 5 minutes partially effective at removing external cake layers formed by the yeast suspensions, with flux recoveries of 94 - 80% produced after backflushing and 58 - 34% following crossflushing. In contrast crossflushing was reported to be completely ineffective and backflushing only slightly effective for removal of internal fouling formed during BSA filtration.

Brans *et al.,* (2004) described other methods that could be used to decrease fouling during MF of milk; these include using air slugs, scouring particles, acoustic or ultrasonic waves and sonication. Air slugs and scouring particles improve mixing close to the membrane surface which leads to improved backtransport into the bulk feed. But air slugs may cause unwanted milk foaming and denaturation of milk and scouring

particles have to be cleaned and cause extra wear within rigs i.e. to the pump and damage membranes.

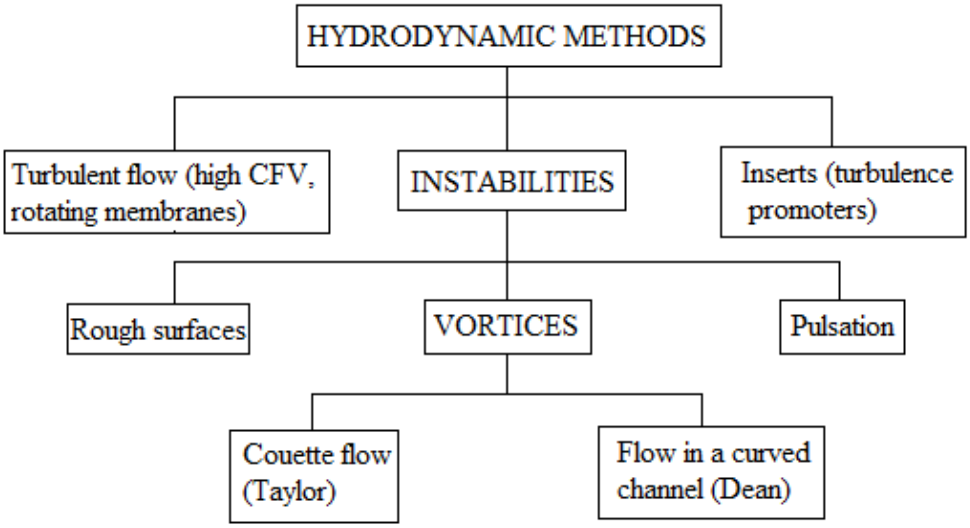

Figure 14. Methods of flow manipulation that aim to reduce concentration polarisation and fouling (Taken from Winzeler and Belfort, 1993)

The use of acoustic or ultrasonic waves and sonication also leads to improved back transport as the energy of the waves is transformed into kinetic energy, this causes foulant particles to vibrate and cavitations allowing them to break free from the membrane. Low frequency ultrasound has been found to facilitate the ultrafiltration of 6 wt% whey solutions through flat sheet polysulfone membranes, producing a 20 – 70% increase in permeate flux (Muthukumaran *et al.*, 2005). Additional studies using the same feed and membrane arrangement showed that continuous as opposed to intermittent low frequency (50 kHz) ultrasound was most effective and the use of intermittent high frequency (1 MHz) ultrasound was detrimental resulting in a lower permeate flux than in the absence of ultrasound (Muthukumaran *et al.*, 2007).

1.20 VISCOSITY MEASUREMENTS

Rheology can be defined as the study of the deformation and flow of matter under the influence of an applied force; it deals with the relationship between three variables stress, strain and time (Steffe, 1996). The relationship between the applied force and the resulting flow is related by shear stress (σ) and shear rate (γ) respectively, with the ratio between shear stress and shear rate called the apparent viscosity, μ_a, this is shown below in equation 12.

$$\sigma = \mu_a \gamma \qquad (12)$$

When an external force is applied to an ideal solid or a truly elastic material it will deform, whereas an ideal liquid or truly viscous material will flow (Gunasekaran and Mehmet 2003).

A material is described as an ideal solid if it obeys Hooke's law. In order to follow Hooke's law when a force is applied the resulting stress against strain plot must be a straight line that goes through the origin. This relationship can be described in terms of shear stress and shear strain by the equation 13, where G is the shear modulus. The stress will remain constant in these types of materials until the strain is removed, after which it will return to its original shape.

$$\sigma = G\,\gamma \tag{13}$$

When an external force is applied to a fluid at rest the resulting flow can be described as either Newtonian or non-Newtonian. A sample is said to be Newtonian if it behaves like water, where its shear stress is linearly proportional to its shear rate with a zero intercept, and the viscosity of the fluid is independent from shear. Honey and fruit juice are two food products known to behave as Newtonian fluids.

Non-Newtonian fluids are those that do not exhibit a linear relationship on a shear stress shear rate plot. On shearing they either thin or thicken, if they thin i.e. the viscosity decreases they are termed shear thinning or pseudoplastic and if they thicken i.e. the viscosity increases they are termed shear thickening or dilatant.

Bingham plastics are a third type of non-Newtonian fluid; these types of materials are only able to flow and behave in a Newtonian fashion after they have had a certain amount of shear stress applied to them, this amount of stress is known as the yield stress, below this value the material behaves as a solid. Toothpaste and tomato puree are two products known to exhibit Bingham plastic behaviour (Steffe, 1996). Materials that behave in a non-Newtonian fashion by shear thinning after their yield stress is exceeded are known as Herchel-Bulkley materials. Minced fish paste and raisin paste have been shown to exhibit Herchel-Bulkley type flow behaviour. Simple schematics showing shear stress against shear rate and viscosity against shear rate expected for typical Newtonian and non-Newtonian fluid can be seen in Figures 15 and 16 respectively.

Using units of N, m^2, m, and m/s for force, area, length and velocity respectively gives viscosity units of Nm^{-2} s, which are known as Pascal seconds (Pa s). With 1 Pa s = 1000 centipoise (cP) = 1000 mPa s and 1 P = 100 cP. All of the viscosity values collected during this project will be reported using cP units.

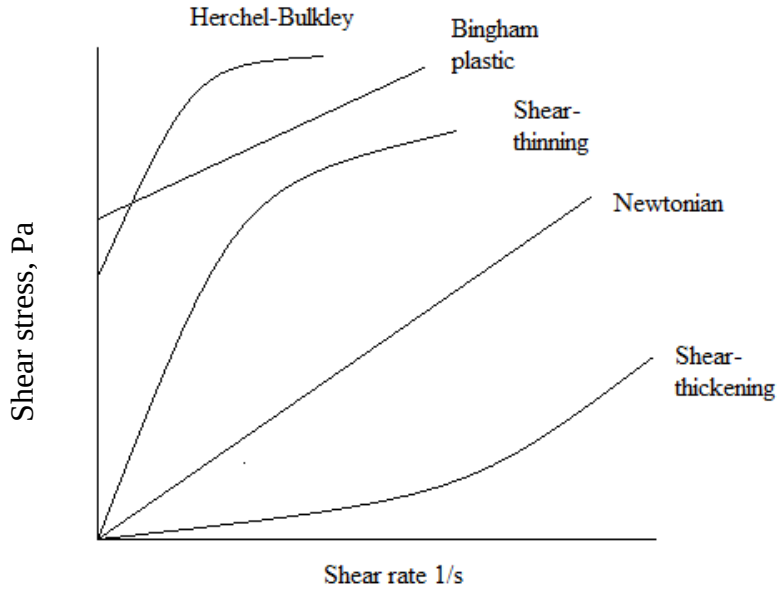

Figure 15. Typical shear stress against shear rate plots for both Newtonian and non-Newtonian materials (Taken from Steffe, 1996).

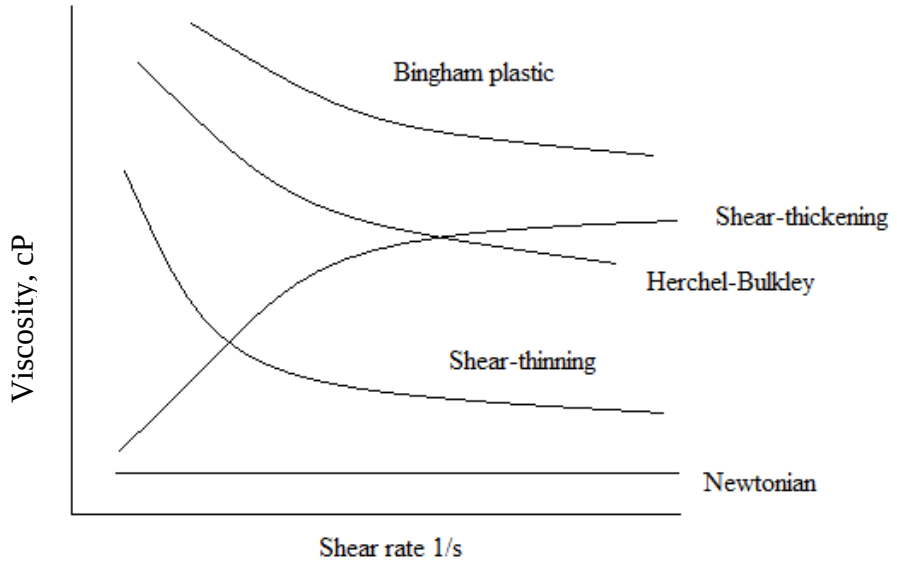

Figure 16. Typical viscosity against shear rate plots for both Newtonian and non-Newtonian materials (Taken from Steffe, 1996).

1.21 PROTEIN DETERMINATION- BRADFORD ASSAY

The Bradford assay is a simple colorimetric technique used to quantify the amount of protein within a sample. This technique is very popular as it is relatively easy and

inexpensive to carry out and produces rapid and sensitive results (Olson and Markwell [online, accessed 15/09/12]).

The assay is based on a dye known as Coomassie Brilliant Blue G-250, the structure of which is shown in Figure 17, this dye interacts with proteins and stains blue under acidic conditions. The dye has three forms; cationic which is red / brown in colour, neutral which is green and anionic which is blue (Compton and Jones, 1985). When the dye interacts with protein an absorbance shift occurs as the dye changes from being in its cationic form, which has an absorbance maximum at 465 nm into its anionic form, which has an absorbance maximum at 610 nm. The maximum difference in absorbance between the two forms is greatest at 595 nm (Bradford, 1976). The staining reaction is complete within about a minute and the colour remains constant for about an hour, which allows plenty of time for the absorbance to be recorded.

It should be noted that the absorbance spectra of the cationic (before protein interaction) and anionic (after interaction) forms of the dye overlap. This causes the assay to respond non-linearly when carrying out a calibration curve and is the reason why a second order curve fits the plot better than a linear treadline.

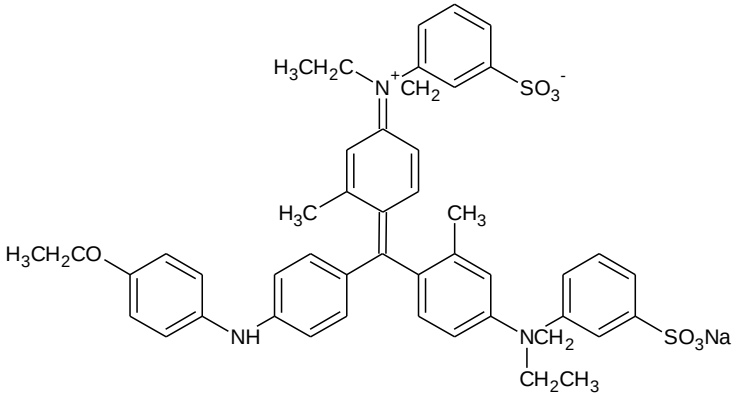

Figure 17. Coomassie Brilliant Blue G

Unlike many other techniques the Bradford assay is not susceptible to interference by chemicals that may be present within samples to be tested, with the only notable exception being the presence of a high concentration of detergent. But the assay does have disadvantages caused by the fact that the dye only interacts with basic and aromatic residues namely arginine, lysine, tryptophan, tyrosine, histidine and phenylanine within proteins. Proteins containing arginine residues create more of an issue as they can respond eight times higher than the other basic and aromatic residues listed. This results in the technique being susceptible to protein-protein variation. As a

result it is advised that if the protein you want to detect for using the assay contains a large amount of arginine residues it may be necessary to use the same protein to produce the calibration curve.

2 MATERIALS AND FILTRATION METHODS

2.1 MATERIALS

2.1.1 Milk Protein Isolate (MPI) powder

Spray dried *Ultranor*^{TM} 9075 Milk Protein Isolate (MPI) powder was supplied by *Kerry Ingredients*, Listowel, Ireland. The amino acid content, chemical composition and mineral profile of the MPI is shown in Tables 7, 8 and 9 respectively.

Table 7. Amino acid content for MPI

Amino acid	g/100g of amino acids
Alanine	3.09
Arginine	3.28
Aspartic acid	7.13
Cysteine	0.63
Glutamic acid	19.72
Glycine	1.80
Histidine	2.57
Isoleucine	5.19
Leucine	8.93
Lysine	7.77
Methionine	2.49
Phenylalanine	4.55
Proline	9.95
Serine	5.47
Threonine	4.71
Tryptophan	1.56
Tyrosine	4.98
Valine	6.18

Table 8. Chemical composition data for *Ultranor*^{TM} 9075 Milk Protein Isolate (MPI)

Component	% Unless otherwise stated
Fat	1.5
Cholesterol (mg / 100 g)	50.0
Protein	86.0
Moisture	4.0
Ash	6.0
Carbohydrates	<1.0

Table 9. Typical mineral profile

Mineral	%
Calcium	1.7
Sodium	0.08
Potassium	0.35
Phosphorus	1.1
Chloride	0.25
Magnesium	0.08

Ideally milk prior to being both pasteurised and spray-dried would have been used during this project but due to issues of safety and practicality spray dried milk powder was instead selected for use. Safety would be a concern as if not pasteurised potentially dangerous bacteria could still be present within the milk. Practical issues would have arisen as MPI powder can be stored for years, but if a liquid MPI feed was used deliveries would have had to be made regularly to the laboratory throughout the

duration of the experimental work. During filtration experiments spray dried MPI powder was resolubilised by addition of the required mass of powder to the required mass of reverse osmosis (RO) water at 60 ºC inside 5 litre plastic beakers placed inside a water bath (NE2-14D series, *Nickel-Electro Ltd*, Weston-Super-Mare). A water bath was used in order to maintain the temperature of the solution at 60 ºC throughout the duration of the resolubilisation. The MPI powder was added in small amounts that were allowed to dissolve before further powder was added in order to aid resolubilisation. Once all the powder was added the solution was left to stir for a further 60 minutes. Ideally MPI was wanted to be resolubilised using the protocol developed in section 2.4, where it was stirred using an overhead stirrer at 125 rpm. But this was only possible when small volumes of a low wt% solution (< 5 wt%) were required. When either a large feed volume or a solution of high wt% (> 5 wt%) was required a faster stirrer speed of 700 rpm had to be used to aid resolubilisation. When large volumes of MPI feed were required during filtration experiments multiple 3 litre solutions were prepared. Once prepared, solutions were sieved using a conventional kitchen sieve in order to remove any powder that had not fully dissolved before being placed into the feed tank.

2.1.2 Chemical cleaning agents

Sodium hydroxide (Technical grade, *Fischer Scientific*, Loughborough, UK) was used to clean the rig in between long periods of inactivity, before each filtration experiment and to clean MPI fouled membranes using the conditions shown in Table 13. Bird and Bartlett (1995) reported optimal cleaning conditions similar to those used in this work in order to remove whey protein concentrate fouling from polymeric microfiltration membranes of a concentration of 0.5 wt% NaOH, a temperature of 50 °C and no TMP and a CFV of 1.6 m s^{-1}. Sodium hydroxide (NaOH) was chosen for use due to its ability to hydrolyse peptide bonds that link amino acids monomers in protein polypeptide chains together. Sodium hydroxide solutions were prepared by addition of the desired mass of powder to the required mass of RO water. Nitric acid (68 – 72%, 1.42 S.G, *Fischer Scientific*) solutions of 0.3 wt% were used to clean MPI fouled tubular ceramic *Membralox*^{TM} membranes after they were subjected to alkali cleaning by NaOH in order to remove any precipitated calcium or magnesium or any other deposited minerals. Both before and after *Bacillus mycoides* was used within the rig, solutions of sodium hypochlorite (NaOCl) at a concentration of 0.02 wt%, 200 ppm were passed through the filtration system for 15 minutes at room temperature, 0.3 bar and 0.73 m s^{-1} in order to

remove any contaminating bacteria from the system. The efficiency of this disinfection procedure was tested and found to be satisfactory as shown within section 4.1.

2.1.3 Reverse Osmosis (RO) water

Water that had been put through a reverse osmosis (RO) unit was used for all experimentation. The RO unit (Intercept RO-S, *Elga Ltd*, High Wycombe) that was initially used during this work was replaced with a Midi-RO (10-200-EP, *Veolia Water*) machine. This RO unit produced water of a very low salt content of between 8 – 10 μS cm^{-1}. In contrast the conductivity of mains water was measured (Oakton, RS232 con 110 series) to be 680 μS cm^{-1}.

2.1.4 *Bacillus mycoides*

The strain of *Bacillus mycoides* used within this project was 13305 (*NCIMB*, Aberdeen, UK). It arrived as a chemically inactive freeze-dried bacterial culture inside an ampoule that needed to be revived before it could be used. This was achieved by firstly opening the ampoule by making a file cut along the middle point of the cotton wool plug and then cracking the glass using the 'ampoule snappers' provided. Once broken the upper part of the ampoule and the cotton wool were discarded into a disinfectant solution of sodium hypochlorite where it was left to soak overnight. The exposed end of the ampoule was then flamed and 0.5 ml of Tryptone soya broth (TS) was added and the contents were mixed. It is generally recommended that bacterial suspensions such as this be subcultured at least twice before they are used experimentally and this was carried out. Two types of all-inclusive media namely *Difco*™ nutrient broth (NB) and Tryptone soya broth (TS) were used to prepare agar plates, slopes and liquid media in order to subculture the bacterial suspension.

To establish which of the two growth media TS or NB the bacteria grew most abundantly within the optical density (OD) of each was recorded at 600 nm after the bacteria had been left to grow inside each for 24 hours. After which NB gave a reading of 0.502, whereas the TS produced a much larger amount of growth having an OD reading of 0.933 nearly twice that of NB. With an acceptable reading being ~1, TS was selected as an acceptable growth media to use during this work when culturing cells of *Bacillus mycoides*.

2.2 METHODS

2.2.1 Developed method for cell culture and sporulation of *Bacillus mycoides*

Bacterial cell and spore culture methods used for *Bacillus mycoides* were adapted from those used by Bowen *et al.*, (2002 a). Initially a 'seed' culture of bacterial cells was grown overnight inside liquid Tryptone soya broth (10 ml, 30g L^{-1}) inside a static incubator at 25 °C. The 'seed' culture (1 ml) is then transferred to a shaking flask containing Tryptone soya broth (100 ml, 30g L^{-1}) and left overnight at 140 rpm, 25 °C. The cells (5 ml) are then transferred into sporulation media (100 ml) consisting of *Difco*™ nutrient broth (8g L^{-1}), $MgSO_4$ (0.25g L^{-1}), KCl (0.97g L^{-1}), $CaCl_2$ (0.15g L^{-1}), $MnCl_2$ (2×10^{-3} g L^{-1}) and $FeSO_4$ (3.0×10^{-4} g L^{-1}). This is then placed back inside the shaking incubator for four days at 140 rpm, 25 °C. Finally, the spores are harvested from the sporulation media using a method adapted from Seale *et al.*, (2008). Where the media was centrifuged (4000 rpm, 20 minutes at 4 °C) the supernatant is then decanted off and the remaining pellet is resuspended and washed in sterile distilled water. This process is repeated three times but is centrifuged for only 10 minutes after the initial centrifuge. Spore suspensions are then stored in water inside a cold room at 4 °C until they are needed. All media was made up using RO water and autoclaved before use and all microbiological work was carried out inside a biological safety cabinet.

Photographs have been taken of the bacteria when in both cell and spore form using a camera attached to an optical microscope and using Scanning Electron Microscopy (SEM). The optical microscope pictures can be seen below in Figure 18 and the SEM images in Figures 19 and 21. Figure 18 (a) - (d) are of *Bacillus mycoides* cells and (e) and (f) are of the bacteria once the cells had been left to spore.

SEM images were taken using a JSM-6480LV machine (*JEOL*, Munich, Germany). Two samples of *Bacillus mycoides* cells were prepared, one of which was freeze-dried and the other prepared using a HMDS evaporation technique. The sample preparation protocols and the parameters used when taking SEM images can be found within Appendices 2.1 and 2.4. As can be seen from the images, *Bacillus mycoides* cells have a rod type structure and tend to line up together forming long chains of cells.

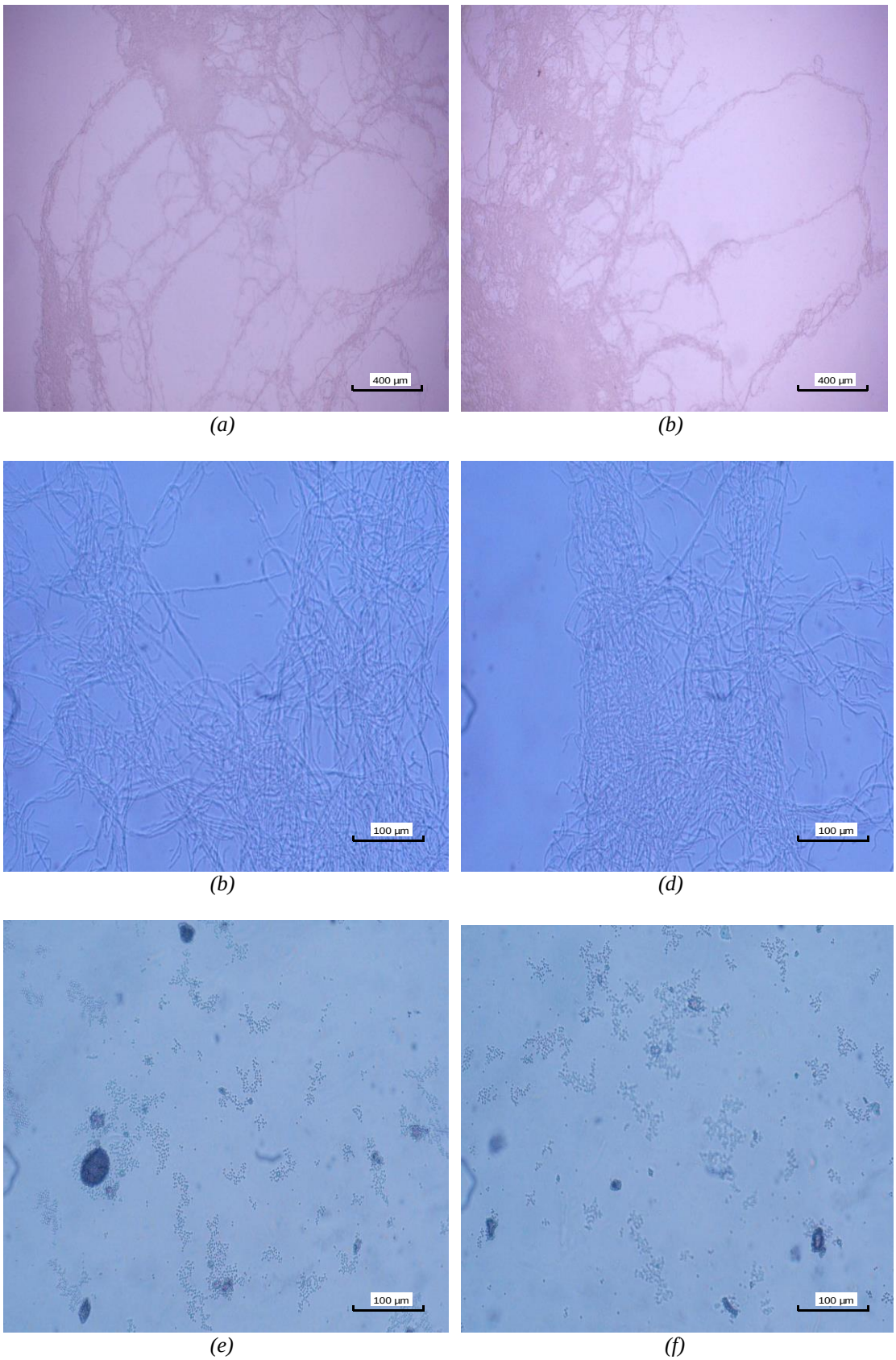

Figure 18. Photographs taken using a digital camera attached to an optical microscope (a) - (d) are of cells of Bacillus mycoides *and (e) and (f) are of* Bacillus mycoides *spores in media.*

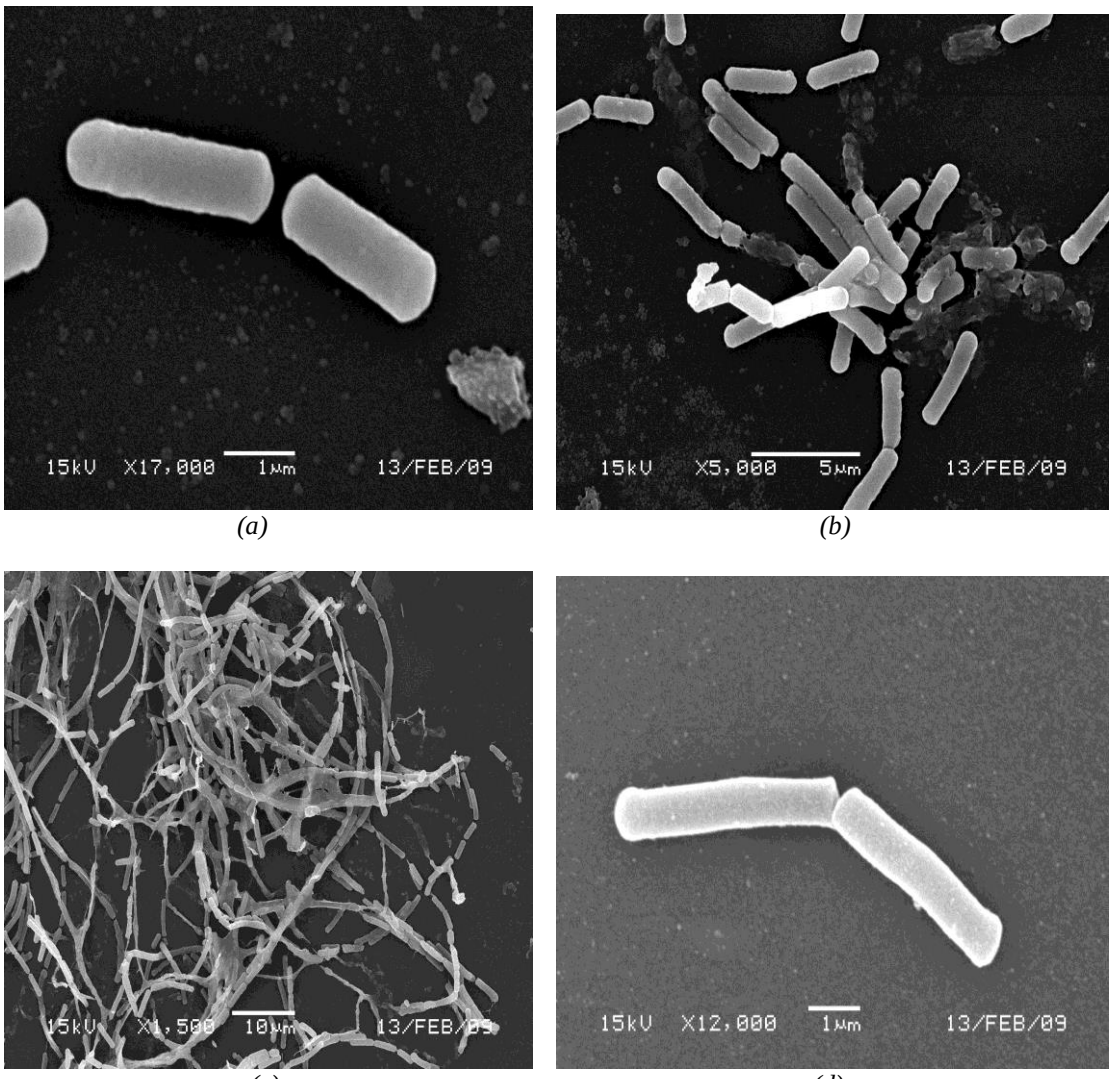

(a) *(b)*

(c) *(d)*

Figure 19. SEM photographs taken on a JSM-6480LV machine a), b), and c) are of Bacillus mycoides *cells prepared by freeze-drying and d), prepared by HMDS evaporation.*

In order to establish whether the method adopted for harvesting the spores from the sporulation media was damaging or altering the structure of the spores photographs were taken of the spore before it had been centrifuged, after centrifuging and after the three washing steps. This was done using both a camera attached to an optical microscope and also using SEM images. The sample preparation protocol used for these samples for SEM can be found within Appendices 2.2 and 2.4. The optical microscope and SEM pictures taken can be found in Figures 20 and 21 respectively. As can be seen from both sets of photographs this method of harvesting does not adversely affect the spores, as they appear unchanged between the photographs taken of the media before centrifuging and those taken after centrifuging and after washing. The only difference that can be seen between the pictures is that the amount of media debris decreases from the pictures taken of the spores before harvesting, after centrifuging and after each washing step as it is being washed away. This is highlighted when comparing Figure 21

(b) and (h) as the spore in (b) is largely covered in media resulting in it having a very ‘bumpy’ surface but the spore in (h) has a much ‘smoother’ surface.

The SEM images of Figure 21 also show the natural state of the *Bacillus mycoides* spores. In particular, Figure 21 (a), (c), (e) and (f) show the preference of such spores to cluster together. This clustering behaviour can be attributed to the hydrophobic nature of the spore’s surface, and is an important characteristic to consider when performing microfiltration (which is a size-exclusion processing technique). For example this clustering effect may be the reason why the large pore size tubular ceramic *Membralox*^{TM} membranes of 2.0 and 12.0 µm were able to give reasonable spore reductions between 1.4 – 3.9 and 1.4 – 2.6 log orders respectively across all experiments, these results are described in more detail within sections 4.6 and 4.7. The filtration process in this thesis was considered to only act on individual spores, as the amount of clustering was unknown between samples.

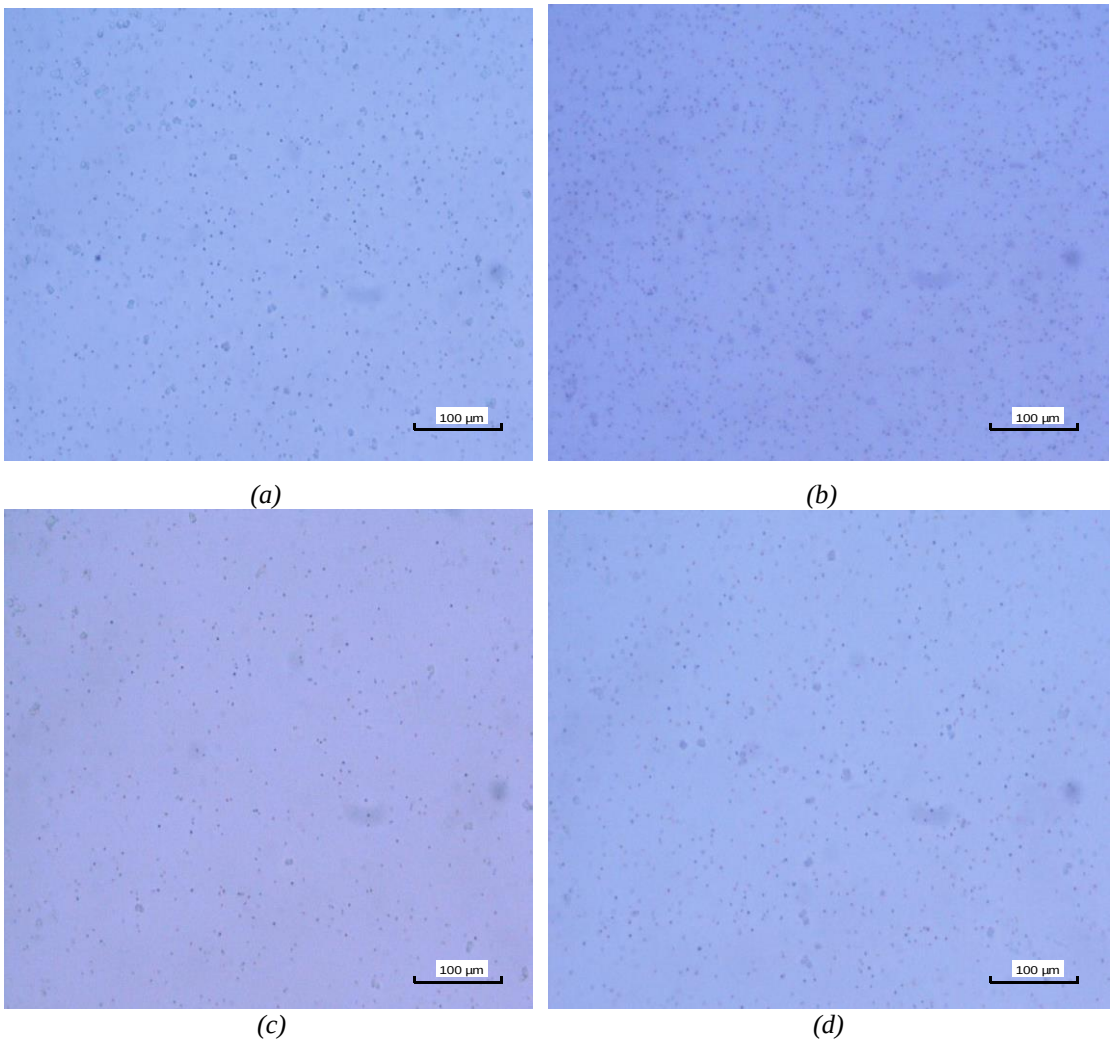

(a) *(b)*

(c) *(d)*

Figure 20. Photographs taken using a digital camera attached to an optical microscope a) supernatant after centrifuging for 20 minutes at 4000 rpm at 4 °C b) supernatant after washing in autoclaved distilled water for 10 minutes at 4000 rpm at 4 °C c) after second washing and d) after third washing step

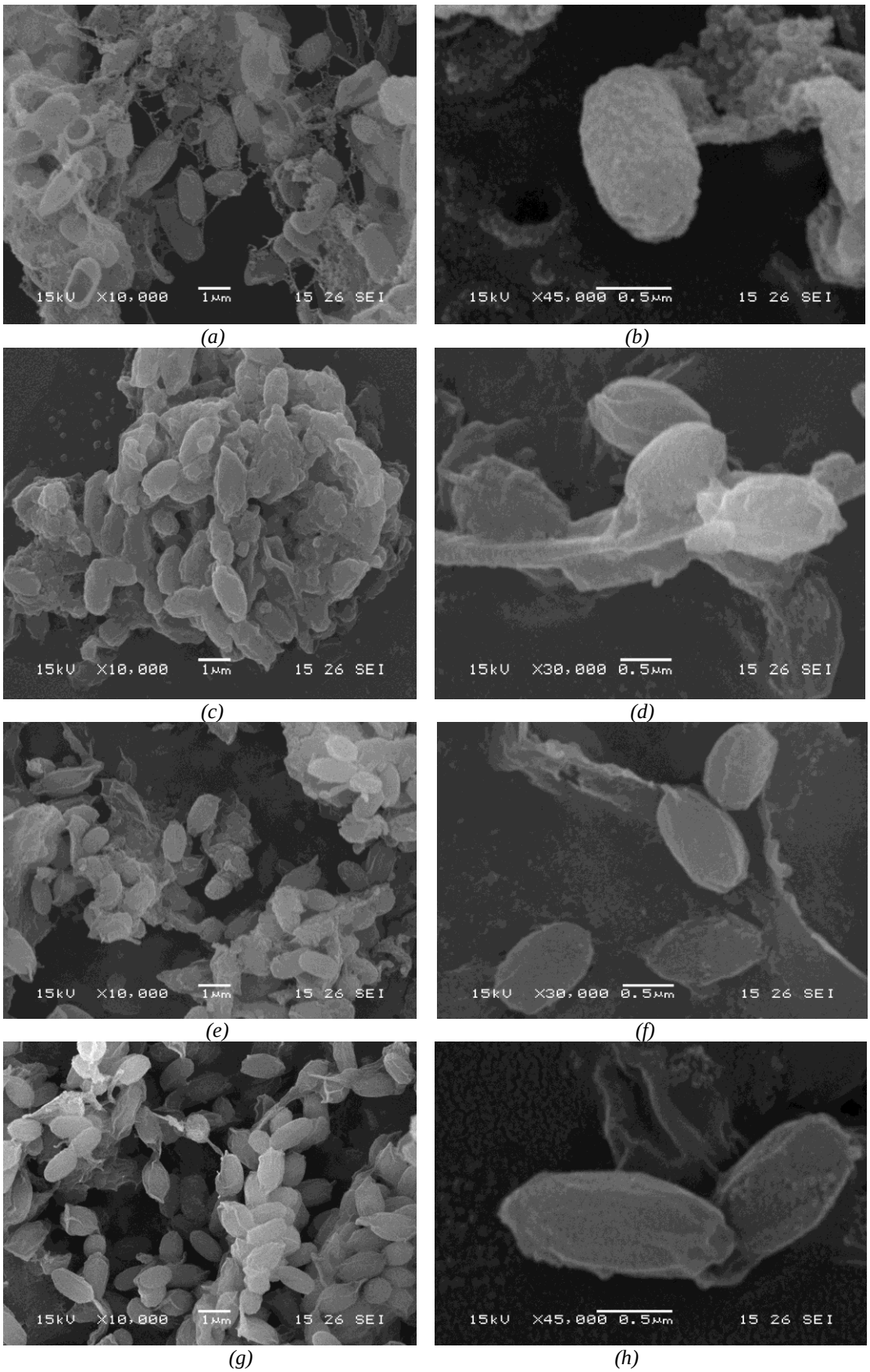

(a) *(b)* *(c)* *(d)* *(e)* *(f)* *(g)* *(h)*

Figure 21. SEM photographs taken on a JSM-6480LV machine, spot size = 26, z distance = 15, accelerating voltage = 15 kV and magnification of either x10,000, x30,000 or x40,000, the magnification used is indicated on the image. a) and b) Bacillus mycoides *spores before they have been centrifuged c) and d) supernatant after centrifuging for 20 minutes at 4000 rpm at 4 °C e) and f) supernatant after washing in autoclaved distilled water for 10 minutes at 4000 rpm at 4 °C and g) and h) after third washing step.*

2.2.2 Handling and storage of *Bacillus mycoides*

All media was prepared using RO water and autoclaved before use, all agar plates and slopes were prepared inside a laminar flow hood and all work involving *Bacillus mycoides* was carried out inside a biological safety cabinet.

A long-term store of *Bacillus mycoides* was prepared after it had undergone the two initial subcultures by making up a solution containing 8 ml TS culture and 2 ml glycerol within a universal bottle. This was then vortexed to ensure adequate mixing and then separated into 10 cryovials, these were then placed in liquid N_2 for an hour before being transferred to a freezer. The glycerol was added as an additional nutrient for the bacteria when frozen.

2.2.3 Size of *Bacillus mycoides* spores

The size of a harvested sample of *Bacillus mycoides* spores prepared following the protocol described in section 2.2.1 was measured using SEM images and a light microscope technique involving the use of an eyepiece graticule and a stage micrometer slide. Scanning Electron Microscopy images were taken using a JSM-6480LV SEM (*JEOL*, Munich, Germany). The sample preparation protocol and parameters used when taking the SEM images can be found within Appendices 2.2 and 2.4. In regards to the light microscope technique both the eyepiece graticule and the stage micrometer slide had a size scale on them but they were in different units with the eyepiece scale in graticule units (GU) and the slide in mm. In order to measure the size of the spores the eyepiece graticule had to be calibrated with respect to the scale on the slide. This was done by firstly replacing the microscope eyepiece with the graticule eyepiece and placing the stage micrometer slide onto the microscope stage. The microscope was then set at the required magnification and focused so that the stage micrometer slide was clearly in view. The eyepiece was then rotated and the stage moved so that the scales superimposed each another. Finally the number of divisions on the eyepiece that were equivalent to 100 µm (the size of each small division of the micrometer slide) on the stage micrometer were counted and the length that one eyepiece division was equivalent to could then be calculated. An example of one such calibration can be found in Appendix 3. Once complete the stage micrometer slide could then be replaced by a specimen slide that contained a sample of spores.

2.2.4 Hydrophobicity of *Bacillus mycoides* spores

The surface hydrophobicity of a harvested sample of *Bacillus mycoides* spores prepared following the protocol described in section 2.2.1 was determined using the microorganism adhesion to hexadecane (MATH) assay used by Seale *et al.,* (2008). Harvested spores were suspended in 0.1M KCl at a pH of 6.8 to an optical density at 600 nm between 0.6 - 1.0 using RO water as the reference sample. This spore suspension (2 ml) was then added to hexadecane (1 ml), vortexed for 1 minute, incubated at 37 °C for 10 minutes and finally vortexed again for 2 minutes. The suspension was then left to settle at room temperature for 30 minutes after which the aqueous phase was separated and its absorbance at 600 nm recorded using RO water as the reference sample.

2.3 Enumeration of *Bacillus mycoides* spores: 3M™ *Petrifilm*™ Aerobic Count Plates (ACP)

Initially, during the preliminary spore rejection experiments carried out using the Danish separation systems (DSS) labunit M10 rig where the feed was an inoculated aqueous suspension, a counting chamber could be used to determine the amount of spores present in both the permeate and feed streams. But when the feed was an inoculated MPI solution the squares that made up the counting area on the counting chamber were no longer visible when looking down a light microscope. This meant that in order to establish the membrane rejection ratios when using MPI feed solutions a counting chamber could not be used and an alternative technique had to be found. A relatively new plating technique namely *Petrifilm*™ Aerobic Count Plates (ACP's) was researched and used to enumerate samples taken from feed and permeate streams for their *Bacillus mycoides* spore contents throughout the duration of the project.

2.3.1 *Petrifilm*™ Aerobic Count Plates

Petrifilm™ Aerobic Count Plates (ACP's) are one in a series of plates developed by 3M™ laboratories. They are a small, sample ready, dehydrated version of the conventionally used agar plate method for bacteria enumeration. They contain growth nutrients, a coloured dye 2, 3, 5-triphenyltetrazolium chloride (TTC), which colours all bacterial colonies red, and a cold water soluble gelling agent. They have various advantages for use over agar plates in that they themselves require no preparation and are ready for use immediately after taking them out of the packet. In contrast agar plate

preparation is lengthy involving the reconstitution of dehydrated media, sterilisation, pouring of the media into Petri dishes and waiting for the agar to harden before it can be inoculated and incubated. *Petrifilm*™ plates are also very easy to use and interpret and require less room when incubated, with about 10 *Petrifilm*™ plates taking up the same space as just one agar plate. Due to these advantages they are increasing in acceptance in food microbiology laboratories (Tavolaro *et al.*, 2005). They have also been validated as an alternative to standard methods for the enumeration of aerobic bacteria by various authorities such as the American Public Health Association (APHA, 1992) and by the Association of Analytical Communities (AOAC), Association française de Normalisation (AFNOR) and Nordic Validation System (NordVal) (*Petrifilm*™ ACP instruction manual).

2.3.2 Instructions for use

Enumeration using *Petrifilm*™ plates involves carrying out three simple steps plating, incubation and interpretation. Before plating, the sample has to be diluted to a suitable dilution so that the plate will display a countable number of colonies; plates containing 25 - 250 colonies are considered countable. Suitable sterile diluents suggested for use are Butterfield's phosphate buffer, 0.1% peptone water, peptone salt diluent, buffered peptone water, saline solution (0.85 - 0.90%), bisulfite-free letheen broth or distilled water. Within this work distilled water was used as the dilutent.

Once prepared the sample can be plated, this involves firstly placing the plate on a flat level surface, the upper film of the plate is then lifted up and 1 ml of the sample suspension to be tested is then pipetted onto the centre of the bottom film. The upper film is then repositioned and a plastic spreader is gently pressed onto the plate in order to distribute the sample evenly over the plate. It is then left undisturbed for at least a minute in order to allow the gel to form.

The plates are then incubated. It is stated in AOAC Official Methods (986.33 Bacteria and Coliform Counts in Milk, Dry Rehydrated Film Methods and 989.10 Bacterial and Coliforms Counts in Dairy Products, Dry Rehydrated film methods) (*Petrifilm*™ ACP instruction manual) that plates used to measure bacteria counts for milk and other dairy products should be incubated for 48 hours ± 3 hours at 32 °C ± 1 °C. But it was found during this work (section 3.2.5) that incubation for 24 hours at 32 °C is sufficient with no further change visible after 48 hours. This observation has also been reported within

the literature. Ellender *et al.*, (1993) used *Petrifilm*^{TM} ACP plates incubated at room temperature and 35 °C for 24, 48 and 72 hours and found there was no significant difference in counts at any of the time points but just that incubation at room temperature gave slightly higher counts. Also, Blackburn *et al.*, (1995) found no difference in counts between 48 and 72 hours incubation at 30 °C.

Finally, interpretation once removed from the incubator plates should be counted within one hour and if the sample has been suitably diluted, then the plate can be counted by eye. As a 1 ml was always plated this allowed the spore ml^{-1} count to be easily calculated. If a plate contains greater than 300 colonies it is suggested that an estimate is made. Estimates were achieved by counting the number of colonies in two or more representative squares and determining the average number per square. As the growth area of a plate was approximately 20 cm^2 this calculated average could then be multiplied by 20 to determine the estimated count for a plate. When too high a concentration was plated this resulted in the whole circular growth area turning pink, in this case the sample was plated again at a higher dilution.

Sterile distilled water was used as the diluent to dilute samples by serial dilution to a suitable dilution for plating. An example of a plate that had been inoculated with a sample diluted to a suitable dilution (so that it can be counted by eye) is shown in Figure 22. The incubator used during this project to incubate the *Petrifilm*^{TM} ACP's was a 30 Litre fan assisted static incubator (Mini/30/F) that had a temperature range from + 5 to 100 ºC, (Townsend Mercer, *Record Electrical Associates*, Manchester, UK).

In order to help aid plate counting (especially when a large amount of colonies were present and an estimate had to be taken) a *Helphand* magnifying glass commonly used for needlework was used. This was a very useful tool as it had two clips that could be used to hold plates, it was freestanding and both of the clips and the magnifying glass were fully adjustable.

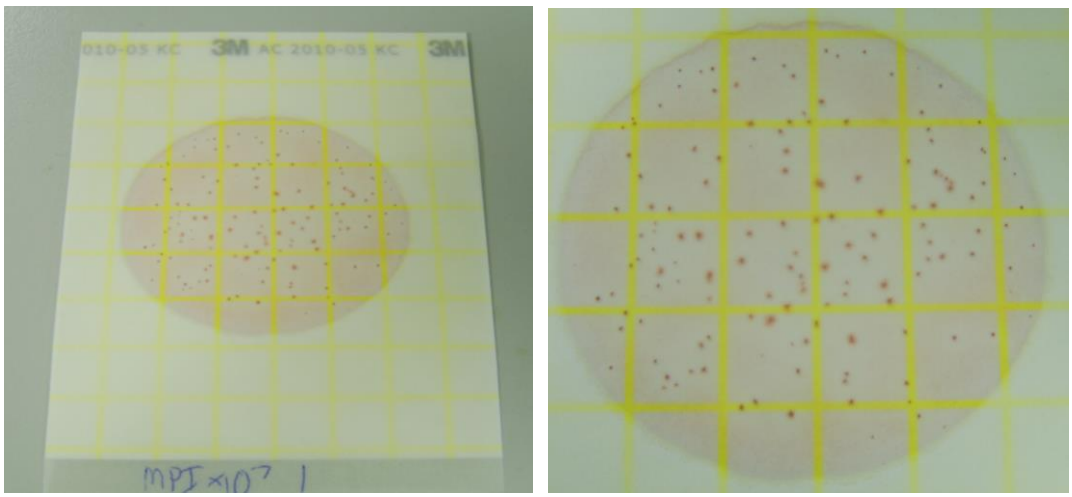

(a) *(b)*

Figure 22. Photographs of a) a Petrifilm^{TM} *Aerobic Count Plate (ACP) after being plated with 1 ml x10^{7} MPI solution containing* Bacillus mycoides *spores after incubation at 32 °C for 24 hours. b) Showing zoomed in picture of the circular growth area of* Petrifilm^{TM} *plate.*

2.4 DEVELOPMENT OF MPI RESOLUBILISATION PROTOCOL

One of the first issues that had to be addressed during this project was the development of a suitable resolubilisation protocol for the spray dried *Ultranor*^{TM} 9075 milk protein isolate powder. The parameters initially believed to affect resolubilisation were temperature, stirrer speed, time, concentration of MPI and potentially the depth at which a sample was taken from the container used to hold the solution.

As discussed in section 1.7, MPC and MPI powders are known to be more readily resolubilised at elevated temperatures. But it is also commonly known that heat treatment of milk above 70 °C causes whey protein denaturation. More specifically Bernal and Jelen (1985) found that WPC powders denaturate at 76.9 ºC ± 5 ºC at pH 6.5 (the closest pH to that of water that was tested). Considering this it was decided that a temperature of 60 ºC would be a sensible temperature to use for resolubilisation as this takes into account the experimental error of the study and allows for human error when resolubilising MPI.

In order to test whether the remaining variables stirrer speed, time and the depth at which a sample is taken and MPI concentration did affect resolubilisation and if so to what extent, a series of solutions were prepared. A description of the prepared solutions can be found within Table 10. These solution preparations were designed so that each variable could be evaluated by comparing two results, for example the effect of stirrer speed could be determined by comparing solutions 1 and 4, stirring time by comparing

solutions 1 and 3, concentration by 3 and 5 and lastly, depth by comparing 1 and 2, as well as 5 and 6. Particle size distribution measurements were used to determine the effectiveness of each resolubilisation method.

Table 10. Detailing solution preparations designed to test the effect that the variables stirrer speed, stirrer time concentration of MPI and the depth at which a sample is taken have on the resolubilisation of MPI.

Expt. no	Temp (°C)	Concentration (wt %)	Stirrer speed (rpm)	Stirring time (minutes)	Depth sample taken (cm)
1	60	20	300	30	25
2	60	20	300	30	5
3	60	20	300	10	25
4	60	20	125	30	25
5	60	15	300	10	25
6	60	15	300	10	5

All particle size distribution analysis was carried out using a Zetasizer nano series, nano S model ZEN 1600 (*Malvern instruments*, Malvern, UK) machine located in the Biological sciences department at the University of Bath. This type of instrument uses a process known as Dynamic Light Scattering (DLS) in order to measure a samples particle size and distribution. It can measure particles ranging from 0.5 nm – 6 μm in size (Malvern [online, accessed 15/9/11]). For each measurement ~1 ml of sample was pipetted into a low volume disposable sizing cuvette

For each sample three consecutive measurements were recorded. If a sample were a monodisperse solution in which the particles have a similar size, shape and mass you would expect the three correlation functions to be very similar to each other. But if the sample were instead a polydisperse suspension in which the particles have a broad range of sizes, shapes and mass then three different correlation function graphs would be produced. If a sample is too polydisperse then the zetasizer software is unable to produce an intensity distribution graph. This was the case for most of the prepared solutions described within Table 10, apart from the 20 wt% MPI solution prepared using the slower stirrer speed of 125 rpm (experiment number 4) and the two 15 wt% solutions (numbers 5 and 6). The correlation against time graphs produced by prepared solutions 1 - 6 can be found in Appendix 4 (Figure 88) and the volume distribution graphs for solutions 4 - 6 in Figure 23.

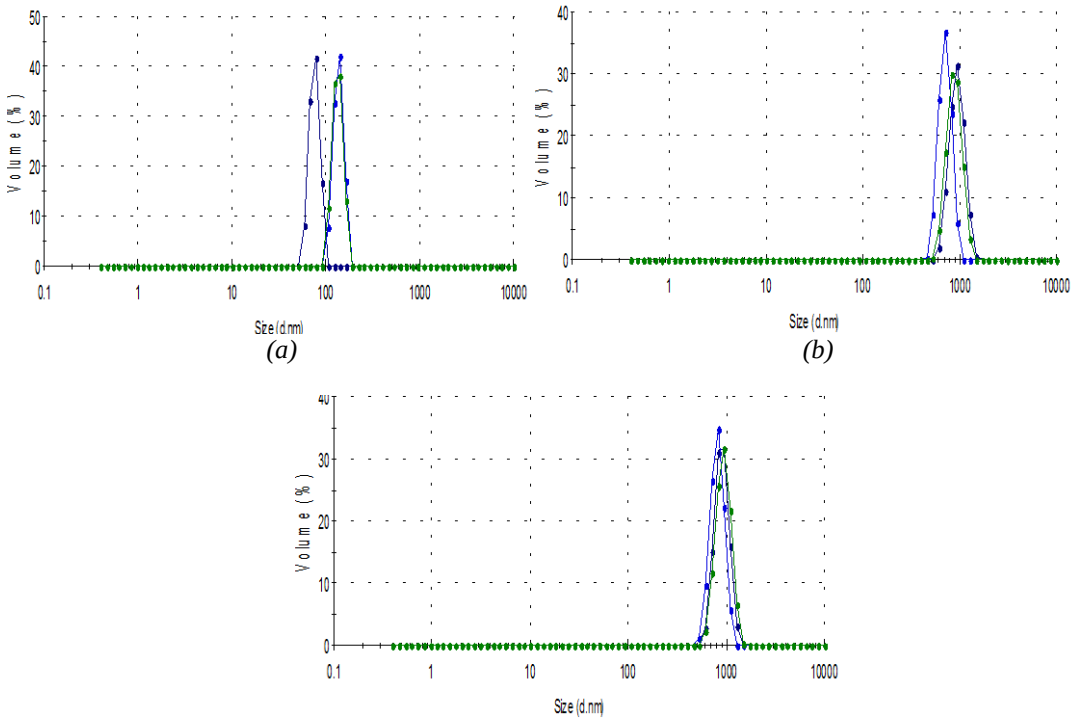

Figure 23. Volume distribution graphs for solutions 4 (graph a), 5 (b) and 6 (c) these graphs have volume % on the y-axis and particle diameter size on the x-axis.

The only three solutions that were monodisperse enough to produce volume distribution data were the two 15 wt% MPI solutions and the 20 wt% solution prepared at the slower stirring speed of 125 rpm. This suggested that MPI concentration and stirrer speed are the most important variables in MPI resolubilisation. The two 15 wt% solutions showed very similar size distribution data with particles having a diameter around 1000 nm whereas the 20 wt% solution contained particles of a much smaller size around 100 nm. This implies that the faster stirring speed tested caused the MPI particles to aggregate together.

In order to check that this observation was valid and to investigate whether stirring time and depth had an affect at this slower stirrer speed another series of solutions were prepared and analysed using particle size distribution. A description of the prepared solutions can be found within Table 11 and their produced volume distribution graphs in Figure 24.

Table 11. Detailing solutions prepared to test the effect that the stirrer time and depth has when using a stirrer speed of 125 rpm on the resolubilsation of MPI.

Expt . no	Temp (°C)	Concentration (wt %)	Stirrer speed (rpm)	Stirring time (minutes)	Depth sample taken (cm)
1	60	20	125	10	25
2	60	20	125	10	5
3	60	20	125	20	25
4	60	20	125	20	5
5	60	20	125	30	25
6	60	20	125	30	5

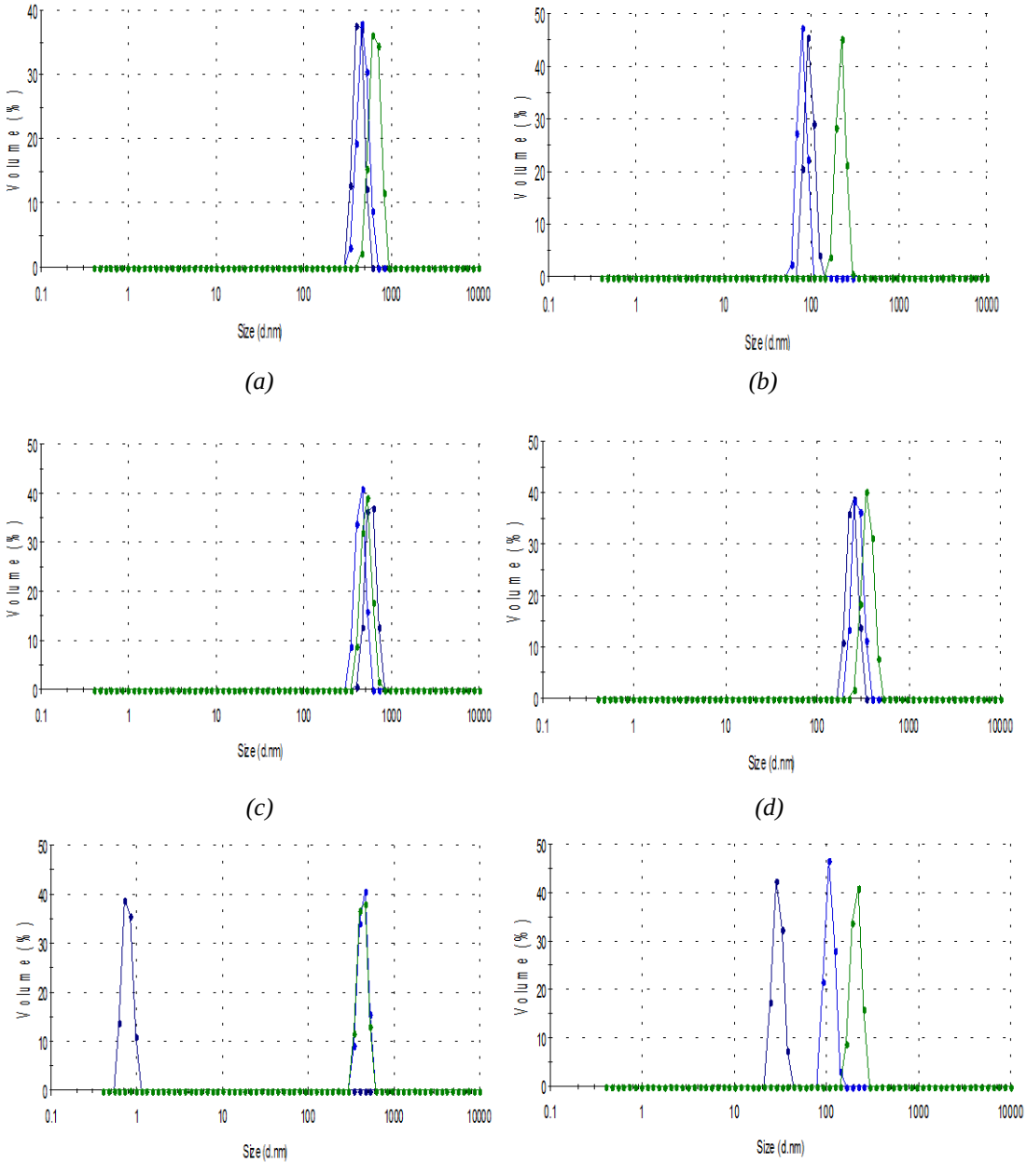

Figure 24. a – f) Volume distribution data for solutions 1 - 6 respectively.

This particle size data supported the previously collected data and showed that both the stirring time and the depth at which a sample was taken do have a noticeable effect at this slower stirrer speed. Generally smaller particles were found at a depth of 5 cm and after 30 minutes of stirring. From these results the following ideal resolubilisation protocol for MPI was developed; a temperature of 60 °C, stirrer speed of 125 rpm and stirrer time of at least 30 minutes.

Scanning Electron Microscopy (SEM) images were used to examine the spray dried *Ultranor*™ 9075 Milk Protein Isolate powder before and after resolubilisation using the ideal resolubilisation protocol. The sample preparation protocol for SEM of both the spray dried powder and resolubilised MPI samples can be found in Appendices 2.3 and 2.4. The samples were examined and photographs taken using a JSM-6480LV SEM using an accelerating voltage of 10 kV, a spot size of 20 and a z value of 20.

The images of the MPI powder and resolubilised solution taken as shown in Figure 25 provided additional qualitative evidence for the success of the developed resolubilisation protocol. As the MPI particles that are clearly visible in the images shown in (a) and (b) of the spray dried powder before resolubilsation cannot be seen within images (c) and (d) of the resolubilised solution. This implies that this resolubilised sample had no suspended particles present and that they were instead fully resolubilised in solution.

As stated previously, this ideal resolubilisation protocol could only be used when small volumes of a low wt% solution (< 5 wt%) were required. When either a large feed volume or a solution of high wt% (> 5 wt%) was required a faster stirrer speed of 700 rpm had to be used to aid resolubilisation. Particle size distribution analysis was carried out on MPI samples of 5, 10 and 15 wt% (MPI wt%'s mainly used during filtration experiments) resolubilised MPI solutions using a stirrer speed of 700 rpm. The volume statistics graphs for these solutions can be found in Figure 26 and the correlation against time and volume statistics tables in Appendix 5 (Figure 89 and Tables 48, 49 and 50).

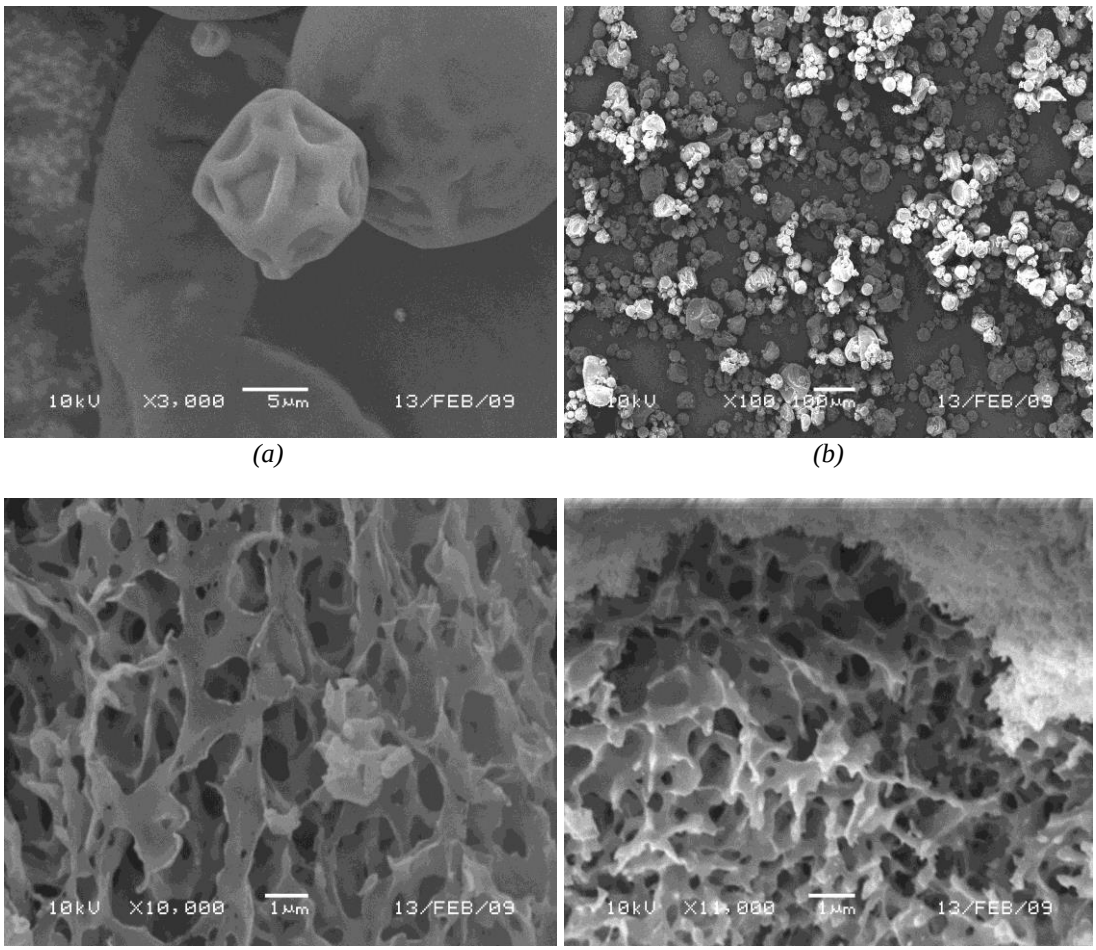

(a) *(b)*

(c) *(d)*

Figure 25. SEM photographs taken on a JSM-6480LV machine a, b, and c) are of Bacillus mycoides *cells prepared by freeze-drying, d)* Bacillus mycoides *cells prepared by HMDS evaporation.*

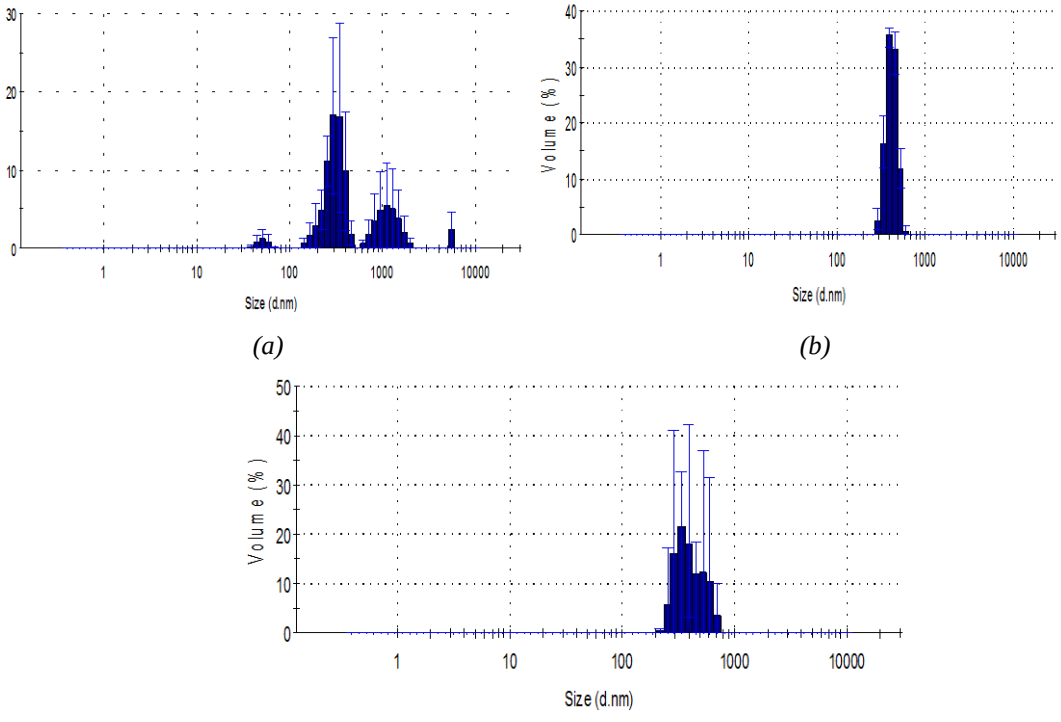

(a) *(b)*

(c)

Figure 26. Volume statistics graphs for a) 5, b) 10 and c) 15 wt% MPI resolubilised at 700 rpm.

2.5 VISCOSITY AND SHEAR STRESS MEASUREMENTS OF MPI

The viscosity of a series of MPI solutions was measured, all rheological measurements were performed using a Bohlin C-Vor Gemini rheometer and a 4° / 40 mm cone measuring system. All experiments were carried out at ambient temperature unless otherwise stated; temperature was controlled using a water bath with an accuracy of ± 0.1 °C. The rheological data were analysed with supporting rheometer software C-Vor 200. Samples of MPI were placed onto the bottom plate of the rheometer using either a plastic pastuer pipette or a spatula depending on the fluidity of the sample.

The flow behaviour of samples was evaluated by controlling shear rate over the range 1 - 20 s^{-1} and measuring shear stress and viscosity. For each sample the shear rate was ramped up and then down over this range. A delay time of ten seconds was used, this is the time between taking each measurement and an integration time of twenty seconds was set, this is the time the rheometer takes to reach the required shear rate. Three replicates of each individual rheological measurement were made using a fresh sample each time, in order to eliminate any hysteresis properties that the sample may possess.

2.6 SYNTHETIC MEMBRANES

Two different flat sheet polymeric membranes *(Alfa Laval)* were initially evaluated, each of which was made of polysulfone but had different pore sizes. A 0.5 µm (GRM-RT5) and a 1.5 µm (PSU-RT8) average pore size membrane.

Five *Membralox*^{TM} α-alumina tubular ceramic membranes (*Pall Filtration)* of 0.8, 1.4, 2.0, 5.0 and 12.0 µm pore sizes were also tested. Membranes of pore sizes 0.8 and 1.4 µm were comprised of a double layer and GP modification. Membranes of pores sizes 2.0 and 5.0 µm were comprised of a single layer without GP modification. Finally, the 12.0 µm pore diameter membrane was comprised of a support layer only (no active layer) without GP modification. Membranes with GP modification have a longitudinal permeability gradient built into their support structure. This eliminates the natural pressure drop that occurs from the inlet to the outlet of flow channels and ensures a stable TMP is maintained across the entire length of the membrane. Each membrane was 1020 mm in length consisted of 19 channels that were 4 mm in diameter producing a filtration area of 0.244 m^2 per membrane. These membranes were chosen as they had a large variation in pore size but were made of the same material, this allowed the effect

of pore size on both the rejection of *Bacillus mycoides* spores and the permeate flux and solid transmission of MPI to be determined. Polymeric membranes were also tested to see the effect of using a different type of membrane material and membrane.

2.7 MODULES

Three different modules were used to house the different membranes, a flat sheet stainless steel square module and two stainless steel tubular housings. The flat sheet module was fitted with a polycarbonate insert, the dimensions of which are shown in Figure 27. The total membrane filtration area for the flat sheet membranes fitted within this module was 7.4 x 10^{-3} m^2. A polyethylene support material was used to support the membrane that had an average pore size of 40 – 100 µm and a thickness of 3.00 ± 0.25 mm. The two stainless steel tubular modules were used to house the ceramic *Membralox*™ microfiltration membranes. One of these modules was used to house the 0.8 and 1.4 µm membranes that were manufactured with rounded ends and the 2.0, 5.0 and 12.0 µm membranes that had hexagonal ends were housed inside the second tubular module. In order to secure the tubular membranes inside their respective housings plastic gaskets were fitted to the ends of each membrane. The total membrane filtration area for each ceramic membrane was 0.24 m^2. Pictures of the ceramic membranes and module can be seen within Figure 28.

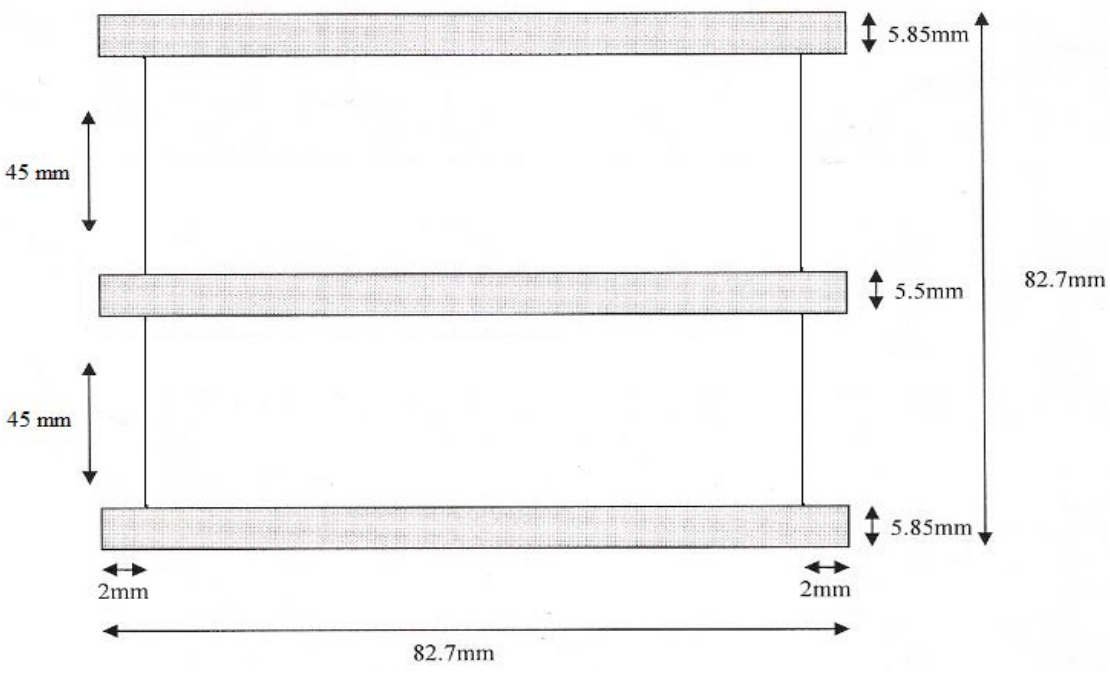

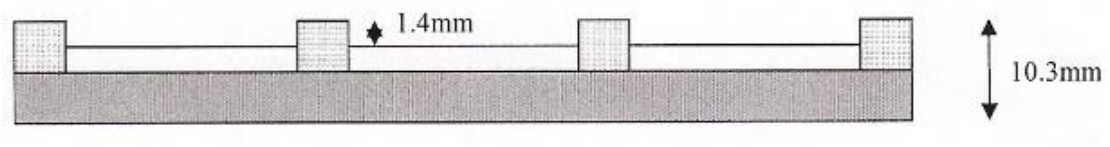

Figure 27. Schematic showing the dimensions for the polycarbonate insert used within the flat sheet stainless steel module

(a)

(b)

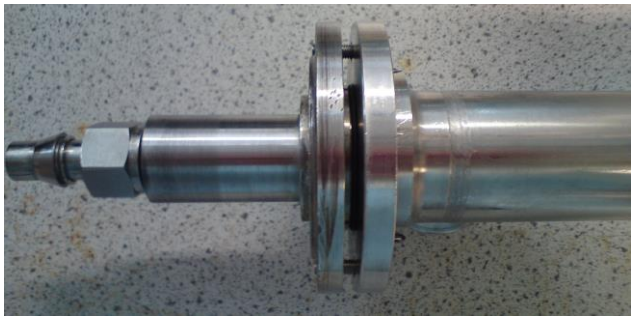

(c)

(d)

(e)

Figure 28. Pictures showing a) Membralox™ *stainless steel tubular module, b) ceramic* Membralox™ *microfiltration membrane, c) close up of a* Membralox™ *module fitting d) close up of a membrane gasket and e) close up of a ceramic membrane fitted with a gasket.*

2.8 DSS LABUNIT M10 RIG

Initial MPI (low solids) filtration and *Bacillus mycoides* spore rejection experiments

were carried out using a DSS LabUnit M10 unit. This rig consisted of a plate and frame module in which four pre-cut flat sheet polysulfone membranes supported by four polysulfone module plates are held together in series using stainless steel supports providing a membrane filtration area of 336 cm^2.

2.9 NEWLY CONSTRUCTED FILTRATION SYSTEM (SET-UP 1)

Because of the issues of low flux discovered when filtering MPI of low solids (3.5 wt%) content through the M10 an alternative filtration system had to be constructed. A fellow PhD student within Dr Michael Bird's research group Peter Bechervaise took the lead in the construction of a new filtration system that was used to carry out the main MPI filtration experiments during this project. A picture and schematic of the initial set-up of this system can be seen within Figures 29 and 30 respectively. This system was made up of a reciprocating pump (CAT 1051, capable of generating up to 2.3 $m^3 h^{-1}$), a shell and tube heat exchanger that maintained temperatures within the system using controlled temperature transcal N oil heated and pumped by an oil circulation pump and heater. The flow within the system was measured using an electromagnetic flow meter (Magflo MAG 1100) and the transmembrane pressure (TMP) within the module was calculated using equation 14.

$$TMP = \frac{(P_1 + P_2)}{2} - P_p \qquad (14)$$

Where P_1 is the feed inlet pressure, P_2 the retentate outlet pressure and P_p the permeate pressure. P_1, P_2 and P_p were measured using pressure transducers. The flux of permeate through the membrane was determined gravimetrically from the mass recorded by the balance (College B3001-S) g at regular time intervals of 20 seconds, the balance had an accuracy of ± 0.1g. Filtration data such as run time, feed, retentate and permeate pressures, mass and mass difference and temperature was logged by LabView and analysed using Microsoft Excel 2000 software. An example flux calculation can be found in Appendix 1. The rig was fitted with a 20 litre feed tank and with sampling points both before and after the module allowing feed and retentate samples to be collected in addition to permeate samples during filtration experiments.

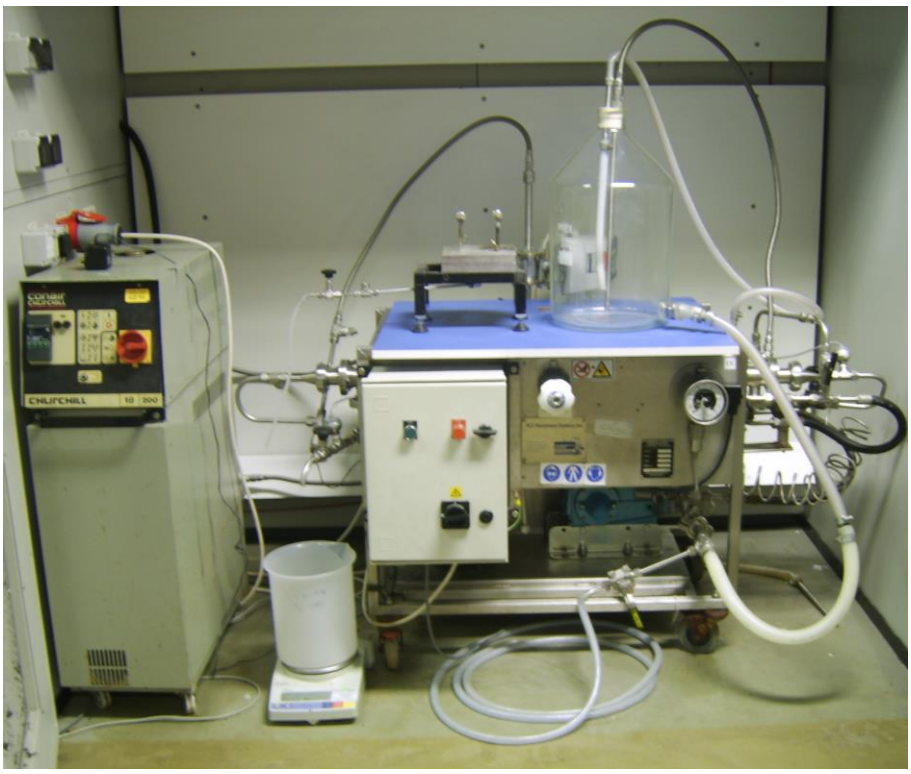

Figure 29. Photograph of the newly constructed filtration system (set-up 1)

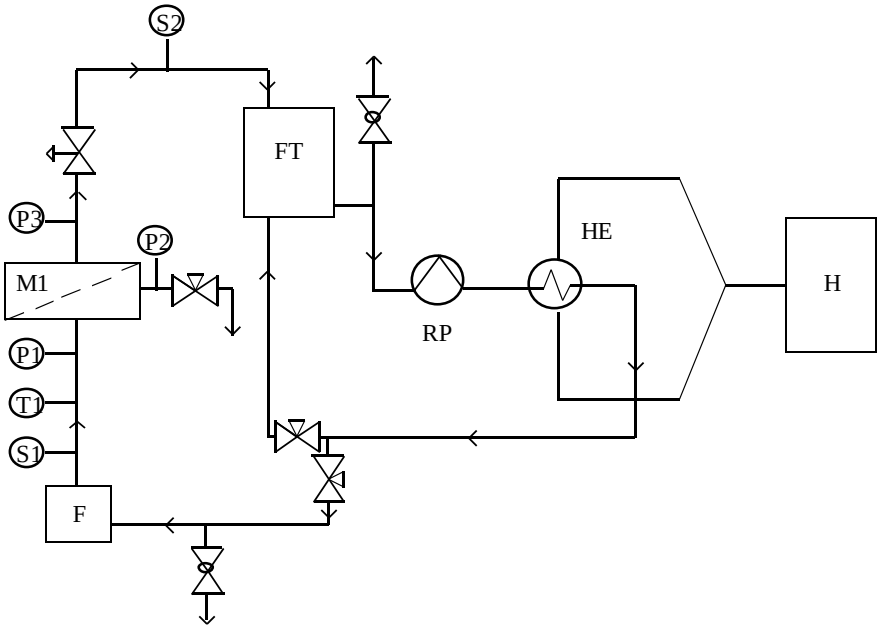

Figure 30. Schematic of the constructed filtration system (set-up 1), C1-feed tank, RP-reciprocating pump, H1-oil circulation pump and heater, F1-electromagnetic flow meter, M1-membrane module, S1 and 2- sample collection taps, T1- thermocouple and P1, 2 and 3- pressure transducers.

2.9.1 Modifications to the filtration system (Set-up 2)

Several modifications were made to the filtration system due to the low fluxes and solid transmissions produced using the initial set-up. The reciprocating pump was replaced with a triplex plunger positive displacement pump the specifications of which stated that it was capable of producing a much higher flow rate of 2.4 – 8.0 m^3 hr^{-1} to try and

increase the CFV's able to be produced within the system. But unfortunately when this pump was fitted onto the rig and tested it wasn't able to produce any significant increase in CFV when filtering MPI with the maximum CFV able to be produced during filtration using 5 wt% MPI increasing by only 0.3 m s^{-1} to 1.7 m s^{-1}. The increase during 10 and 15 wt% filtration was less than this so it was decided to conduct experiments using only 5 wt% at 1.7 m s^{-1} as well as at 1.4 m s^{-1} and using 10 and 15 wt% at the previous maximum CFV of 1.4 m s^{-1}.

The change of pump caused for other modifications to be made. As the new pump added more heat into the feed a cooling coil was needed and the feed tank had to be changed in order to accommodate the coil. A new balance (Ohaus, Scout Pro, SPU4001) was also added to the system, which was able to measure a higher weight of up to 4 kg with an accuracy of ± 0.1g. A constant MPI filtration temperature of 50 °C was maintained in this rig set-up by using the heat exchanger that was connected to an oil circulation heater and pump as in set-up 1 to heat the feed, and the coil within the feed tank connected to the mains water supply to cool the feed when required. Figures 31 and 32 show a photograph and schematic of the modified filtration system (set-up 2).

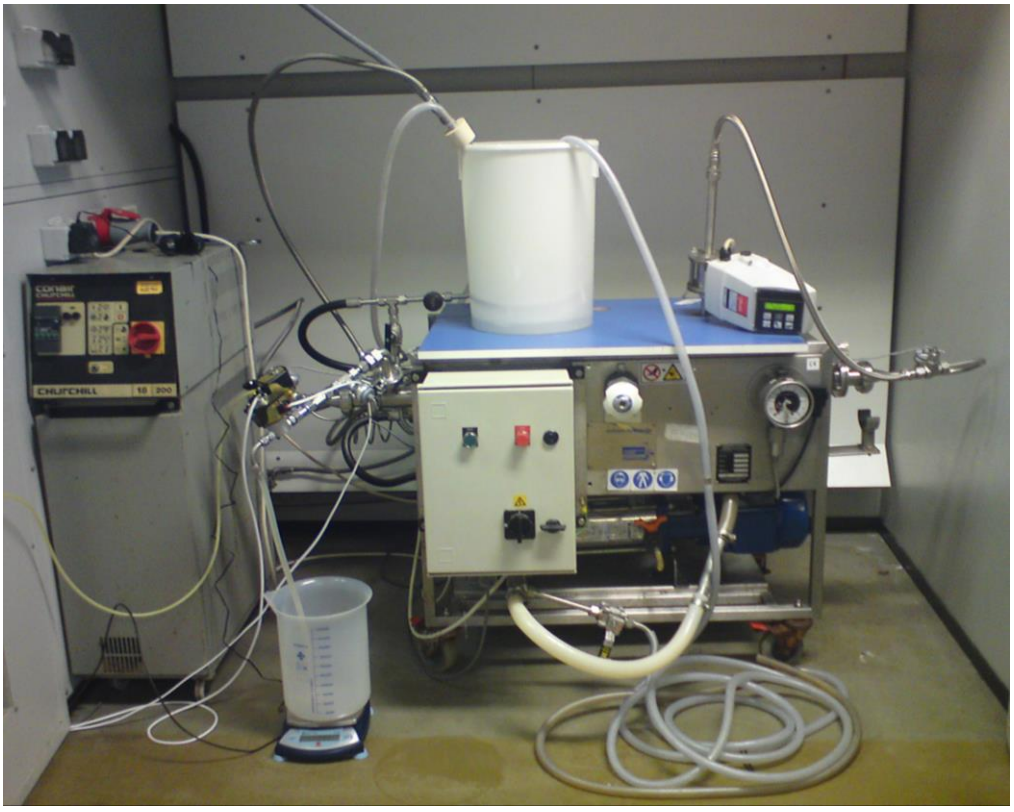

Figure 31. Photograph of the newly constructed filtration system (set-up 2).

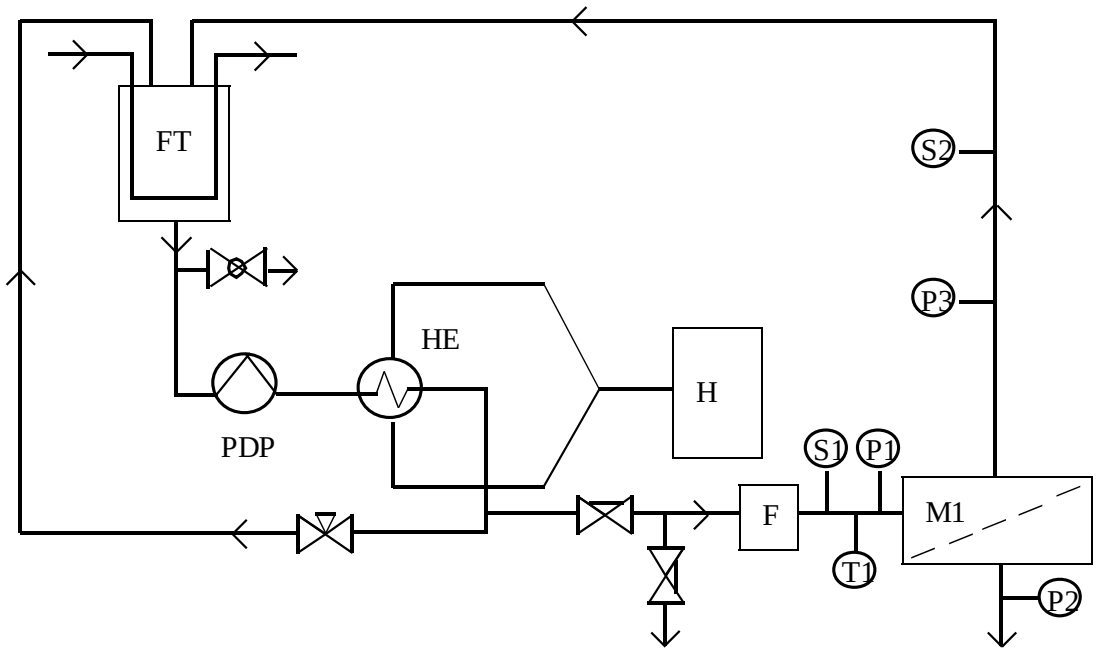

Figure 32. Schematic showing set-up 2 of the constructed filtration system. Where FT- feed tank, H- oil circulation pump and heater, M- membrane module, F-electromagnetic flow meter, HE- heat exchanger, PDP- positive displacement pump, T- thermocouple, S- sampling point and P- pressure transducer.

2.9.2 Modifications to the filtration system (Set-up 3)

As the new pump was not able to produce any significant increase in CFV the problem of low flux and solid transmission still remained. Further modifications were made to the system in order to try and increase CFV as well as to allow backwashing to be carried out. Increasing the produced CFV's involved the addition of a centrifugal pump into the feed loop of the rig as well as the positive displacement pump that was within the bypass loop, changing the cooling coil into a heating coil and the heat exchanger into a cooling unit that was connected to the mains. This was necessary as having two pumps on the rig added more additional heat into the system. These changes increased the CFV able to be reached within the system to 2.0 m s^{-1}. A constant MPI filtration temperature of 50 °C was maintained within this set-up by heating the feed using the heating coil within the feed tank connected to the oil circulation pump and heater and cooling the feed by passing mains water through the heat exchanger that was connected to the mains water supply. The backwashing modifications involved attaching a cylinder filled with nitrogen gas and a pressurised tank to the module as well as adding a solenoid valve and replacing the permeate needle valve with a solenoid valve. The pressurised tank was placed onto a balance so that the amount of water backwashed into the system could be measured and the LabView program was modified so that the frequency and duration that the solenoid valves were open and closed for could be

controlled. A photograph and schematic of the new set up complete with backwashing modifications (set-up 3) can be seen in Figures 33 and 34 respectively.

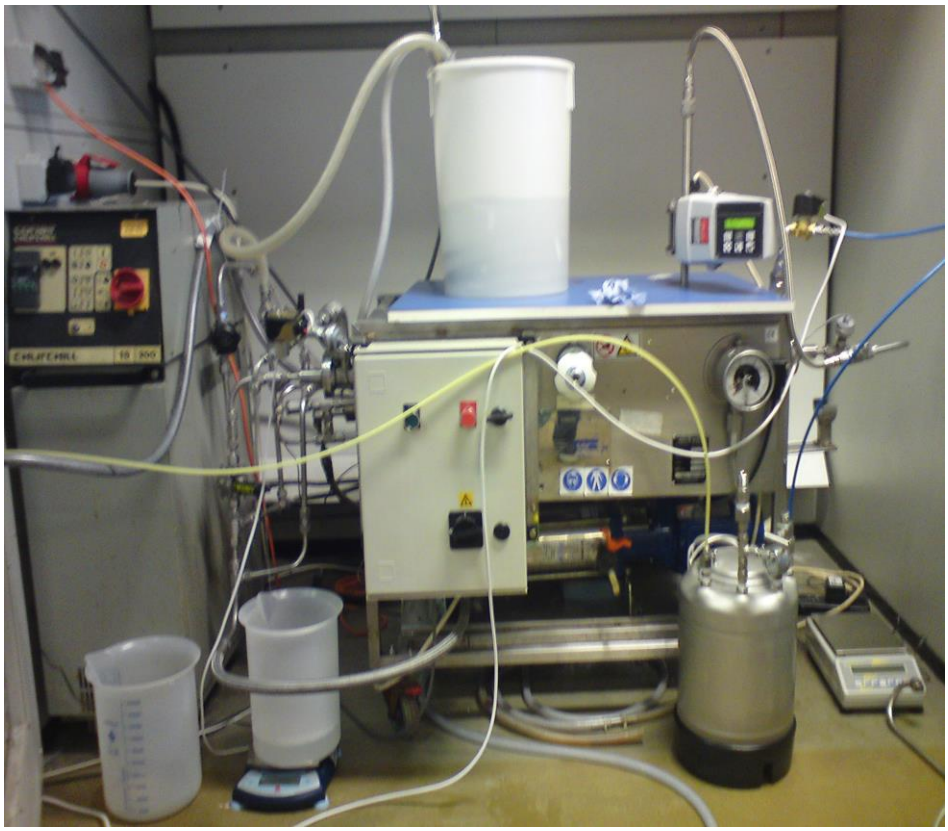

Figure 33. Photograph of the newly constructed filtration system (set-up 3)

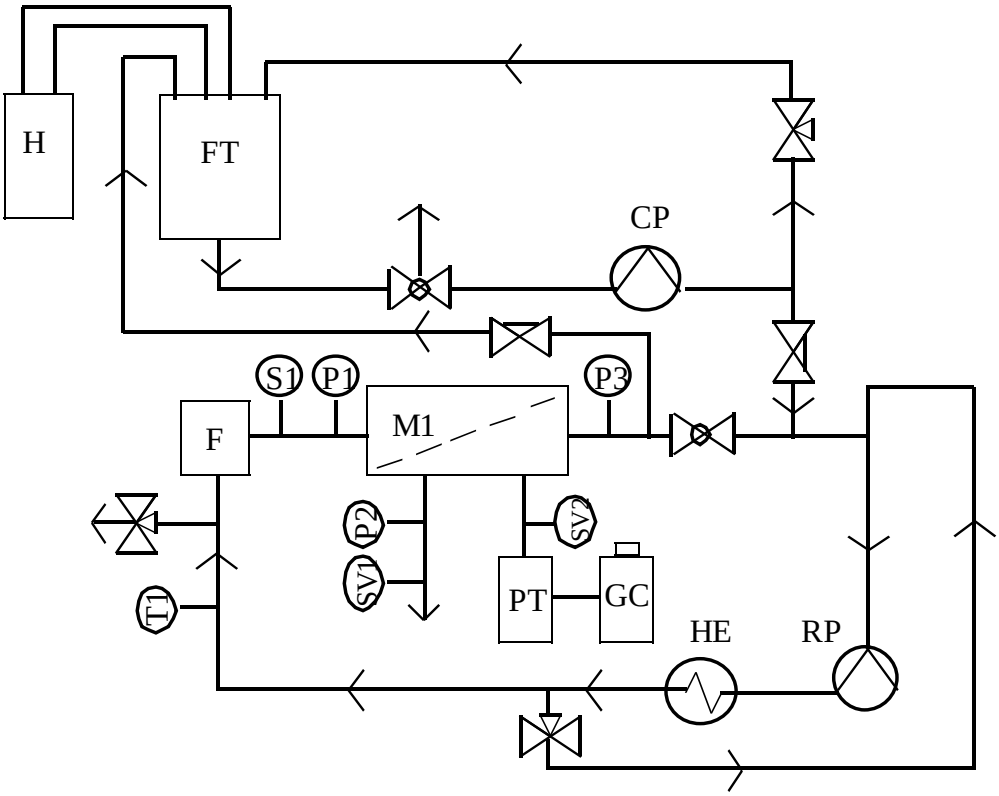

Figure 34. Schematic showing set up 3 of the constructed filtration system. Where FT- feed tank, H- oil circulation pump and heater, M- membrane module, F- electromagnetic flow meter, HE- heat exchanger, PDP- positive displacement pump, CP- centrifugal pump T- thermocouple, S- sampling point, P- pressure transducer, SV- solenoid valve, PT- pressurised tank and GC- nitrogen gas cylinder.

2.10 FILTRATION EXPERIMENT PROTOCOL

Initial filtration experiments using MPI feeds of high solid contents (> 5 wt%) were carried out using filtration set up 1. These initial experiments used a 12 kg feed solution (prepared as described within section 2.4) made up of either 5, 10 or 20 wt% spray dried powder, and 95, 90 or 80 wt% RO water respectively. But this was diluted by RO water already in the system when the feed was added resulting in a feed solid content of 4, 8 or 16 wt%. During subsequent experiments in order for 5, 10 or 15 wt% MPI to be filtered the dead volume of the rig had to be established and used to calculate the wt% of MPI needed to be resolubilised in order to be diluted appropriately when added to the system. The calculated dead volumes of the different filtration system set-ups used along with the MPI wt% wanted within the rig and the respective MPI wt% that had to be resolubilised and added to the system in order to achieve this concentration are shown in Table 12. During backwashing experiments in order to compensate for the additional water added to the system during backwashes an extra 3 kg portion of MPI was resolubilised at an appropriate concentration.

Table 12. Showing the dead volume, MPI wt% wanted within the system and the respective required amount needed to be added to produce this feed wt%.

Rig setup (no.)	Dead volume (litres)	MPI wt% wanted within system	MPI wt% required to be added to system
1	2.82	5 10 15	6.1 12.1 17.9
2	3.99	5 10 15	6.6 12.9 19.0
3	7.79	5 10 15	8.0 15.5 22.5

A summary of the conditions used for pure water flux (PWF) measurements, MPI filtration, rinsing, cleaning and sanitising during experiments using the five tubular ceramic *Membralox*^{TM} microfiltration membranes can be found in Table 13.

Table 13. Filtration experimental conditions used for PWF measurements during fouling, rinsing and cleaning operations

	PWF	Sanitising	Fouling	Rinsing	Alkali cleaning	Acid cleaning
Test liquor	RO water	200 ppm NaOCl	4 – 16 wt% MPI with / without BW and with / without *Bacillus mycoides* spore inoculation	RO water	0.25 or 0.5 wt% NaOH	0.3 wt% HNO_3
Temp (ºC)	18	18	50	18 or 50	18 or 50	50
TMP (bar)	0.1	0.1	1 or 2	0 or 1.0	0, 0.3 or 1.0	0 or 0.3
CFV (m s^{-1})	0.73	0.73	0.7, 1.4 or 2.0	0.7 or 1.4	0.7 or 1.4	1.4
Run time (mins)	5	15	40	10	10	10

Before each experiment was conducted the filtration system was cleaned with a 0.5 wt% sodium hydroxide solution for 10 minutes at 50 °C, 0.3 bar and 0.7 m s^{-1} CFV. After which at the start of every experiment, as well as after fouling and after each stage of cleaning the membrane was characterised by pure water flux (PWF) measurement using a RO water feed volume of 10 litres, ambient temperature, a TMP of 0.1 bar and a CFV of 0.73 m s^{-1} for a period of 5 minutes. The same conditions were used each time so that the membrane performance could be compared at these different stages.

Before and after each experiment involving an MPI feed inoculated with *Bacillus mycoides* spores the system was run for 15 minutes at ambient temperature using a TMP of 0.1 bar and a CFV of 0.73 m s^{-1} with a 200 ppm solution of sodium hypochlorite in order to sanitise the system and membrane to minimise bacterial contamination. Fritsch and Moraru (2008) used these conditions to sanitise a filtration system before and after filtering raw skim milk. Young and Setlow (2003) found that a NaOCl concentration as low as 50 ppm after NaOH treatment was able to destroy 100% of *Bacillus subtilis* spores when suspended within liquid growth media.

During a run once the initial flux of the membrane had been recorded and if required the filtration system sanitised, the resolubilised MPI solution was added to the feed tank, inoculated (if required) and heated to the desired filtration temperature of 50 °C. This was achieved either by running the feed through the heat exchanger on the system bypass loop (set-ups 1 and 2) or by using the heating coil within the feed tank whilst

pumping the feed around the bypass loop (set-up 3). The feed line was then opened allowing the solution to pass through the membrane module. When using set-up 3 when a CFV higher than 0.7 m s^{-1} was required the second positive displacement pump was started.

During backwashing (BW) experiments (carried out using set-up 3) backwashes were performed by controlling the solenoid valves on the permeate and backwashing sides, shown as SV1 and SV2 respectively on Figure 34. During normal crossflow filtration, the permeate valve is open and the backwash valve closed. In contrast, the permeate valve is closed and the backwash valve is open during backwashing. These valves were controlled using LabView software. An average TMP of 2 bar was maintained for forward filtration periods and a reverse TMP of 1 bar was used during backwashing periods. A lower TMP was used during reverse filtration in order to reduce permeate loss during each backwash. Backwashes were carried out using nitrogen gas pressurised to 3 bar to force RO water within the pressurised tank back through the membrane in the reverse direction.

All MPI filtration experiments were carried out for 40 minutes. This was deemed long enough for steady state to be reached according to criteria stated within Evans and Bird (2006). During this time both retentate and permeate streams were recycled back to the feed tank to maintain a constant feed concentration, with the exception of small samples taken for analysis. During backwashing experiments the additional MPI solution was also gradually added to the feed tank to maintain a constant feed concentration. Once filtration was complete the system was then drained and flushed with RO water before being rinsed and cleaned.

When required 5 ml samples of *Bacillus mycoides* spore suspensions were used to inoculate resolubilised MPI producing feeds, resulting in a bacterial content of between 10^4 - 10^5 cfu ml^{-1}. Spore samples were kept within sterile containers and added to the feed within the feed tank. This was done when the feed stream was being heated to the required filtration temperature of 50 °C whilst being circulated through the bypass loop. This ensured adequate mixing of the spores within the MPI feed solution before the membrane was exposed to the feed.

2.10.1 Feed and permeate sample collection

During normal crossflow MPI fouling runs samples of the feed and permeate streams were taken after 5, 15 and 40 minutes, during backpulsing experiments samples were also collected after 30 minutes. During backflushing experiments using an MPI feed not inoculated with spores of *Bacillus mycoides* samples were collected after 40 minutes and those involving inoculated feeds, samples were taken 1, 2 and 4 minutes after the 1st, 5th and 8th backflushes. All collected samples were analysed for total solids concentration by oven drying at 55 °C. Percentage solid transmissions were calculated using equation 15, where DM_P and DM_F are the wt% dry masses of permeate and feed samples respectively. The total MPI collected was calculated using the measured solid transmissions and equation 16.

$$Transmission = \left(\frac{DM_P}{DM_F} \right) \times 100 \tag{15}$$

$$Mass\ of\ MPI\ collected\ (g's) = \frac{(Sum\ of\ permeate)\ x\ Solid\ transmission}{100} \tag{16}$$

The mass of permeate collected directly after a backwash had occurred was not included in the sum of permeate. Equation 16 was used for each of the measured solid transmissions and the calculated weights were added together to give the total MPI weight collected during a run. The protein content of selected samples was determined using a Bradford assay (Bradford, 1976) and the spore content of selected samples using the *Petrifilm*™ Aerobic Count Plate (ACP) technique. Spore rejection was calculated using equations 17a and 17b, where C_{sp} and C_{sf} are the average spore ml^{-1} *Petrifilm*™ plate counts for collected permeate and feed samples respectively. Both the protein determination and spore enumeration techniques along with the development of the oven drying protocol used are described in more detail within sections 2.10.4, 2.3.2 and 2.10.5 respectively.

$$\%\ \text{Reduction (spore ml}^{-1}) = \left(1 - \left(\frac{C_{sp}}{C_{sf}} \right) \right) x100 \tag{17a}$$

$$\log_{10}\ \text{Spore reduction} = \log_{10} C_{sf} - \log_{10} C_{sp} \tag{17b}$$

2.10.2 Membrane fouling resistance measurement

Total resistances (R_T) were calculated at steady state after 40 minutes of filtration for each filtration experiment using equation 18. Where TMP is the average transmembrane pressure during the experiment (Pa), μ_P is the viscosity of the permeate solution at 50 °C (Pa.s) and J_v is the steady state permeate flux (m s^{-1}).

$$R_T = \frac{TMP}{(J_V \times \mu_P)} \tag{18}$$

In an ideal system the resistance of the membrane itself is the only resistance acting on the filtration process. But when a membrane is fouled a number of various other resistances act on the process. These can be characterised by the resistance in series model (Evans and Bird, 2006) as shown in equations 19, 20 and 21. Where R_m is the membrane resistance, R_p resistance due to pore plugging, R_a resistance due to adsorption of feed onto the membrane surface, R_g resistance due to gel layer formation, R_c resistance due to cake layer formation and lastly R_{cp} is the resistance caused by concentration polarisation.

$$R_{TOT} = R_m + R_p + R_a + R_g + R_c + R_{cp} \tag{19}$$

A fouling resistance R_F, can be shown as:

$$R_F = R_p + R_a + R_g + R_c \tag{20}$$

And the total hydraulic resistance can be summarised as:

$$R_{TOT} = R_m + R_F + R_{CP} \tag{21}$$

R_m is calculated from the initial PWF measurement taken before fouling and R_F from the PWF measurement taken after fouling. R_F can be broken down into a reversible R_R and irreversible fouling resistance R_I as shown by equation 22. R_R and R_I are calculated from the PWF taken after rinsing, with R_R defined within this study as that which is removed by rinsing using conditions of a RO water feed at 50 °C a CFV of 1.4 m s^{-1} and no TMP for 10 minutes, R_I was defined as fouling that is not removed by rinsing. These terms are relative and depend upon the rinsing conditions used (Shorrock and Bird, 1998), but can be compared within the data set as the rinsing conditions were kept constant.

$$R_F = R_R + R_I \tag{22}$$

2.10.3 Selection of MPI filtration temperature

All MPI filtration experiments were conducted at 50 °C; this temperature was selected as a compromise between process advantages over pasteurisation and MPI viscosity. One of the benefits of using membrane filtration is the possibility of operating at ambient temperatures. But as the viscosities found at ambient temperature for MPI solutions (5 – 15 wt%) were so high (as discussed in more detail within section 3.4.1) this was not possible. Additional measurements indicated a feed temperature of 50 °C would have to be used, in order to decrease MPI viscosity into a range that could be filtered (as discussed in more detail within section 3.4.2). The difference between these high solid MPI streams compared to skim milk (low solids) is highlighted by these measured viscosities. Whilst operating at an elevated temperature of 50 °C this reduces the benefit of microfiltration over pasteurisation, but it still offers the advantage of being able to remove all types of microorganisms present in raw milk including spore-forming bacteria that are resistant to pasteurisation. Moreover, product quality improvements and the possible savings in energy achieved by subjecting the feed to a temperature of 50 ^{o}C rather than the usual pasteurisation conditions of 73 ^{o}C could also be significant. Madaeni *et al.,* (2011) investigated the effect of temperature on filtration performance during the filtration of raw whole and skim milk and concluded that 50 °C was the optimum filtration temperature.

2.10.4 Protein determination- Bradford assay

The following protocol was used to carry out the Bradford assay on selected feed and permeate samples. This method was adapted from the instructions supplied with the Protein Quantification Kit-Rapid assay (*Sigma Aldrich,* UK).

1. Bovine Serum Albumin (BSA) standard stock solution (4000 μg ml^{-1}) was diluted with RO water to prepare various concentrations of BSA standard stock by multiple dilutions; 2000, 1000, 500, 250, 125, 62.5, 31.25 and 0 μg ml^{-1} inside sterile universal bottles.
2. 50 μL of each BSA solution (prepared as above) was added to a low volume sizing cuvette
3. 2.5 ml Coomassie Brilliant Blue (CBB) solution was then added to each cuvette.
4. The absorbance of each solution at 600 nm was measured using a Shimadzu UV-1601 spectrophotometer.

5. A calibration curve of absorbance against concentration for BSA was then plotted
6. A 2000 μg ml^{-1} solution of MPI was then prepared by dissolving 0.1g in 50 ml of RO water, from which as with the BSA a series of MPI solutions were prepared by multiple serial dilutions; 2000, 1000, 500, 250, 125, 62.5, 31.25 and 0 μg ml^{-1} inside sterile universal bottles.
7. Steps 2 - 5 were then carried out on these MPI solutions.

As discussed in section 1.21, arginine responds eight times higher to the assay dye compared to other basic and aromatic residues and as a result it is advised that if the protein you want to detect for using the assay contains a large amount of arginine residues it may be necessary to use the same protein to produce the calibration curve. There is not a large amount of arginine within the spray dried *Ultranor*™ 9075 milk protein isolate powder as can be seen in Table 7, but as a precaution a second calibration curve in addition to the BSA curve was produced using the MPI powder itself. UV-Visible spectra were obtained using a double beam Shimadzu UV-1601 spectrophotometer and UV probe 2.10 software. Spectra were recorded between 400 - 800 nm with typical curves for both MPI and BSA of concentrations ranging from 32 - 4000 μg ml^{-1} shown in Figures 35 and 36 respectively. The absorbance at 600 nm was then used to construct a standard curve of absorbance against concentration, which can be seen in Figure 37. Samples were placed into the instrument inside disposable plastic cuvettes, using Coomassie Brilliant Blue as the reference sample.

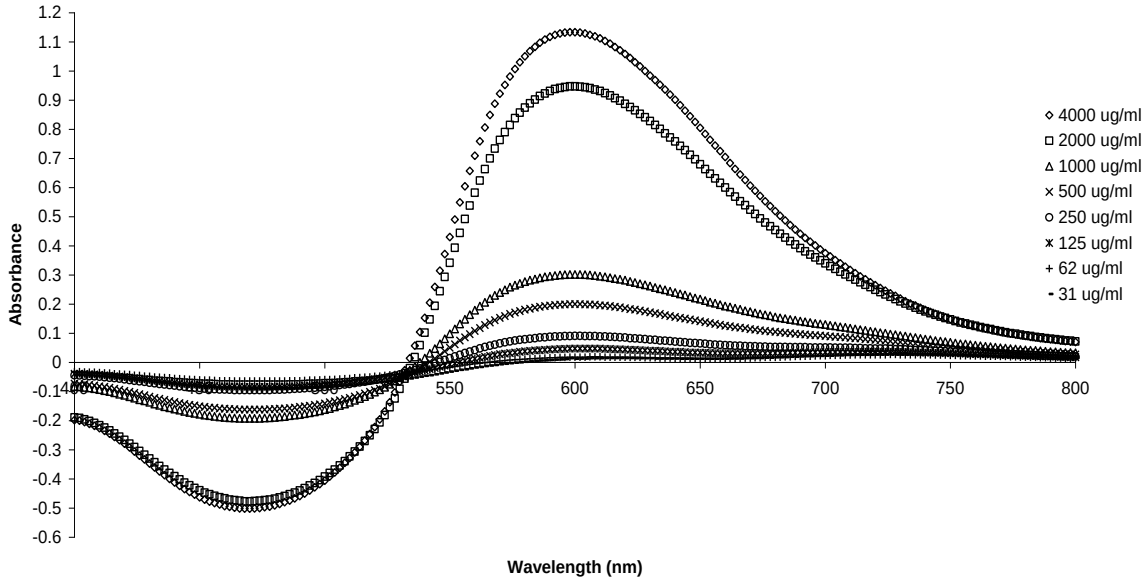

Figure 35. Typical curves produced by MPI solutions of different concentrations within the range 4000 - 31μg ml^{-1}, after being treated with Coomassie Brilliant Blue dye (the Bradford assay), the absorbance at 600nm was used to construct a calibration curve for protein quantification.

The average absorbance curves produced from triplicated averages for both the BSA standard and MPI solutions can be found in Figure 37. The treadlines put through each of the data sets are second order polynomials. As can be seen the error bars of the two curves do not overlap meaning that BSA and MPI respond significantly different to each other, with the MPI responding to a lesser extent to the dye. As a result the MPI calibration curve and not the BSA standard curve was used to detect for protein within feed and permeate samples collected during filtration experiments.

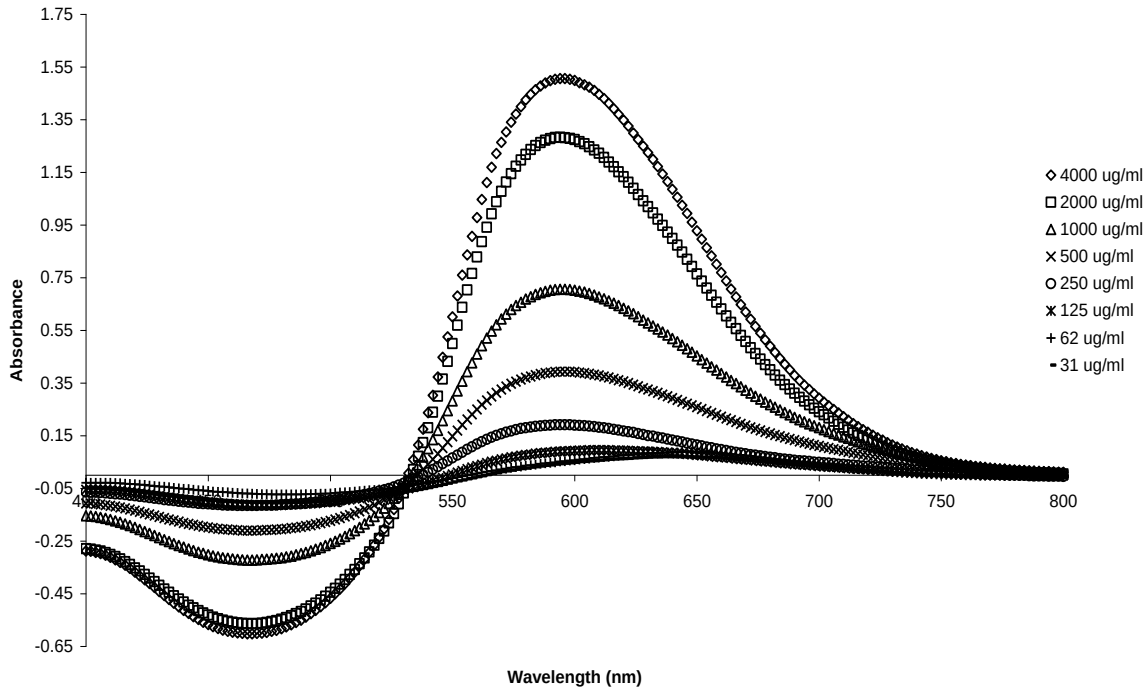

Figure 36. Typical curves produced by solutions of the Bradford assay standard BSA at different concentrations within the range 4000 - 31μg ml^{-1}.

MPI solutions ranging from 32 to 1000 μg ml^{-1} produced a linear response to the dye as can be seen in Figure 38. As a result the equation of this plot was used to determine the protein content of feed and permeate samples, in order for a samples absorbance to be within this plot samples had to be diluted using RO water by x100. Percentage protein transmission was calculated using equation 23, where C_{pp} and C_{pf} are the concentrations (μg ml^{-1}) of protein in the permeate and feed samples respectively.

$$Transmission = \left(\frac{C_{pp}}{C_{pf}} \right) x100 \qquad (23)$$

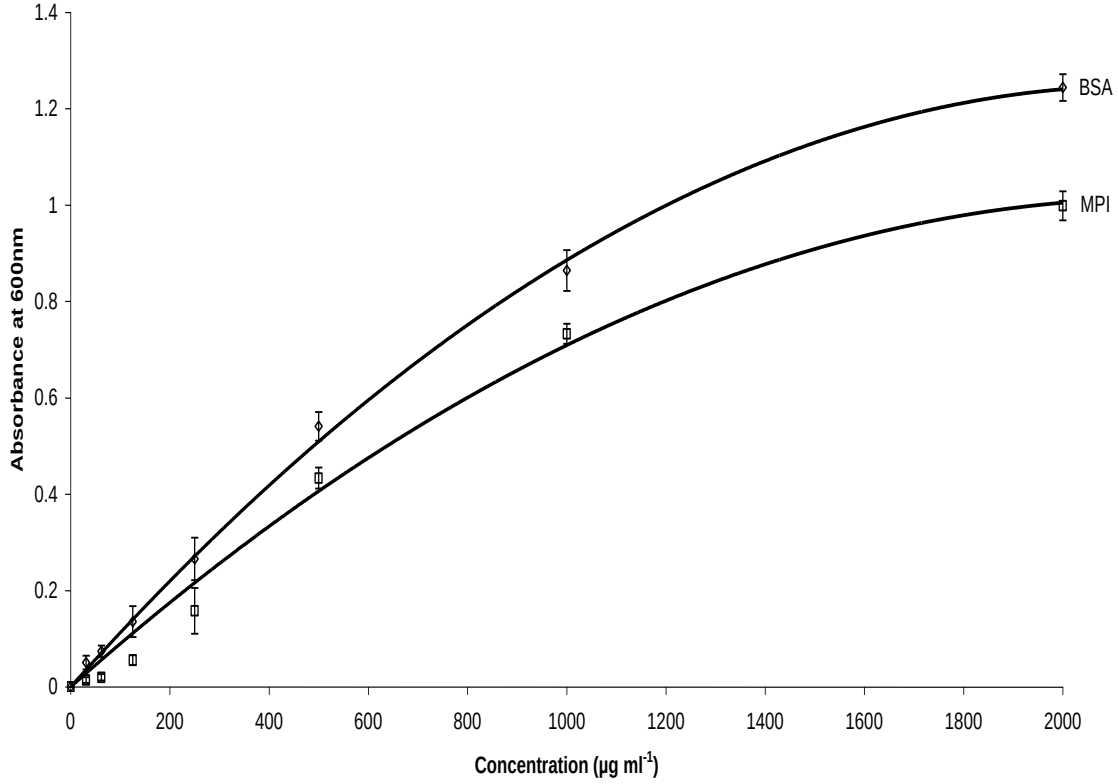

Figure 37. Average absorbance calibration curves for MPI (bottom curve) and BSA (top curve) at 600nm produced using the Bradford assay.

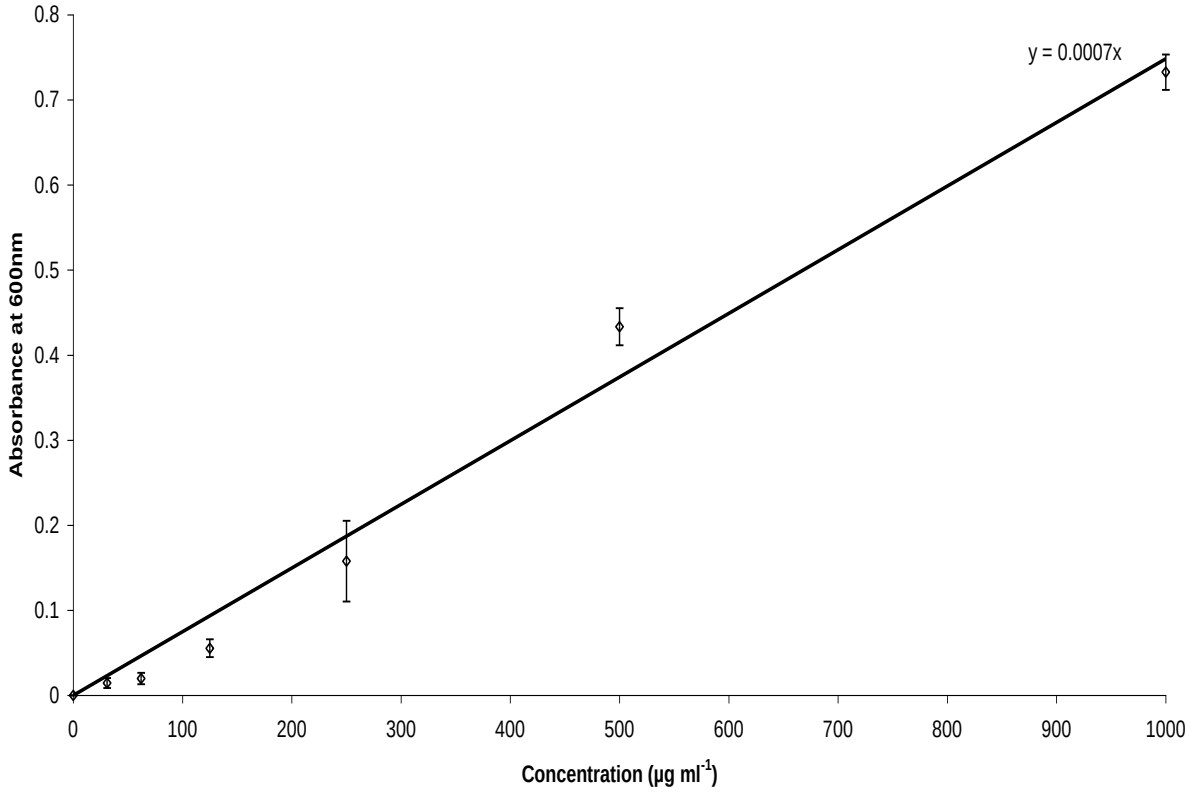

Figure 38. Linear region of MPI calibration curve between 32 - 1000µg ml^{-1} that can be used for determining protein concentration

2.10.5 Development of suitable drying protocol

A suitable oven drying protocol to determine the total solids content of samples taken of feed and permeate streams was developed. In order to find the optimum temperature to use a series of MPI solutions of known concentration were produced in triplicate and dried at 55 and 80 °C. These samples were weighted both before and after drying. As can be seen from Table 14, the drying temperature used did affect the amount of solid recovered, with less solid being recovered at 80 °C. It was concluded that this was the result of whey protein within the MPI becoming thermally denatured at this higher temperature. As a result of this a sample drying temperature of 55 °C was used during this work in order to determine the total solids content of collected feed and permeate samples.

The moisture content of the MPI feed stated to be 4% within the chemical composition data supplied by *Kerry Ingredients* was checked. This was done by drying a ~2g sample of the feed at both 55 and 80 °C for five days weighting them both before and after. As can be seen from Table 14 at 55 ºC the solids recovered were 96.4% meaning that the supplied data could be considered accurate.

The error of the mass balance used to determine the total solids content of feed and permeate samples during this work was established. The standard deviation and standard error calculated were very small being no greater than 0.0005 and 0.0003 respectively. The method used to determine these error values is described in detail within Appendix 6 along with the mass balance error data (Table 51)

Table 14. Weights of MPI recovered at 55 and 80 °C during development of a suitable drying protocol.

Concentration (wt %)	Average wt % left after drying at 55 °C	Percentage difference	Average wt % left after drying at 80 °C	Percentage difference
0.5	0.48	4.8	0.34	32.3
0.75	0.74	1.8	0.66	12.5
1.0	0.95	5.1	0.76	23.5
1.25	1.2	5.2	1.0	23.2
1.5	1.46	2.6	1.3	13.4
Feed	96.4	0.4	94.6	1.4

2.10.6 Filtration experiment errors

In order to establish the errors in the steady state permeate flux, solid and protein transmissions and spore rejection measurements, triplicated averages of each were found. The triplicated experiment was carried out through the 0.8 µm tubular ceramic *Membralox*^{TM} membrane using 15 wt% MPI feed at 50 °C, 2 bar and 1.4 m s^{-1} CFV. The error of each measurement was calculated over the three runs as ± 1 standard deviation. The error in permeate flux (LMH) across the three runs was found to be ± 6.1 %. Errors in solid transmission, protein transmission and spore reduction were found to be 5.1 %, 1.1 % and 0.003 % respectively.

3 CHARACTERISATION

3.1 SPORE CHARACTERISATION

3.1.1 Size of *Bacillus mycoides* spores

The size of a sample of *Bacillus mycoides* spores prepared and harvested following the protocol described in section 2.2.1 has been measured using SEM images and a light microscope technique involving the use of an eyepiece graticule and a stage micrometer slide, which is described in more detail in section 2.2.3.

A total of 50 measurements were taken using the light microscope technique with the average length found to be 2.13 ± 0.86 µm. Using SEM pictures the length and width of a total of 60 individual spores were measured with the average length and width found to be 1.53 ± 0.18 µm and 0.90 ± 0.11 µm respectively.

Both measurements of *Bacillus mycoides* spore length are in good agreement with the stated literature values as discussed in section 1.8.2. These values for spore size are larger than the size of milk protein isolate (MPI) particles measured by particle size distribution described in section 2.4. This implies that during filtration if a suitable membrane pore size is employed the spores should be retained by the membrane and found within the retentate and that the MPI should pass through the membrane and be present predominantly within the permeate. As the spores are ellipsoidal in nature i.e they have a longer length than width this means that the effectiveness of separation using MF depends on the orientation of individual spores as they approach the membrane. A lengthwise orientation of spore would result in a greater separation compared to widthwise orientation (Mukhopadhyay *et al.*, 2010). It is logical to assume that this process would be random and that if a membrane pore size between the spore length and width is used that only a partial separation would occur (this appeared to be what was occurring within filtration experiments as described within section 4.6.2). In addition filtration of protein rich feeds such as MPI often results in the development of a gel layer which reduces the effective membrane pore size and further aids separation, meaning that a larger pore size than expected may be able to provide an effective separation (this again appeared to be what was occurring within filtration experiments as described within section 4.6.2).

3.1.2 Particle size distribution of *Bacillus mycoides* spores

The particle size distribution of a harvested sample of *Bacillus mycoides* spores has been determined using a Zetasizer nano series, nano S model ZEN 1600 machine. A volume distribution graph and a volume statistics graph can be found in Figures 39 and 40 respectively and the particle sizes found, the % of each size and the standard deviation across the three measurements can be found in Table 15. This data mainly agrees with the spore size determination work described in section 3.1.1. Also as implied from SEM pictures taken of harvested spores in Figure 21 shows that there is a large range of spore sizes but that all spores are over 1 µm in diameter. This is much larger than that found for MPI solution particles as can be seen in Figures 23, 24 and 26 and again implies that if the right choice of membrane pore diameter is selected that a good separation is possible.

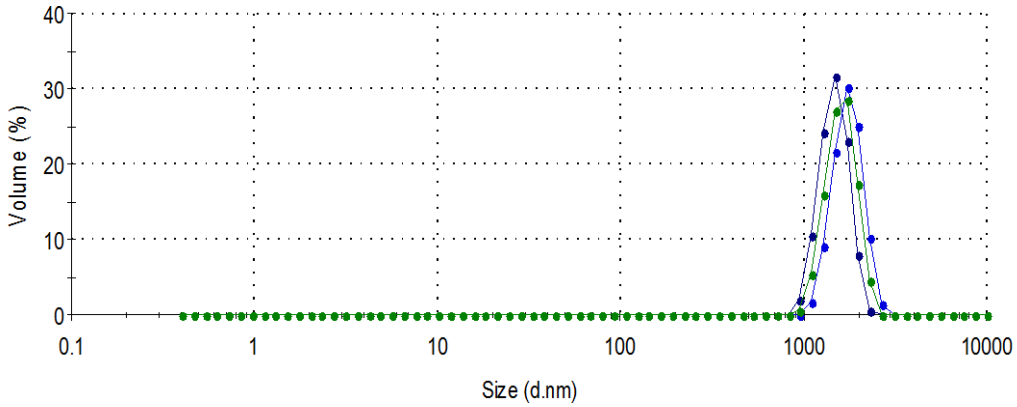

Figure 39. Showing the volume distribution size graph for a harvested sample of Bacillus mycoides *spores.*

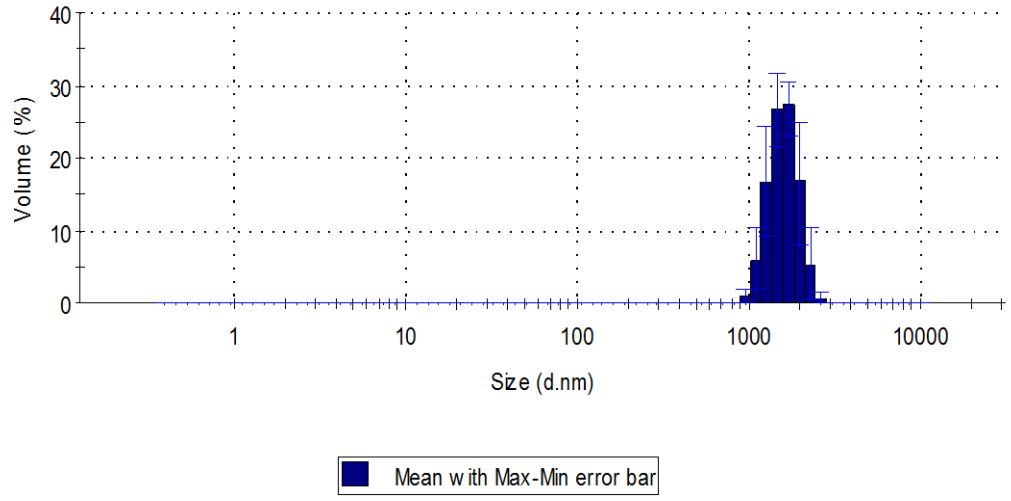

Figure 40. Showing the particle volume statistics size graph for a harvested sample of Bacillus mycoides *spores.*

Table 15. *Bacillus mycoides* particle size volume distribution data

Size (d. nm)	Mean volume (%)	Standard deviation (volume %)
1110	5.9	4.3
1280	16.5	7.5
1480	26.8	5.0
1720	27.4	3.7
1990	16.8	8.6
2300	5.2	4.9
2670	0.5	0.8

3.1.3 Hydrophobicity of *Bacillus mycoides* spores

The surface hydrophobicity of a harvested sample of *Bacillus mycoides* spores prepared following the protocol described in section 2.2.1 has been determined using the microorganism adhesion to hexadecane (MATH) assay used by Seale *et al.*, (2008). The method is described in section 2.2.4. The percentage hydrophobicity was determined using equation 24, where A_i is the absorbance of the original spore suspension and A_f is the absorbance of the aqueous phase after mixing with hexadecane. The percentage hydrophobicity by taking an average of 5 measurements was found to be 45.3% ± 2.6%, the absorbance data can be found within Table 16. This result is similar to that found by Husmark and Ronner (1992) of 41.6% ± 2.2%. They used a similar BATH assay technique involving the use of an organic hexadecane phase but used a saline solution instead of a KCl solution as the aqueous phase.

$$\%h = (Af - \frac{Af}{Ai}) \times 100 \qquad (24)$$

Table 16. *Bacillus mycoides* BATH assay absorbance data

Sample number	A_i - Abs of original sample at 600 nm	A_f – Abs of aqueous phase after mixing at 600 nm
1	0.673	0.134
2	0.621	0.121
3	0.644	0.118
4	0.674	0.131
5	0.654	0.149

As the *Membralox*™ tubular ceramic membranes used within this work are hydrophilic in nature this result suggested that the *Bacillus mycoides* spores measured to be 54.7% ± 2.6% hydrophilic would be attracted to the surface of the membrane. Proteins however are more likely to become adsorbed on to hydrophobic membranes such as polysulfone and polypropylene (Makardij *et al.,* 1999). This is one of the reasons for choosing a hydrophilic membrane for a separation process involving proteins as well as the fact that they produce high fluxes with aqueous solutions.

3.2 3M™ *PETRIFILM*™ AEROBIC COUNT PLATES (ACP)

3.2.1 Comparison of *Petrifilm*™ Aerobic Count Plates (ACP) with the standard spread plate method

Since their launch in 1984 *Petrifilm*™ plates have been extensively tested and compared with standard plate methods for the enumeration of aerobic flora (Tavolaro *et al.,* 2005) this has been done using a variety of different food products including meat, poultry, vegetables (Tavolaro *et al.,* 2005) and various dairy products (Blackburn *et al.,* 1996; Tavolaro *et al.,* 2005; Hayes *et al.,* 2001; Beloti *et al.,* 2002 and De Sousa *et al.,* 2005).

Within this project colony counts produced using *Petrifilm*™ ACP's and the standard spread plate method have been compared. This was achieved using an aqueous solution of *Bacillus mycoides* spores at a dilution of $x10^{10}$. Five *Petrifilm*™ plates and five TS agar plates were inoculated with this solution. The *Petrifilm*™ plates with 1 ml and the agar plates with 0.1 ml, both were then incubated for 24 hours at 32 °C. Five *Petrifilm*™ and five TS agar plates were also inoculated using a solution of $x10^{9}$ dilution but this produced plates that were uncountable. The colony counts for both the *Petrifilm*™ and agar plates were converted to $\log_{10}$ cfu ml^{-1} and linear least squares regression analysis was used to compare the counts found using the two methods, shown in Figure 41. The correlation coefficient found was $R^2 = 0.938$, indicating that there is a strong relationship between the two methods. This correlation coefficient is close to the values found within previous studies, such as Blackburn *et al.,* (1996) who found a correlation coefficient of $R^2 = 0.989$ when testing 84 samples of a variety of chilled, frozen and ambient stored food products. Belotti *et al.,* (2002) found a correlation coefficient of $R^2 = 0.878$ when testing samples of Brazilian milk and lastly,

Hayes *et al.*, (2001) also found a high correlation coefficient of $R^2 = 0.94$ when using raw bovine milk.

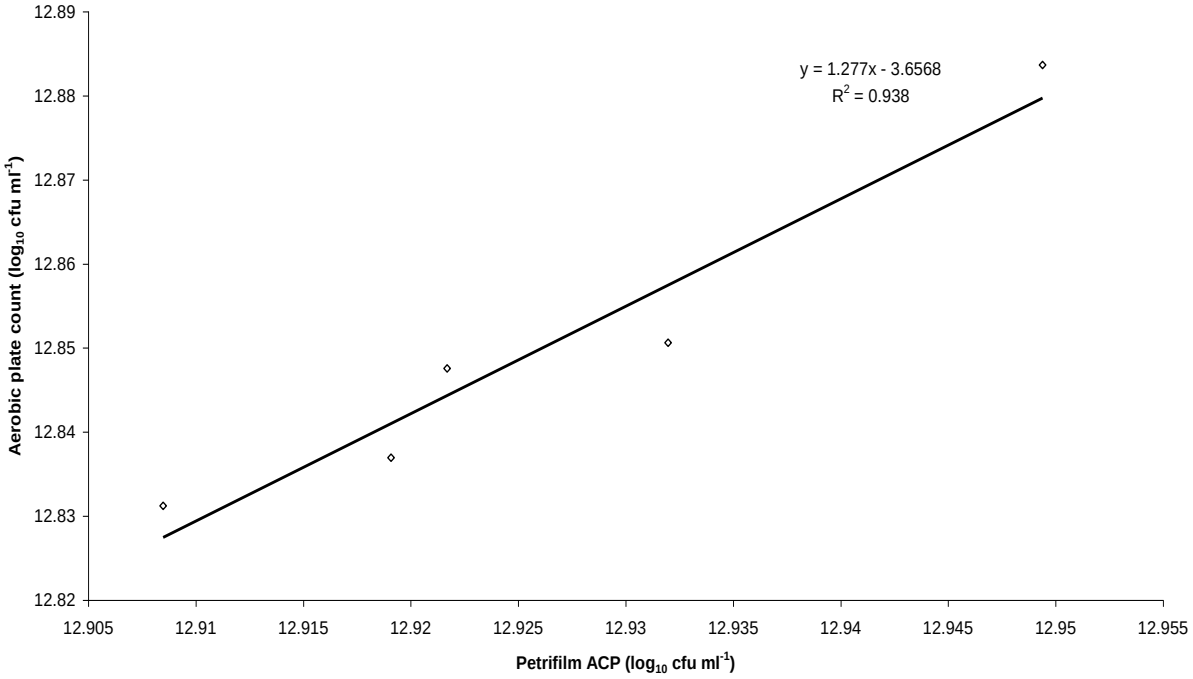

Figure 41. Comparison of Petrifilm^{TM} *Aerobic Count Plate (ACP) with the standard spread plate method for the enumeration of spores of* Bacillus mycoides *in water*

3.2.2 Error between *Petrifilm*^{TM} ACP counts

In order to determine whether changes in the bacterial counts of feed, permeate and retentate streams during filtration were significant, it was necessary to conduct a thorough error analysis to find the error that occurs between plates. This was achieved by measuring the standard deviation between plate counts found during the experiments conducted in sections (3.2.4) in each case the standard deviation was found over five plate counts plated using the same solution.

It was found that when a plate contained between 25 - 250 colonies (and could therefore be accurately counted by eye); the standard deviation was within the range 6.3 – 14.5 actual count or $6.3 \times 10^9 – 1.5 \times 10^{10}$ cfu ml^{-1}. When plates contained more than 300 colonies resulting in an estimate having to be taken by counting two or more representative squares, the standard deviation range was between 1.8 - 4.6 actual count or $3.6 \times 10^{10} – 9.2 \times 10^{10}$ cfu ml^{-1}. Due to the fact that this standard deviation figure is not constant it was concluded it was necessary to calculate a standard deviation for each plate count. Ideally it was intended that a solutions spore count could be measured from a single plate and the error stated as the standard deviation value calculated during this

error analysis work. However, as a range of standard deviations were found solutions needed to be plated in at least triplicate and the standard deviation value stated be calculated for each solutions set of plates.

3.2.3 Comparison of *Petrifilm*^{TM} ACP counts of *Bacillus mycoides* spores when suspended in both water and MPI

In theory the presence of MPI in solution should not have a detrimental effect on spores of *Bacillus mycoides* if this bacterium is a good analogue to *Bacillus cereus* but to be certain this was tested. This was achieved by comparing colony counts produced by inoculating five *Petrifilm*^{TM} plates with an aqueous solution of *Bacillus mycoides* spores at a dilution of $x10^9$ with five plates inoculated with a 20 wt% MPI solution containing spores at the same dilution. In order to ensure that there was as little variation as possible in spore counts between both solutions before plating, a single 1 ml sample of spores was taken from the sporulation media. This was then diluted down in water to a dilution of $x10^8$ and at the same time the MPI solution was diluted as if it had been inoculated with spores to a dilution of $x10^8$. 1 ml of this MPI solution was then discarded and replaced with 1 ml of the inoculated $x10^8$ water solution. Both sets of *Petrifilm*^{TM} plates were incubated for 24 hours at 32 °C before being counted.

In theory if the MPI had little or no effect on the *Bacillus mycoides* spores then the plate counts between solutions would be similar. In Table 17, the average of each solutions set of five *Petrifilm*^{TM} plate counts are shown along with the SD across these and the cfu ml^{-1} counts ± 1 SD. The ± 1 SD counts do not overlap but are very close to each other, this indicates that the counts do not differ significantly meaning that the presence of MPI does not have a negative effect on the *Bacillus mycoides* spores. In addition to this linear least squares regression analysis was carried out on the counts after they had been converted to $\log_{10}$ cfu ml^{-1} as shown in Figure 42. The correlation coefficient found was $R^2 = 0.9154$, as this value is close to 1 this also indicates that the counts do not differ considerably and that MPI does not have a negative effect on the spores.

Table 17. Spore count data for two sets of *Petrifilm*^{TM} plates one inoculated with an aqueous solution and the other a 20 wt% MPI solution both contained *Bacillus mycoides* spores at a dilution of x10^9.

Solution	Average (cfu ml^{-1})	SD (cfu ml^{-1})	+ 1 SD (cfu ml^{-1})	- 1 SD (cfu ml^{-1})
x 10^9 water	4.8 x 10^{11}	3.9 x 10^{10}	5.2 x 10^{11}	4.3 x 10^{11}
x 10^9 20 wt% MPI	4.1 x 10^{11}	1.9 x 10^{10}	4.4 x 10^{11}	4.0 x 10^{11}

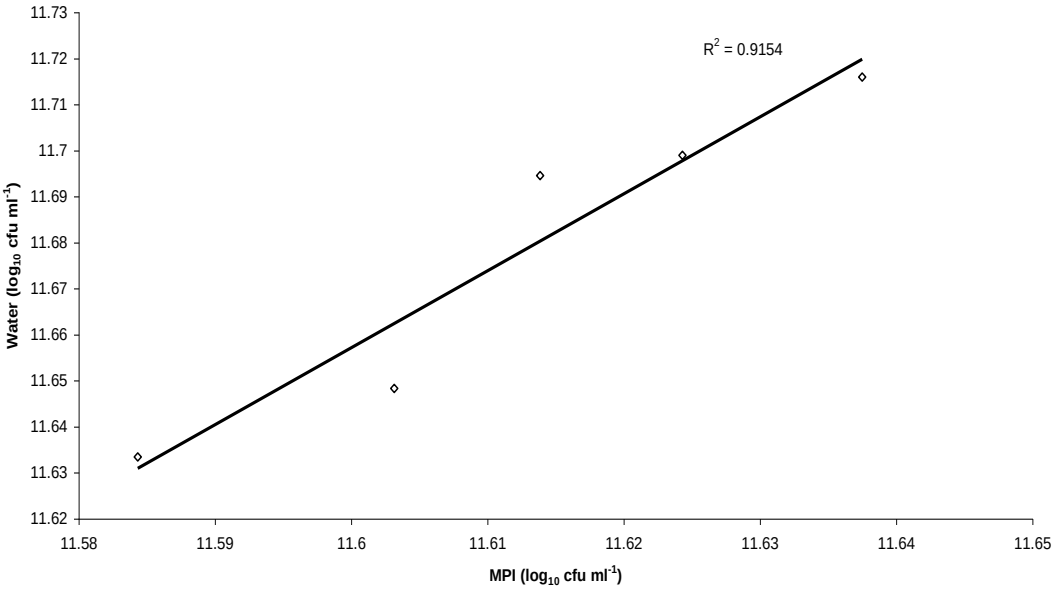

Figure 42. Comparison of the enumeration of Bacillus mycoides *spores using* Petrifilm^{TM} *Aerobic Count Plate (ACP) counts when the bacteria are in either water or MPI at a dilution of x10^9.*

3.2.4 Comparison of *Petrifilm*^{TM} ACP counts of *Bacillus mycoides* spores with time when stored in water and MPI

To investigate the effect of leaving *Bacillus mycoides* spores over a period of time when suspended in both water and MPI solutions two sets of solutions were prepared. One of sterile water and a 20 wt% MPI solution both of which contained spores of *Bacillus mycoides* at a dilution of x10^8. In contrast to the experiment carried out in section 3.2.3, the aqueous and MPI solutions were prepared by taking separate 1 ml spore samples from the sporulation media. This meant that their bacterial counts could have differed quite significantly from each other, as a result the water and MPI solutions could not be compared to each other within this experiment only between themselves with time.

Every day for four days each solution was used to inoculate five *Petrifilm*^{TM} ACP's, each plate was incubated for 24 hours at 32 °C and the average count for each set of five plates was calculated. Between plating both solutions were kept at 4 ºC inside a cold room. The change in plate counts observed for both solutions over the four days can be

seen within Figure 43. Both solutions plate counts varied between days over the entire duration of the experiment. As both solutions behaved in a similar fashion this provides further evidence suggesting that the presence of MPI does not have a negative effect on the spores even with time. It also shows that spores can be kept inside either MPI or water for at least four days. The variation in counts can be attributed to both errors within the plate counts themselves and the fact that spore numbers can often vary significantly between samples.

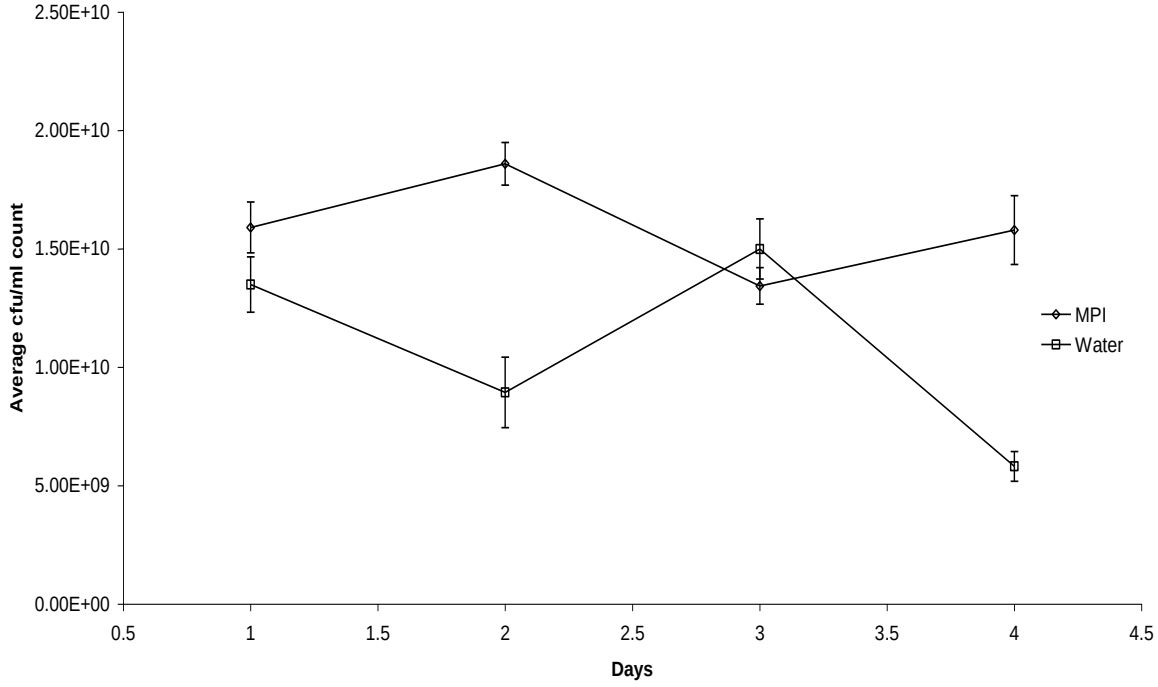

Figure 43. Comparison of Petrifilm ™ *Aerobic Count Plate (ACP) counts of* Bacillus mycoides *spores when the bacteria are in either water or a MPI solution at a dilution of x10^{8} over a period of 4 days when stored in a cold room (< 5 °C).*

After this spore stability experiment was conducted the sample of spores suspended in sterile water was left at 4 ºC over a period of three months. During this time the spore structure and numbers were monitored every two weeks. A light microscope was used to check spore structure and the sample was enumerated using *Petrifilm*™ ACP's. Both spore structure and numbers appeared unchanged over the three month period meaning that once spores have been harvested from the sporulation media they could be kept for at least three months before being used for experimentation.

3.2.5 Comparison of bacterial counts produced using 'old' and 'new' *Petrifilm*™ ACP's

It is recommended that *Petrifilm*™ ACP's be used within one month of their packet being opened. In order to see whether inoculating these plates after this time makes a

significant difference to the counts produced, two sets of plate counts were compared. One set from a newly opened packet termed 'new' and the other from a packet that was first opened two months previous termed 'old'. Both sets of plates were made up of five *Petrifilm*™ ACP's and each plate was inoculated with the same aqueous solution that contained *Bacillus mycoides* spores at a dilution of $x10^{11}$. Each plate was incubated for 24 hours at 32 °C before being counted.

Detailed in Table 18 are the average counts produced using both sets of *Petrifilm*™ plates along with the SD across these and the cfu ml^{-1} counts ± 1 SD. As the ± 1 SD counts overlap, this indicates that the counts do not differ significantly and that using these plates one month over the manufacturers one month guideline for usage once opened does not have a significant effect on the count produced. This meant that it was not necessary to adhere to this guideline too strictly and that plates could be used up to two months after the packet had been opened. In addition linear least squares regression analysis was carried out on the counts after they had been converted to $\log_{10}$ cfu ml^{-1}, as shown within Figure 44. The correlation coefficient was found to be $R^2 = 0.8312$, this also indicates that the two sets of plate counts do not differ significantly.

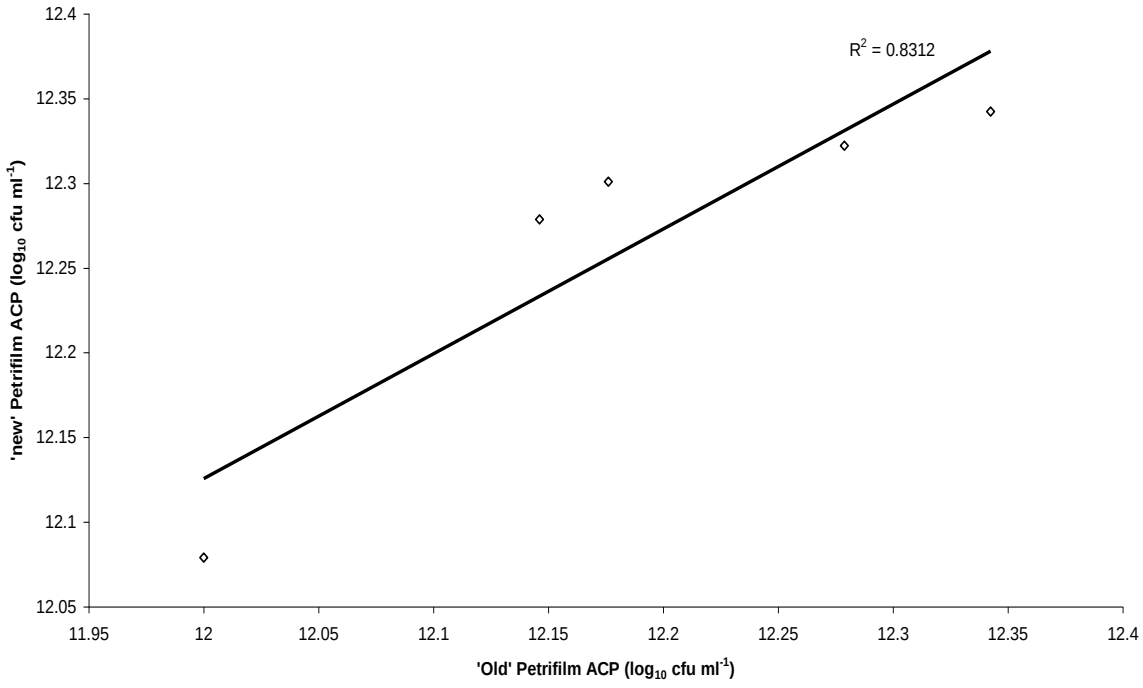

Figure 44. Comparison of Petrifilm™ *Aerobic Count Plate (ACP) counts using plates taken either from a newly opened packet 'new' or from a packet that has been open for two months 'old', a month over the manufacturers stipulated use period*

Table 18. Spore count data for two sets of *Petrifilm*™ plates 'new' set taken from a freshly opened packet, 'old' set taken from a packet that had been open for two months. Both were inoculated with *Bacillus mycoides* spores at a dilution of $x10^{11}$.

Plates	Average (cfu ml^{-1})	SD (cfu ml^{-1})	+ 1 SD (cfu ml^{-1})	- 1 SD (cfu ml^{-1})
'Old' *Petrifilm*™ ACP	1.6×10^{12}	4.6×10^{11}	2.1×10^{12}	1.1×10^{12}
'New' *Petrifilm*™ ACP	1.9×10^{12}	4.0×10^{11}	2.3×10^{12}	1.5×10^{12}

3.3 INCUBATOR VALIDATION

It has been found during this project and previously by Ellender *et al.*, (1993) that counts obtained from *Petrifilm*™ ACP's are largely temperature dependent. This meant it was necessary to ensure that the temperature within the whole of the incubator being used within this project was constant. This was achieved by inoculating six *Petrifilm*™ plates with an aqueous solution containing spores of *Bacillus mycoides* at a dilution of $x10^{8}$, and placing them inside the incubator so that they were evenly distributed, these were then left for 24 hours at 32 °C. The colony counts from these plates indicated that the temperature over the whole of the incubator was constant as the standard deviation over the plates was ± 1.53 actual count or ± 3.1×10^{10} cfu ml^{-1}, which is below the error range found in section 3.2.2.

3.4 VISCOSITY AND SHEAR STRESS MEASUREMENTS OF MPI

Understanding the relationships between MPI viscosity with changing temperature and concentration is critical when filtering high solids content dairy feeds. All viscosity and shear stress values stated within this thesis are the average of triplicate measurements with each experiment carried out using a new sample. The error bars are ± one standard deviation.

3.4.1 Concentration

The change in viscosity of MPI with concentration at ambient temperature (18 ºC) was found using both a single shear rate of 6.45 s^{-1} for MPI concentrations between 1 - 30 wt% and over a range of shear rates between 1 - 20 s^{-1} for MPI concentrations of 10 - 25 wt%, as shown in Figures 45 and 46 respectively. It was found that as the concentration of MPI was increased the viscosity of the solution increased. Any increase in concentration over 15 wt% was found to cause a large increase in viscosity. This is

highlighted with the log scale that has been used on the y-axis of both graphs. For example when comparing a 15 wt% solution with that of a 20 wt% solution at 6.45 s^{-1} (Figure 45) the viscosity increases from ~200 to ~1600 cP and again between a 20 wt% and a 25 wt% solution from ~1600 to ~7100 cP. This large increase in viscosity is the reason why MPI solutions of up to only 15 wt% were used within the filtration rig for experimentation. This meant resolubilising MPI solutions between 6.1 – 22.5 wt% to produce feeds of 5 - 15 wt% within the system to take into consideration the dead volume of the filtration system as shown within Table 12.

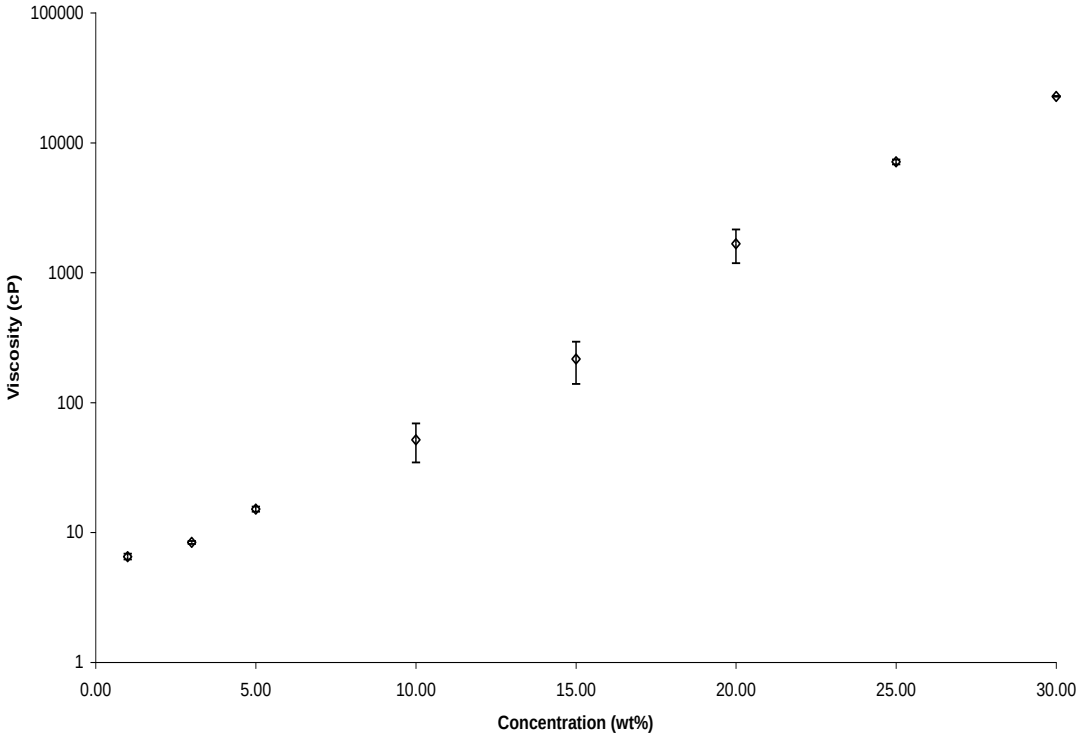

Figure 45. Change in MPI viscosity with concentration of MPI solutions between 1 - 30 wt% using single shear rate of 6.45 s^{-1} at ambient temperature (18 ºC).

Van Wazer *et al.*, (1963) studied the sensitivity of the eye in judging the viscosity of Newtonian liquids and found it was difficult to distinguish between fluids in the range of 0.1 - 10 cP. But found that small differences in viscosity could be clearly seen between samples of approximately 100 - 10,000 cP. But above 100,000 cP it was difficult to make visual distinctions as these materials do not pour and appear as solids unless closely inspected. This was seen with MPI solutions of 15 – 25 wt% that are within the 100 to 10,000 cP range as they can be easily identified from one another. 15 wt% MPI solutions are water-like free flowing solutions, 20 wt% solutions are still able to be poured but with less ease and 25 wt% are more gel-like only able to be slowly poured when heated.

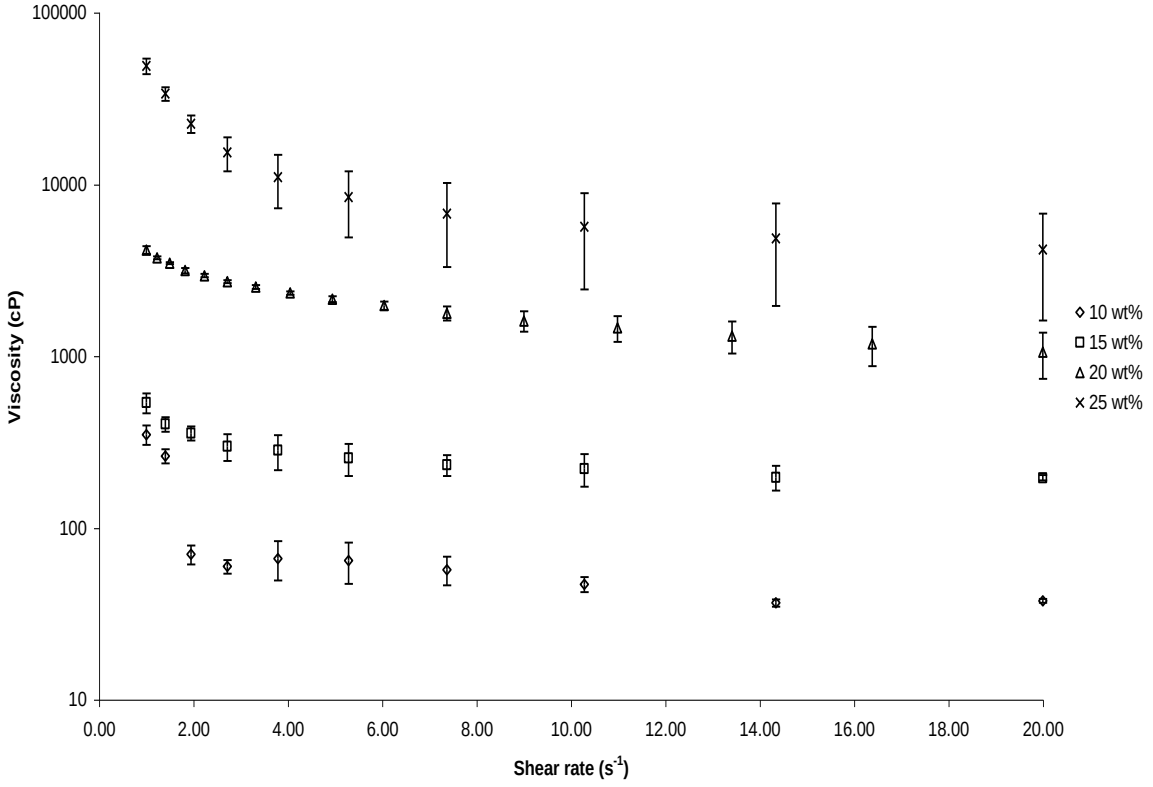

Figure 46. Change in MPI viscosity with concentration of MPI solutions between 10 - 25 wt% over a range of shear rates between 1 - 20 s^{-1} at ambient temperature (18 ºC).

The viscosity against shear rate plots in Figure 46 show that MPI solutions are non-Newtonian materials, as on shearing they do not show a linear viscosity against shear rate relationship but are instead shear thinning materials as with increasing shear their viscosity decreases. The shear stress against shear rate plots shown in Figure 47 were produced using the same MPI solutions as were used to construct the plot in Figure 46.

A shear stress against shear rate plot produced by an ideal shear thinning fluid would contain three distinct regions as shown in Figure 48. The first region is termed the 'lower Newtonian region' where the apparent viscosity is constant with changing shear, region 2 is called the 'middle Newtonian region' where viscosity decreases with increasing shear and lastly region 3 is called the 'upper Newtonian region' where the slope of the curve is constant with changing shear. These different regions are displayed by the MPI shear stress against shear rate plots shown in Figure 47.

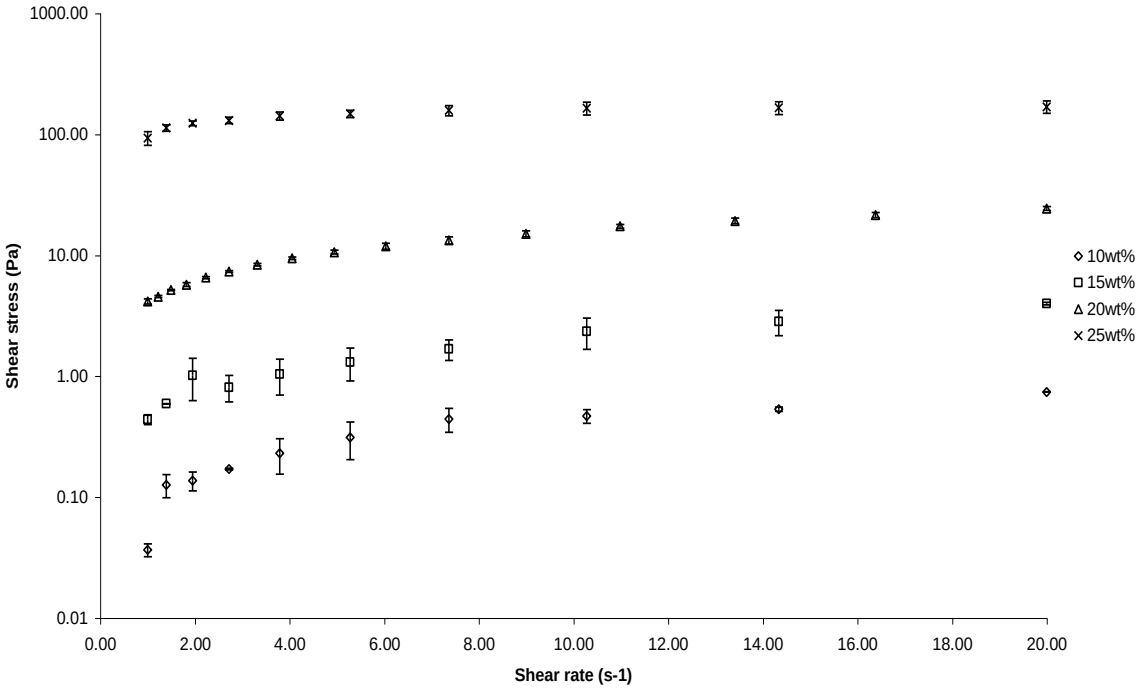

Figure 47. Shear stress against shear rate plots for MPI solutions of concentrations 10 – 25 wt% at ambient temperature (18 ºC).

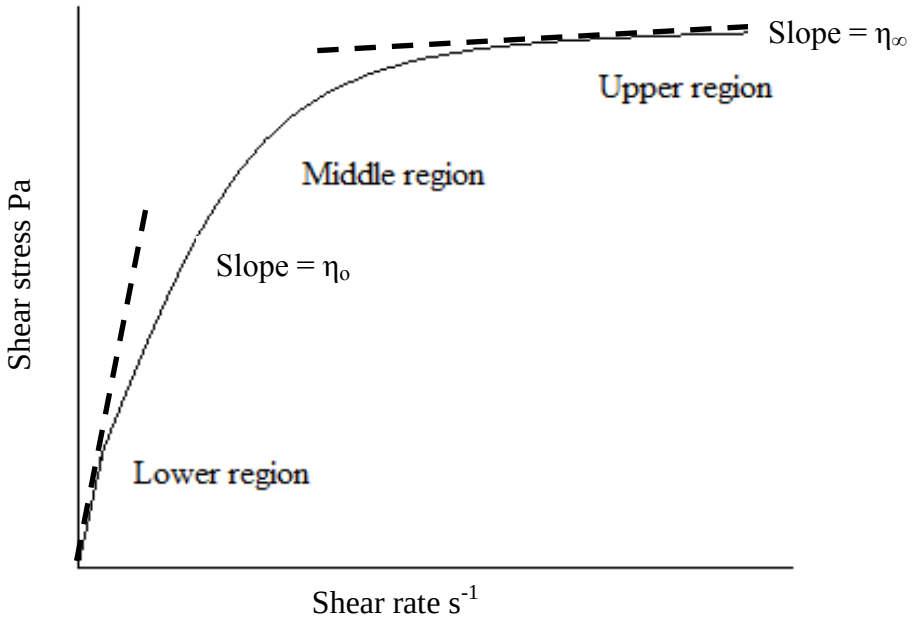

Figure 48. A shear stress against shear rate plot produced by an ideal shear thinning fluid (Taken from Steffe, 1996).

3.4.2 Temperature

Initially it was intended that MPI solutions of up to 25 wt% would be inoculated and filtered, but due to the very high viscosity found at 18 °C (ambient temperature) for 20 and 25 wt% (shown previously in Figures 45 and 46) and because of resolubilisation problems with the MPI, solutions of up to only 15 wt% (in system) were actually used

requiring MPI of up to only 22.5 wt% (rig set-up 3) to be resolubilised compared to 35.5 wt% in order for 25 wt% to be in the system (rig set-up 3) as shown previously in Table 12.

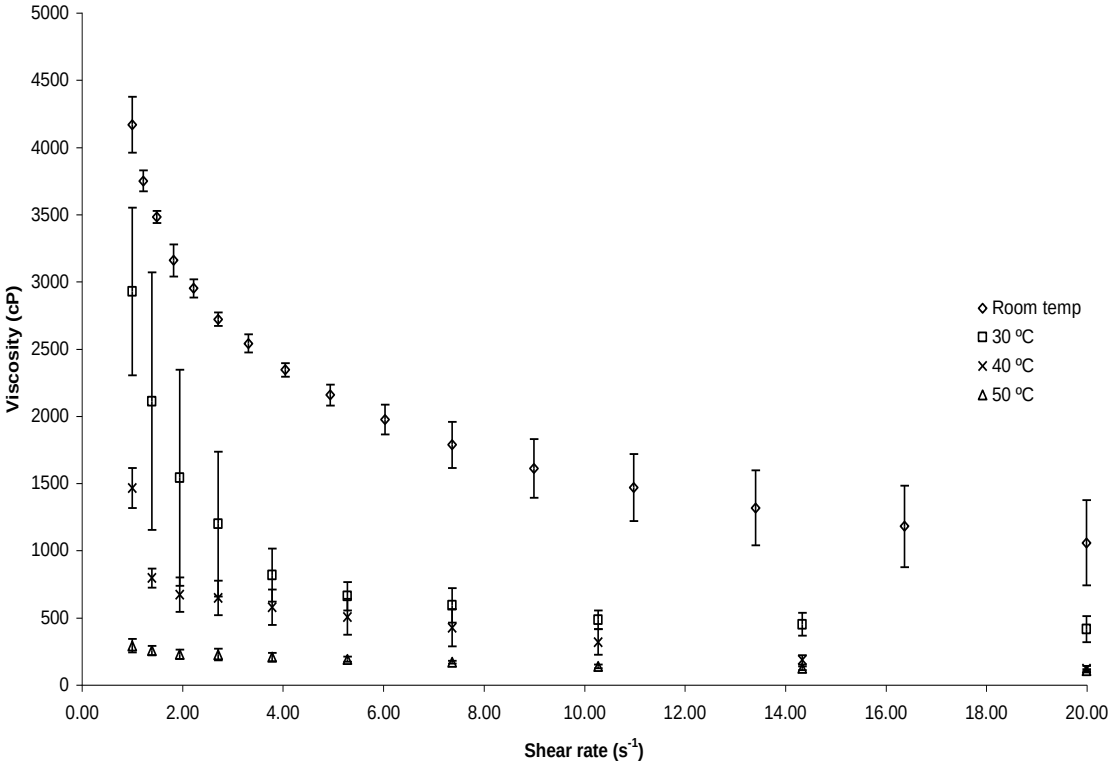

Figure 49. Change in viscosity of a 20 wt% solution (calculated with respect to the amount of powder present) with temperature, from 18 °C (ambient temperature) up to 50°C, over a range of shear rates from 1 - 20 s^{-1}.

The change in viscosity with temperature has been found for MPI solutions of 20 wt%. Two types of experiment were carried out, which differed in how the wt% was calculated. MPI wt% was calculated with respect to both the amount of powder in the solution and the amount of protein with the change in viscosity with shear rate at 18 °C (ambient temperature), 30 °C and 40 °C for these solutions shown in Figures 49 and 50 respectively, the change in viscosity is also shown at 50 °C for the powder calculated solution. This was done as it was initially thought that calculating concentration with respective to the amount of protein present as opposed to the amount of powder would be a good way of displaying collected data. But as can be seen in Figures 49 and 50 the viscosities found for the 20 wt% solution calculated with respect to the amount of protein are much larger than those found for the solution calculated with respect to powder. This again shows the large increase that occurs between 20 and 25 wt% solutions and as a result meant that wt% was calculated with respect to the amount of powder present throughout the rest of the project.

The change in MPI viscosity with temperature was found for MPI solution concentrations between 5 – 20 wt% and for all was found to be highly temperature dependent, with viscosity significantly decreasing with each incremental increase in temperature. The viscosity of a 15 and 20 wt% MPI solution was measured over a range of temperatures as shown in Figures 51 and 49 respectively over a range of shear rates between 1 - 20 s^{-1}. At 20 s^{-1} viscosities were found to decrease by 61% (20 wt%) and 79% (15 wt%) when temperature was increased from ambient to 30 ºC, by a further 28% (20 wt%) when increased to 40 ºC and by another 2% (20 wt%) and 11.7% (15 wt%) when increased to 50 ºC. As a result as stated in section 2.10.3 a temperature of 50 ºC was selected for MPI filtration experiments as this is below the 71.7 ºC used during pasteurisation making microfiltration more favourable in terms of energy requirements and product quality. This is because as stated previously if a lower temperature is used there is less chance of protein denaturation occurring that will decrease the nutritional benefits and taste of the product. But as shown in these experiments 50 ºC is a temperature high enough to decrease the viscosity of high solids content MPI solutions into a region able to be filtered.

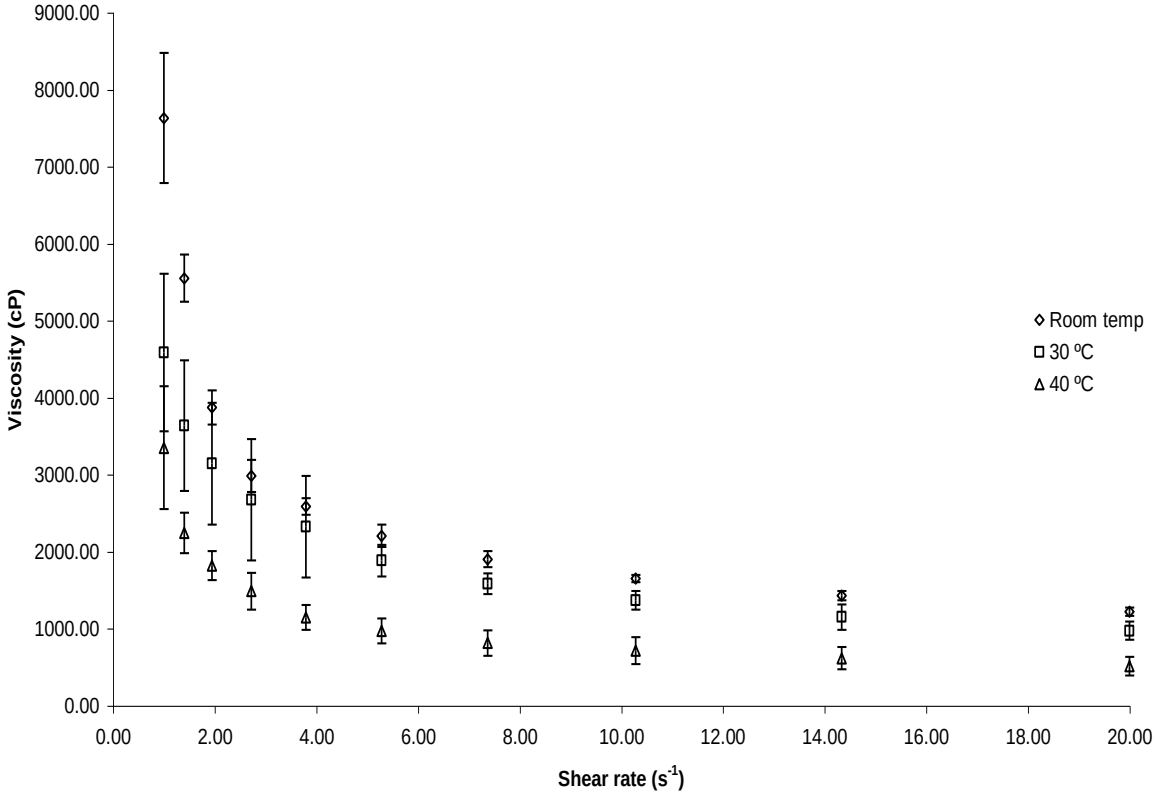

Figure 50. Change in viscosity of a 20 wt% solution (calculated with respect to the amount of protein present) with temperature, from 18 °C (ambient temperature) up to 40°C, over a range of shear rates from 1 - 20 s^{-1}.

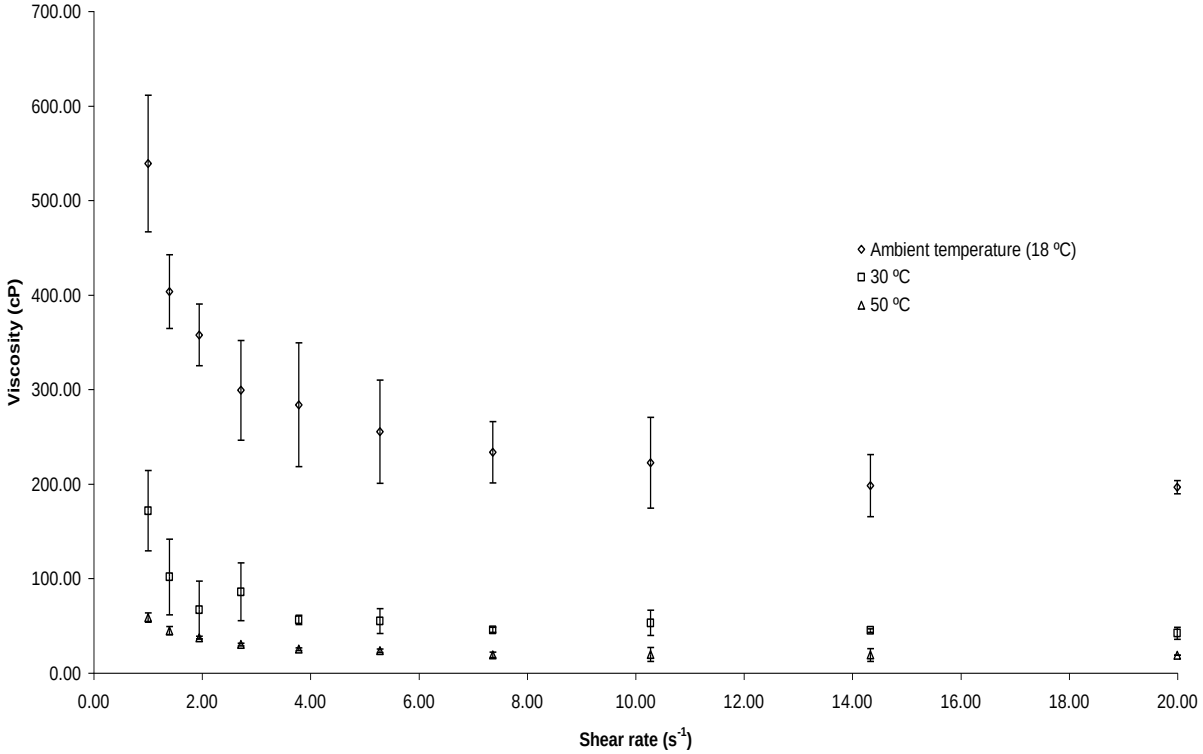

Figure 51. Change in viscosity with temperature of a 15 wt% MPI solution (calculated with respect to the amount of powder present) between ambient (18 °C) - 50 °C, over a range of shear rates from 1 – 20 s^{-1}.

Figure 52 shows the change in viscosity with MPI concentration between 5 – 20 wt% at 50 ºC over a range of shear rates between 1 – 20 s^{-1}. The shear rate applied to the MPI feed streams during filtration within the rig was not able to be calculated but would be above 20 s^{-1}. As the viscosity appears to plateau with increasing shear up to 20 s^{-1} the assumption was made that the viscosity of MPI measured at 20 s^{-1} would be the same as that of the MPI within the rig during a filtration experiment. As a result the viscosity at 20 s^{-1} was used during calculations, the equation of the plot shown in Figure 53 was used to establish the viscosity of collected permeate stream samples needed to calculate total and fouling resistances.

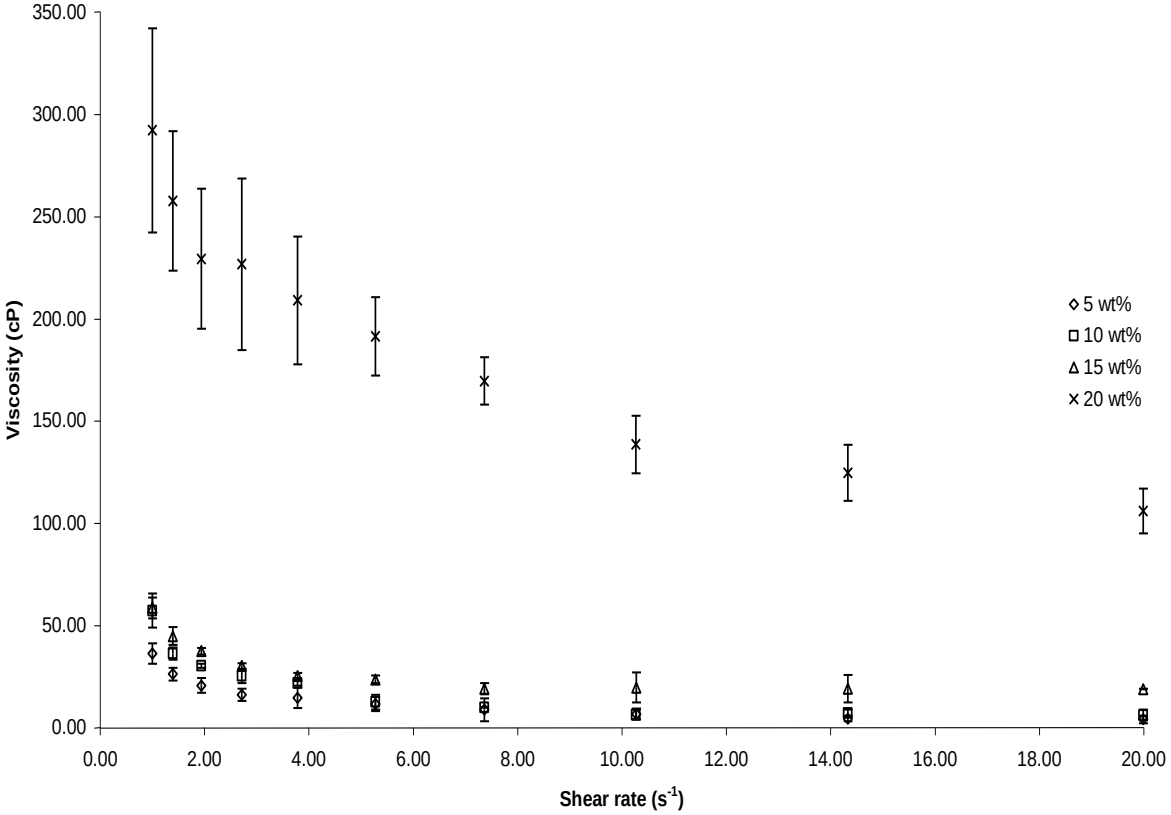

Figure 52. Change in viscosity with increasing MPI concentration, solutions of 5, 10, 15 and 20 wt% (calculated with respect to the amount of powder present) were tested at 50°C over a range of shear rates from 1 –20 s^{-1}.

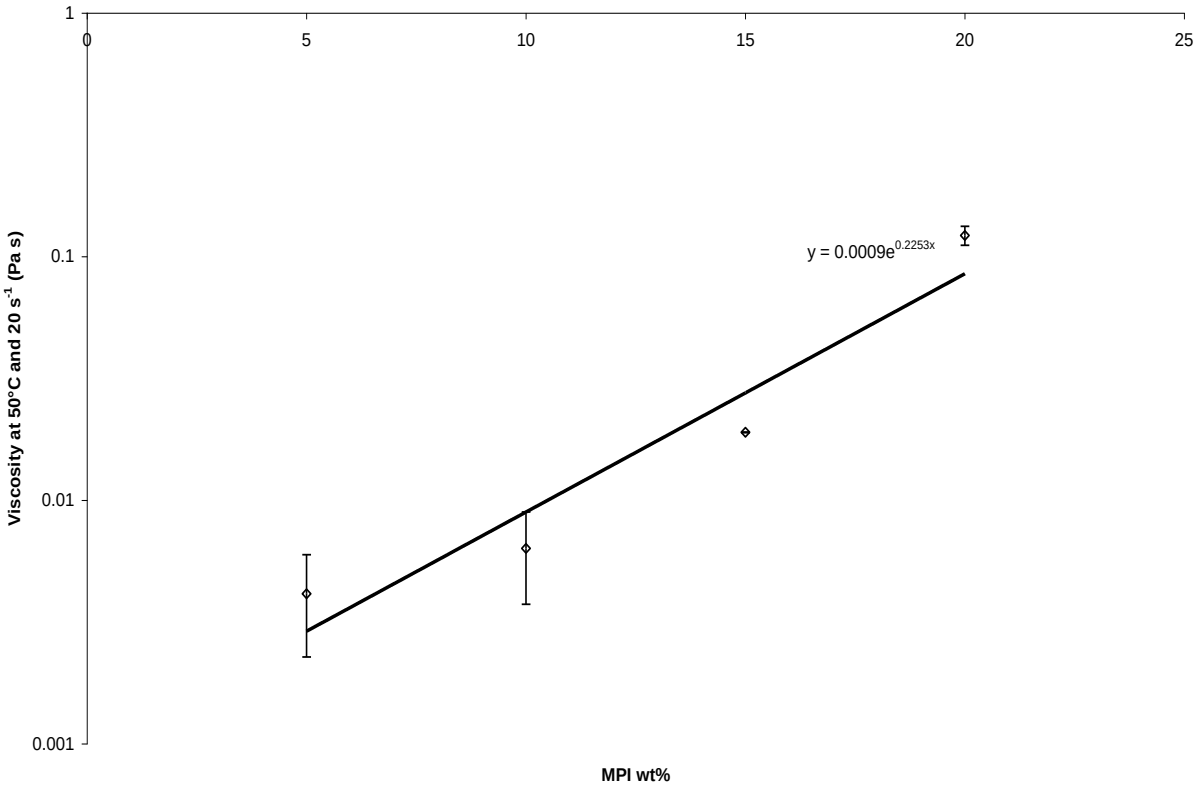

Figure 53. Plot showing the change in viscosity with increasing MPI concentration at 50 °C and 20 s^{-1} used to calculate the viscosity of permeate solutions.

3.4.3 Time

The change in viscosity of MPI solutions with time was found by comparing the viscosity of a solution tested within an hour of being prepared and after it had been left to stand at ambient temperature for 20 hours. The viscosity against shear rate plots found at ambient temperature for a 20 wt% MPI calculated by both the amount of powder and protein they contain, within an hour of being prepared and after 20 hours of standing can be found within Figures 55 and 56 respectively.

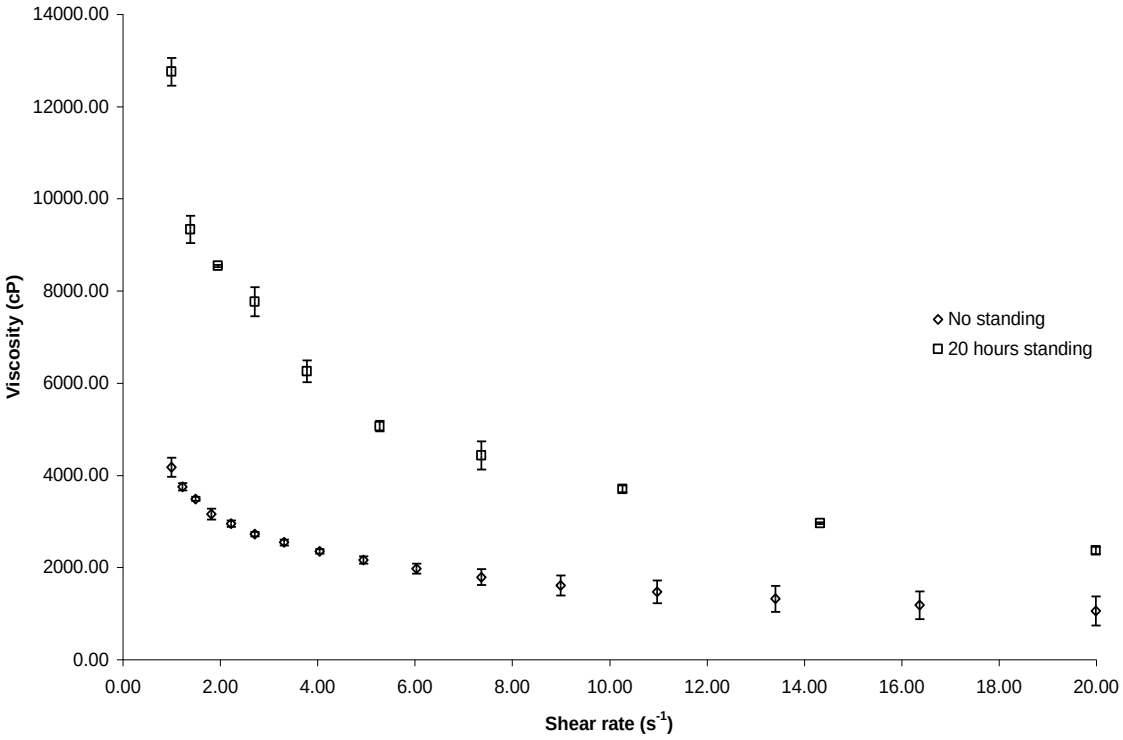

Figure 54. Change in viscosity of a 20 wt% solution (calculated with respect to the amount of powder present) with time, by comparing a solution within an hour of being prepared and after being left to stand for 20 hours at ambient temperature (18 °C). Both tested at ambient temperature, over a range of shear rates between 1 – 20 s^{-1}.

As can be seen a large increase in viscosity was found for both 20 wt% solutions after being left to stand. This standing caused an irreversible change in the structure of the MPI occurs as even when the standing solution was heated to both 30 and 40 °C the viscosity was found to be higher than that measured for the solution before standing. This is shown by comparing Figures 49 and 56 as before being left to stand the maximum viscosity at 30 °C was 2928 cP but after standing the viscosity went up to 9671 cP. The same pattern was observed at 40 °C with the maximum viscosity found before standing 482 cP and after standing 3782 cP. As a result it was decided that resolubilised MPI solutions had to be used for experimentation within an hour of being prepared as otherwise the solution would become too viscous and unusable.

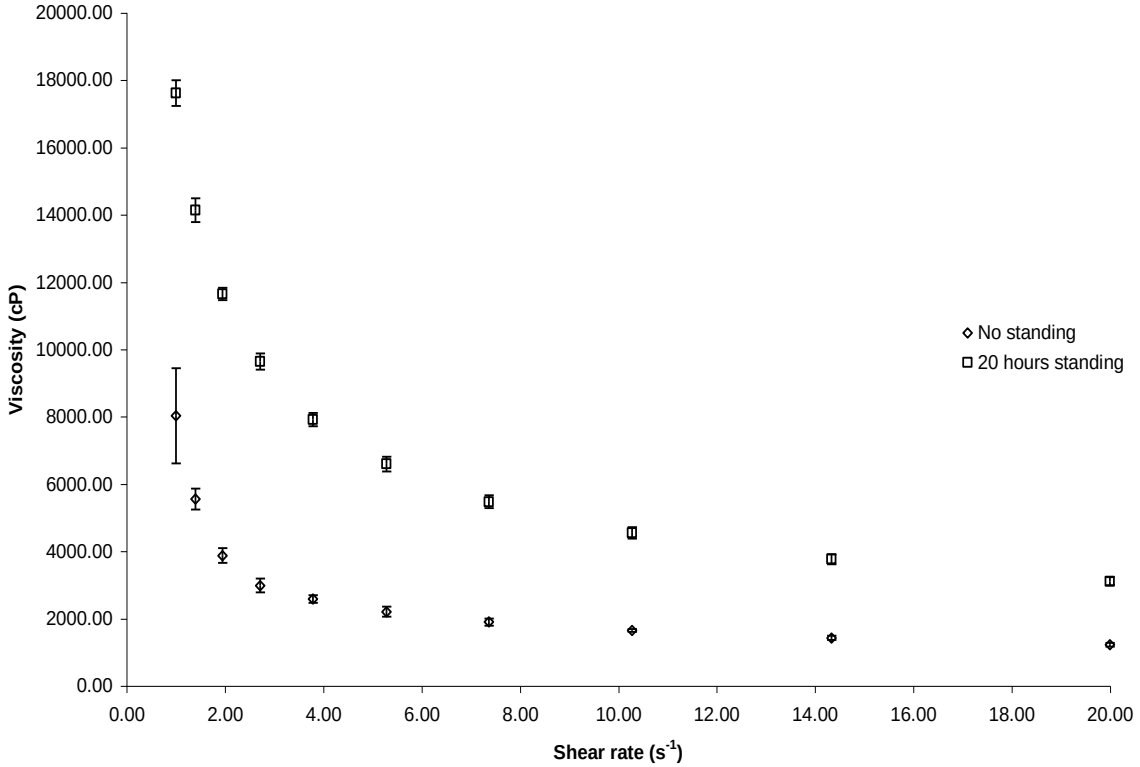

Figure 55. Change in viscosity of a 20 wt% solution (calculated with respect to the amount of protein present) with time, by comparing a solution within an hour of being prepared and after being left to stand for 20 hours at ambient temperature. Both tested at ambient temperature (18 °C), over a range of shear rates between 1 – 20 s^{-1}.

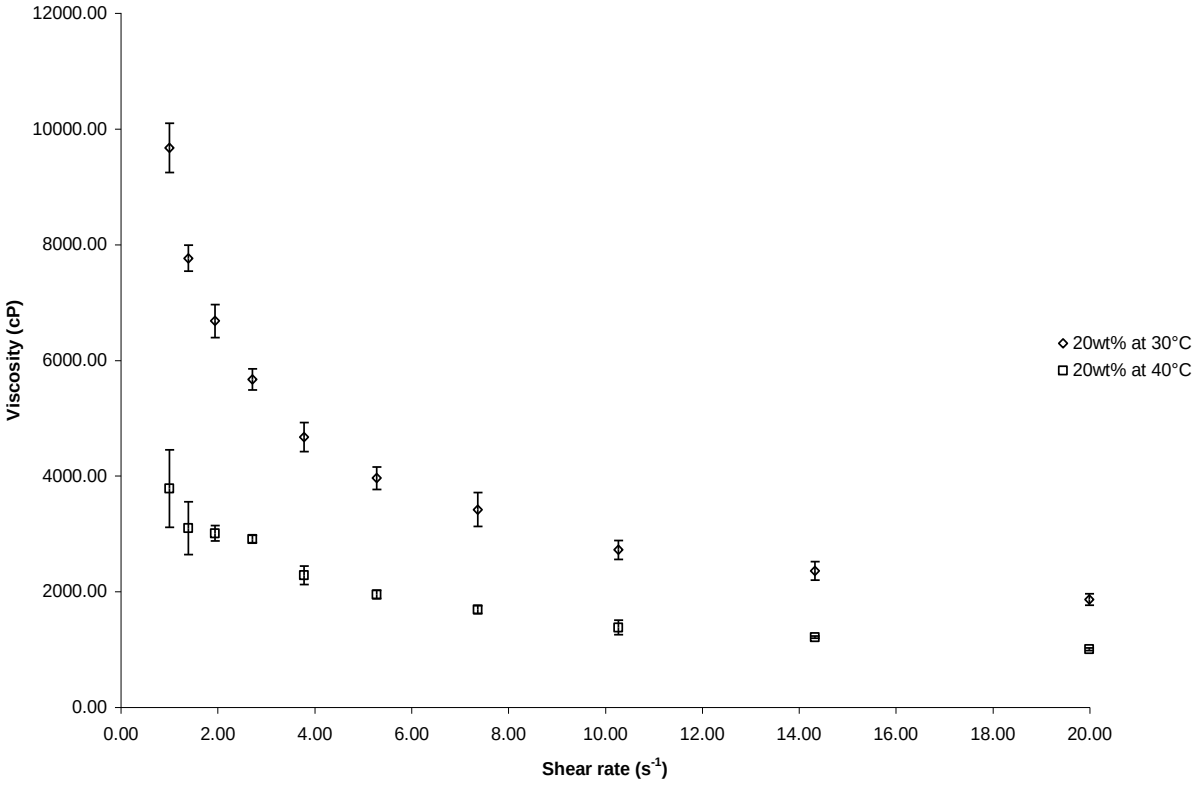

Figure 56. Change in viscosity of a 20 wt% solution (calculated with respect to powder present) left to stand at ambient temperature for 20 hours at 30 and 40 °C over a range of shear rates between 1 – 20 s^{-1}.

4 FILTRATION RESULTS

4.1 EFFICIENCY OF SELECTED SODIUM HYDROXIDE CLEANING AND SODIUM HYPOCHLORITE DISINFECTION PROTOCOLS AT SPORE REMOVAL

In order to test the efficiency of the selected cleaning and disinfection protocols used during a filtration experiment (as described in section 2.10) at removing *Bacillus mycoides* spores along with any unwanted contaminating bacteria from the system, the cleaning and disinfection protocols were carried out on static inoculated solutions of RO water and 5, 10 and 15 wt% milk protein isolate (MPI) inside beakers outside the rig. In order to recreate the cleaning and disinfection that occurs within the rig during this experiment the same concentrations of sodium hydroxide (NaOH) and sodium hypochlorite (NaOCl) were used 0.5 wt% and 200 ppm, the same temperatures 50 ºC and ambient and the same times 10 and 15 minutes as that used during a run were applied to the solutions but were scaled down to replicate a run as closely as possible. A sample was taken from each of the four solutions once they had been inoculated with spores, after being treated with NaOH and after NaOCl disinfection. Each of these solutions was then plated in triplicate onto *Petrifilm*^{TM} plates using the protocol described in section 2.3.2. The initial spore count of each solution, along with the log reduction and % reduction (cell ml^{-1}) found after each treatment along with the respective plate standard deviation (%) can be found within Table 19.

Table 19. Showing initial spore counts along with log reductions, % cell ml^{-1} reductions and SD (%) of RO water, 5, 10 and 15 wt% MPI solutions after being treated with NaOH and NaOCl as they would be during a filtration experiment.

Feed	Initial spore count (log cfu ml^{-1})	After NaOH treatment			After NaOCl treatment		
		Log reduction	% reduction (cells ml^{-1})	SD (%)	Log reduction	% reduction (cells ml^{-1})	SD (%)
Water	4.8	0.8	84.6	6.6	2.0	98.9	0.5
5 wt% MPI	5.8	1.1	91.9	5.4	1.7	98.2	0.05
10 wt% MPI	6.0	1.0	89.0	5.5	1.9	98.8	0.5
15 wt% MPI	6.3	0.9	87.6	6.7	2.3	99.5	0.2

The spore reductions found provide evidence that the combined NaOH and cleaning disinfection procedures used before and after fouling runs involving inoculated feeds

were effective at spore removal with total reductions found between 98 - 99.9%. As a result this protocol was considered suitable for use when filtering both inoculated RO water and 5 – 15 wt% MPI feeds. This shows that a suitable sterilisation procedure was developed in order to ensure that the filtration system was always sterile before inoculated feeds were added and that the system was returned to a sterile state after filtration runs were complete. As expected the spore reduction after NaOH treatment decreased with increasing MPI wt% as interfering organics lead to higher concentrations of chemicals being required to achieve the same effect. But this decrease in spore reduction was only slight and all solutions spore reduction after NaOH treatment was within the standard deviation of the solutions plates. The RO water solution average spore count reduction after NaOH treatment was low compared to that of the three MPI solutions but was not significantly different when considering the standard deviation.

4.2 DSS LABUNIT M10 RIG

Initial MPI filtration and *Bacillus mycoides* spore rejection experiments were carried out using a Danish separation systems (DSS) LabUnit M10 unit. This was found to produce insufficient fluxes when filtering MPI solutions of 3.5 wt% producing fluxes as low as < 30 litres m^{-2} hr^{-1} (LMH), as shown in Figure 57. As a result of the CFV's able to be produced by the positive displacement pump being too low (pump capable of generating 0.24 m^3 h^{-1}), the membrane filtration area provided by the module being relatively small 336 cm^2 and the fact that only flat sheet membranes could be used in the system meaning that hydraulic cleaning methods i.e. backwashing cannot be used. It was concluded that a new filtration system able to provide a more powerful pump, a larger membrane surface area and be able to be used with ceramic membranes was required.

In addition to initial MPI filtration experiments, initial spore rejection experiments were carried out using the M10 to try and determine whether or not the separation was possible. This involved filtering RO water inoculated with spores of *Bacillus mycoides* at ambient temperature (20 °C), a TMP of 0.5 bar and a CFV of 0.8 m s^{-1} for 30 minutes. The changes in permeate flux with time through both a 0.5 and 1.5 µm polysulfone membrane are shown in Figure 58. As can be seen the permeate flux remained relatively constant with time when using a 0.5 µm membrane but decreased through the 1.5 µm membrane. This decrease in flux can be explained when considering the size of the spores, (measured in section 3.1.1 using SEM images to be 1.53 ± 0.18

µm in length and 0.90 ± 0.11 µm in width) as they are a similar size to that of the membrane pores they may be fouling the membrane through pore blocking. The flux through the 0.5 µm membrane remains constant as the spores take up very little volume within the feed, so if they don't block the pores it is unlikely that a decrease in flux would occur. Spore counts of samples taken from both the permeate and feed streams after 15 and 30 minutes of filtration were measured using a counting chamber. The spore counts weren't considered to be accurate but provided evidence to imply that the separation was physically possible.

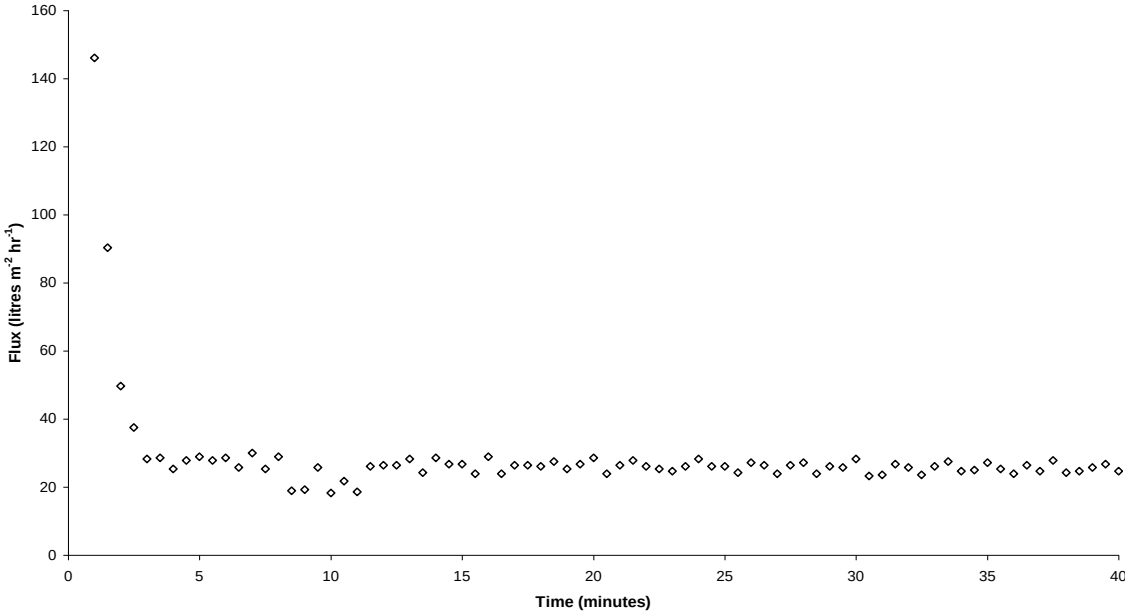

Figure 57. Change in permeate flux with time when filtering a 3.5 wt% MPI solution through a 0.5 µm flat sheet PS membrane at 25 °C, 1 bar and 0.6 m s^{-1}.

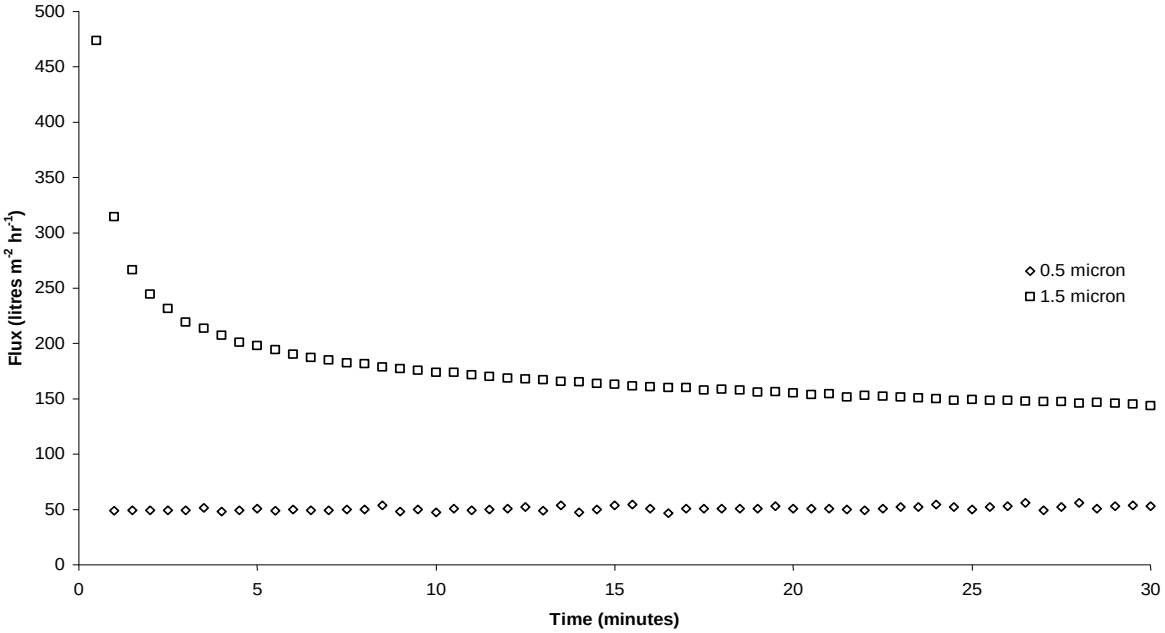

Figure 58. Change in permeate flux with time when filtering RO water inoculated with spores of Bacillus mycoides *through a 0.5 and 1.5µm flat sheet PS membrane at 20 °C, 0.5 bar and 0.8 m s^{-1}.*

4.3 VIRGIN MEMBRANES PURE WATER FLUX (PWF) MEASUREMENTS

Pure water flux (PWF) measurements were determined for each tubular ceramic *Membralox*™ microfiltration membrane prior to initial fouling. This was in addition to before and after fouling and after rinsing and cleaning during each filtration cycle. The change in the virgin PWF values obtained for the 0.8, 1.4, 2.0, 5.0 and 12.0 µm *Membralox*™ membranes with varying TMP can be seen in Figure 59. As expected from equation 33 these are linear plots that have an intercept that passes through the origin. Only one PWF value was recorded at a low TMP of 0.002 bar for the 12.0 µm membrane, as the flux was so high 682.4 LMH. This meant it was not possible to measure the PWF at higher TMP's. Membrane resistances (R_M) were calculated from these plots using equation 32 for the single PWF (J_v) measured for the 12.0 µm membrane and using the gradient of the other membranes plots and equation 34. These were calculated to be 9.97 x 10^{11}, 4.99 x 10^{11}, 1.66 x 10^{10}, 1.42 x 10^{10} and 1.48 x 10^{9} m^{-1} for the 0.8, 1.4, 2.0, 5.0 and 12.0 µm membranes respectively.

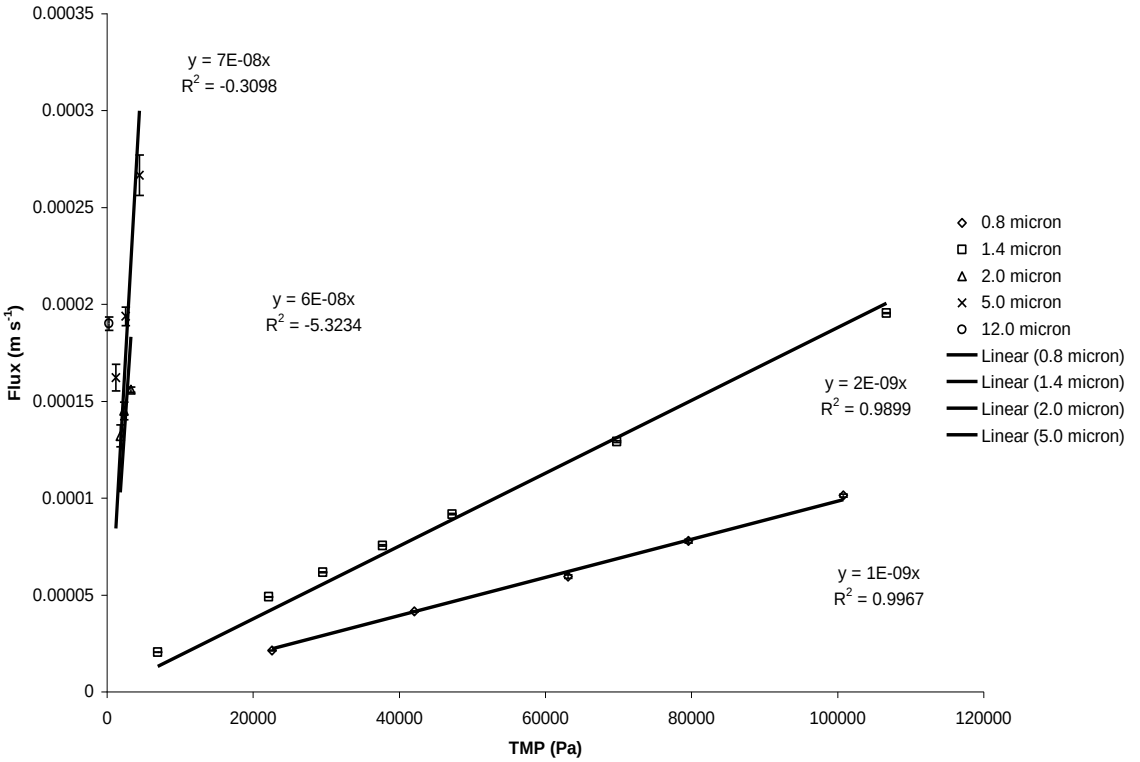

Figure 59. Change in pure water flux of virgin ceramic Membralox™ *membranes of 0.8, 1.4, 2.0, 5.0 and 12.0 µm pore diameter with increasing TMP.*

4.4 OSMOTIC PRESSURE EFFECTS

As explained in section 1.16, generally during microfiltration experiments the effect of osmotic pressure on flux is ignored as it is assumed that the osmotic pressure for macromolecules is negligible compared to the applied hydraulic pressure $\Delta P - \pi_M \approx \Delta P$.

During RO and NF this effect is more pronounced as the molecules being filtered are much smaller. It was initially thought that osmotic pressure might have an effect on filtration during this work, as the feed concentrations being used were so high. Using equation 35 the osmotic pressure difference between typical experimental feed and permeate streams during filtration through a 1.4 µm membrane has been calculated to be 2.77×10^{-5} bar. As this osmotic pressure difference is so small in comparison to even the lowest TMP of 0.5 bar used during experimentation it was considered to have a negligible effect during this work. The full calculation can be found in Appendix 7.

4.5 FILTRATION EXPERIMENTS USING FILTRATION SET UP 1

4.5.1 Difference in spore rejection values with membrane pore size and type of inoculated feed.

Initial spore rejection experiments were carried out using set-up 1 of the newly constructed filtration system. Spore counts (using *Petrifilm*™ Aerobic Count Plate's described within section 2.3) were recorded for feed and permeate samples taken after 5 and 40 minutes during the filtration of an inoculated 5 wt% MPI solution at 50 °C, 0.7 m s^{-1} and 0.3 bar, through both the 0.8 and 1.4 µm *Membralox*™ tubular ceramic membranes. A low concentration of MPI was initially tested to establish the principle of spore and MPI separation. The results produced demonstrated that the separation was possible. Spore counts were also recorded during the filtration of inoculated RO water after 5 and 20 minutes of filtration through the 1.4 µm ceramic membrane. Thus the effect of spores on the membrane has been analysed separately from the effect of the MPI feed. Table 20 shows the spore counts measured for all feed and permeate samples taken and the spore reduction achieved by both membranes.

These results show that both the membrane pore size and the feed type employed have an effect upon membrane spore retention. When inoculated RO water was run through the 1.4 µm membrane, the spore retention remained constant throughout the filtration with a reduction of 3.4 log orders measured. When inoculated 5 wt% MPI was filtered through the 1.4 µm membrane under the same conditions a slightly higher spore reduction of 3.6 log orders was found. However, when the 0.8 µm pore size was employed much larger spore reduction values were found when filtering 5 wt% MPI of 7.3 log orders after 5 minutes and 6.4 log orders after 40 minutes. This was expected,

due to the size of the spores, which have been measured using SEM pictures (described within section 3.1.1) to be 1.53 ± 0.18 µm in length and 0.90 ± 0.11 µm in width.

Table 20. Spore counts of feed and permeate samples during filtration of a RO water and 5 wt% MPI feed solutions through either a 0.8 or 1.4 µm *Membralox*^{TM} membrane.

	Spore counts (Log_{10} cfu ml^{-1})					
Membrane and feed	Feed 5 min	Permeate 5 min	Log order reduction after 5 min	Feed 20 min (RO water) or 40 min (MPI)	Permeate 20 min (RO water) or 40 min (MPI)	Log order reduction after 20 min (RO water) or 40 min (MPI)
0.8 µm 5 wt% MPI	9.1	1.8	7.3 ± 0.1	7.2	0.7	6.4 ± 0.3
1.4 µm 5 wt% MPI	6.6	2.9	3.6 ± 0.1	6.8	2.8	4.0 ± 0.4
1.4 µm RO water	6.7	3.3	3.4 ± 0.1	6.7	3.3	3.4 ± 0.1

The feed spore counts during the MPI run through the 0.8 µm ceramic membrane decreased from 9.1 to 7.2 log orders after 5 and 40 minutes of filtration respectively. This may be caused by spore denaturation, aggregation or adhesion to various surfaces within the filtration system. These preliminary studies showed that the separation was physically possible.

4.5.2 Effect of TMP on porosity of spore fouling cake layers

Experiments have been carried out using inoculated RO water feeds to find the effect that varying pore size and TMP have on the porosity of the fouling cake layer that the spores form on the membrane surface. Experiments were carried out using either a 0.8 or 1.4 µm membrane at 0.7 m s^{-1}, 50 ºC and either 0.5, 1.0 or 1.5 bar for 40 minutes, the change in permeate flux with time for each of the experiments can be seen in Figure 60. As can be seen when filtering at 0.5 bar through the 0.8 µm membrane the flux remains relatively constant with time but with increasing TMP flux decreases to a greater extent decreasing by 3% at 0.5 bar, 11% at 1.0 bar and by 15% at 1.5 bar and through the 1.4 µm membrane at 1.0 bar by 18%. This could be because as TMP is increased more spores are forced towards and onto the surface of the membrane resulting in a larger amount of fouling. The higher decrease in flux with time that occurred when filtering through the 1.4 µm membrane at 1 bar than through the 0.8 µm membrane can be explained when considering the size of the spores as with this pore size more spores would be able to penetrate into the membrane pores themselves and absorb onto the

surface decreasing the effective pore diameter as well as blocking the pores which would decrease flux. The porosity of the cake layers was found by firstly calculating the specific resistance of the cake (r) using equation 25. Where R_c is the resistance of the cake (m^{-1}) calculated from PWF measurement after fouling, A_m is the membrane area (m^2) and V_s is the volume of spores deposited (m^3) calculated from the spore rejection.

$$r = \frac{R_c A_m}{V_s} \tag{25}$$

The specific resistance (r) was then used to calculate the porosity (ε) of the fouling layer using equation 26, where d_s is the mean spore diameter (m^2). This equation can be rearranged into equation 27 a cubic equation that when plotted can be used to calculated porosity. The plots used to calculate the porosity of the different formed cake layers are shown in Figure 61 and the values in Table 21. Porosity values are between 0 - 1 with 0 meaning that no cake layer is present and 1 that the membrane is completely covered in cake and the layer has no porosity. As can be seen from Table 21 the porosity decreased with increasing TMP when filtering through the 0.8 µm membrane. This was expected as when TMP is increased this leads to a greater compaction of the cake layer with the spores being forced closer together decreasing the porosity of the layer. It should be noted however that there are limitations to these measurements as the diameter of the spores was calculated from SEM images. SEM images are taken within a vacuum and this would have caused the spore structure to alter. For example, the exosporium layer could have contracted resulting in a smaller diameter being measured; this would have therefore altered the porosities calculated.

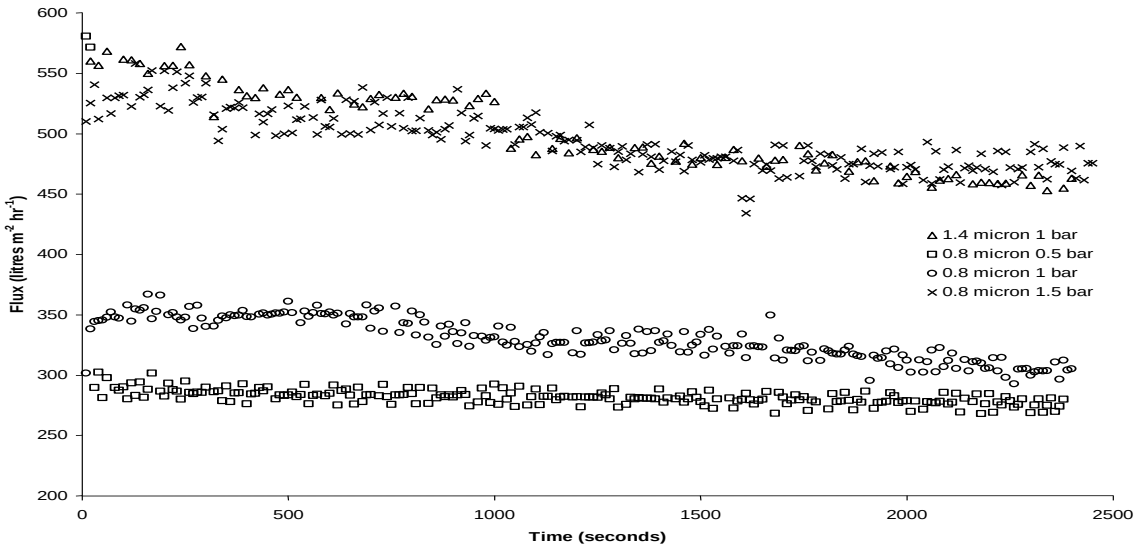

Figure 60. Change in permeate flux with time during filtration of inoculated RO water feeds through either a 0.8 or 1.4 µm membrane at 0.7 m s^{-1}, 50 ºC and either 0.5, 1.0 or 1.5 bar for 40 minutes.

$$r = 180\frac{(1-\varepsilon)}{\varepsilon^3}\frac{1}{d_s{}^2} \tag{26}$$

$$\varepsilon^3 - a\varepsilon - a = 0 \tag{27}$$

Table 21. Calculated porosities of spore cake layers formed during filtration through either 0.8 or 1.4 µm membrane at either 0.5, 1.0 or 1.5 bar.

Membrane (µm)	TMP (bar)	Porosity (ε)
0.8	0.5	0.58
0.8	1.0	0.22
0.8	1.5	0.17
1.4	1.0	0.19

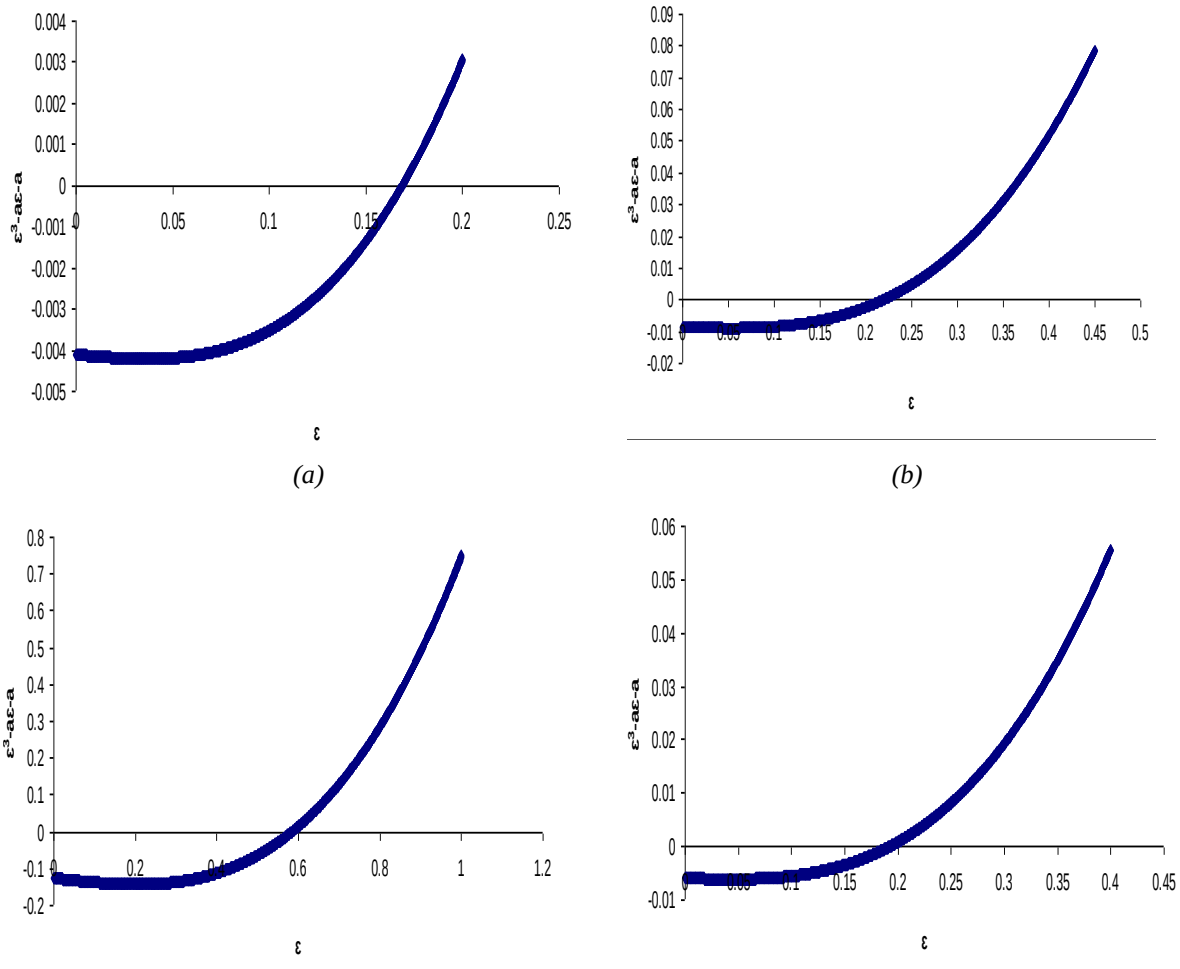

Figure 61. Plots used to establish the porosities of the spore cake fouling layers formed on the surface of a 0.8 µm membrane when using TMP's of either a) 0.5, b) 1.0 or c) 1.5 bar and d) on the surface of a 1.4 µm membrane at 1 bar.

4.5.3 Change in permeate flux, solids and protein transmission with varying process conditions, feed concentration and inoculation during filtration through a 0.8 µm membrane.

Milk Protein Isolate (MPI) filtration experiments were carried out using filtration system set-up 1 on both the 0.8 and 1.4 µm *Membralox*™ membranes. 'Sterile' feed streams (that have not been inoculated with spores of *Bacillus mycoides*) between 4 – 16 wt% were filtered using two different CFV's at 1 bar TMP and 50 °C for 40 minutes, in order to determine the effect of varying the solids content and process conditions. The MPI feed concentrations and CFV's used and the resulting steady state permeate flux, solid transmission and protein transmissions found during filtration through the 0.8 µm membrane can be seen in Table 22.

Table 22. Experimental conditions used and the steady state permeate flux, solid and protein transmission found during experiments carried out using 'sterile' MPI feeds through a 0.8 µm membrane (rig set-up 1).

		At steady state (After 40 minutes)		
MPI wt%	CFV ($m\ s^{-1}$)	Flux (LMH)	Solids transmission (%)	Protein transmission (% of feed protein content)
4	1.4	41.2	25.2	42.2
5	0.7	22.4	12.4	26.4
5	1.4	46	26.3	39.4
8	0.7	12.2	18.8	32.1
8	1.4	30.2	27.2	36.9
16	1.4	12.2	22.6	31.4

Figure 62 shows the permeate flux curves obtained for the 4, 8 and 16 wt% 'sterile' solutions filtered at 1.4 $m\ s^{-1}$ CFV, 1 bar and 50 °C through the tubular ceramic 0.8 µm *Membralox*™ membrane. Each curve displays the same typical trend found for permeate flux behaviour when filtering dairy based feeds. The flux is high at the start of the experiment but decreases rapidly to low terminal flux decline values. As expected it was found that the lower the solutions solids content the higher the permeate flux with the 4 wt% solution producing a flux of 41.2 litres $m^{-2}\ hr^{-1}$ (LMH), this decreased by 11 LMH (26.7%) to 30.2 LMH when filtering 8 wt% MPI and by 18 LMH (59.6%) to 12.2 LMH when filtering 16 wt% MPI. Liu *et al*., 2012 found report a similar trend during the filtration of $CaCO_3$ suspensions of 0.5, 2 and 5 wt% through a polyurethane based hollow fibre membrane. With each curve displaying the same rapid decrease in

permeate flux at the start of filtration regardless of feed concentration with the steady state permeate flux values decreasing with increasing feed concentration namely 73, 52 and 49% of the original flux for 0.5, 2 and 5 wt% respectively.

Filtration experiments were also carried out using set-up 1 of the filtration system through the 0.8 µm membrane using inoculated feeds, to determine the effect that the presence of spores has on the steady state permeate flux, solids and protein transmission values. Table 23 shows the MPI feed concentrations and CFV's used and the resulting steady state permeate flux, spore reductions, solid and protein transmissions found during filtration experiments. As can be seen when comparing Tables 22 and 23 that filtering solutions of MPI which have been inoculated with spores of *Bacillus mycoides* results in a lower steady state permeate flux than when comparable 'sterile' solutions are filtered. With flux decreasing when filtering 5 wt% MPI at 0.7 m s^{-1} by 3.8 LMH (17.0%), by 2.5 LMH (5.4%) at 1.4 m s^{-1} and by 1.1 LMH (9.0%) when filtering 8 wt% MPI at 0.7 m s^{-1}. It can also be seen that generally higher solids and protein transmission values are found when filtering inoculated solutions apart from the solid transmission value for the 8 wt% solution filtered at 0.7 m s^{-1}.

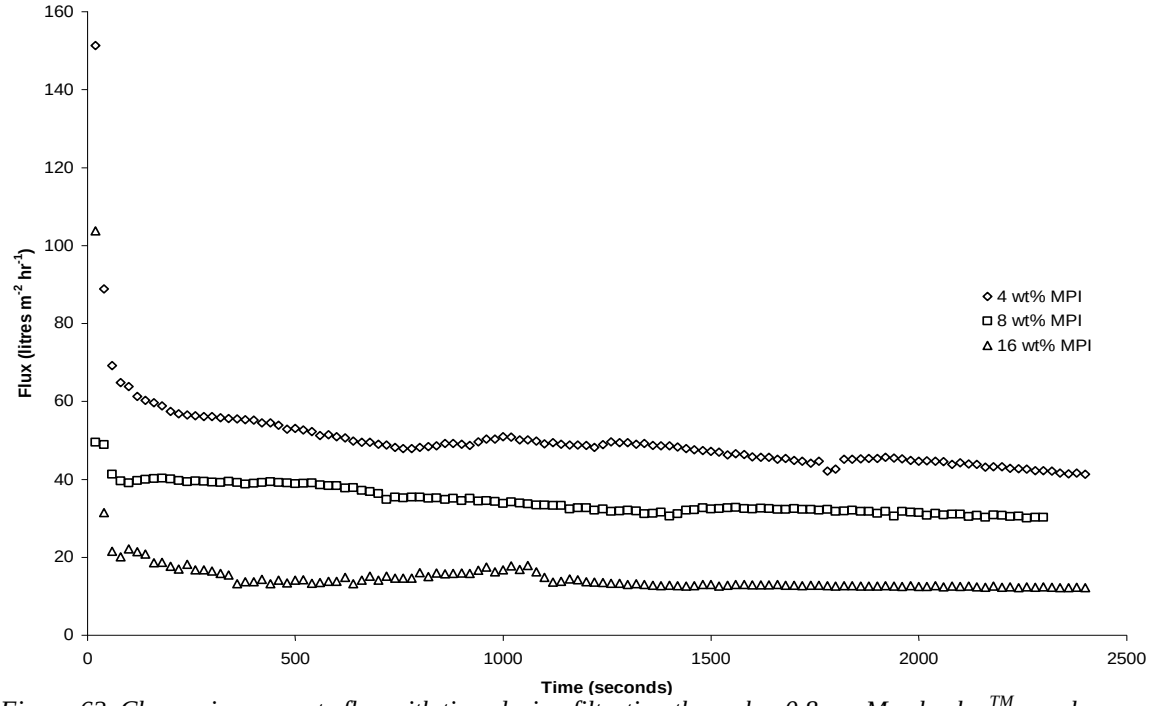

Figure 62. Change in permeate flux with time during filtration through a 0.8 µm Membralox™ membrane of 'sterile' 4, 8 and 16 wt% MPI solutions at 1 bar TMP, 1.4 m s^{-1} CFV and 50 °C.

4.5.4 Spore rejection analysis

In regards to the spore reductions shown in Table 23, all measured reductions were very high between 3.8 – 5.6 log orders equating to a 99.9% decrease. This was expected as

spores of *Bacillus mycoides* are larger in size compared to that of the membranes pore diameter, with the average length and width found to be 1.53 ± 0.18 µm and 0.90 ± 0.11 µm respectively as discussed in section 3.1.1. Also it was found that as MPI feed concentration increased and CFV decreased this led to an increase in spore reduction. As a log order value of 3.8 was measured when filtering 5 wt% MPI at 1.4 m s^{-1} and this increased to 4.7 log orders and to 5.1 log orders when the MPI wt% was increased to 10 and 15 wt% respectively. In regards to CFV when this was decreased from 1.4 to 0.7 m s^{-1} when filtering 5 wt% MPI this led to an increase in 0.9 log orders from a 3.8 to 4.7 log order reduction. This was caused because both an increase in feed concentration and a decrease in CFV result in a larger amount of MPI fouling as shown by the associated decreases in permeate flux values. This fouling acts as an additional separation layer and so increases the amount of both spore and MPI solid rejection. It appears that changes in CFV and MPI concentration have similar effects on spore reduction as when CFV is doubled from 0.7 to 1.4 m s^{-1} when filtering 5 wt% MPI this causes a 0.9 log order decrease from 4.7 to 3.8 log orders and this same decrease is observed when MPI concentration is halved from 10 to 5 wt% when filtering at 1.4 m s^{-1} decreasing from 4.7 to 3.8 log orders.

Table 23. Experimental conditions used and the steady state permeate flux, spore rejection and solid and protein transmission found during experiments carried out using inoculated MPI feeds through a 0.8 µm membrane (rig set-up 1).

		At steady state (after 40 minutes)				
MPI wt%	CFV (m s^{-1})	Flux (LMH)	Solids transmission (%)	Spore reduction		Protein transmission (% of feed protein content)
				%	log	
5	0.7	18.6	28.3	99.9	4.7 ± 0.4	48.2
5	1.4	43.5	29.4	99.9	3.8 ± 0.3	53.6
8	0.7	11.1	16.4	99.9	5.6 ± 0.2	38.8
10	1.4	28.4	16	99.9	4.7 ± 0.2	34.6
15	1.4	20.7	2.7	99.9	5.1 ± 0.6	21.6

4.5.5 Change in permeate flux, spore reduction, solids and protein transmission with varying solution solids content and process conditions during filtration through a 1.4 µm membrane.

Filtration experiments involving inoculated feeds were also carried out at 1 bar TMP using filtration set-up 1 through the 1.4 µm membrane. Experiments as with the 0.8 µm

membrane were carried out using different MPI concentrations between 5 – 15 wt% and CFV's between 0.7 – 1.4 m s^{-1} as shown in Table 24, along with the produced steady state permeate flux, spore reduction, solid and protein transmission values.

As with the 0.8 µm membrane increases in MPI concentration and decreases in CFV were found to result in a decrease in steady state permeate flux, solid and protein transmission. With an increase in MPI concentration from 5 to 10 wt% resulting in a 14.4 LMH (42.6%) decrease in permeate flux to 19.4 LMH, along with a 13.6 and 7.7% decrease in solids and protein transmission respectively. A decrease in CFV from 1.4 to 0.7 m s^{-1} when filtering 5 wt% MPI was found to result in a 20.5 LMH (60.7%) decrease in permeate flux and a 8.0 and 13.0% decrease in solids and protein transmission respectively. When comparing the 1.4 µm to the 0.8 µm membrane all of the comparable steady state permeate flux values are lower as well as the solid and protein transmission values found when filtering 5 wt% MPI at 0.7 m s^{-1} CFV. But the 5, 10 and 15 wt% experiments carried out at the higher CFV of 1.4 m s^{-1} produced higher values for solids and protein transmission of 3.3 and 2.2% for 5 wt%, 3.1 and 3.5% for 10 wt% and 6.2 and 6.8% for 15 wt% MPI respectively.

Table 24. Experimental conditions used and the steady state permeate flux, spore rejection and solid and protein transmission found during experiments carried out using inoculated MPI feeds through a 1.4 µm membrane (rig set-up 1).

		At steady state (after 40 minutes)				
MPI wt%	CFV (m s^{-1})	Flux (LMH)	Solids transmission (%)	Spore reduction		Protein transmission (% of feed protein content)
				%	log	
5	0.7	13.3	24.7	99.9	4.0 ± 0.4	32.8
5	1.4	33.8	32.7	99.2	2.1 ± 0.1	55.8
10	1.4	19.4	19.1	99.8	2.8 ± 0.1	38.1
15	1.4	10.4	8.9	99.1	2.0 ± 0.3	28.4

In regards to spore reductions for the 1.4 µm membrane the same trends were found as with the 0.8 µm membrane with spore reductions increasing with increasing MPI concentration and decreasing CFV. This effect is more pronounced with this membrane with an increase of 1.9 log orders found when increasing CFV from 0.7 to 1.4 m s^{-1} during 5 wt% MPI filtration compared to only a 0.9 log order increase found with the 0.8 µm membrane. This is because as pore size increases the membrane becomes less of

a barrier and the effect that additional filtration layers have in the form of MPI fouling have on spore reduction increases.

In conclusion although the spore reduction values were high between 3.8 – 5.6 log orders for the 0.8 µm membrane and between 2.1 – 4.0 log orders for the 1.4 µm membrane when filtering between 5 – 15 wt% MPI solutions at 1 bar, the steady state permeate flux and solid transmission values found for both membranes when using filtration set-up 1 were not commercially viable. This meant that different process conditions needed to be tested and as a result the filtration system was modified to set-up 2 as described in section 2.9.1.

4.6 FILTRATION EXPERIMENTS USING FILTRATION SET UP 2

4.6.1 Effect of TMP (1 bar- set up 1, 2 bar- set up 2) on permeate flux and solids transmission during filtration of inoculated MPI.

As discussed in section 2.9.1, the modifications made to the filtration system were intended to increase the CFV at which MPI filtration experiments could be conducted, but unfortunately the changes did not improve the CFV. But using this set-up filtration experiments that had been carried out using 5 – 15 wt% MPI, 1.4 m s^{-1} CFV and 50 °C through the 0.8 and 1.4 µm membranes at 1 bar were repeated using 2 bar TMP. Tables 25 and 26 show the wt% MPI filtered and the resulting steady state permeate flux, solid transmissions and total resistances (R_T) at 1 and 2 bar TMP and Figures 63 and 64 show the change in permeate flux with time and corresponding change in membrane resistance graphs for the 0.8 and 1.4 µm membrane respectively. When filtering 5, 10 and 15 wt% MPI using both the 0.8 and 1.4 µm membrane total resistance was found to increase with increasing TMP. Also when filtering the lower solids content solutions of 5 and 10 wt% MPI steady state permeate flux and solid transmissions decreased with the TMP increase, apart from the permeate flux produced during filtration of 10 wt% through the 0.8 µm membrane. These results suggest that the higher TMP is causing the fouling layer to become more compacted leading to an increase in total resistance and as a result a lower permeate flux and solid transmission with the lower wt% feed solutions of 5 and 10 wt%. As such it could be argued that a lower TMP of 1 bar should be used during MPI filtration experiments using feeds up to 10 wt%.

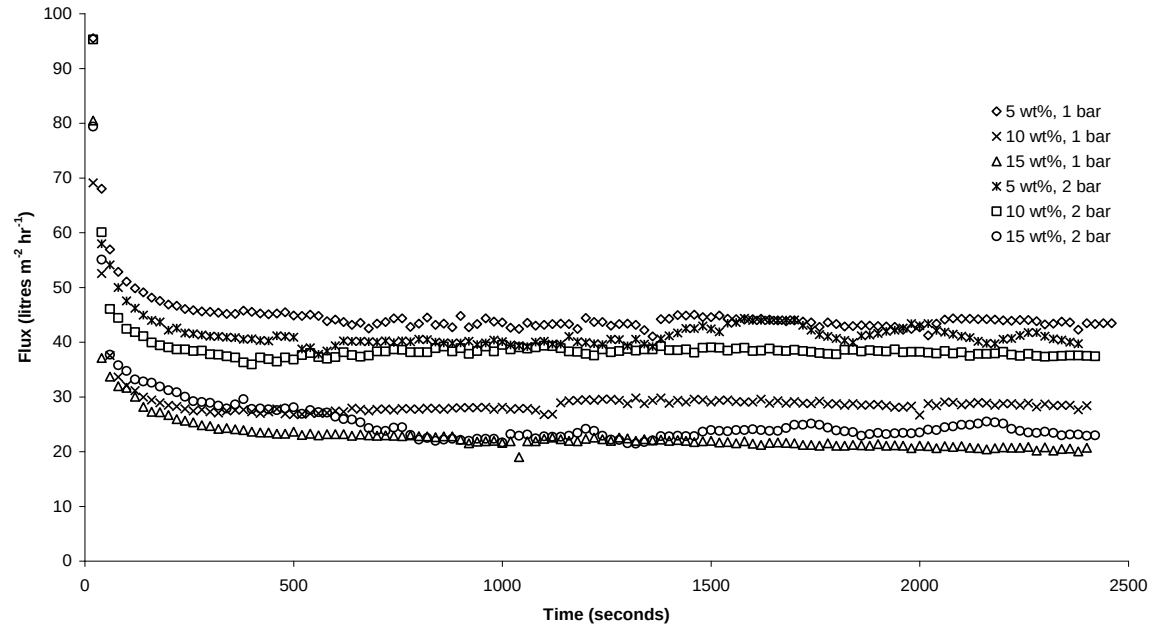

(a)

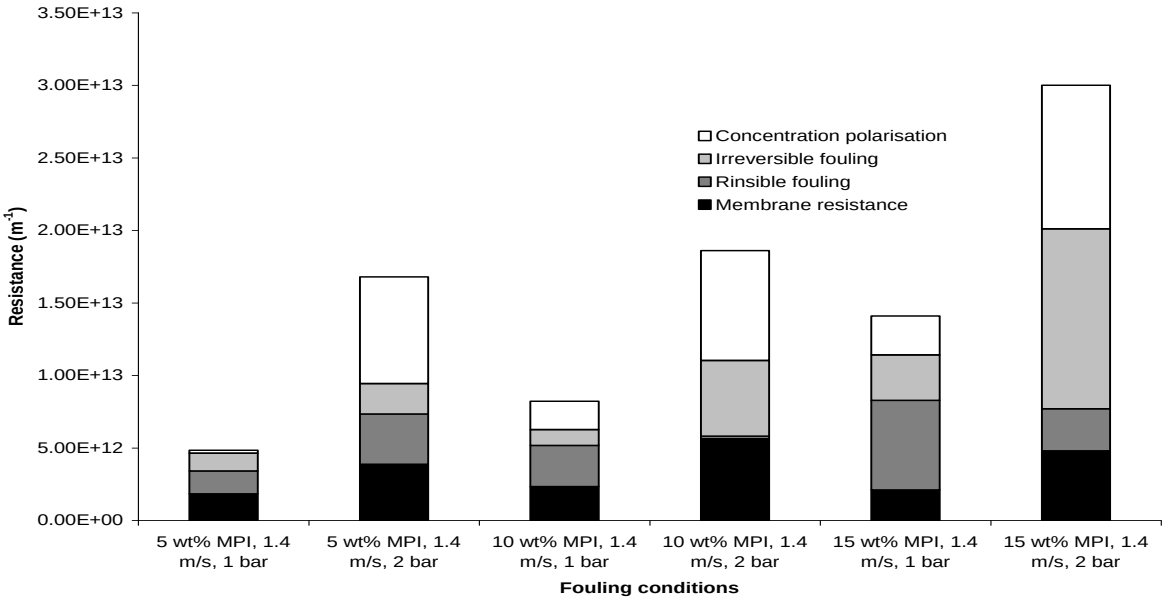

(b)

Figure 63. a) Change in permeate flux with time during filtration through a 0.8 µm Membralox^{TM} *membrane of 5, 10 and 15 wt% MPI inoculated solutions using either 1 or 2 bar TMP, 1.4 m s^{-1} CFV at 50 °C, b) corresponding change in membrane resistance.*

But during the filtration of 15 wt% MPI through both membranes increasing TMP led to an increase in both permeate flux and solids transmission suggesting that although the total resistance increases the increase in TMP forces more permeate through the membrane and that this permeate contains more MPI. As this work was concerned with the optimisation of the filtration of as high a MPI feed solids content as possible the remaining experiments conducted within this work were carried out using a TMP of 2 bar. Madaeni *et al.,* (2011) investigated the effect of TMP on filtration performance

during the filtration of raw whole and skim milk and concluded that 2 bar was the optimum filtration TMP.

Table 25. Comparison of the steady state permeate fluxes and solid transmissions through the 0.8 µm membrane using either 1 or 2 bar TMP, 1.4 m s^{-1} CFV, and 50 °C.

		Steady state		
MPI (wt%)	TMP (bar)	Flux (LMH)	Solids transmission (%)	R_T (m^{-1}) x10^{12}
5	1	43.5	29.4	3.00
10	1	28.4	16.0	5.88
15	1	20.7	8.7	12.0
5	2	39.7	19.8	12.9
10	2	37.5	7.5	13.0
15	2	23.0	3.8	25.2

Table 26. Comparison of the steady state permeate fluxes and solid transmissions through the 1.4 µm membrane using either 1 or 2 bar TMP, 1.4 m s^{-1} CFV, and 50 °C.

		Steady state		
MPI (wt%)	TMP (bar)	Flux (LMH)	Solids transmission (%)	R_T (m^{-1}) x10^{12}
5	1	33.8	32.7	3.74
10	1	19.4	19.1	8.19
15	1	10.4	8.6	15.9
5	2	36.2	31.4	18.5
10	2	16.3	16.1	30.1
15	2	12.3	10.7	47.2

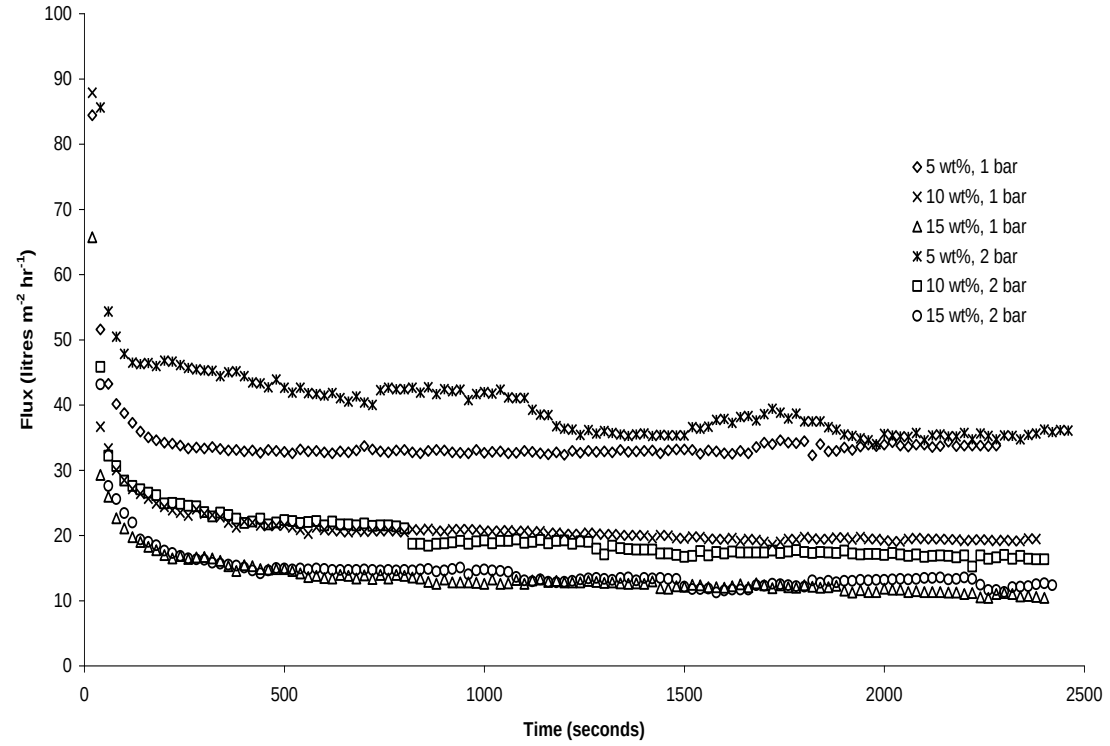

(a)

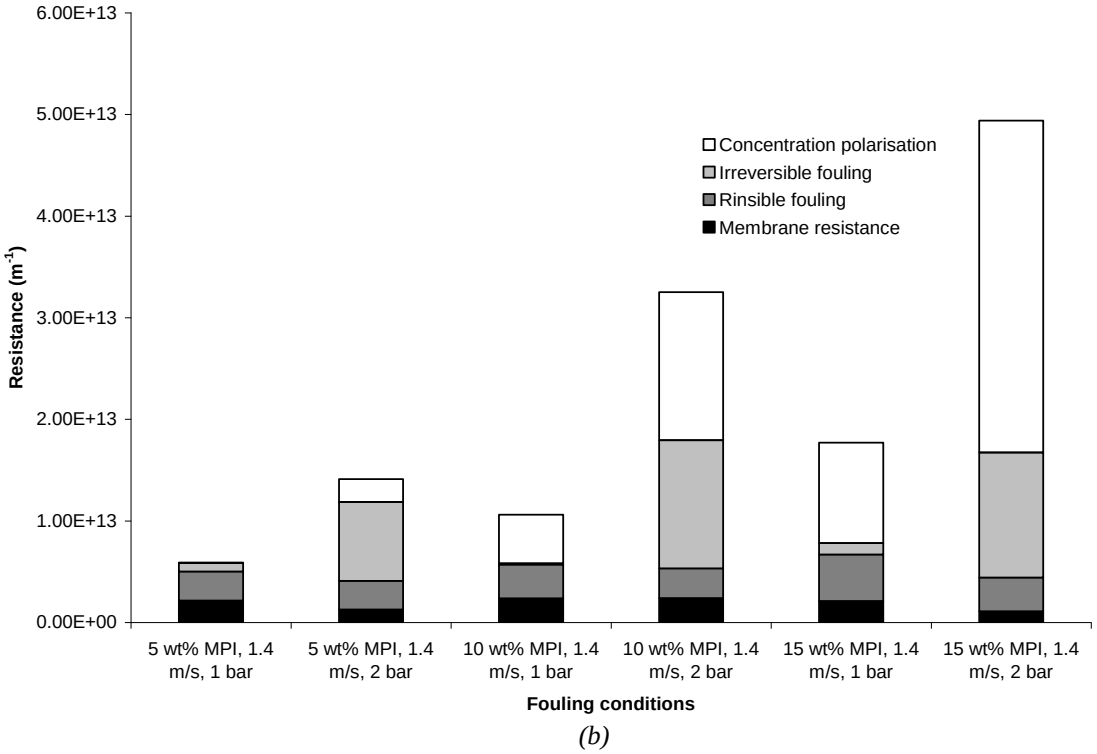

(b)

Figure 64. a) Change in permeate flux with time during filtration through a 1.4 µm Membralox^{TM} *membrane of 5, 10 and 15 wt% MPI inoculated solutions using either 1 or 2 bar TMP, 1.4 m s^{-1} CFV at 50 °C, b) corresponding change in membrane resistance*

4.6.2 Determination of optimum membrane pore size and filtration conditions.

Five tubular ceramic *Membralox*^{TM} membranes were used to filter MPI feeds of between 5 and 15 wt%. CFV values of 0.7 and 1.4 m s^{-1} were used, at a temperature of

50 °C and a TMP of 2 bar. Results for these five membranes (0.8, 1.4, 2.0, 5.0 and 12.0 µm) are summarised in Tables 27 – 31, the change in permeate flux with time graphs for each membrane are shown in Figures 65, 67, 69, 71, 73 respectively along with each membranes resistance data in Figures 66, 68, 70, 72, 74 respectively.

Table 27. Performance of a 0.8 µm pore size ceramic membrane. Steady state permeate flux, spore rejection, solids transmission and protein transmission during filtration.

		At steady state (After 40 minutes)					
				Spore reduction		Protein transmission (% of feed protein content)	
MPI wt%	CFV ($m\ s^{-1}$)	Flux (LMH)	Solids transmission (%)	%	log		R_F (m^{-1}) x10^{13}
5	1.4	39.1	19.8	99.996	4.4 ± 0.2	40.8	1.35
10	1.4	37.4	7.5	99.954	3.3 ± 0.5	17.9	1.57
15	0.7	18.6	7.0	99.611	2.4 ± 0.5	3.3	3.32
15	1.4	23.0	3.8	99.966	3.5 ± 0.1	7.8	2.83

Table 28. Performance of 1.4 µm pore size ceramic membrane. Steady state permeate flux, spore rejection, solids transmission and protein transmission during filtration.

		At steady state (After 40 minutes)					
				Spore reduction		Protein transmission (% of feed protein content)	
MPI wt%	CFV ($m\ s^{-1}$)	Flux (LMH)	Solids transmission (%)	%	log		R_F (m^{-1}) x10^{13}
5	1.4	30.9	31.4	98.4	1.8 ± 0.2	40.4	2.15
10	1.4	16.3	16.1	98.567	1.8 ± 0.4	31.2	3.01
15	0.7	13.2	6.4	99.471	2.3 ± 0.2	15.0	4.81
15	1.4	12.3	10.7	98.245	1.8 ± 0.4	19.0	4.83

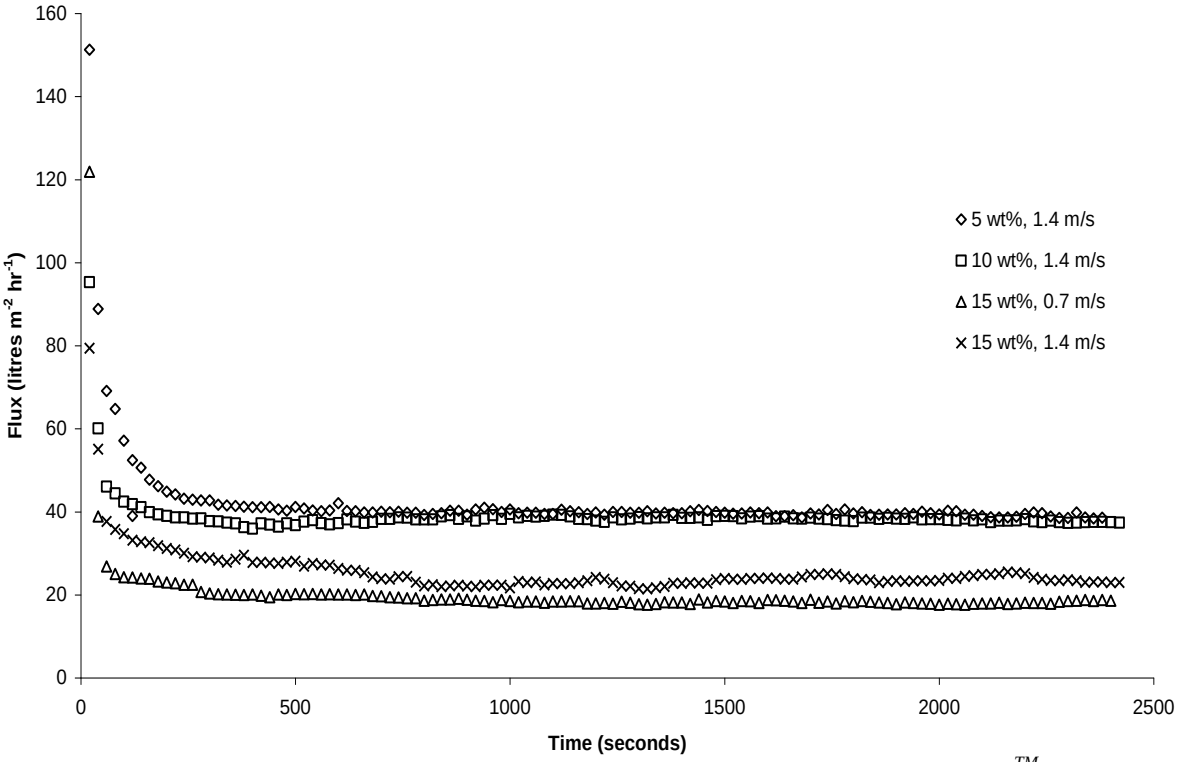

Figure 65. Change in permeate flux with time during filtration through a 0.8 µm Membralox^{TM} *membrane of 5, 10 and 15 wt% MPI solutions using either 0.7 or 1.4 m s^{-1} CFV at 50 °C and 2 bar TMP.*

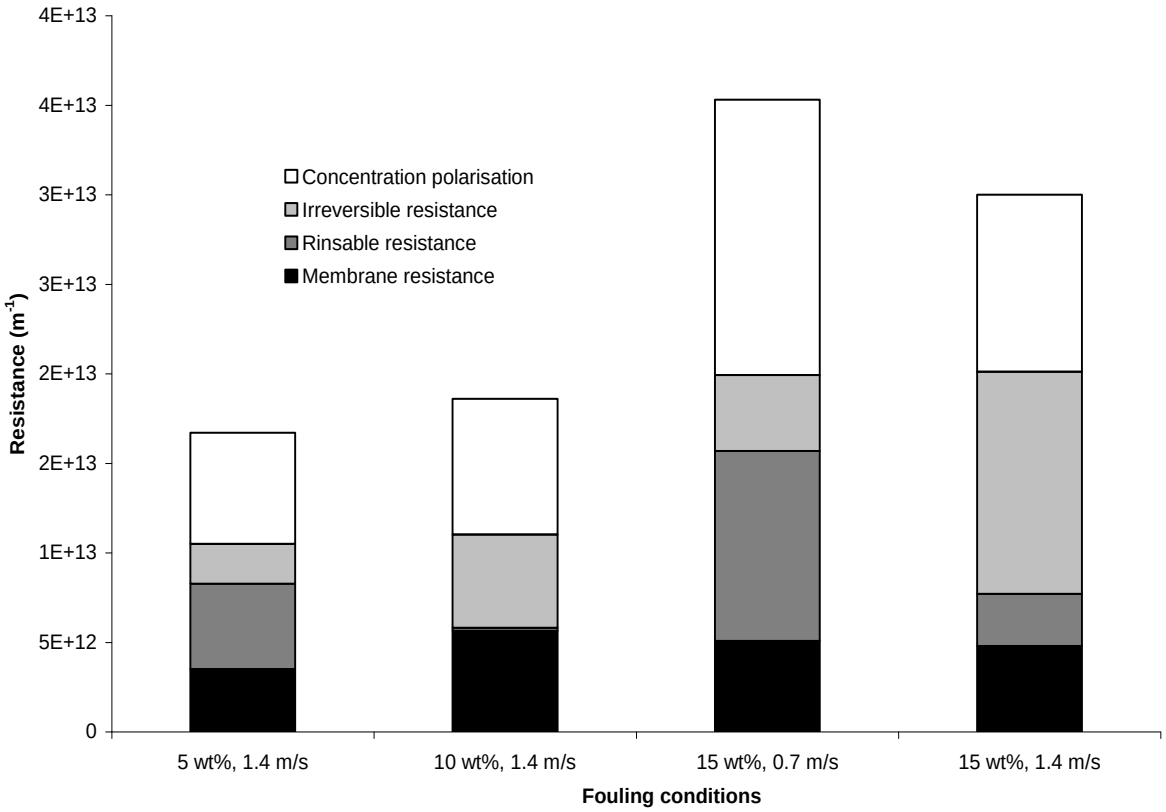

Figure 66. Change in membrane resistance with MPI concentration and filtration conditions during filtration through a 0.8 µm Membralox^{TM} *membrane at 50 °C and 2 bar TMP.*

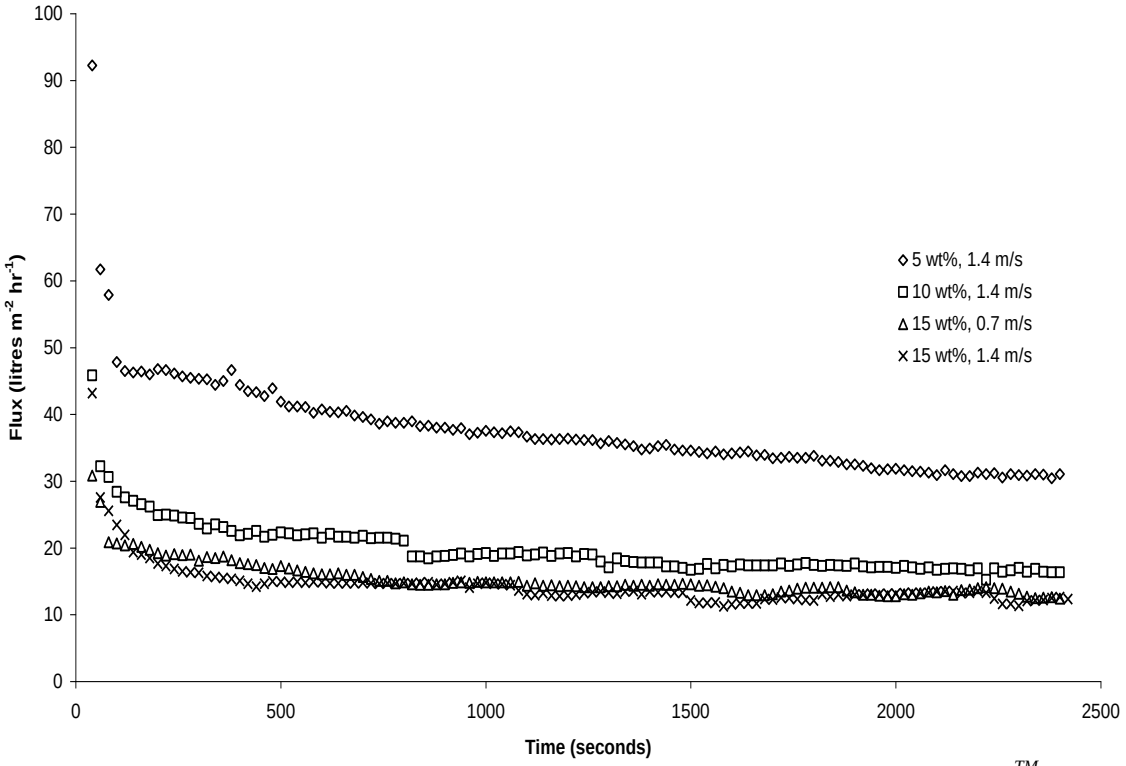

Figure 67. Change in permeate flux with time during filtration through a 1.4 µm Membralox^{TM} *membrane of 5, 10 and 15 wt% MPI solutions using either 0.7 or 1.4 m s^{-1} CFV at 50 °C and 2 bar TMP.*

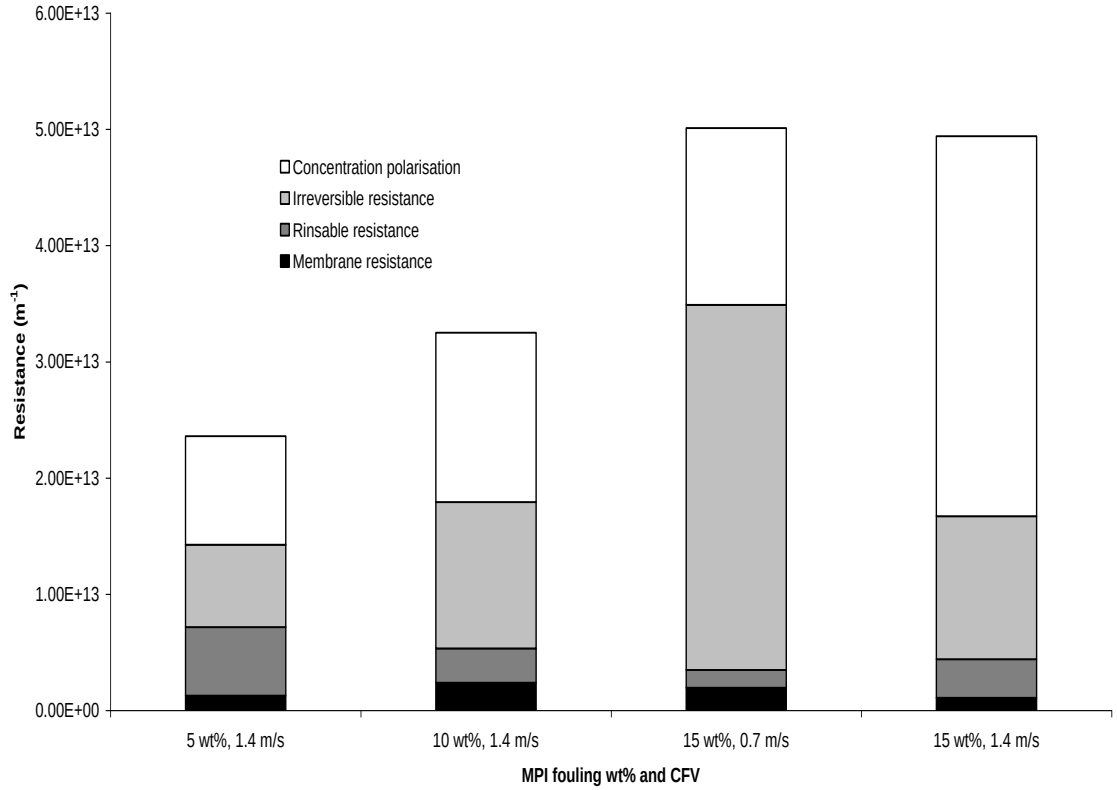

Figure 68. Change in membrane resistance with MPI concentration and filtration conditions during filtration through a 1.4 µm Membralox^{TM} *membrane at 50 °C and 2 bar TMP.*

Table 29. Performance of 2.0 µm pore size ceramic membrane. Steady state permeate flux, spore rejection, solids transmission and protein transmission during filtration.

		At steady state (After 40 minutes)					
				Spore rejection		Protein transmission (% of feed protein content)	R_F (m^{-1}) x10^{12}
MPI wt%	CFV (m s^{-1})	Flux (LMH)	Solids transmission (%)	%	log		
5	1.4	69.5	40.1	99.160	2.1 ± 1.1	56.9	6.40
10	1.4	23.1	25.2	99.640	2.4 ± 0.8	42.8	17.7
15	0.7	11.8	8.5	99.989	3.9 ± 1.0	23.2	53.6
15	1.4	12.9	11.1	99.874	2.9 ± 0.6	38.6	49.2

Figure 69. Change in permeate flux with time during filtration through a 2.0 µm Membralox™ *membrane of 5, 10 and 15 wt% MPI solutions using either 0.7 or 1.4 m s^{-1} CFV at 50 °C and 2 bar TMP.*

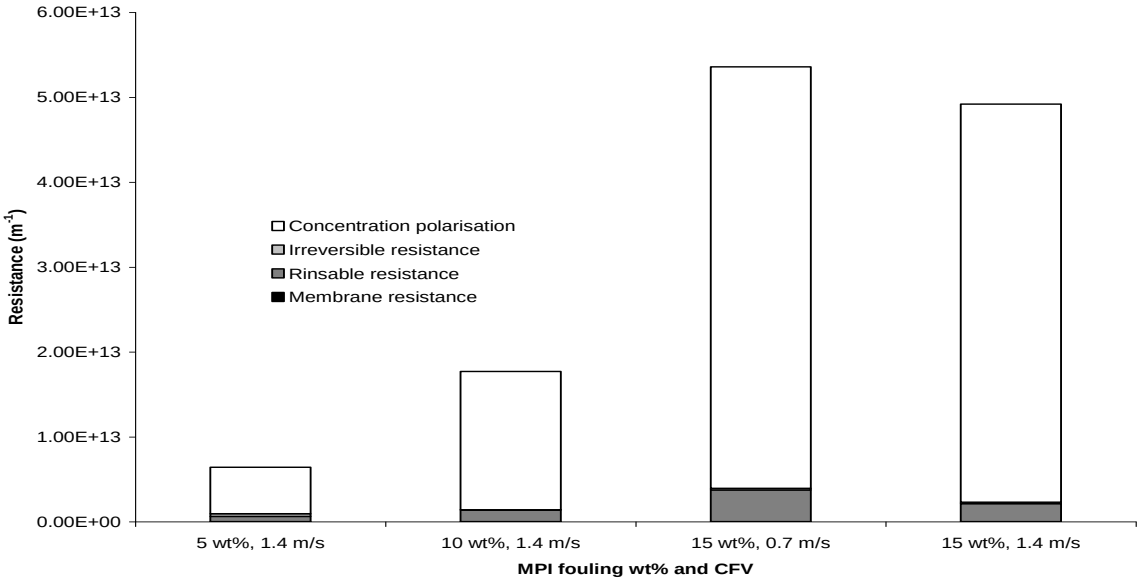

Figure 70. Change in membrane resistance with MPI concentration and filtration conditions during filtration through a 2.0 µm Membralox^{TM} *membrane at 50 °C and 2 bar TMP*

Table 30. Performance of 5.0 µm pore size ceramic membrane. Steady state permeate flux, spore rejection, solids transmission and protein transmission during filtration.

		At steady state (After 40 minutes)					
				Spore rejection		Protein transmission (% of feed protein content)	
MPI wt%	CFV (m s^{-1})	Flux (LMH)	Solids transmission (%)	%	log		R_F (m^{-1}) x10^{11}
5	1.4	371.7	61.1	92.474	1.1 ± 0.7	74.6	9.66
10	1.4	137.3	64.2	94.265	1.2 ± 0.8	73.8	14.5
15	0.7	14.0	64.6	99.067	2.0 ± 0.7	86.7	75.6
15	1.4	22.9	66.0	93.9	1.2 ± 0.8	67.0	37.9

Table 31. Performance of 12.0 µm pore size ceramic membrane. Steady state permeate flux, spore rejection, solids transmission and protein transmission during filtration.

		At steady state (After 40 minutes)					
				Spore rejection		Protein transmission (% of feed protein content)	
MPI wt %	CFV (m s^{-1})	Flux (LMH)	Solids transmission (%)	%	log		R_F (m^{-1}) x10^{12}
10	1.4	122.8	70.2	99.728	1.4 ± 0.3	90.2	1.42
15	0.7	9.8	65.0	96.110	2.6 ± 0.6	42.1	9.69
15	1.4	26.6	68.7	98.362	2.1 ± 0.7	96.5	3.80

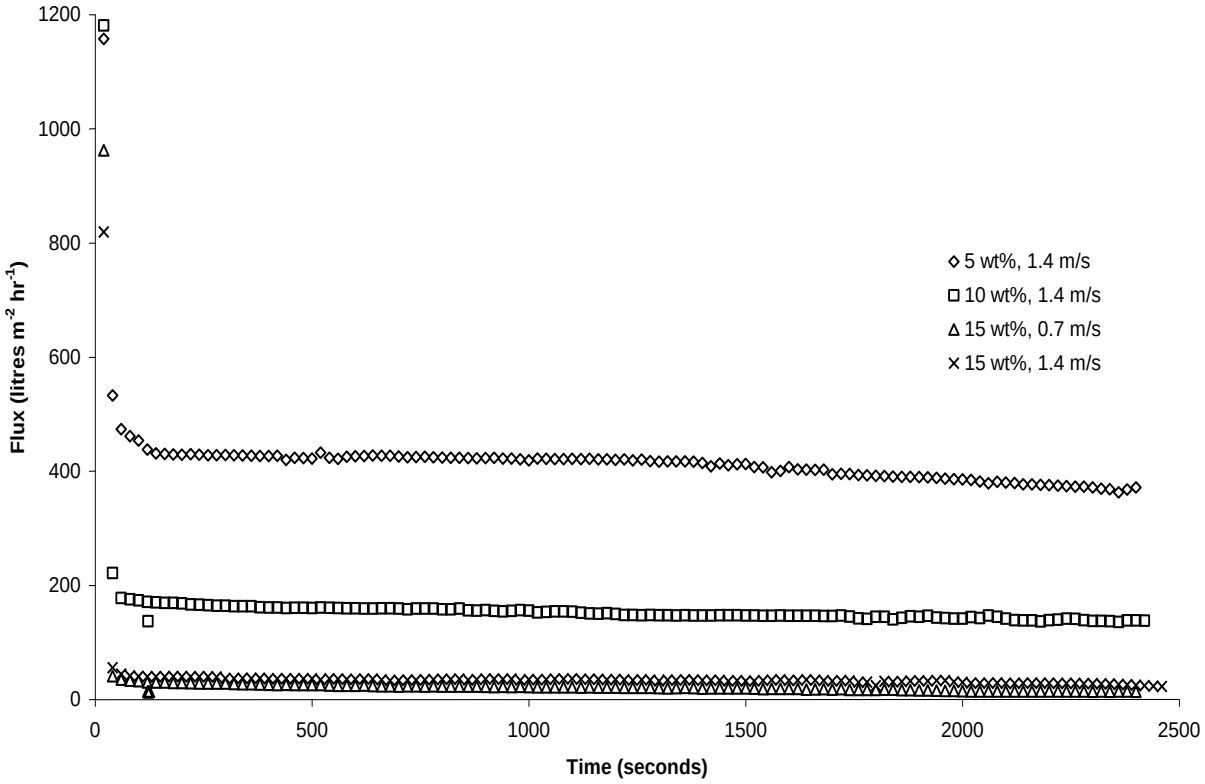

Figure 71. Change in permeate flux with time during filtration through a 5.0 µm Membralox^{TM} *membrane of 5, 10 and 15 wt% MPI solutions using either 0.7 or 1.4 m s^{-1} CFV at 50 °C and 2 bar TMP.*

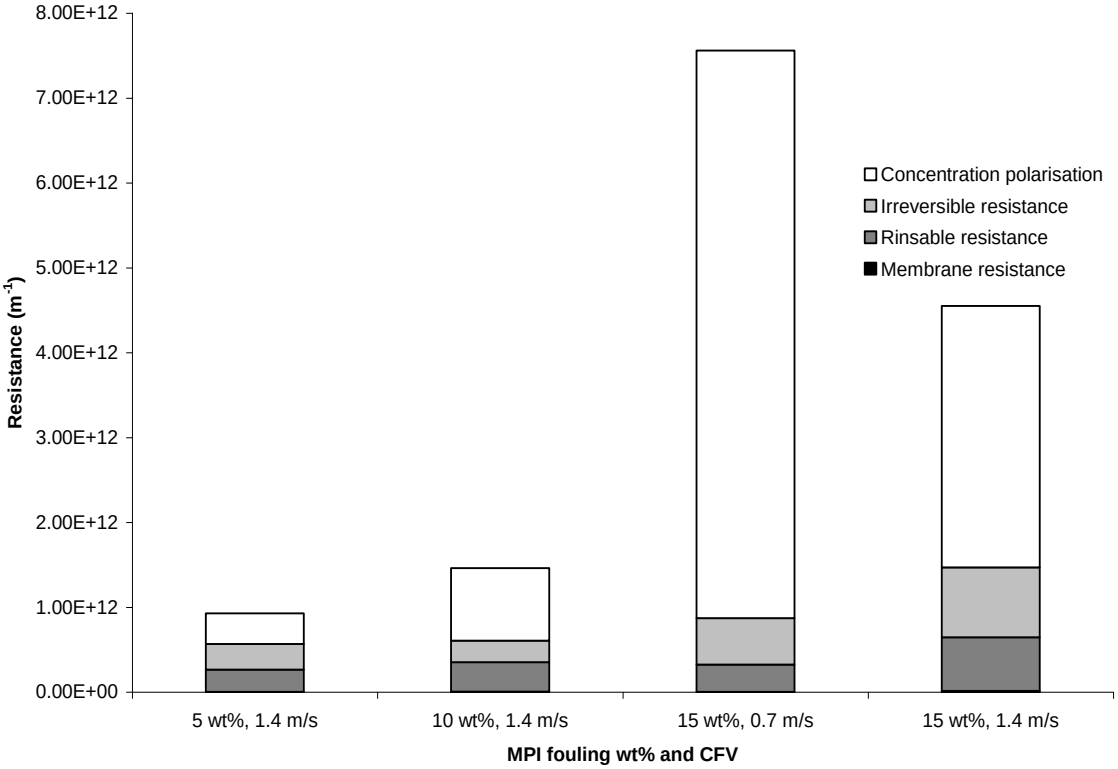

Figure 72. Change in membrane resistance with MPI concentration and filtration conditions during filtration through a 5.0 µm Membralox^{TM} *membrane at 50 °C and 2 bar TMP*

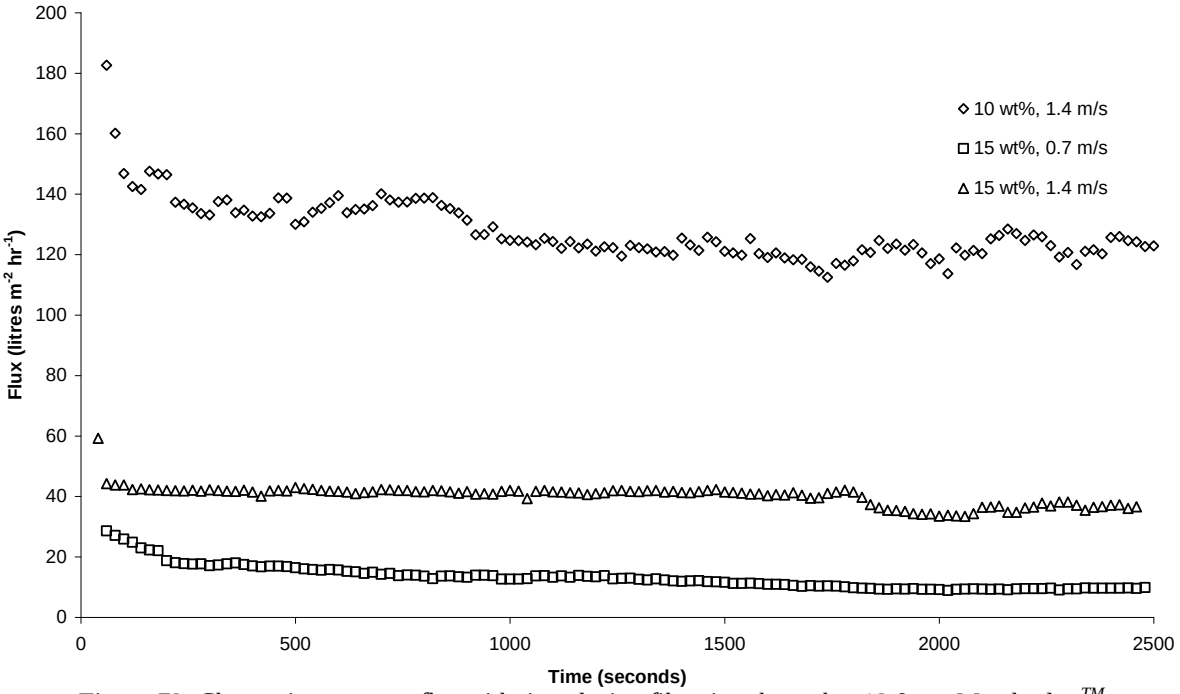

Figure 73. Change in permeate flux with time during filtration through a 12.0 µm Membralox^{TM} *membrane of 5, 10 and 15 wt% MPI solutions using either 0.7 or 1.4 m s^{-1} CFV at 50 °C and 2 bar TMP.*

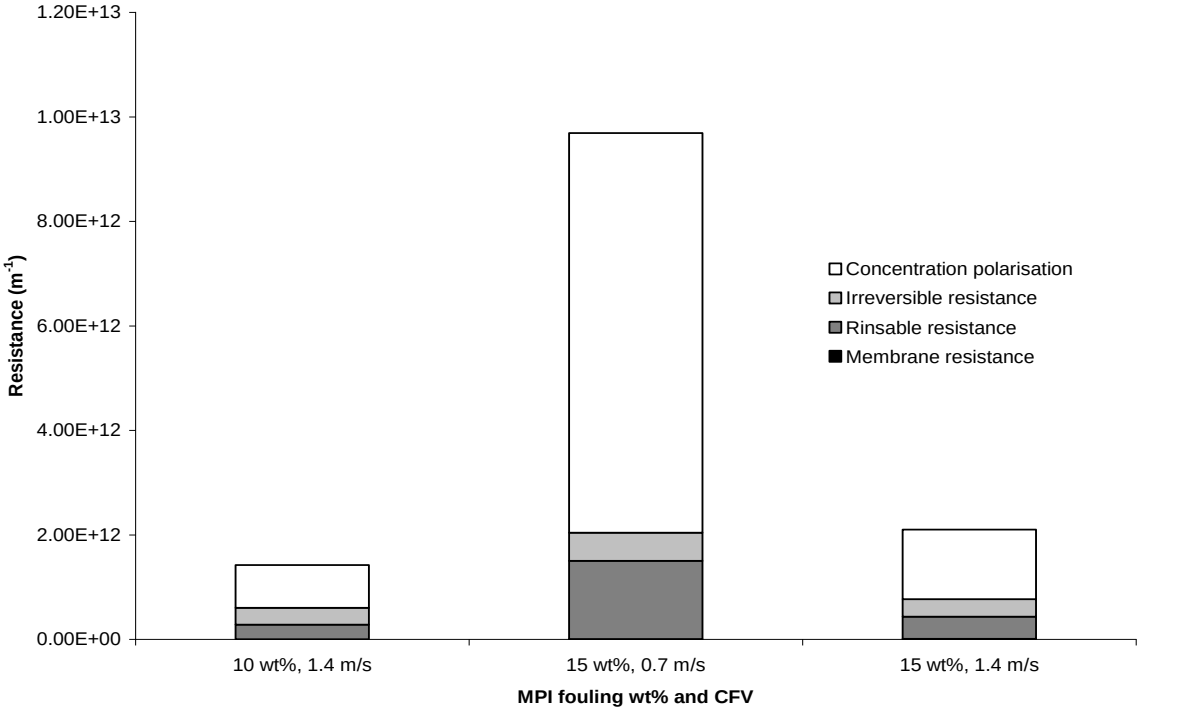

Figure 74. Change in membrane resistance with MPI concentration and filtration conditions during filtration through a 12.0 µm Membralox^{TM} *membrane at 50 °C and 2 bar TMP.*

For each of the membranes tested, it was found that as MPI concentration was increased, permeate flux decreased along with solids and protein transmission values. Moreover, as CFV was increased during the filtration of the 15 wt% MPI solution, this led to increases in some or all of the permeate fluxes, solids and protein transmission values achieved. Specifically, for the 0.8 and 5.0 µm membranes permeate flux increased by 4.4 LMH (or 23.7%) and 8.9 LMH (63.6%) respectively and solids

transmission increased by 4.5 and 1.4% respectively. For the 1.4 µm membrane, solids and protein transmission increased by 3.3 and 4.0% respectively. Lastly, for the 2.0 and 12.0 µm membranes respectively, permeate flux increased by 1.1 LMH (9.3%) and 16.8 LMH (171.4%), solids transmission increased by 2.6 and 3.7% respectively, and protein transmission increased by 15.4 and 54.4% respectively. This is due to a reduction in the fouling resistances as a result of increases in CFV. Abadi *et al*, 2011 reported a similar effect during the filtration of oil-in-water emulsions through a tubular ceramic 0.2 µm microfiltration membrane. They report an increase in permeate flux and a decrease in fouling resistance with increasing CFV between 0.75 – 2.25 m s^{-1}. They state this is due to a reduction of feed component aggregation within the gel layer that leads to a greater proportion of particles being returned to the bulk stream, which in turn weakens the effect of concentration polarisation.

The 5.0 and 12.0 µm membranes tested gave commercially viable fluxes of over 100 LMH when filtering 5 and 10 wt% MPI. Permeate flux was lowest for the 1.4 µm membrane between 12.3 - 30.9 LMH (for 5 – 15 wt%) with the 0.8 µm membrane having the next highest between 18.6 - 39.1 LMH (for 5 – 15 wt%), flux continued to increase with pore size with the 12.0 µm membrane having the highest between 9.8 - 122.8 (for 10 – 15 wt%). The 1.4 µm membrane displayed the lowest flux. As this membrane has pores of a similar size to those of a *Bacillus mycoides* spore, it seems likely that pore plugging is occurring during fouling, resulting in a lower steady state permeate flux than that seen for the 0.8 µm membrane. The 1.4 µm membrane produced a flux of 12.3 LMH, compared to a flux value of 23.0 LMH produced through the 0.8 µm membrane, when filtering 15 wt% MPI at 1.4 m s^{-1}. Solids and protein transmission both increased with increasing membrane pore size. If considering flux alone, both the 5.0 or 12.0 µm membranes would be suitable for the filtration of MPI, however spore rejection also needs to be considered.

For the 2.0, 5.0 and 12.0 µm membranes (all of a pore size larger than that of the spores), spore rejections were found to increase with increasing MPI concentration and to decrease with increasing CFV. This increase in spore rejection was 1.8 log orders when increasing the MPI concentration from 5 to 15 wt% for the 2.0 µm membrane, a 0.9 log order increase for the 5.0 µm membrane, and a 1.2 log order increase for the 12.0 µm membrane. The decrease in spore rejection when filtering 15 wt% MPI with increasing CFV from 0.7 to 1.4 m s^{-1} was 1.0 log orders for the 2.0 µm membrane, 0.8

log orders for the 5.0 µm membrane and 0.5 log orders for the 12.0 µm. Mechanistically, increases in MPI concentration and reductions in CFV both lead to a greater amount of fouling on the membrane surface. Such fouling layers act as an additional (secondary) filtration layer, thereby increasing spore rejection. In contrast for the 0.8 and 1.4 µm membranes (those of a smaller or similar size to the spores) the spore rejection values were relatively unchanged with increasing CFV and MPI concentration.

In certain membrane systems it is possible to selectively absorb key foulants onto the filter surface, leading to the generation of a beneficial fouling layer. Such a layer can lead to improvements in permeate flux and selectivity (Jones *et al.,* (2011); Evans and Bird, 2010; Wu and Bird, 2007). Within the filtration systems used in this thesis MPI foulant adsorption does not appear to increase permeate flux but in larger pore sized membranes it does lead to a greater selectivity in the form of a higher spore log reduction as the MPI foulant acts as an additional (secondary) filtration layer. The development of a beneficial secondary layer for bacteria removal through ceramic microfiltration membranes does not always occur. Bendick *et al*., 2005 reported during the filtration of primary sewage effluent through ceramic membranes between 0.05 – 1.4 µm that as pore size increased this lead to an increase in bacteria transmission regardless of variation in process conditions.

When analysing each of the membranes data sets in terms of permeate flux, solid and protein transmission, and spore rejection it was concluded that both the 1.4 and 5.0 µm membranes were unsuitable, and were eliminated from further testing. The 1.4 µm membrane was deemed unsuitable for further trials, as it produced low fluxes of between 12.3 and 30.9 LMH along with low solid and protein transmission values of between 6.4 - 31.4 % and 15 - 40.4 % respectively. In addition, the 1.4 µm membrane gave a low spore reduction of between 1.8 & 2.3 log orders. This may have been the result of this membrane pore size being between the *Bacillus mycoides* spore length and width resulting in only a partial separation (Mukhopadhyay *et al.,* 2010). The 5.0 µm membrane was discarded even though it produced relatively high fluxes between 14.0 - 371.7 LMH and solid and protein transmissions of between 61.1 - 66.0 % and 67.0 – 86.7 % respectively. This was due to the very low spore reduction achieved of between 1.1 & 2.0 log order reductions. It was therefore concluded that the 0.8, 2.0 and 12.0 µm membranes showed the most promising results under the conditions tested.

4.6.3 Fouling resistance (R_F) variation with changing MPI concentration and membrane pore size

The membrane resistance (R_m) values calculated from the PWF measured at the start of each experiment and the total resistances (R_T) calculated using the steady state permeate fluxes were used to calculate the fouling resistance (R_F) using equation 28, for each experiment and can be found in Tables 27 – 31.

$$R_F = R_T - R_M \quad (28)$$

As expected, for each of the membranes tested, fouling resistance (R_F) increased with increasing MPI feed concentration. When filtering 15 wt% MPI, R_F tended to decrease with increasing CFV apart from when filtering through the 1.4 µm membrane. When filtering 15 wt% MPI using the 0.8 µm membrane, R_F decreased from 3.32 x 10^{13} m^{-1} when filtering at 0.7 m s^{-1} to 2.83 x 10^{13} m^{-1} when filtering at 1.4 m s^{-1} (Table 27)

When filtering 15 wt% MPI using the 2.0 µm membrane, R_F decreased from 5.36 x 10^{13} m^{-1} at 0.7 m s^{-1} to 4.92 x 10^{13} m^{-1} at 1.4 m s^{-1} (Table 29). Filtering 15 wt% MPI using the 5.0 µm membrane, R_F decreased from 7.56 x 10^{12} m^{-1} at 0.7 m s^{-1} to 3.79 x 10^{12} m^{-1} at 1.4 m s^{-1} (Table 30). Lastly, when using the 12.0 µm membrane to filter 15 wt% MPI, R_F values decreased from 9.69 x 10^{12} m^{-1} at 0.7 m s^{-1} to 3.8 x 10^{12} m^{-1} at 1.4 m s^{-1} (Table 31).

The effect of pore size upon R_F value was examined, but did not show a clear trend, reflecting the combination and relative magnitude of in-pore and cake fouling mechanisms likely to be dominating the filtration process at different membrane pore sizes. The lowest value of R_F was 9.66 x 10^{11} m^{-1}, found when filtering 5 wt% MPI using the 5.0 µm membrane. The highest value of R_F was 5.36 x 10^{13} m^{-1}, found for the filtration of 15 wt% MPI solution using a 2.0 µm membrane.

4.6.4 Spore rejection values

The 5.0 µm membrane produced very low spore reductions between 1.1 - 2.0 log orders, and as a result was not selected for further trials. However, the 2.0 and 12.0 µm membranes both produced acceptable spore reduction values of 2.1 – 3.9 and 1.4 - 2.6 log orders respectively, and so were tested with backwashing in order to try and achieve

a higher permeate flux value. The 0.8 µm membrane was also subjected to additional trials as it showed a high log order reduction of 2.4 - 4.4 log orders. As a result it was thought the use of backwashing might be able to increase the solid transmission closer to the values achieved for the 2.0 and 12.0 µm membranes.

4.6.5 Calculation of mass transfer coefficients (*k*) and membrane surface concentrations (C_M)

Mass transfer coefficients (*k*) and membrane surface concentrations (C_M) were determined at steady state fluxes. Experiments were carried out at a CFV of 1.4 m s^{-1}, a temperature of 50 °C and a TMP of 2 bar, using a range of MPI concentrations. Equation 30 (derived from film-layer theory) indicates that a plot of ln $[(1-R_{coeff})/R_{coeff}]$ against permeate flux (J_v) generates a straight line (R_{coeff} is the observed rejection coefficient calculated from equation 29), where C_p is the MPI wt% in the permeate and C_B is the MPI concentration in the bulk stream. The mass transfer coefficient (*k*) is calculated from the slope of this plot (1/*k*). The maximum rejection coefficient, R_{max}, can be determined from the intercept, and used to calculate the value of the membrane surface concentration (C_M) (Mulder, 2000). Table 8 shows the resulting mass transfer coefficients and membrane surface concentrations so determined, in addition to the bulk stream concentration values (C_B), permeate concentration values (C_p) and R_{coeff} and R_{max} for each experiment.

$$R_{coeff} = 1 - \frac{C_p}{C_B} \tag{29}$$

$$\ln\left[\frac{1-R_{coeff}}{R_{coeff}}\right] = \ln\left[\frac{1-R_{\max}}{R_{\max}}\right] + \frac{J_v}{k} \tag{30}$$

The mass transfer coefficients (*k*) get larger as membrane pore size increases (Table 32). This was expected, as the larger the pore size the easier it is for solute to pass through the membrane. The concentration at the membrane surface, C_M, was much larger for 0.8 and 1.4 µm membranes, compared to the other membranes tested. The values of C_M obtained were 35.7 - 36.6 and 41.7 - 35.8 wt% higher than that of C_B for the two pore sizes respectively. By comparison, for the 12.0 µm membrane the value of C_M was only 0.27 - 0.45 wt% higher than the value obtained for C_B. This difference is reflected in the permeate flux, solids and protein transmission values found for the membranes tested,

all of which were much lower for the 0.8 and 1.4 µm membranes when compared to the larger pore sized membranes tested.

Table 32. Mass transfer coefficients (*k)* and membrane surface concentrations (C_m) during filtration through five tubular ceramic membranes with varying MPI feed wt% (C_B) using a CFV of 1.4 m s^{-1}, a TMP of 2 bar and a filtration temperature of 50 °C.

Membrane (µm)	C_B (wt%)	C_P (wt%)	R_{coeff}	R_{max}	*k* (m s^{-1})	C_M (wt%)
0.8	9.81	0.74	0.93	0.98	6.77 x 10^{-6}	46.41
	15.70	0.82	0.96	0.98	6.77 x 10^{-6}	51.43
1.4	10.16	1.64	0.84	0.97	2.57 x 10^{-6}	51.81
	15.10	1.61	0.89	0.97	2.57 x 10^{-6}	50.86
2.0	4.97	1.99	0.6	0.89	1.1 x 10^{-5}	18.00
	10.09	2.54	0.75	0.89	1.1 x 10^{-5}	22.97
	16.34	1.82	0.89	0.89	1.1 x 10^{-5}	16.46
5.0	4.76	2.91	0.39	0.34	4.64 x 10^{-4}	4.75
	9.54	6.13	0.36	0.34	4.64 x 10^{-4}	10.01
	15.41	10.17	0.34	0.34	4.64 x 10^{-4}	16.60
12.0	9.74	6.84	0.3	0.33	2.53 x 10^{-4}	10.19
	15.15	10.35	0.32	0.33	2.53 x 10^{-4}	15.42

4.6.6 Effect of increasing CFV from 1.4 to 1.7 m s^{-1} during filtration of 5 wt% MPI solutions

The modifications made to filtration set-up 1 were intended to increase the CFV able to be reached during filtration of 15 wt% MPI solutions but only increased the CFV that 5 wt% MPI could be filtered at from 1.4 to 1.7 m s^{-1}. The difference in steady state permeate flux, solids transmission, spore rejection and R_F values found at 1.7 compared to 1.4 m s^{-1} during filtration of 5 wt% MPI through the 0.8 and 1.4 µm *Membralox*™ membrane can be found in Table 33. Figures 75a and 76b show the change in permeate flux with time and the membrane resistance data graphs.

Table 33. Change in steady state permeate flux, spore rejection, solids transmission and protein transmission during filtration of 5 wt% MPI through a 0.8 and 1.4 µm membrane at 1.4 or 1.7 m s^{-1}.

Pore size (µm)	CFV (m s^{-1})	Flux (LMH)	Solids transmission (%)	Spore reduction		R_F (m^{-1}) x10^{13}
				%	log	
0.8	1.4	39.1	19.8	99.996	4.4 ± 0.2	1.35
0.8	1.7	39.7	21.4	99.997	4.5 ± 0.1	1.35
1.4	1.4	30.9	31.4	98.4	1.8 ± 0.2	2.15
1.4	1.7	36.1	34.2	98.65	1.9 ± 0.2	1.86

As can be seen from Table 33 the increase in CFV from 1.4 to 1.7 m s^{-1} produced a slight increase in permeate flux and solids transmission for both tested membranes. Permeate flux and solid transmission increased by 0.6 LMH (1.5%) and 1.6% for the 0.8 µm membrane and by 5.2 LMH (16.8%) and 2.8% for the 1.4 µm membrane. In contrast spore reductions remained relatively unchanged for both membranes along with the fouling resistance for the 0.8 µm membrane but decreased by 2.9 x 10^{12} m^{-1} for the 1.4 µm membrane. These results were expected as increases in CFV result in a higher shear stress at the membrane surface causing more of the rejected material that has become loosely attached to the membrane surface to be removed and transported back to the bulk flow. As more fouling material is removed as long as the remaining material does not reorganise itself into a more compact cake this should lead to a decrease in fouling resistance and as a result an increase in permeate flux and solid transmission.

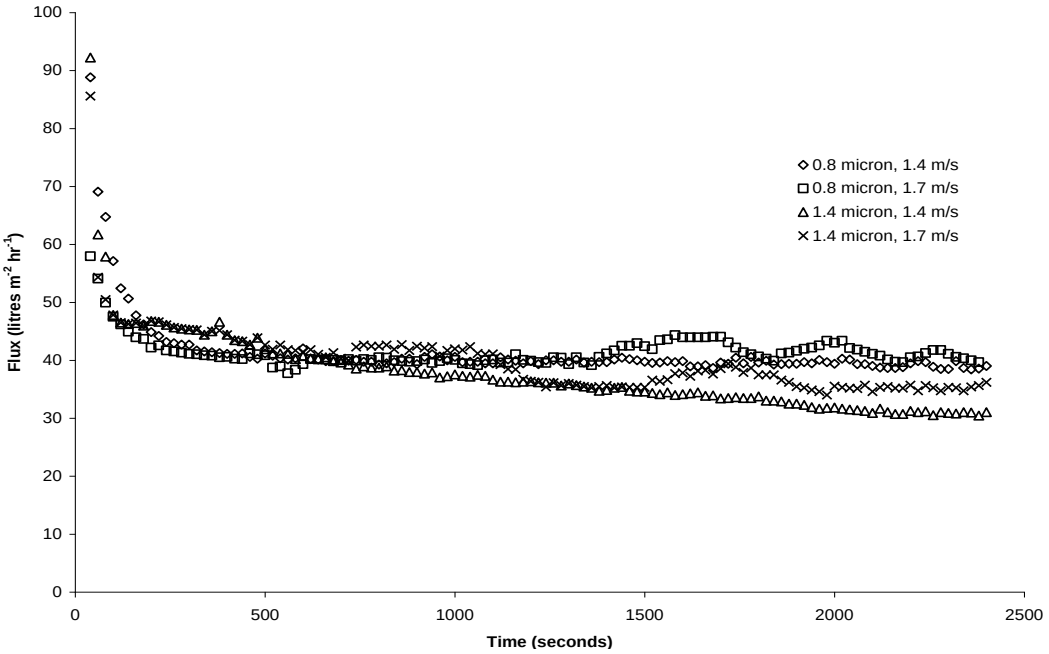

(a)

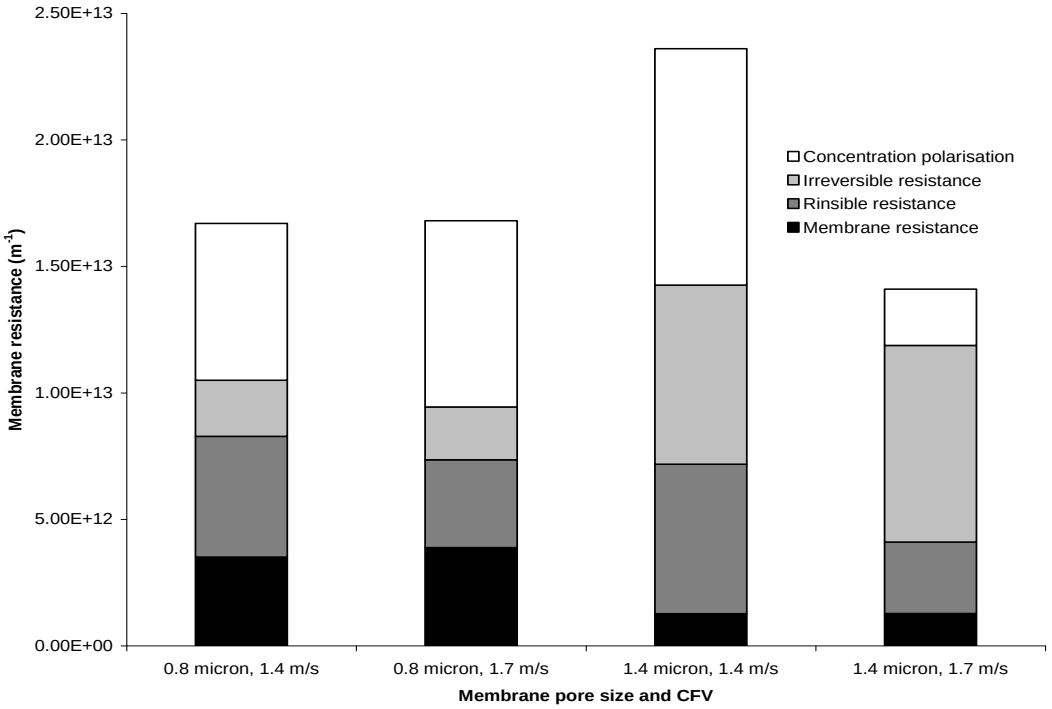

(b)

Figure 75. a) Change in permeate flux with time during filtration of 5 wt% MPI through a 0.8 and 1.4µm Membralox™ *membrane using either a 1.4 or 1.7 m* s^{-1} *CFV, 50 °C and 2 bar TMP, b) corresponding change in membrane resistance.*

4.6.7 Summary of results

When analysing each of the membranes data sets using set-up 2 (Tables 27 - 31) in terms of permeate flux, solid and protein transmission, and spore rejection it was concluded that both the 1.4 and 5.0 µm membranes were unsuitable, and were eliminated from further testing. The 1.4 µm membrane was deemed unsuitable for further trials, as it produced low fluxes of between 12.3 and 30.9 LMH along with low solid and protein transmission values of between 6.4 - 31.4 % and 15 - 40.4 % respectively. In addition, the 1.4 µm membrane gave a low spore reduction of between 1.8 & 2.3 log orders. The 5.0 µm membrane was discarded even though it produced relatively high fluxes between 14.0 - 371.7 LMH and solid and protein transmissions of between 61.1 - 66.0 % and 67.0 – 86.7 % respectively. This was due to the very low spore reduction achieved of between 1.1 & 2.0 log order reductions. It was therefore concluded that the 0.8, 2.0 and 12.0 µm membranes showed the most promising results under the conditions tested.

4.6 FILTRATION EXPERIMENTS USING FILTRATION SET UP 3

4.7.1 Filtration of 15 wt% MPI using a CFV of 2.0 m s^{-1} through 0.8, 2.0 and 12.0 µm membranes

As detailed in section 2.9.2 the modifications made to set-up 2 producing set-up 3 of the filtration system resulted in a higher CFV value of 2.0 m s^{-1} being able to be tested. Experiments were performed on each of the 0.8, 2.0 and 12.0 µm membranes that showed the most promising results at the lower CFV values, using a 15 wt% MPI feed at 2.0 m s^{-1}, 50 °C and 2 bar TMP. Table 34 shows the permeate flux, solids and protein transmission and spore rejection measured at steady state for the 0.8, 2.0 and 12.0 µm membranes respectively. Figures 77a and 77b show the respective change in permeate flux with time and the membrane resistance data graphs.

Table 34. Effect of ceramic membrane pore size upon 15 wt% MPI filtration performance at a CFV of 2.0 m s^{-1}, 50 ºC temperature and a TMP of 2.0 bar.

	At steady state (After 40 minutes)					
Pore size (µm)	Flux (LMH)	Solids transmission (%)	Spore reduction		Protein transmission (% of feed protein content)	R_F (m^{-1}) x10^{12}
			%	log		
0.8	21.8	5.3	99.992	4.2 ± 0.6	12.6	13.5
2.0	17.9	20.0	96.182	1.4 ± 0.5	46.3	18.3
12.0	26.2	67.9	96.918	1.5 ± 0.9	88.2	2.61

Increasing the CFV from 1.4 to 2.0 m s^{-1} when filtering 15 wt% MPI through the 0.8 µm membrane led to an increase in solids and protein transmission values of 1.5 and 4.8 % respectively (comparison of Tables 27 and 34). The permeate flux remained low, and the spore reduction remained high. Results obtained for the 2.0 µm membranes show that the permeate flux, solids and protein transmission all increased by 5.0 LMH, 7.1 and 7.7 % respectively, with the increase in CFV but were all still relatively low and the spore reduction decreased dramatically by 1.5 log orders (comparison of Tables 29 and 34). Lastly, the 12.0 µm membrane showed a slight decrease in permeate flux, solid and protein transmission and a 0.6 lower log order reduction at a CVF of 2.0 m s^{-1} (comparison of Tables 31 and 34).

Increasing CFV led to a large decrease in spore reduction during filtration through the 2.0 and 12.0 µm membranes. This can be explained as increasing CFV leads to a decrease in the amount of fouling on the membrane surface. When the *Bacillus mycoides* spores are smaller than the membrane pores, and the rejection is still high, the fouling layer must provide an additional filtration resistance. Decreasing the thickness of this fouling layer leads to a desirable effect of increasing the permeate flux and solid and protein transmission shown by the 2.0 µm membrane, but can also lead to a decrease in the spore reduction values achieved. This implies that an optimal amount of membrane surface fouling is needed if the membrane pores are significantly larger than the size of the spores.

For the 0.8 µm membrane, solids and protein transmission values increased when the CFV was increased from 1.4 - 2.0 m s^{-1}, but these values along with the permeate flux are still too low to be considered to be commercially viable. The spore rejection remained high due to the fact that the pores were smaller than the size of the spores. Increasing the CFV above 2.0 m s^{-1} appeared unlikely to improve the flux, with the highest solids transmission of 7.3% found at the lowest CFV of 0.7 m s^{-1} tested. However, the use of backwashing as another method of flux enhancement was investigated as discussed in sections 4.7.3, 4.7.4, 4.7.5 and 4.7.6.

Bendick *et al*., 2005 reported a similar effect during the filtration of primary sewage effluent through ceramic microfiltration membranes between 0.05 – 1.4 µm. Permeate flux was found to increase with increasing CFV from 0.5 – 1.8 m s^{-1} but when CFV was increased further up to 3.7 m s^{-1} any further increase in permeate flux was negligible.

4.7.2 Fouling resistance (R_F) variation with increasing CFV

Fouling resistances (R_F) for each filtration experiment using a 15 wt% MPI feed carried out at 2.0 m s^{-1} can be found within Table 34. The decrease in R_F trend found with increasing CFV from 0.7 to 1.4 m s^{-1} continued when CFV was increased further to 2.0 m s^{-1} for each of the membranes tested. With R_F decreasing from 2.83 x 10^{13} m^{-1} when filtering at 1.4 m s^{-1} to 1.35 x 10^{13} m^{-1} at 2.0 m s^{-1} through the 0.8 µm membrane (comparison of Tables 27 and 34). For the 2.0 µm membrane R_F decreased from 4.92 x 10^{13} m^{-1} at 1.4 m s^{-1} to 1.83 x 10^{13} m^{-1} at 2.0 m s^{-1} (comparison of Tables 29 and 34). Lastly, when using the 12.0 µm membrane to filter a 15 wt% MPI solution, R_F values

decreased from 3.8 x 10^{12} m^{-1} at 1.4 m s^{-1} to 2.61 x 10^{12} m^{-1} at 2.0 m s^{-1} (comparison of Tables 31 and 34).

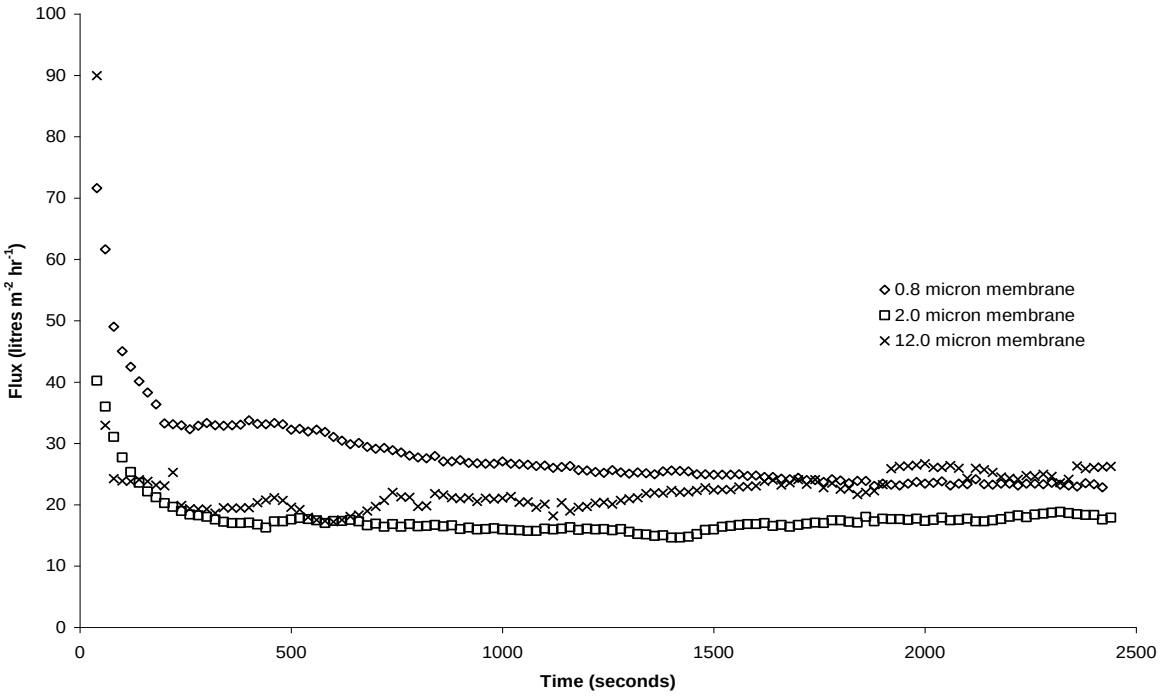

(a)

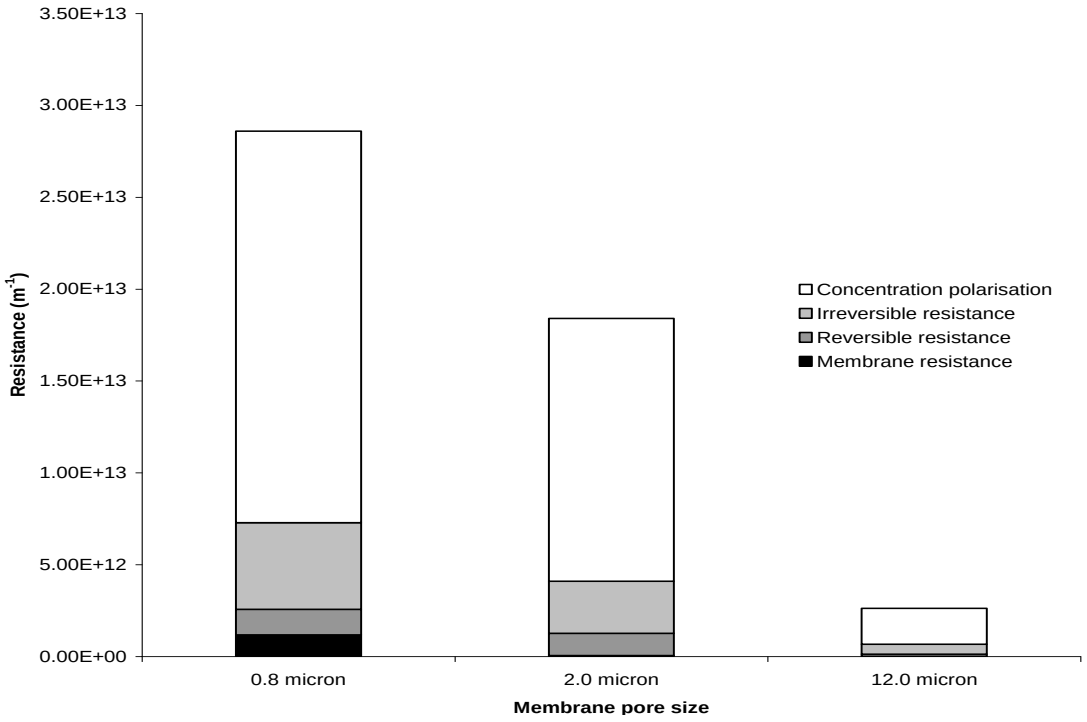

(b)

Figure 76.a) Change in permeate flux with time during filtration of 15 wt% MPI through a 0.8, 2.0 and 12.0 µm Membralox^{TM} *membrane at 2.0 m s^{-1} CFV, 50 °C and 2 bar TMP, b) Corresponding change in membrane resistance.*

4.7.3 Effects of backflushing on steady state permeate flux, solid transmission and total MPI collected during filtration using 0.8, 2.0 and 12.0 µm membranes.

Filtration experiments have been carried out using a 15 wt% MPI feed, 50 °C temperature and 2 bar TMP, through a 0.8, 2.0 and 12.0 µm membrane. These three membranes as well as the CFV's used were selected based on the initial filtration results found during the experiments carried out to try and determine the optimum membrane pore size and filtration conditions for high solids content MPI solution filtration. Experiments were carried out under normal crossflow conditions and also using backflushing for 10 seconds every 5 minutes at 1 bar. Table 35 shows the experimental conditions used and the resulting steady state permeate flux, solid transmission and total resistance (R_T) values as well as the total MPI collected for each run carried out through the 0.8 µm membrane. Figure 77 shows the corresponding change in permeate flux with time and membrane resistance graphs for each CFV tested with and without backflushing.

Table 35. Comparison of the steady state permeate fluxes and solid transmissions along with the total MPI collected during experiments through the 0.8 µm membrane using optimum experimental conditions with and without backflushing.

		Steady state			
Backwashing conditions	CFV ($m\ s^{-1}$)	Flux (LMH)	Solids transmission (%)	$R_T\ (m^{-1})\ x10^{13}$	Total permeate collected during run (g's)
No backwashing	0.7	10.9	4.6	6.41	94.3
1 bar-10 seconds every 5 minutes	0.7	12.0	2.1	6.09	28.6
No backwashing	1.4	14.0	4.8	4.60	132.7
1 bar-10 seconds every 5 minutes	1.4	17.0	4.7	3.99	107.9
No backwashing	2.0	22.8	5.5	3.22	191.3
1 bar-10 seconds every 5 minutes	2.0	28.8	3.5	2.44	129.2

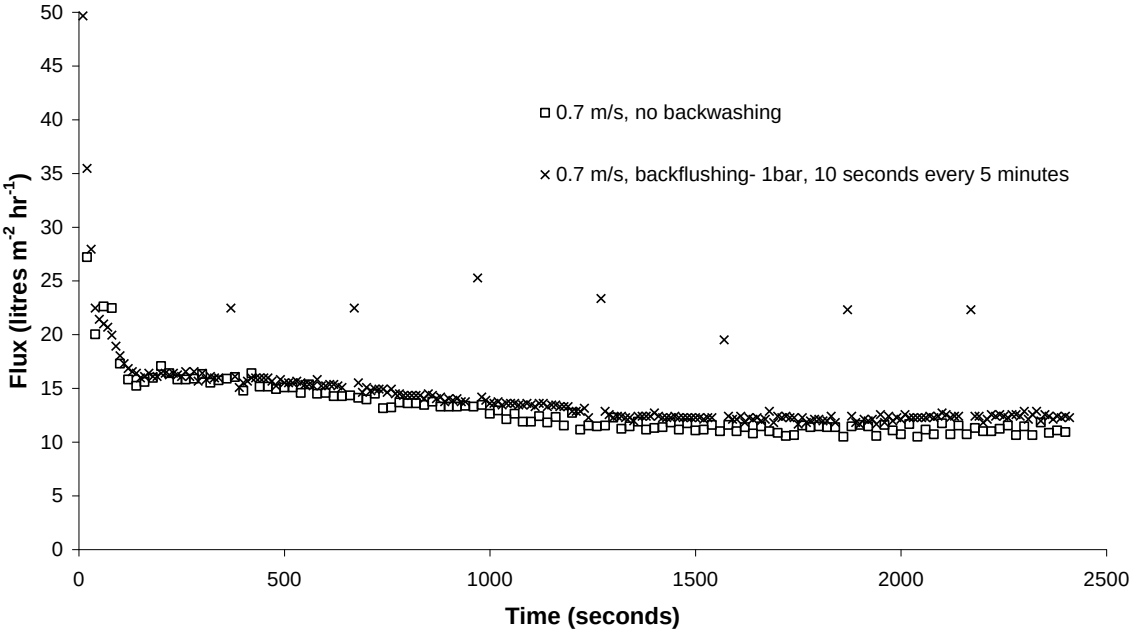
0.7 m/s, no backwashing
0.7 m/s, backflushing- 1bar, 10 seconds every 5 minutes
Flux (litres m-2 hr-1)
Time (seconds)

(a)

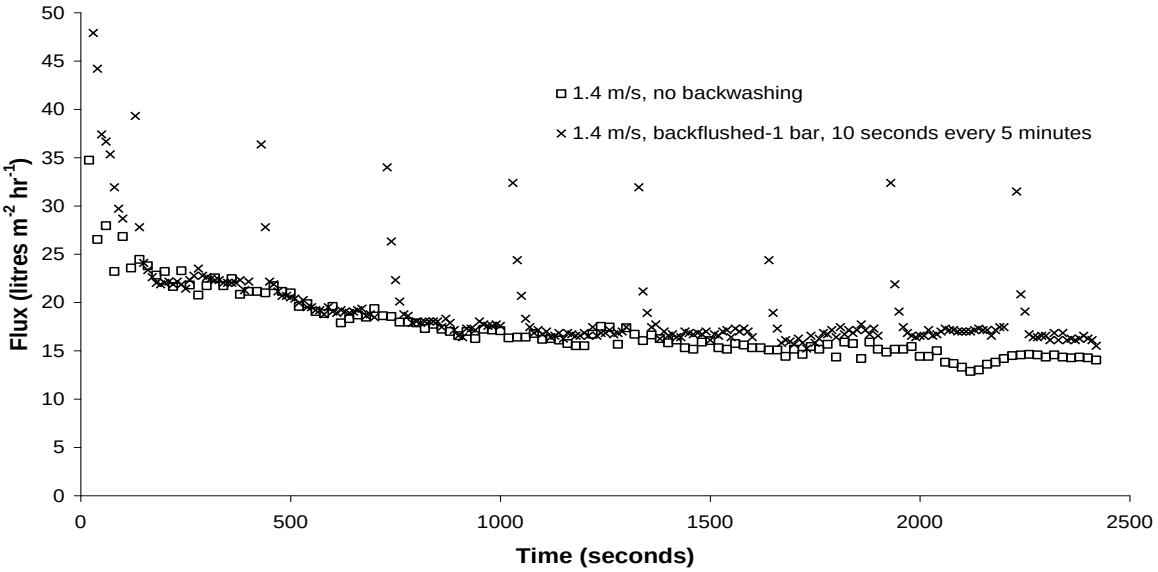
1.4 m/s, no backwashing
1.4 m/s, backflushed-1 bar, 10 seconds every 5 minutes
Flux (litres m-2 hr-1)
Time (seconds)

(b)

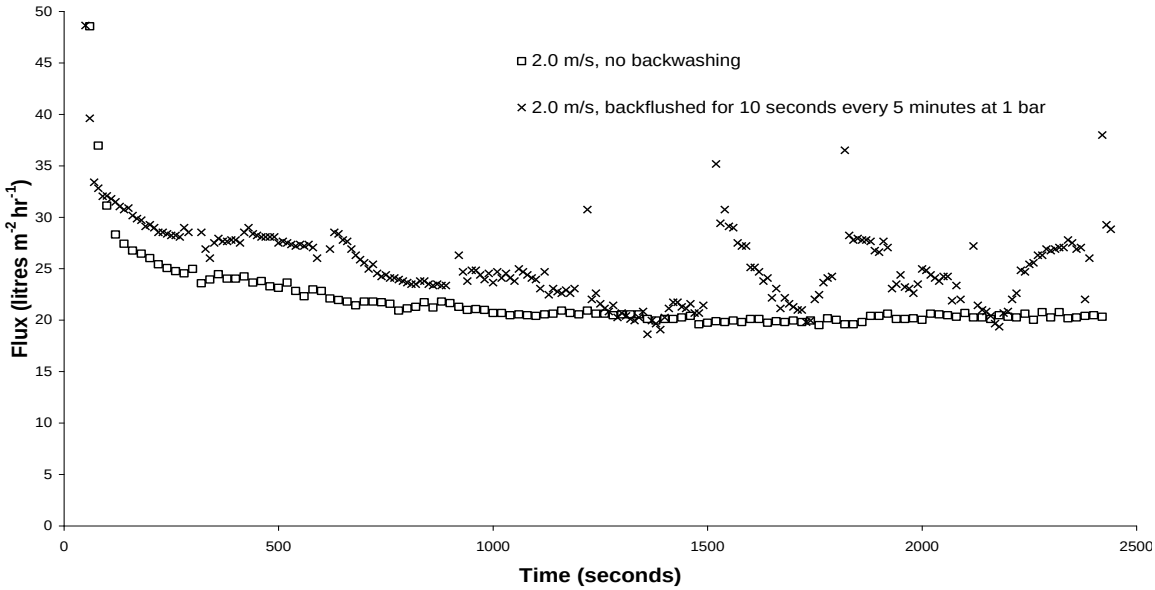
2.0 m/s, no backwashing
2.0 m/s, backflushed for 10 seconds every 5 minutes at 1 bar
Flux (litres m-2 hr-1)
Time (seconds)

(c)

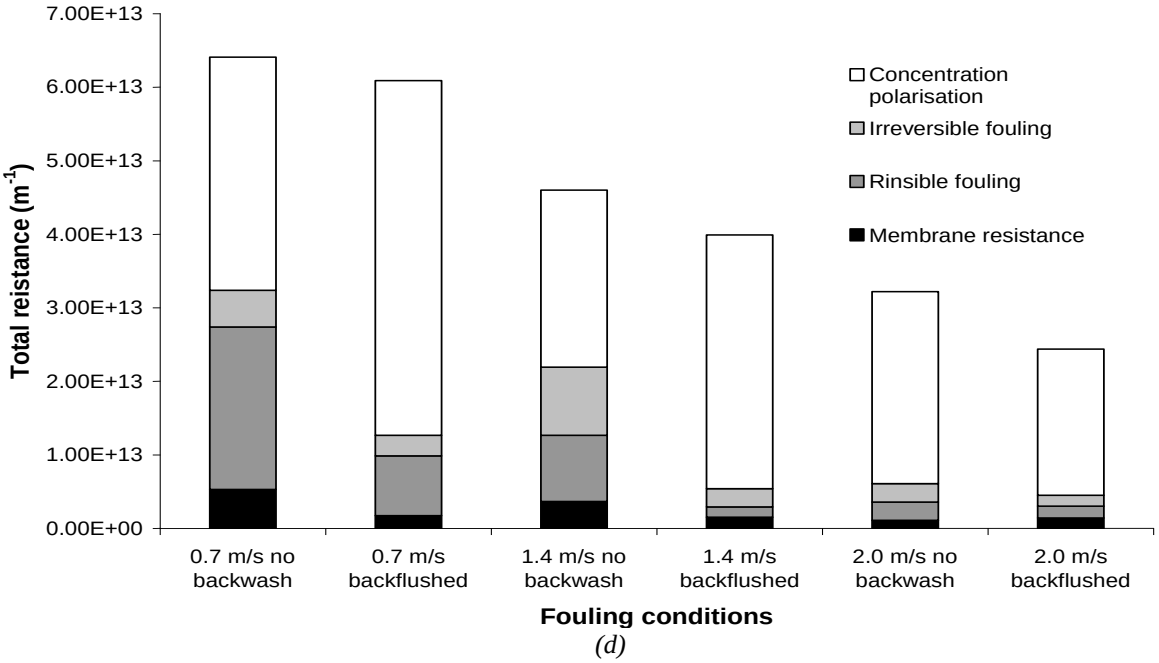

(d)

Figure 77. a) Comparison of the change in permeate with time with and without backflushing (30 seconds every 5 minutes at 1 bar) 0.7 m s^{-1} CFV, 50 °C, 2 bar through a 0.8 µm Membralox^{TM} *membrane,* b) 1.4 m s^{-1} CFV, c) 2.0 m s^{-1} CFV and d) the change in membrane resistances with different filtration conditions.

Backflushing for each CFV tested through the 0.8 µm membrane resulted in an increase in steady state permeate flux 1.1 LMH (10.1%) for 0.7 m s^{-1}, 3.0 LMH (21.4%) for 1.4 m s^{-1} and 6.0 LMH (26.3%) for 2.0 m s^{-1} but led to a decrease in solid transmission and therefore also a decrease in the total MPI collected during the run. This implies that backflushing forces more water from the feed through the membrane leading to a higher permeate flux but that the permeate contains less MPI solid compared to without BF. Total membrane resistance was found to decrease with increasing CFV and also with BF. Specifically at the lower CFV's (0.7 and 1.4 m s^{-1}) BF led to a decrease in reversible (R_R) and irreversible (R_I) fouling resistances from 2.21 x 10^{13} to 8.13 x 10^{12} m^{-1} and 4.99 to 2.8 x 10^{12} for R_R and R_I respectively at 0.7 m s^{-1} and 9.02 to 1.39 x 10^{12} and 9.25 to 2.48 x 10^{12} m^{-1} for R_R and R_I respectively at 1.4 m s^{-1} CFV but an increase in concentration polarisation (R_{CP}) 3.17 to 4.82 x 10^{13} m^{-1} for 0.7 m s^{-1} and 2.41 to 3.45 x 10^{13} for 1.4 m s^{-1}. This may be because BF causes any adhering reversible and irreversible fouling deposits to be removed from the membrane surface but as the CFV is not high enough, these deposits are not swept effectively back into the bulk stream and remain in the vicinity of the surface, thereby increasing the effect of concentration polarisation. At CFV values of 2.0 m s^{-1} the reversible, irreversible and concentration polarisation resistances are all decreased with the application of BF 2.48 to 1.61 x 10^{12} m^{-1} for R_R 2.50 to 1.49 x 10^{12} m^{-1} for R_I and 2.61 to 1.99 x 10^{13} m^{-1} for R_{CP}.

At the higher CFV value of 2.0 m s^{-1}, the reversible and irreversible resistances do not decrease as much as with the other lower CFV's tested (0.7 and 1.4 m s^{-1}). This is because the higher CFV values resulted in reduced foulant deposition on the membrane surface, with BF still leading to an enhanced removal of the deposition that has occurred.

Table 36. Comparison of the steady state permeate fluxes and solid transmissions along with the total MPI collected during experiments through the 2.0 µm membrane using optimum experimental conditions with and without backflushing.

		At steady state			
Backwashing conditions	CFV (m s^{-1})	Flux (LMH)	Solids transmission (%)	R_T (m^{-1}) x10^{13}	Total permeate collected during run (g's)
No backwashing	0.7	11.8	8.5	5.36	161.9
1 bar-10 seconds every 5 minutes	0.7	12.7	7.1	4.70	113.3
No backwashing	1.4	13.2	11.1	4.92	216.5
1 bar-10 seconds every 5 minutes	1.4	26.2	23.7	1.32	521.2

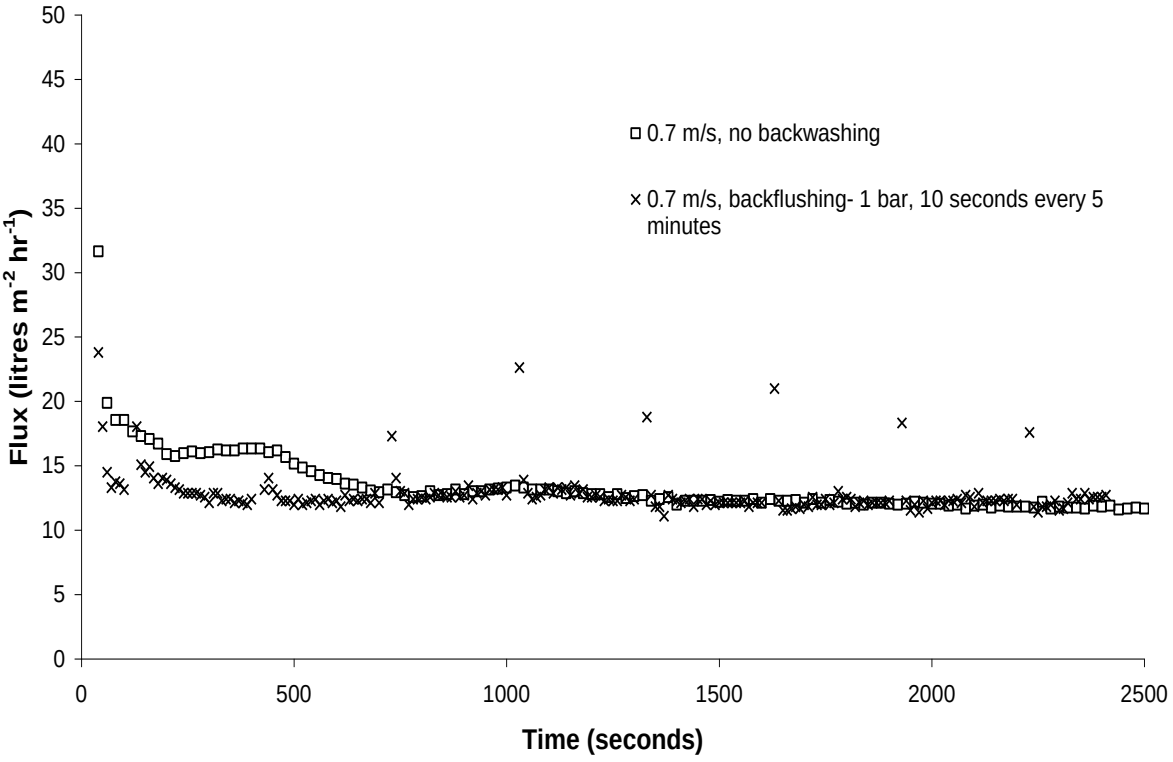

(a)

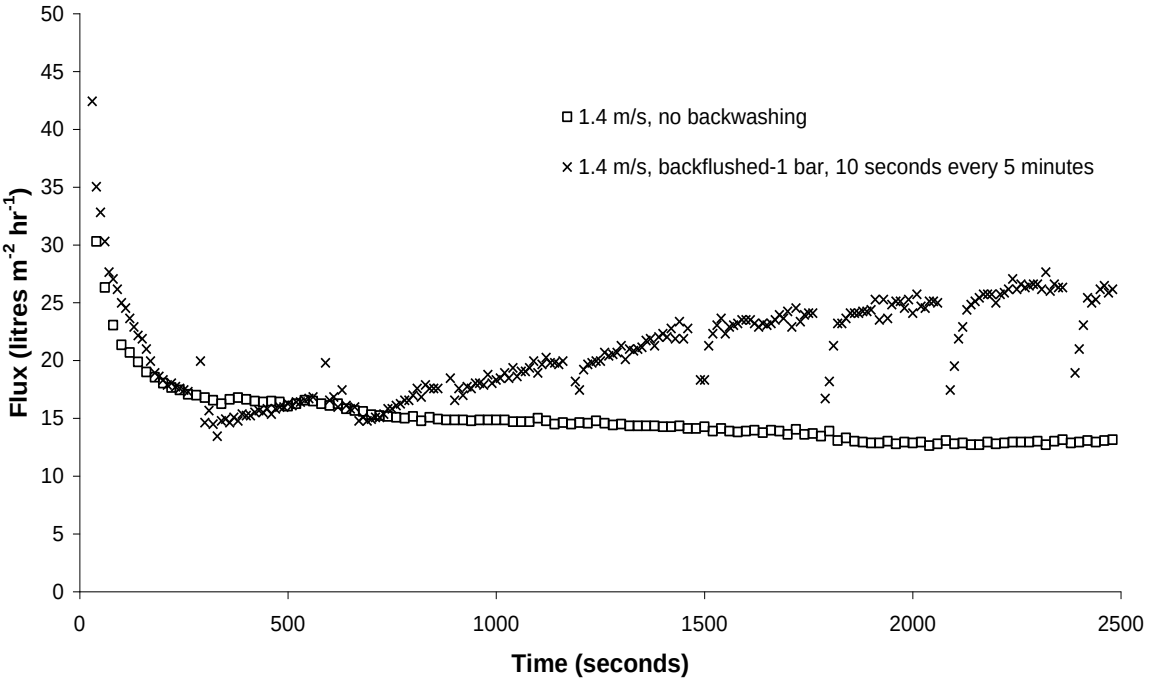

(b)

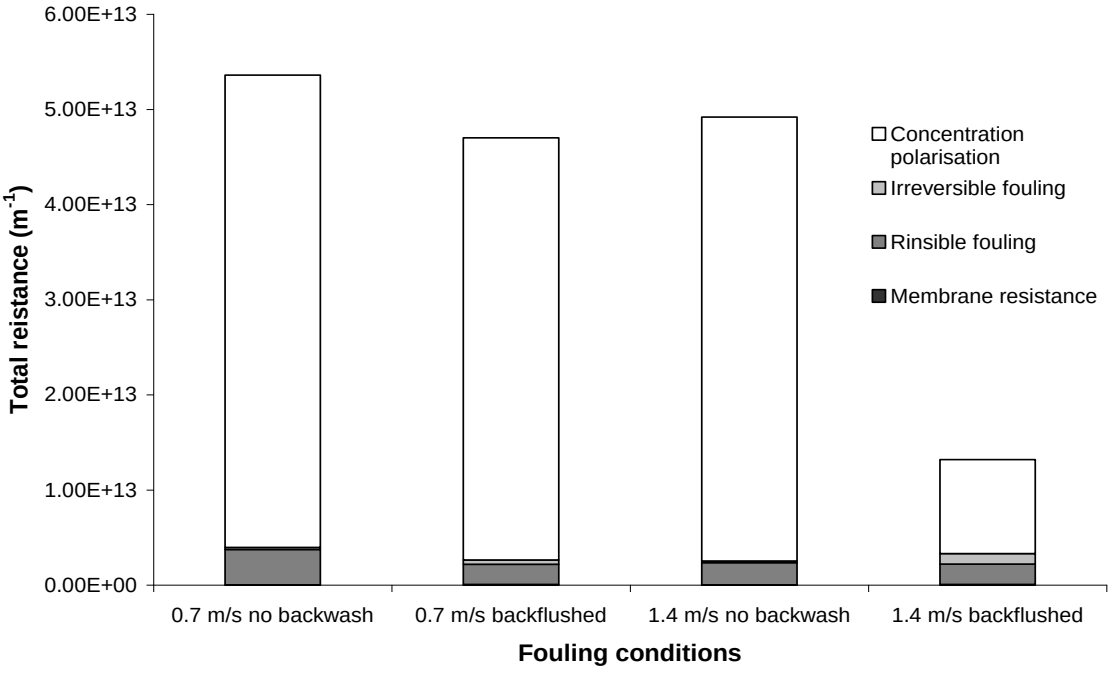

(c)

Figure 78. a) Comparison of the change in permeate with time with and without backflushing (30 seconds every 5 minutes at 1 bar) 0.7 m s^{-1} CFV, 50 °C, 2 bar through a 2.0 µm membrane, b) 1.4 m s^{-1} CFV, and c) the change in membrane resistances with different filtration conditions.

Similar experiments were carried out using the 2.0 µm membrane but using just 0.7 and 1.4 m s^{-1} CFV as it was found previously during this work (section 4.7.1) that using a 2.0 m s^{-1} CFV led to only a very low spore reduction of 1.4 ± 0.5 cfu ml^{-1} (log order reduction) compared to 3.9 ± 1.0 and 2.9 ± 0.6 log order reductions for 0.7 and 1.4 m s^{-1}

respectively. Table 36 shows the experimental conditions used and the resulting steady state permeate flux, solid transmission and total resistance (R_T) values as well as the total MPI collected for each run carried out using the 2.0 µm membrane. Figure 78 shows the corresponding change in permeate flux with time and membrane resistance graphs for each CFV tested with and without BF. BF led to an increase in permeate flux when filtering using both 0.7 and 1.4 m s^{-1} CFV's producing a 0.9 LMH (7.6%) and 13.0 LMH (98.5%) increase respectively. Similar to the 0.8 µm membrane 0.7 m s^{-1} experiment this increase was associated with a decrease in solid transmission at 0.7 m s^{-1} of 1.4% and total MPI collected of 48.6g. However, the application of BF at 1.4 m s^{-1} CFV led to an increase in solid transmission of 113.5% and total MPI collected 304.7g (140.7%). The change in permeate flux with time plot for the BF filtration experiment using 1.4 m s^{-1} CFV has a very different shape compared to the other permeate flux graphs. At the start of the filtration permeate flux decreases and follows a similar pattern to that produced without BF, but after the first BF permeate flux increases and continues to increase with each BF. It appears that under these conditions BF is very effective and that each BF is gradually removing the foulant that is deposited at the start of the filtration. This may be because this membranes pore diameter is larger than the 0.8 µm membrane, which allows a much easier passage of the backwashed water back through the pores, causing more foulant to be removed from the membrane surface.

As with the 0.8 µm membrane total membrane resistance was found to decrease with increasing CFV and also with BF. For both CFV's tested BF was found to decrease both reversible fouling and concentration polarisation resistance by 3.73 to 2.13 x 10^{12} m^{-1} for R_R and 4.97 to 4.44 x 10^{13} m^{-1} for R_{CP} at 0.7 m s^{-1} CFV and by 2.35 to 2.13 x 10^{12} m^{-1} for R_R and 4.67 x 10^{13} to 9.88 x 10^{12} m^{-1} at 1.4 m s^{-1} CFV but increased irreversible resistance by 2.03 to 4.48 x 10^{11} m^{-1} and 1.66 x 10^{11} to 1.12 x 10^{12} m^{-1} for 0.7 and 1.4 m s^{-1} CFV respectively. This may be because the application of BF has caused any loosely adhering reversible fouling to be removed and the concentration polarisation layer to be disturbed but through clearing the membrane surface of these loosely adhering or surrounding deposits allowed the remaining foulant to become more compacted either on the membrane surface, or indeed in the membrane pores, and thereby converted into irreversible fouling.

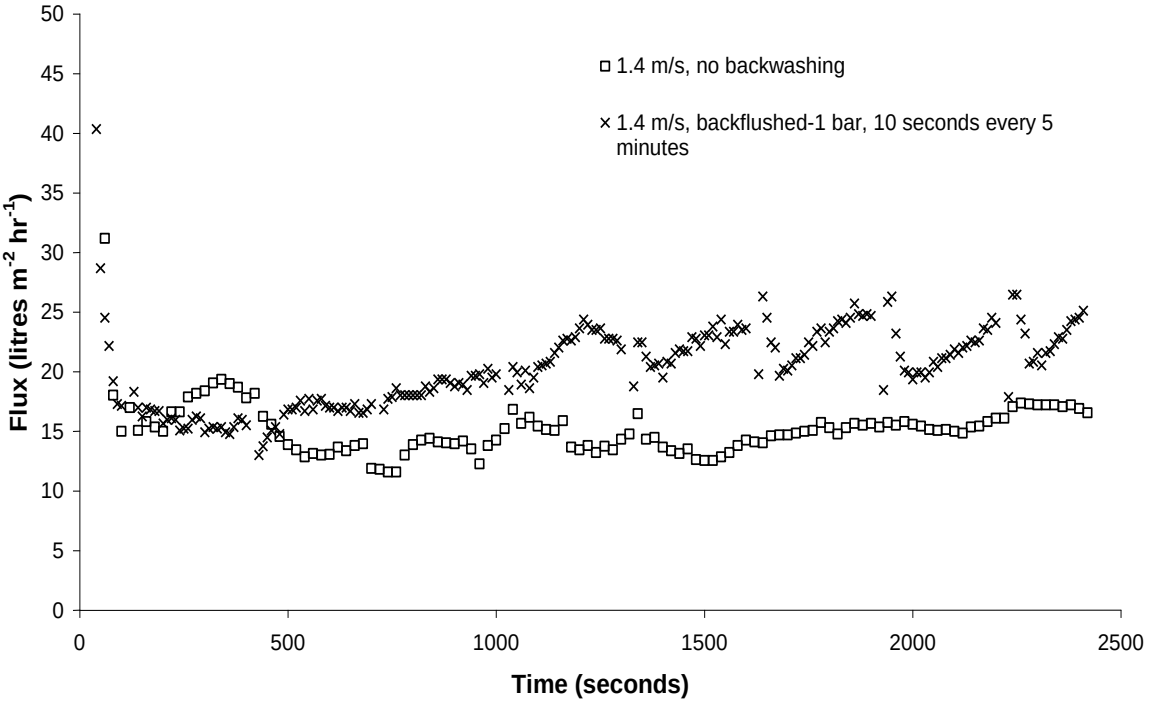

(a)

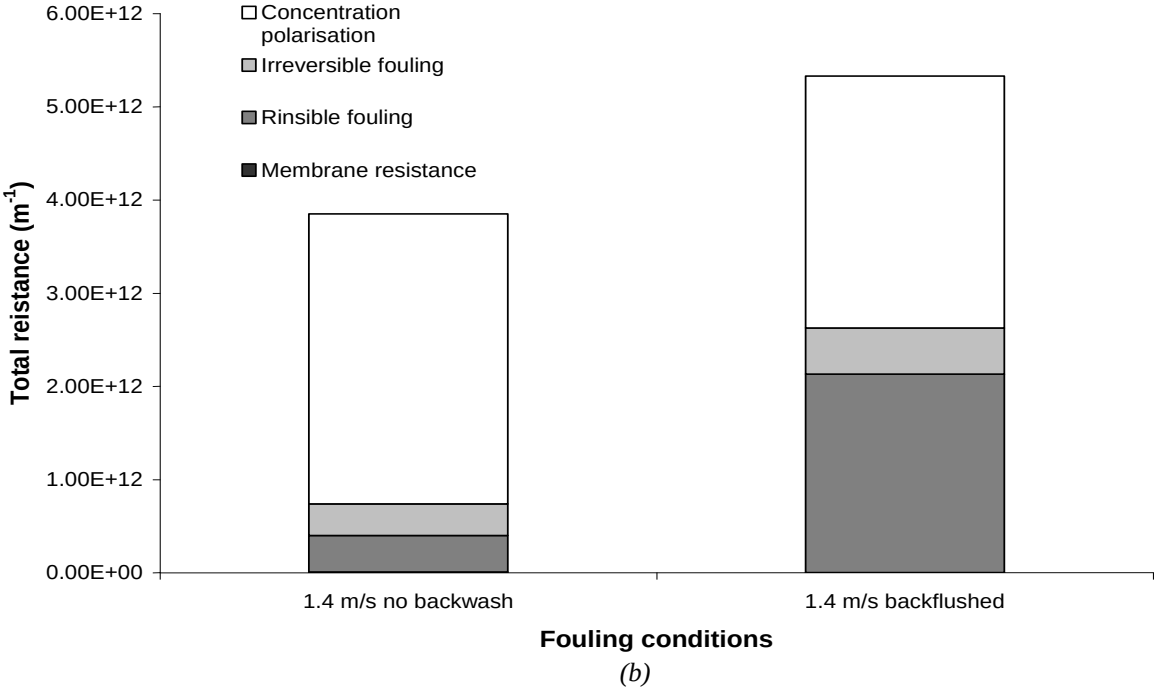

(b)

Figure 79a) Comparison of the change in permeate with time with and without backflushing (30 seconds every 5 minutes at 1 bar) 1.4 m s^{-1} CFV, at 50 °C, 2 bar through a 12.0 µm membrane and b) the change in membrane resistances with different filtration conditions.

The effect of BF has also been tested during filtration through a 12.0 µm membrane at a CFV value of 1.4 m s^{-1}. This CFV was tested as it was found previously during this work that using both a 0.7 and 2.0 m s^{-1} CFV led to low spore reductions of 1.4 ± 0.6 and 1.5 ± 0.9 log orders respectively compared to a 2.1 ± 0.7 log order reduction using a 1.4 m s^{-1} CFV. Table 37 shows the experimental conditions used and the resulting steady state permeate flux, solid transmission and total resistance (R_T) values as well as

the total MPI collected for each run carried out through the 12.0 µm membrane. Figure 79 shows the corresponding change in permeate flux with time and membrane resistance graphs for the 1.4 m s^{-1} CFV tested with and without BF. As with the 0.8 µm membrane backflushing led to an increase in permeate flux of 8.5 LMH (an increase of 51.2% compared to in the absence of BF) but a decrease in solids transmission of 17.6% and the associated total MPI collected 108.4g (6.8%). This again implies that backflushing forces more water from the feed through the membrane but this permeate contains less MPI solid compared to in the absence of BF. Clearly this is not a desirable outcome. In contrast to the other membranes BF was found to increase total membrane resistance, this was mainly the result of an increase in reversible resistance from 3.9 x 10^{11} to 2.1 x 10^{12} m^{-1}.

Table 37. Comparison of the steady state permeate fluxes and solid transmissions along with the total MPI collected during experiments through the 12.0 µm membrane using optimum experimental conditions with and without backflushing.

		At steady state			
Backwashing conditions	CFV (m s^{-1})	Flux (LMH)	Solids transmission (%)	R_T (m^{-1}) x10^{12}	Total MPI collected during run (g's)
No backwashing	1.4	16.6	69.0	3.85	1605.3
1 bar-10 seconds every 5 minutes	1.4	25.1	51.4	5.33	1496.9

4.7.4 Effect of backflushing on spore reduction

The most promising improvements with backflushing in terms of steady state permeate flux and solid transmissions were found with the (i) 0.8 µm membrane at 2.0 m s^{-1} CFV, (ii) 2.0 µm membrane at 1.4 m s^{-1} CFV and (iii) 12.0 µm membrane at 1.4 m s^{-1} CFV experiments. Consequently these conditions were repeated using an inoculated 15 wt% MPI feed. The spore log order reductions found 1, 2 and 4 minutes after the 1^{st}, 5^{th} and 8^{th} backflush can be found in Tables 38, 39 and 40 for the 0.8, 2.0 and 12.0 µm membranes respectively and the corresponding experiments conducted without backflushing.

The highest spore reduction values obtained were those recorded through the 0.8 µm membrane between 2.8 – 4.1 log orders. These values were largely unaffected with backflushing as can be seen in Table 38. Samples were collected after 1, 2 and 4 minutes after the 1^{st}, 5^{th} and 8^{th} flush in order to establish if the spore reduction values changed as a function of filtration time and / or between backflushes as a result of

foulant removal by the backflush and subsequent redeposition of material, which may act as a secondary filtration layer. For the 0.8 µm membrane, spore reduction remained relatively constant between 2.8 and 3.3 log orders throughout the filtration process, implying that BF did not interfere with the reduction of spores achieved in the permeate. The size of the *Bacillus mycoides* spores (length: 1.53 ± 0.18 µm and width: 0.90 ± 0.11 µm, as measured in section 3.1.1) means that they are larger than the pores, so substantial spore rejection is always likely, irrespective of the hydraulic conditions.

Spore reductions through the 2.0 µm membrane unsurprisingly were lower than that found through the 0.8 µm membrane between 1.9 and 3.0 log orders as can be seen in Table 39 but are still relatively high equating to a 99.9% reduction. As with the 0.8 µm membrane, spore reduction does not seem to vary as a function of filtration time and BF does not significantly affect the spore reduction achieved. However, in contrast to the 0.8 µm membrane results, spore reduction does seem to vary with time after a backflush has occurred, with spore reduction increasing with increasing time after a backflush has occurred. This effect is not statistically significant, as the errors overlap but may still be a genuine phenomenon caused as a result of the increase in irreversible fouling resistance with BF found with this membrane. Such fouling may be acting a secondary filtration layer responsible for the spore reduction, as this membrane is composed of pores larger in size than the *Bacillus mycoides* spores. This layer may be being partially removed by backflushes but then is gradually redeposited onto the membrane following the backflush.

Table 38. Comparison of the spore reductions achieved during filtration experiments using 15 wt% MPI at 50 °C, 2.0 m s^{-1}, 2 bar through the 0.8 µm membrane with and without backflushing at 1 bar for 10 seconds every 5 minutes.

	1st Backflush			5th Backflush			8th Backflush		
Log order spore reduction	1 min after BF	2 min after BF	4 min after BF	1 min after BF	2 min after BF	4 min after BF	1 min after BF	2 min after BF	4 min after BF
Backwashing conditions: 10 seconds every 5 minutes	3.3 ± 0.5	2.9 ± 0.5	3.3 ± 0.8	3.1 ± 0.6	3.0 ± 0.6	2.9 ± 0.4	2.8 ± 0.7	2.9 ± 0.4	3.0 ± 0.5
	After 5 minutes of filtration			After 15 minutes			After 40 minutes		
No backwashing	4.1 ± 0.7			No measurement			4.0 ± 0.6		

As size exclusion considerations would indicate, spore reduction values recorded through the 12.0 µm membrane were indeed found to be the lowest of the three membranes tested. But the values obtained were still relatively high with the lowest spore reduction at any time being 1.6 log orders, which equates to a 98% spore reduction. As with the other two membranes backflushing does not appear to affect spore reduction and although it appears that spore reduction decreases with filtration time, the spore reduction found at the start of filtration 2.2 ± 0.7 log orders is not significantly different to that found at the end of filtration 1.6 ± 0.4 log orders.

Table 39. Comparison of the spore reductions achieved during filtration experiments using 15 wt% MPI at 50 °C, 1.4 m s^{-1}, 2 bar through the 2.0 µm membrane with and without backflushing at 1 bar for 10 seconds every 5 minutes.

	1st Backflush			5th Backflush			8th Backflush		
Log order spore reduction	1 min after BF	2 min after BF	4 min after BF	1 min after BF	2 min after BF	4 min after BF	1 min after BF	2 min after BF	4 min after BF
Backwashing conditions: 10 seconds every 5 minutes	2.0 ± 0.2	2.3 ± 0.3	2.4 ± 0.4	1.9 ± 0.8	2.6 ± 0.7	2.8 ± 0.5	3.0 ± 0.4	2.9 ± 0.1	3.0 ± 0.3
	After 5 minutes of filtration			After 15 minutes			After 40 minutes		
No backwashing	2.7 ± 0.5			No measurement			2.9 ± 0.6		

Table 40. Comparison of the spore reductions achieved during filtration experiments using 15 wt% MPI at 50 °C, 1.4 m s^{-1}, 2 bar through the 12.0 µm membrane with and without backflushing at 1 bar for 10 seconds every 5 minutes.

	1st Backflush			5th Backflush			8th Backflush		
Log order spore reduction	1 min after BF	2 min after BF	4 min after BF	1 min after BF	2 min after BF	4 min after BF	1 min after BF	2 min after BF	4 min after BF
Backwashing conditions: 10 seconds every 5 minutes	2.2 ± 0.7	2.5 ± 0.5	2.3 ± 0.4	2.1 ± 0.5	1.9 ± 0.3	1.9 ± 0.2	1.8 ± 0.4	1.7 ± 0.5	1.6 ± 0.4
	After 5 minutes of filtration			After 15 minutes			After 40 minutes		
No backwashing	2.0 ± 0.8			No measurement			2.1 ± 0.7		

4.7.5 Effects of backpulsing on steady state permeate flux and solid transmissions through the 2.0 and 12.0 µm membrane.

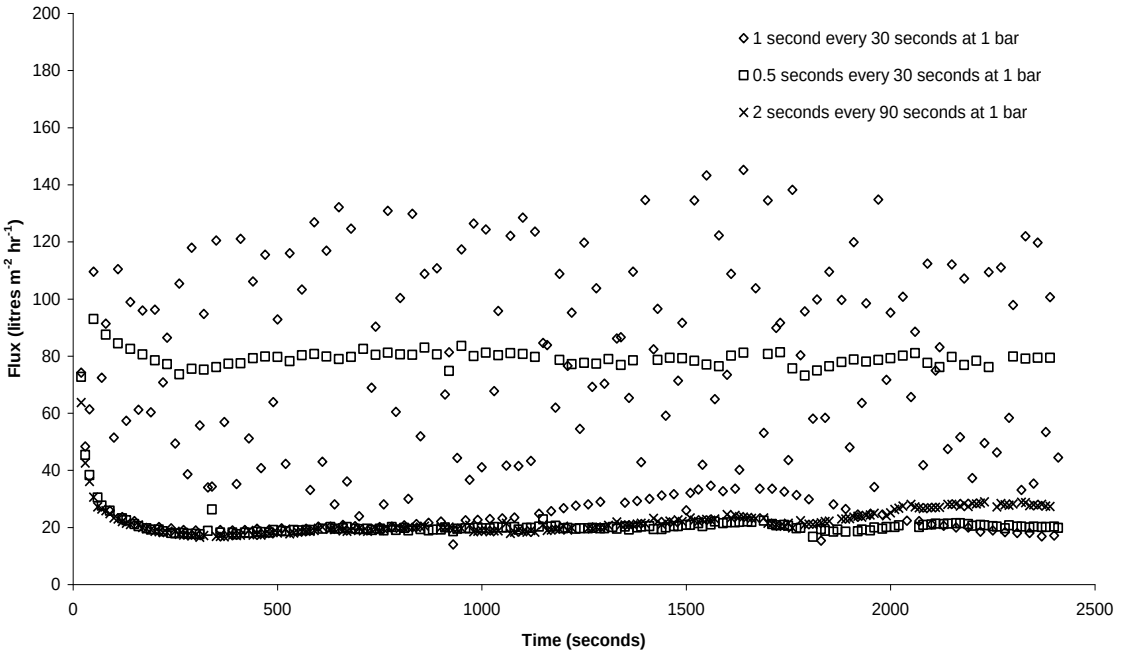

(a)

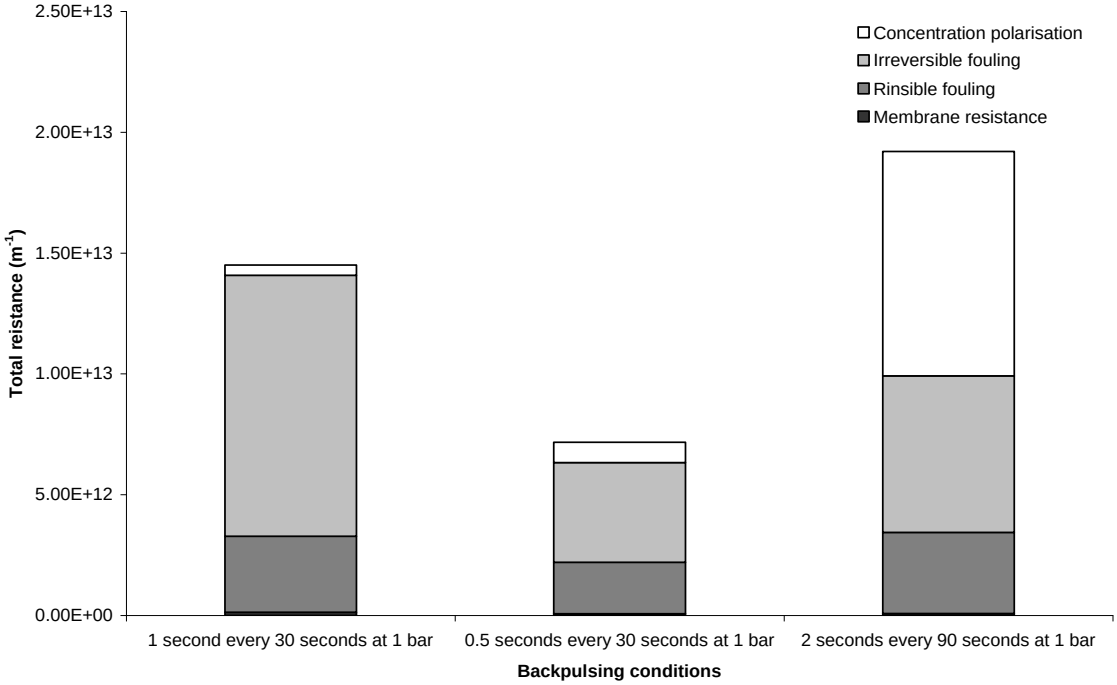

(b)

Figure 80. a) Comparison of the change in permeate with time with different backpulsing conditions at 1.4 m s^{-1} CFV, 50 °C and 2 bar through a 2.0 µm membrane and b) the change in membrane resistances with different filtration conditions.

As the steady state permeate fluxes and solid transmissions found through the 0.8 µm membrane were so low and backflushing did not result in a significant increase, actually causing a decrease in solids transmission. Backpulsing experiments were only carried out on the 2.0 and 12.0 µm membranes at 1.4 m s^{-1} CFV, 2 bar and 50 °C with

backpulsing at 1 bar. A series of backpulsing experiments were carried out on both the membranes that differed in the backpulse duration and frequency in order to try and optimise the filtration process further. Experiments involved backpulsing every 30 seconds for 1 second, every 30 seconds for 0.5 seconds or every 90 seconds for 2 seconds. The steady state permeate fluxes and solid transmissions values found for the 2.0 and 12.0 µm membranes set of BP experiments can be found in Tables 41 and 42 respectively. The corresponding change in permeate flux with time and membrane resistance graphs can be seen in Figure 80 a) and Figure 80 b) respectively for the 2.0 µm membrane and in Figure 81 a) and Figure 81 b) respectively for the 12.0 µm membrane.

For the 2.0 µm membrane, BP for 2 seconds every 90 seconds (the closest conditions to that used during BF experiments) produced the highest steady state permeate flux of 27.9 LMH and solid transmission of 13.1%. As can be seen when comparing Tables 36 and 41 the permeate flux recorded was slightly higher than that found using BF at 1.4 m s^{-1} CFV by 1.7 LMH (6.5%) but the solid transmission was 10.6% lower. This is an undesirable effect, as although increases in permeate flux are sought after this is only the case when it is associated with an increase in the amount of solid being passed through the membrane. For the 12.0 µm membrane BP for 1 second every 30 seconds produced the highest solid transmission of 31.7% and BP for 2 seconds every 90 seconds produced the highest permeate flux of 17.3 LMH. But when comparing Tables 37 and 42 it can be seen that both of these values are lower than that found during BF experiments. With permeate flux being 7.8 LMH (31.1%) and solid transmission 19.7% lower. This implies that when filtering high solids content MPI feeds of 15 wt% through large pore sized tubular ceramic membranes, backwashing using longer and less frequent flushes produces the most desirable results in terms of steady state permeate flux and solids transmission values.

Table 41. Comparison of the steady state permeate fluxes and solid transmissions during experiments through the 2.0 µm membrane with different backpulsing conditions.

		At steady state	
Backpulsing duration	Backpulsing frequency	Flux (LMH)	Solids transmission (%)
1 second	Every 30 seconds	17.1	6.8
0.5 seconds	Every 30 seconds	19.8	11.0
2 seconds	Every 90 seconds	27.9	13.1

Table 42. Comparison of the steady state permeate fluxes and solid transmissions during experiments through the 12.0 µm membrane with different backpulsing conditions.

		At steady state	
Backpulsing duration	Backpulsing frequncy	Flux (LMH)	Solids transmission (%)
1 second	Every 30 seconds	14.8	31.7
0.5 seconds	Every 30 seconds	12.7	22.9
2 seconds	Every 90 seconds	17.3	23.1

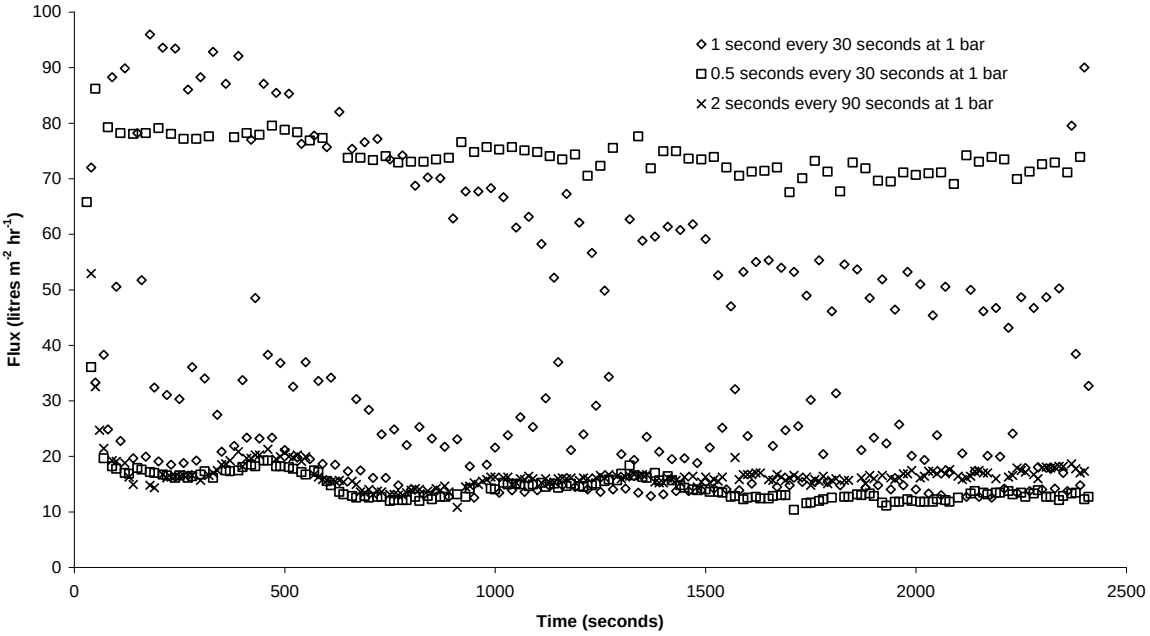

(a)

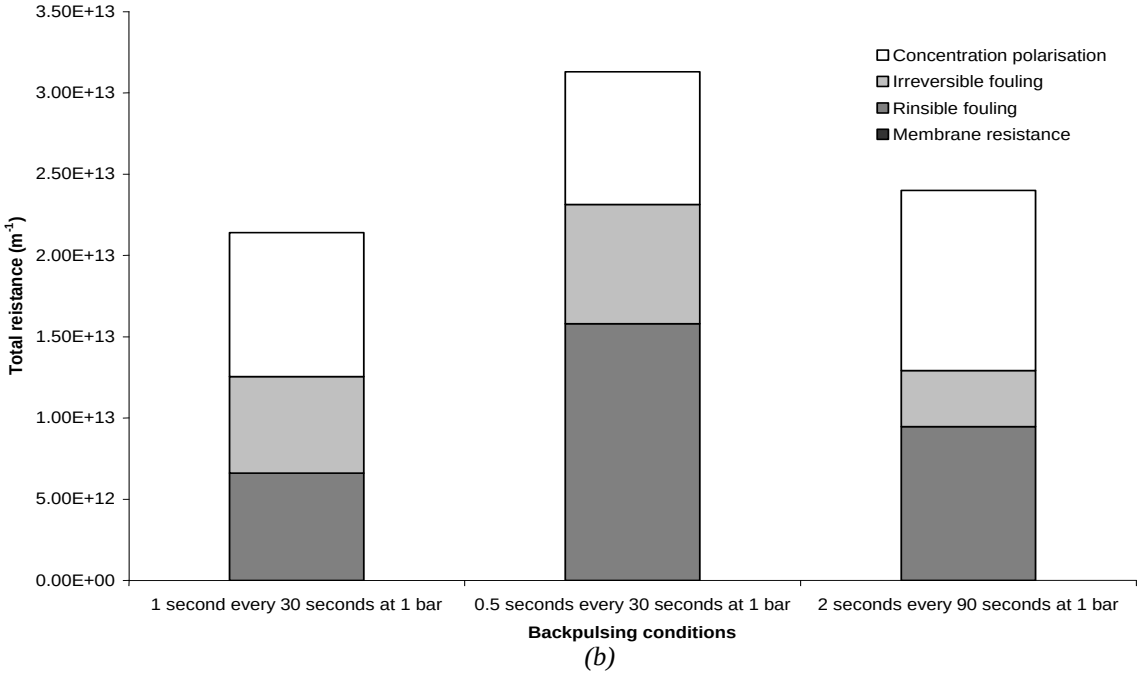

(b)

Figure 81a) Comparison of the change in permeate flux with time with different backpulsing conditions at 1.4 m s^{-1} CFV, 50 °C and 2 bar through a 12.0 µm membrane and b) the change in membrane resistances with different filtration conditions.

4.7.6 Comparison between 15 wt% MPI solution filtration carried out through a 2.0 and 12.0 µm membrane with no backwashing, backflushing and optimum backpulsing conditions.

Within Tables 43 and 44 are the steady state permeate flux, solid transmission and total resistance (R_T) values along with the total amount of MPI collected within the run found during 15 wt% MPI filtration at 1.4 m s^{-1} CFV, 2 bar and 50 °C for the 2.0 and 12.0 µm membranes when filtering with no backwashing, backflushing at 1 bar for 10 seconds every 5 minutes and the optimum backpulsing conditions found. For the 2.0 µm membrane this was 2 seconds every 90 seconds at 1 bar and for the 12.0 µm membrane this was 1 second every 30 seconds at 1 bar. Figures 82 and 83 show the change in permeate flux with time and the corresponding change in membrane resistance graphs found during each experiment using the 2.0 and 12.0 µm membrane respectively.

As can be seen from Table 43 and as mentioned previously backwashing during MPI filtration through the 2.0 µm membrane appears to be advantageous in terms of increasing steady state permeate flux, solid transmission and total MPI collected and by decreasing total resistance (R_T). Also indicated by these experiments is that longer and less frequent backflushes are more effective at removing MPI foulant as opposed to shorter and more frequent backpulses. With a 13.0 LMH (98.5%) and 304.7g (140.7%) increase measured in permeate flux and total MPI collected respectively during 15 wt% MPI filtration with backflushing compared to filtration with no backwashing. Solid transmission and total MPI collected during filtration with backflushing was 12.6% higher and 3.6 x 10^{13} m^{-1} (73.2%) lower compared to without backwashing and 10.6% higher and 6.0 x 10^{12} m^{-1} (31.3%) lower compared to backpulsing.

Table 43. Comparison of the steady state permeate fluxes, solid transmissions and total MPI collected during a run during experiments through the 2.0 µm membrane with either no backwashing, backflushing or optimum backpulsing conditions.

	At steady state			
Backwashing conditions	Flux (LMH)	Solids transmission (%)	R_T (m^{-1}) x 10^{13}	Total MPI collected during run (g's)
No backwashing	13.2	11.1	4.92	216.5
1 bar-10 seconds every 5 minutes	26.2	23.7	1.32	521.2
1 bar- 2 seconds every 90 seconds	27.9	13.1	1.92	---

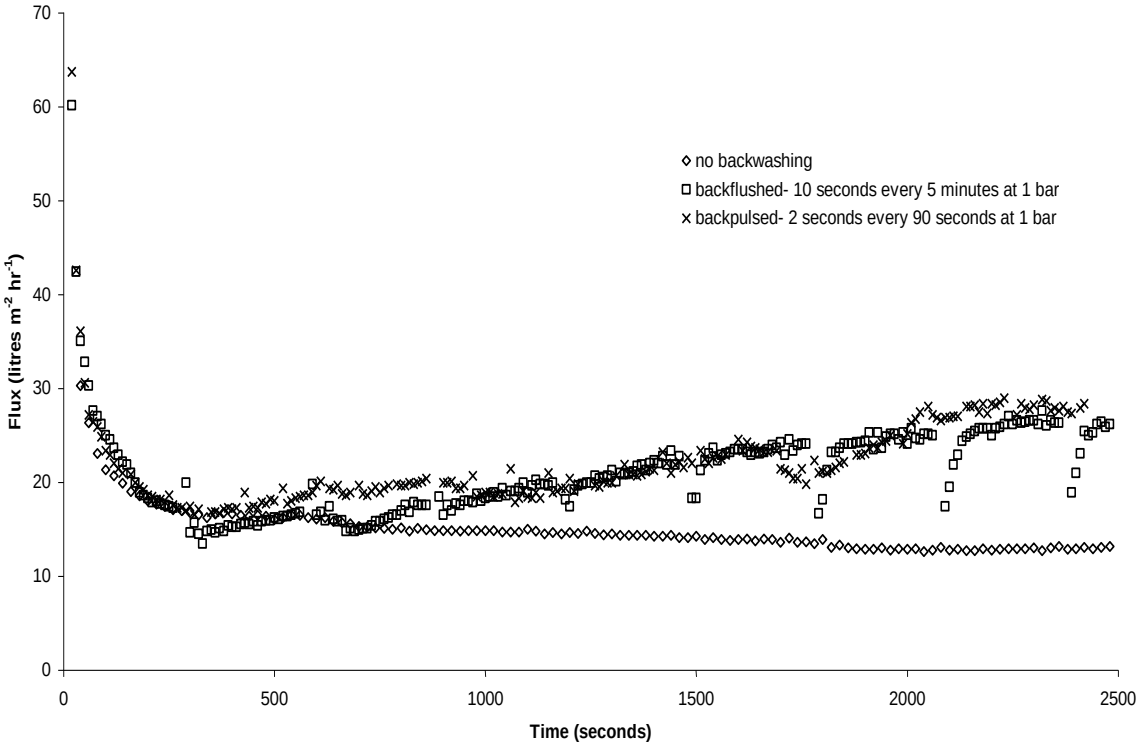

(a)

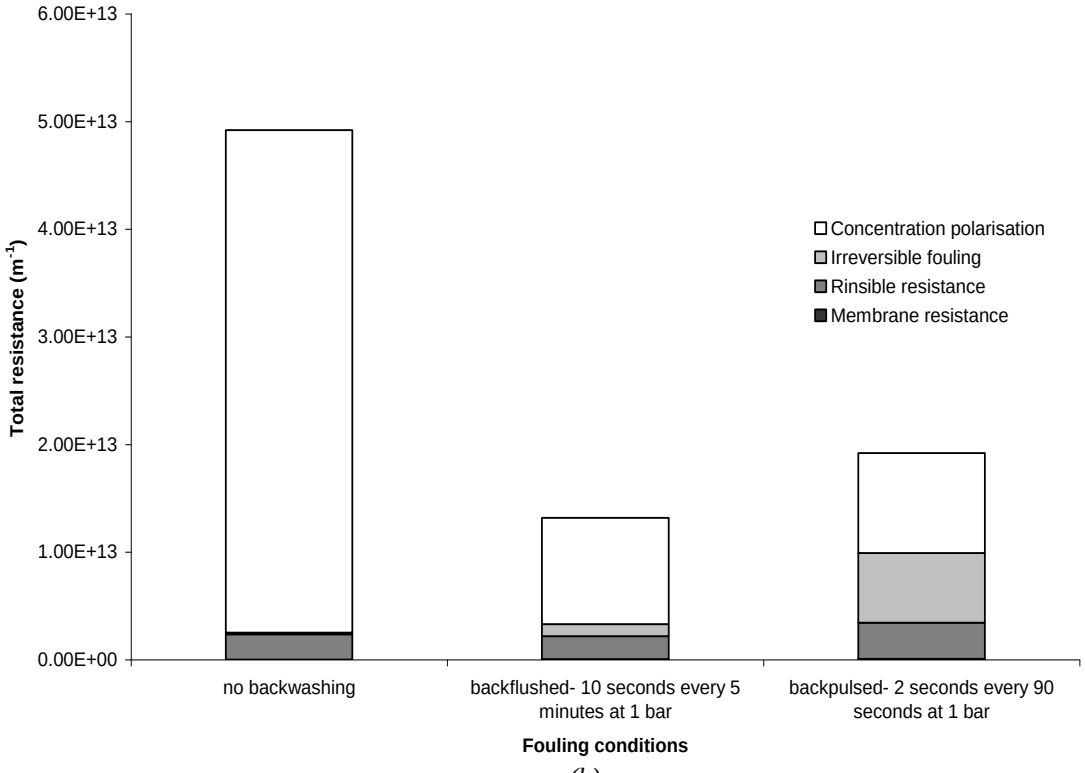

(b)

Figure 82a) Comparison of the change in permeate flux with time when filtering 15 wt% MPI through a 2.0 µm membrane at 1.4 m s^{-1}, 50 °C and 2 bar with either no backwashing, backflushing for 10 seconds every 5 minutes at 1 bar or optimum backpulsing for 2 seconds every 90 seconds at 1 bar, b) the corresponding change in membrane resistance.

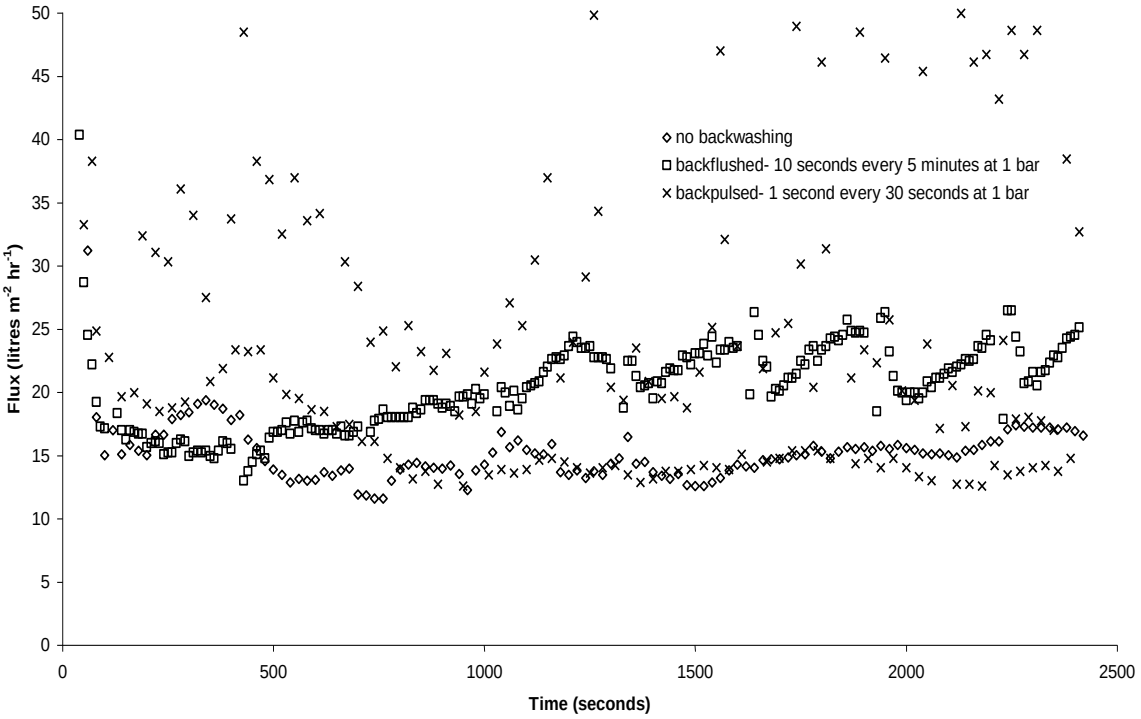

(a)

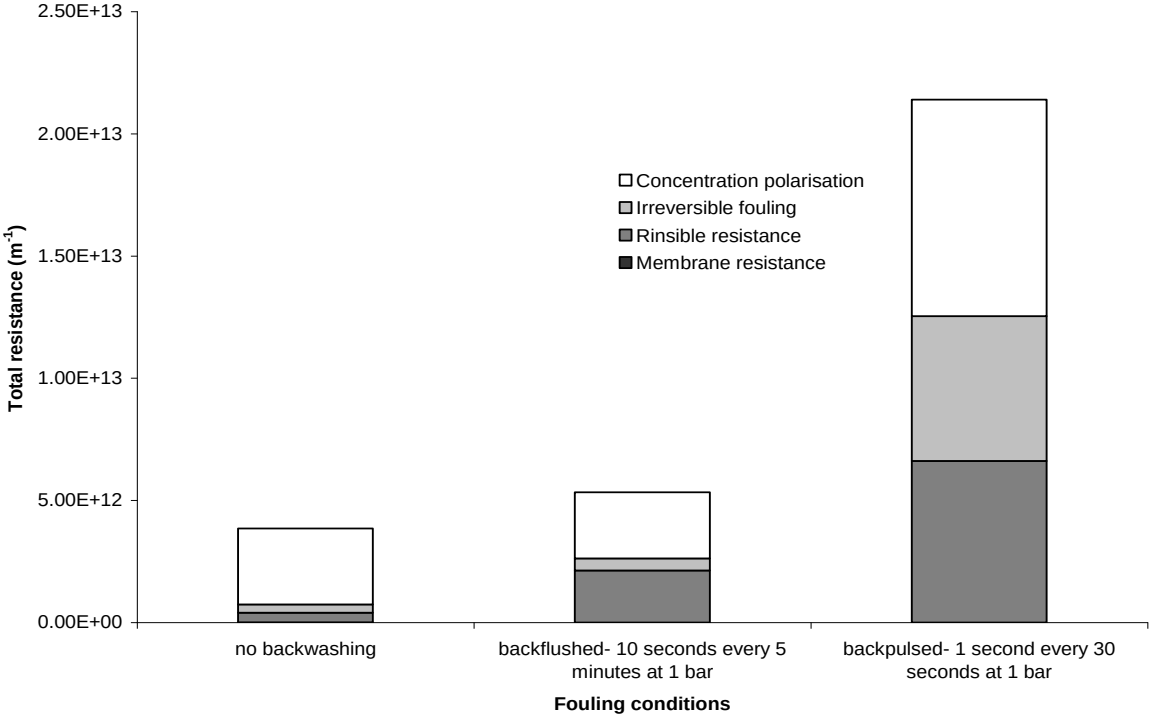

(b)

Figure 83. a) Comparison of the change in permeate flux with time when filtering 15 wt% MPI through a 12.0 µm membrane at 1.4 m s^{-1}, 50 °C and 2 bar with either no backwashing, backflushing for 10 seconds every 5 minutes at 1 bar or optimum backpulsing for 2 seconds every 90 seconds at 1 bar, b) the corresponding change in membrane resistance.

From Table 44 and Figures 84a and b, it appears in contrast to the 2.0 µm membrane that backwashing has a detrimental effect on MPI filtration through the 12.0 µm membrane in terms of steady state permeate flux, solid transmission and total resistance

as well as the total MPI collected during a run. As although backflushing during filtration of 15 wt% MPI led to a 8.5 LMH (51.2%) increase in permeate flux compared to filtration with no backwashing this was associated with a 17.6% and 108.4g (6.8%) decrease in solid transmission and total MPI collected, as well as a 1.48 x 10^{12} m^{-1} (38.4%) increase in total resistance. Backpulsing was found to be even more detrimental, even though the permeate flux measured directly after a backpulse increased it was clear that this permeate consisted mainly of water having only a low MPI content. Backpulsing led to an increase in total resistance of 17.55 x 10^{12} m^{-1} (455.8%) compared to filtration carried out with no backwashing. This can often occur in membrane systems if in the absence of backwashing the fouling layer is only loosely attached and has an open structure. When backwashing occurs this disturbs the fouling layer (a desirable effect) but if the process conditions are not correct and the foulant is not efficiently removed from the membrane surface the layer can reorganise itself and be redeposited as a denser cake that has a higher fouling resistance compared to the initial loosely attached cake.

Table 44. Comparison of the steady state permeate fluxes, solid transmissions and total MPI collected during a run during experiments through the 12.0 µm membrane with either no backwashing, backflushing or optimum backpulsing conditions.

	At steady state			
Backwashing conditions	Flux (LMH)	Solids transmission (%)	R_T (m^{-1}) x 10^{12}	Total MPI collected during run (g's)
No backwashing	16.6	69.0	3.85	1605.3
1 bar-10 seconds every 5 minutes	25.1	51.4	5.33	1496.9
1 bar- 1 second every 30 seconds	14.8	31.7	21.4	---

4.7.6 Optimum MPI cleaning regime

The effect of using a combination of both acid and alkali cycles with and without backflushing to clean ceramic membranes after MPI filtration was investigated, to establish an optimum cleaning regime. Experiments were carried out on the 2.0 µm membrane after it had been fouled with 15 wt% MPI, at 1.4 m s^{-1}, 2 bar, 50 °C, for 40 minutes, with BF at 1 bar. The frequency of BF was every 5 minutes and the duration was 10 seconds. After each MPI filtration, the system was drained and flushed with RO

water and then one of the cleaning cycle combinations shown in Table 45 were tested. After each stage of a cleaning regime was carried out the system was flushed with RO water before a PWF was taken. Within Table 45 BF means that backflushing at 1 bar every 5 minutes for 10 seconds was carried out during that section of the cleaning regime.

Table 45. Showing the different cleaning regimes tested for their effectiveness at removing MPI fouling. Where --- means that part of the cycle was not carried out and 1 - 4 refers to when within the regime that cleaning step was carried out.

	Cleaning regime				
	1	2	3	4	5
Type of cleaning	Step in regime				
Rinsing- RO water, 50 °C, 1.4 m s^{-1}, no TMP for 10 minutes.	1st	2nd	2nd	2nd	2nd
Long backflush- RO water, 1 bar for 30 seconds.	---	1st	1st	1st	1st
Alkali cleaning- 0.5 wt% NaOH, 50 °C, 1.4 m s^{-1}, no TMP, 10 minutes.	2nd	3rd	---	---	---
Alkali cleaning- 0.5 wt% NaOH, 50 °C, 1.4 m s^{-1}, 0.3 bar for 10 minutes with BF at 1 bar every 30 seconds for 1 second.	---	---	3rd	3rd	---
Alkali cleaning- 0.5 wt% NaOH, 50 °C, 1.4 m s^{-1}, 0.3 bar for 10 minutes with BF at 1 bar every 30 seconds for 4 seconds	---	---	---	---	3rd
Acid cleaning- 0.3 wt% HNO_3, 50 °C, 1.4 m s^{-1}, no TMP, 10 minutes.	---	4th	---	---	---
Acid cleaning- 0.3 wt% HNO_3, 50 °C, 1.4 m s^{-1}, 0.3 bar, 10 minutes with BF at 1 bar every 30 seconds for 1 second.	---	---	---	4th	---
Acid cleaning- 0.3 wt% HNO_3, 50 °C, 1.4 m s^{-1}, 0.3 bar, 10 minutes with BF at 1 bar every 30 seconds for 4 seconds.	---	---	---	---	4th

Table 46. Showing the increase in PWF achieved after each cleaning stage of the four different cleaning regimes tested.

Cleaning regime	NaOH flux increase (%)	HNO_3 flux increase (%)	Product flux (LMH)
1	38.2	---	19.4
2	55.5	99.6	20.0
3	10.1	---	20.1
4	13.8	88.1	19.2
5	31.0	92.3	19.5

The effectiveness of each cleaning regime was determined using PWF measurements after each stage and the steady state product flux produced during the following MPI filtration. Figure 84 a, shows the change in product flux with time following each of the

different cleaning regimes and Figure 84 b, shows the corresponding change in membrane resistance. Table 46 shows the percentage flux recovery achieved after each stage and the product flux produced for each tested cleaning regime. Cleaning regime number 2 was found to be the most effective producing a 99.6% flux recovery. This regime involved firstly performing a long RO water backflush at 1 bar for 30 seconds followed by an RO water rinse at 50 °C, 1.4 m s^{-1}, with no TMP for 10 minutes, the membrane was then subjected to an alkali clean using 0.5 wt% NaOH, at 50 °C, 1.4 m s^{-1}, no TMP, for 10 minutes and was lastly acid cleaned with 0.3 wt% HNO_3 using the same conditions as that used during the alkali clean. The PWF data obtained during this optimum cleaning regime can be found in Figure 85.

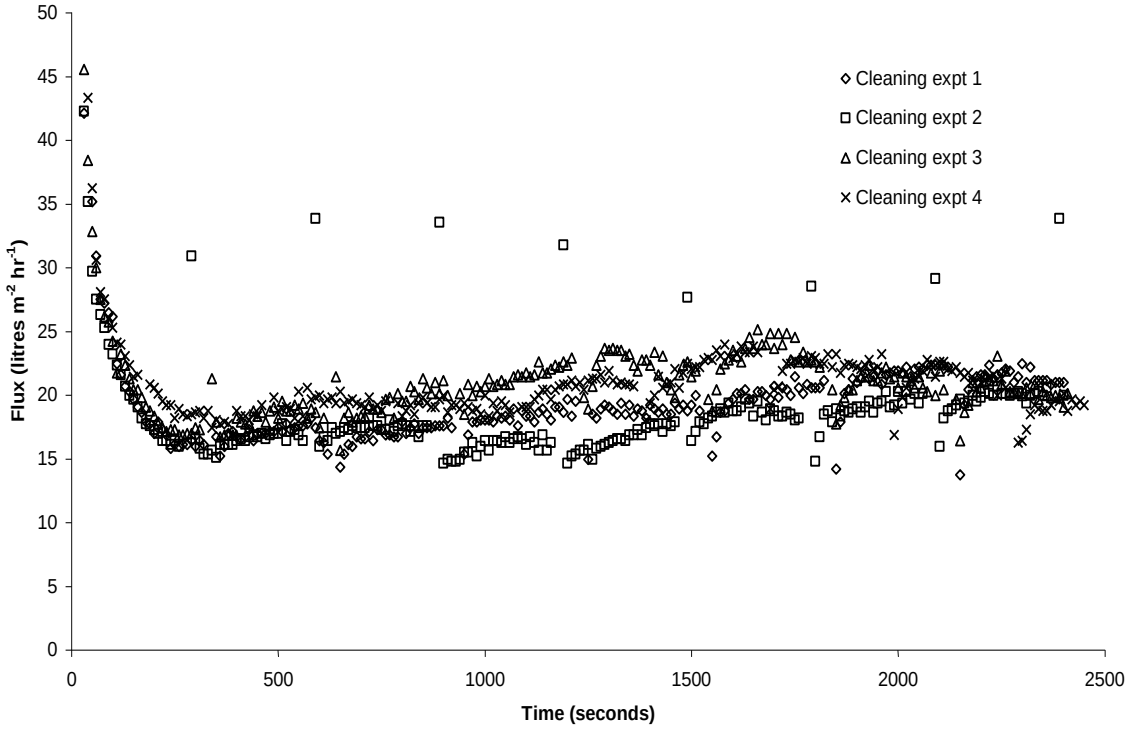

(a)

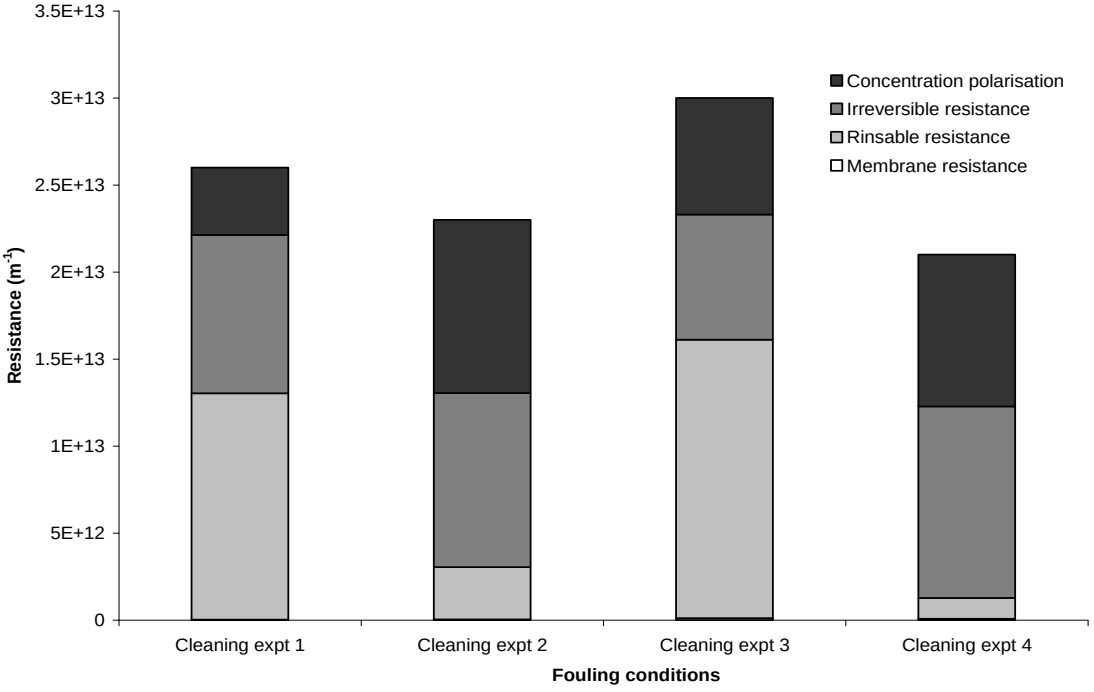

(b)

Figure 84. a) Comparison of the change in product flux with time following different cleaning regimes after filtration of 15 wt% MPI at 1.4 m s^{-1} CFV, 50 °C and 2 bar through a 2.0 µm membrane and b) the corresponding change in membrane resistances.

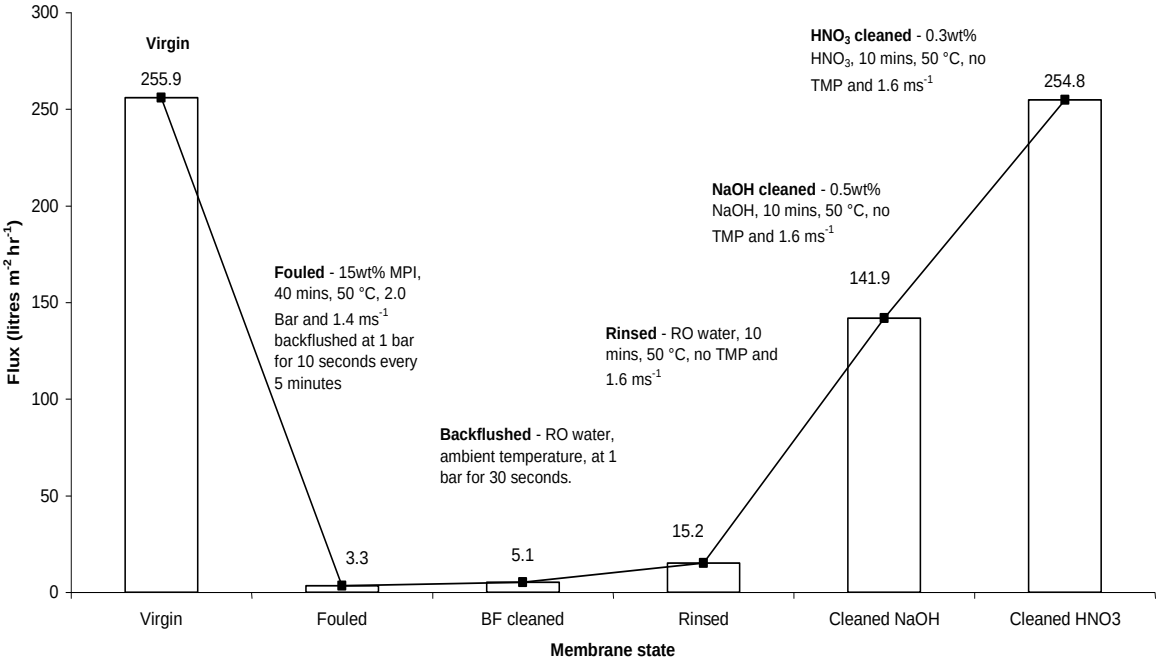

Figure 85. Pure water flux data collected after each stage of the optimum cleaning regime. Found after a 2.0 µm membrane Membralox™ *had been fouled with 15 wt% MPI at 1.4 m s^{-1} CFV, 50 °C and 2 bar for 40 minutes.*

4.8 TRIALS CONDUCTED USING MPI CONCENTRATE AT KERRY FOODS, LISTOWEL

Pilot plant trials were conducted at the Kerry Foods site in Listowel, Ireland using MPI concentrate solutions at 25 wt% taken off the production line before spray drying. This

solution was diluted enabling trials to be carried out using solutions of 10, 17 and 25 wt%. Solutions of 100 litres were prepared and inoculated with spores of *Bacillus mycoides* prepared following the protocol described in section 2.2.7. A schematic of the pilot plant filtration rig used to filter these solutions can be seen in Figure 86. The module was fitted with a PS spiral wound membrane of 0.8 µm pore diameter. Experiments were conducted at 50 ºC using a TMP of 3 bar for two hours. Permeate flux was determined using a rotameter, and the solids content of feed and permeate streams was determined during fouling runs using a handheld refractometer and confirmed using an Atago refractometer. Samples were taken from the permeate and feed streams near the end of each filtration run and spray dried, so that spore counts for each sample could be determined within our Membrane Applications Laboratory at the University of Bath using the *Petrifilm*^{TM} Aerobic Count plating method. After each trial the system was drained, rinsed with water and then cleaned with *Divos ff* at pH 9 for 20 minutes, flushed, cleaned with *Divos 2* at pH 1.5 - 1.8 for 20 minutes, flushed and lastly cleaned with *Divos 110* at pH 10.5 - 11.0 for 20 minutes and flushed. The change in permeate flux with time during each trial is shown in Figure 87 and the steady state flux values as well as solids transmission and spore retention data for each trial can be found in Table 47.

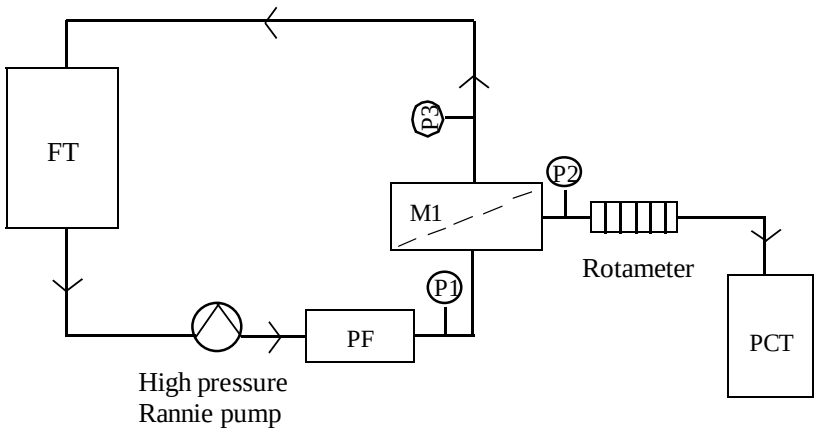

Figure 86. Schematic of the pilot plant filtration rig at Kerry Food, Listowel, Ireland. Where FT- feed tank, PF- pre-filter, M- membrane module, P- pressure transducer and PCT- permeate collection tank.

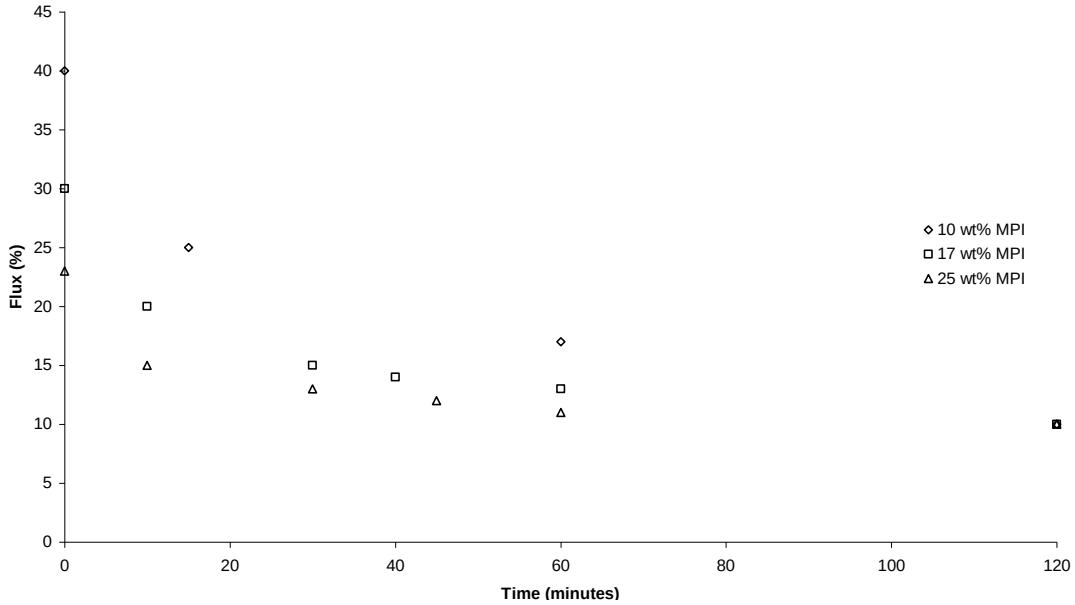

Figure 87. Change in permeate flux with time during each pilot plant trial carried out at Kerry Food, Listowel, using inoculated 10, 17 or 25 wt% MPI concentrate.

Table 47. Steady state permeate flux values, solids transmission and spore retention data for three pilot plant trials carried out at Kerry Food, Listowel.

	At steady state (after two hours of filtration)			
MPI wt%	Flux (% of initial flux)	Solids transmission (%)	Spore reduction	
			%	Log
10	10	45.0	99.82	2.7 ± 0.1
17	10	41.2	99.87	2.9 ± 0.1
25	10	34.0	99.87	2.9 ± 0.1

Results from the pilot trial experiments are particularly noteworthy as the experimental set up represents an important intermediary step between the laboratory filtration experiments carried out at Bath and the large-scale industrial microfiltration of dairy products.

It should be noted that there were various differences between the pilot trials and the experimental work carried out at Bath. At Bath, feeds were prepared by resolubilising spray-dried MPI powder to the desired concentration whereas MPI concentrate solution was taken directly off the production line (and then if required diluted to the desired concentration, 10 or 17 wt%) for the pilot trials. Different TMP's were used; 3 bar

during pilot trials and 2 bar at Bath. At Bath flux was measured gravimetrically using a mass balance and expressed in litres m^{-2} hr^{-1}, but at Kerry Foods it was recorded with a rotameter and expressed as a percentage of the initial filtration flux. Finally, at Kerry Foods a spiral wound membrane was tested, compared to a tubular ceramic *Membralox*™ membrane at Bath. However, there were also significant similarities. A pore size of 0.8 micron was used in both locations and the mode of operation (i.e. cross flow filtration) was also kept constant.

The results from the pilot trials (Table 47) showed the potential of microfiltration using spiral wound membranes over tubular ceramic *Membralox*™ membrane. The highest solid transmissions using a 10 and 15 wt% MPI feed recorded at Bath were 7.5 and 5.3% respectively (measured at 1.4 and 2.0 m s^{-1} CFV as shown within Tables 27 and 34 respectively). However, the spiral wound membrane produced solids transmissions of 45.0 and 41.2% for 10 and 15 wt% MPI concentrate feeds respectively. This increase in solids transmission was accompanied by similar spore rejections to that measured at Bath. With the tubular ceramic membrane producing spore rejections between 2.4 – 4.4 log orders across all conditions tested compared to between 2.7 - 2.9 log orders measured through the spiral wound membrane.

5 CONCLUSIONS AND FUTURE WORK

5.1. Conclusions

The research performed during this PhD project involved the application of microfiltration (MF) to remove spores from high solids content Milk Protein Isolate (MPI) solutions up to 16 wt% in laboratory and 25 wt% in pilot trials. MPI feeds were inoculated with *Bacillus mycoides* spores as a safer alternative to *Bacillus cereus* a psychrotrophic spore forming bacteria commonly found in dairy products.

A large amount of material has been published in regards to microfiltration of low solids content dairy feeds such as raw and skimmed milk that contain generally 3.5 wt%. But to the best of my knowledge (at the time of writing) there was no published material available within the literature apart from the two papers produced from this work in regards to the processing of high solids content dairy feeds via microfiltration. This study therefore represents a significant contribution to the field of dairy filtration and goes some way to filling this gap in knowledge.

If possible microfiltration represents an attractive alternative processing technique to pasteurisation for the treatment of dairy products. Whereas pasteurisation (a heat treatment process) only destroys heat-sensitive spoilage and pathogenic bacteria, microfiltration (a size exclusion based technique) is capable of removing all types of microorganisms found within dairy products including thermoduric and spore forming bacteria that can survive pasteurisation. Moreover, microfiltration can be carried out using lower temperatures. Pasteurisation is an energy intensive process that is expensive to perform and can affect the organoleptic properties of milk and other dairy products. Whilst the application of microfiltration for filtering low viscosity diary feeds is relatively well established being used to produce commercially available products such as Cravendale® milk, the filtration of high solids content, high viscosity feeds has not become well established due to low fluxes and poor transmission of solids.

At the start of the project suitable protocols for MPI resolubilisation, *Bacillus mycoides* cell and spore preparation and feed and permeate sample spore content enumeration (*Petrifilm*™ aerobic count plates) were established and the membranes, MPI and spores were fully characterised by SEM, particle size distribution, hydrophobicity, rheology and pure water flux (PWF) measurements.

Initially it was intended that MPI solutions of up to 25 wt% would be filtered but due to issues encountered during MPI resolubilisation and filtration of these highly viscous feeds (4199.1 cP at 20 s^{-1} and 18 °C, ambient temperature), filtration experiments were conducted using MPI solutions up to only 16 wt% during laboratory trials. As stated in section 4.8 MPI solutions of up to 25 wt% were able to be tested during the pilot scale trials as the MPI concentrate was taken directly from the production line before being spray-dried. An ideal MPI resolubilisation protocol for spray-dried MPI was developed using particle size distribution analysis (section 2.4). This protocol involved stirring the solution using an overhead stirrer at 125 rpm for 30 minutes. Unfortunately using this protocol was only possible when small volumes of a low wt% solution (< 5 wt%) were required. When either a large feed volume or a solution of high wt% (> 5 wt%) was required a faster stirrer speed of 700 rpm had to be used to aid resolubilisation. *Bacillus mycoides* cell and spore culture methods developed for *Bacillus mycoides* were adapted from those used by Bowen *et al.,* (2002 a).

Initially during the preliminary filtration experiments involving an inoculated RO water feed carried out on the Danish separation systems (DSS) labunit M10 rig the spore content of collected feed and permeate samples was able to be analysed using a counting chamber. But when inoculated MPI feeds were filtered the squares that make up the counting area on the counting chamber were no longer visible down a light microscope. A solution in the form of *Petrifilm*™ aerobic count plates was researched and used for sample enumeration throughout the remainder of the project. These plates were subjected to a thorough error analysis necessary in order to determine whether changes in the bacterial counts of feed and permeate streams during filtration were significant. The difference in counts produced by these plates and the traditionally used standard spread plate method was determined along with the effect of using 'old' and 'new' *Petrifilm*™ plates and the difference of *Petrifilm*™ plate counts of *Bacillus mycoides* spores with time when stored within both water and MPI.

Understanding the relationships between MPI viscosity with changing temperature and concentration is critical when filtering high solids content dairy feeds. As a result a large amount of rheology measurements were conducted as a function of changing MPI concentration between 1 – 30 wt%, temperature between 18 °C (ambient) – 50 °C (filtration temperature) and time with varying shear rate (1 – 20 s^{-1}).

In order to try and determine an optimum protocol for high solids content MPI filtration, experiments were carried out using a variety of filtration rigs, modules and membranes. Specifically two different filtration rigs were tested a DSS labunit M10 and a newly constructed filtration rig that was modified throughout the project resulting in experiments being carried out on three different set-ups. Three different modules were used, a flat sheet stainless steel square module and two stainless steel tubular housings. Lastly, inside these modules two different flat sheet polysulfone polymeric membranes of 0.5 and 1.5 µm pore size (*Alfa Laval*) were evaluated along with five *Membralox*^{TM} α-alumina tubular ceramic membranes (*Pall Filtration*) of 0.8, 1.4, 2.0, 5.0 and 12.0 µm pore diameters.

Experiments were carried out at different CFV's (0.7 – 2.0 m s^{-1}), TMP's (1 and 2 bar) and MPI concentrations (4 – 16 wt%) using both 'sterile' and inoculated MPI feeds through these different membranes.

During filtration experiments samples were taken of the feed and permeate streams and analysed for their solids content by oven drying, their protein content using the Bradford assay and spore content using *Petrifilm*^{TM} Aerobic count plates where appropriate.

Experiments carried out through the tubular ceramic membranes produced the most encouraging results with the majority producing high spore reductions. In general successful filtration outcomes for 5 and 10 wt% feeds were achieved, with the most encouraging result for 10 wt% found using the 12.0 µm membrane and 1.4 m s^{-1} cross flow velocity (CFV). This produced a flux of 123 litres m^2 hr^{-1} (LMH), a 90% protein transmission and a 2.6 log spore reduction. The filtration of 15 wt% MPI solutions proved more challenging. The best set of results for this feed during normal crossflow experiments was also obtained using the 12.0 µm membrane at 1.4 m s^{-1}, producing a flux of 26.6 LMH, 96.5 % protein transmission and a 2.1 log spore reduction. These results indicate that large pore ceramic microfiltration may be a suitable technology to replace or augment pasteurisation for high solids content dairy feeds. This finding showed that the process is mechanistically very different when filtering high solids content feeds as opposed to low solids content feeds as the larger sized membranes produced the most successful filtration results within this work as opposed to the 1.4 µm membrane pore size typically employed for skim milk (low solids) microfiltration.

The effect of backwashing using different durations and frequencies during MPI filtration was also established. Backwashing parameters of 10 seconds every 5 minutes at 1 bar were found to be the most effective during filtration experiments. The most encouraging result during 15 wt% filtration was found using the 2.0 µm membrane and a CFV of 1.4 m s^{-1} producing a 13.0 LMH equating to a 98.5% increase in permeate flux and a 12.6 % increase in solid transmissions equating to a 113.5% increase at steady state after 40 minutes of filtration compared to filtration in the absence of backwashing. This was achieved whilst maintaining high spore reductions between 1.9 – 3.0 log order reductions compared to 2.7 – 2.9 log orders without backwashing.

The relative contributions of concentration polarisation, reversible and irreversible fouling resistances to permeate flux decline were calculated during each filtration experiment. This allowed qualitative analysis of the types of fouling mechanisms occurring when different membrane pore sizes and process conditions were tested.

Lastly, an optimum cleaning regime for MPI fouled tubular ceramic *Membralox*^{TM} membranes was investigated involving testing of various combinations of both hydraulic and chemical cleaning methods. A long rinsing backflush at 1 bar and acid and alkali steps without backwashing were found to be most effective producing a 99.6% recovery in pure water flux.

At the start of the project suitable targets were set for spore rejection, permeate flux and solid transmission during the filtration of a 15 wt% MPI feed, by consideration of values achieved within industry and those reported within the literature. As stated within the 'project aims and objectives' section of the introduction; spore rejections of 2.08 ± 0.12 and 2.15 ± 0.10 $\log_{10}$ cfu ml^{-1} have been reported by Fritsch and Moraru, (2008), 3.79 $\log_{10}$ cfu ml^{-1} by Elwell and Barbano (2006), 4.5 $\log_{10}$ cfu ml^{-1} by Tomasula *et al.,* (2011) and 2.28 ± 0.17 $\log_{10}$ units by Madec *et al.,* (1992). All these rejections were found using a feed of raw skimmed milk and a 1.4 µm membrane. A similar minimum reduction target of ~2 $\log_{10}$ orders cfu ml^{-1} was set for 15 wt% MPI filtration during this project. This target was met for all experiments carried out through the 0.8, 2.0 and 12.0 µm membranes that were subjected to the largest amount of testing. With regards to permeate flux and solids transmission in industry steady state permeate fluxes of 500 litres m^{-2} hr^{-1} (LMH) and solids transmissions of > 99% are typically obtained during the filtration of skimmed milk over a 10 hour period (Saboya

and Maubois, 2000). Considering the difference in solids content between skimmed milk (3 - 4 wt%) and the MPI (up to 15 wt%) a realistic target of > 50 LMH for steady state permeate flux and > 80% for solids transmission were set. The permeate flux target was met for 5 wt% through both the 2.0 and 5.0 µm membranes at 1.4 m s^{-1} CFV and for 10 wt% through the 5.0 µm membrane at 1.4 m s^{-1} CFV. Both permeate flux and solid transmission targets were met during filtration of 10 wt% through the 12.0 µm at 1.4 m s^{-1}. Unfortunately, neither of these targets were met during the filtration of 15 wt% MPI. The closest values of 26.6 LMH and 68.7% were obtained through the 12.0 µm membrane at 1.4 m s^{-1} CFV.

5.2. Future work

Ideally, the feed stream used in this project would have been liquid milk (prior to being pasteurised) or MPI concentrate solution (taken directly off the production line at Kerry Foods). This would have removed the issue of powder resolubilisation and the need for spore inoculation (as bacteria are already present). However, due to safety issues such as the presence of harmful microorganisms (see section 1.8), and practicality in terms of transportation and storage of liquid dairy products, a spray dried MPI powder prepared using pasteurised skim milk was used. As detailed in section 4.8 pilot plant trials were conducted using MPI concentrate feed solutions of 10, 17 and 25 wt%. These studies gave promising results in terms of solids transmissions and spore reductions, but as stated previously there were limitations to this work (see section 4.8). It would be interesting to carry out further optimisation experiments using this feed type with the large pore size tubular ceramic *Membralox*™ membranes of 2.0 and 12.0 µm.

Despite various modifications being made to the filtration system during the course of the project aimed at improving the CFV able to be reached during filtration of high solids MPI, the maximum CFV value able to be reached was 2.0 m s^{-1}. This value is low compared to other microfiltration experiments carried out using dairy feeds that often use up to 8 m s^{-1}. In order to increase this value either the general pipework within the filtration rig would have to be replaced with pipework of a larger diameter and / or a bigger pump should be incorporated into the system that would lead to the pressure within the feed loop to be increased. This was too large a task to be carried out during this project but in order to try and improve the permeate flux values and solid

transmission produced during experimentation using this rig this would have to be carried out.

During this work experiments have been conducted using the MPI in its manufactured state but investigations into MPI feed pH modification through the addition of either hydrochloric acid (HCl) to decrease the pH or sodium hydroxide (NaOH) to increase the pH prior to filtration may improve membrane performance and should be investigated. According to Mukhopadhyay *et al.,* (2010) who filtered liquid egg white through a 1.4 µm *Membralox*^{TM} tubular ceramic membrane found that maximum permeate flux occurs at or near the isoelectric point of the feed, which for protein is pH 6. At pH 6 the overall charges of the protein-membrane are neutral. As the protein is positively charged it adsorbs onto the negatively charged membrane surface causing an increase in flux.

This present research work has focused on the effect that variations in membrane pore size, process conditions and MPI concentration have on the steady state permeate flux, solids and protein content and spore rejection. Although the relative contribution that each type of fouling resistance has on the total resistance was calculated and used to give qualitative conclusions on the type of fouling mechanisms occurring no modelling of the fouling process has been conducted. In order to further increase the steady state permeate flux and solid transmission values into commercially viable regions for high solids content MPI solutions, it may be necessary to model the filtration process to determine what type of fouling is dominant and so determine what methods would aid the filtration. Madaeni *et at* (2011) modelled the different mechanisms responsible for fouling during the filtration of raw whole and skim milk through a flat sheet 0.22 µm polyvinylidenefluoride (PVDF) membrane and used SEM images to confirm their conclusions. They reported during whole milk filtration that at the start standard blocking dominated but over time (180 minutes) bacteria, casein and fat particles filled the pores and formed a cake layer. Whereas, during skim milk filtration three fouling mechanisms occurred standard blocking, intermediate blocking and cake deposition.

Due to the limited supply of tubular ceramic *Membralox*^{TM} membranes having only one in each membrane pore size tested, it was not possible to carry out dissections of the membranes for testing at different stages of the filtration cycle such as before and after fouling, after rinsing and cleaning. If more than one pore size of each membrane were

available it would be interesting to carry out analytical techniques on sections of the membranes. These analytical techniques could include Scanning Electron Microscopy (SEM) imaging, Atomic Force Microscopy (AFM) measurements, Fourier Transform Infrared (FTIR) spectroscopy and contact angle measurements. SEM images would allow the morphology of the membrane surface to be visualised at different points of the operational cycle. These images would allow the effectiveness of different fouling and cleaning process conditions to be qualitatively analysed. AFM force measurements could be used to probe the membrane surface topography and interactions and provide quantitative information on the effectiveness of different fouling and cleaning process conditions. Lastly, FTIR analysis would allow the types of chemical bonds and functional groups present on the membrane surface to be determined and contact angle measurement would provide a measure of the hydrophobic / hydrophilic nature of the membrane surface.

It could also prove useful to carry out a combination of Sodium Dodecyl Sulfate Polyacrylamide Gel Electrophoresis (SDS-PAGE) and High performance liquid chromatography (HPLC) on collected feed and permeate samples in addition to measurements of the solid and protein content. This could be used in order to quantify the relative contributions of each amino acid to the solid and protein content values. This data could be collected as a function of filtration time to determine which amino acids are transmitted through the membrane, which amino acids are responsible for membrane fouling and whether this changes as filtration time progresses.

It would also be of interest to determine the long-term effect of multiple fouling and cleaning cycles on the *Membralox*^{TM} ceramic membranes performance. A large amount of work of this nature has been conducted within our research group using different feeds and membranes. Evans (2008) carried out 18 fouling (black tea liquor) and 17 cleaning cycles (sodium hydroxide) on a single 30kDa flat sheet Fluoropolymer membrane and found that both the steady state permeate flux and solids transmission varied insignificantly. Weis (2004) found that flat sheet polyethersulfone and polysulfone membranes fouled with spent sulphite liquor and cleaned with sodium hydroxide showed a steady state permeate flux decline of 45% and 85% respectively after multiple operational cycles. In addition when cleaning with *Ultrasil 11* this difference in flux was found to be even higher.

In the long term once the filtration process for high solids content MPI has been optimised it would be interesting to carry out further pilot plant trails under these conditions to see the effect if any, of scale-up. This would have to be determined if the process were to be used commercially to augment or replace pasteurisation. If achieved this technique could be used to reduce the bacterial load of all types of dairy products that at present are processed via heat treatment.

REFERENCES

Abadi, S.R.H., Sebzari, M.R., Hemati, M., Rekabdar, F., and Mohammadi, T., 2011. Ceramic membrane performancein microfiltration of oily wastewater. *Desalination,* 265, pp.222-228.

ACDP Classification of Pathogens [online]. Available from: http://microblog.me.uk/322 [Accessed: 15th September 2011].

Akpinar-Bayizit, A., Ozcan, T., and YilImaz-Ersan, L., Membrane processes in production of functional whey components. *Mljekarstvo,* 59(4), pp.282-288.

Andersson, A., Rönner, U., and Granum, P.E., 1995. What problems does the food industry have with the spore-forming pathogens *Bacillus cereus* and *Clostidium perfringens*?. *International Journal of Food. Microbiology*, 28, pp.145-155.

APHA, 1992. In: Vanderzant, C., and Spittstoesser, D.F., eds. *Compendium of Standard Methods for the Microbiological Examination of Food. APHA (American Public Health Association) Inc.* Washington, DC, USA.

Barker, M.E., 2003. Contribution of dairy foods to nutrient intake. In: Roginski, H., Fuquay, J.W, and Fox, P.F., eds. *Encyclopedia of Dairy Sciences.* London: Academic Press.

Bartlett, M., Bird, M.R., and Howell, J.A., 1995. Experimental study for the development of a qualitative membrane cleaning model. *Journal of Membrane Science,* 105, pp.147-151.

Baruah, G.L., Nayak, A., and Belfort, G., 2006. Scale-up from laboratory microfiltration to a ceramic pilot plant: Design and performance. *Journal of Membrane Science,* 274, pp.56-63.

Beloti, V., Barros, M.De A.F., Nero, L.A., Pachemshy, J.A.De S., DE Santana, E.H.W., and Franco, B.D.G.M., 2002. Quality of pasteurised milk influences the performance of ready-to-use systems for enumeration of aerobic microorganisms. *International Dairy Journal,* 12, pp.413-418.

Bendick, J.A., Miller, C.J., Kindle, B.J., Shan, H., Vidic, R.D., and Neufeld, R.D., 2005. Pilot scale demonstration of cross-flow ceramic membrane microfiltration for treatment of combined and sanitary sewer overflows. *Journal of Environmental Engineering,* 131, pp.1532-1539.

Bernal, V. and Jelen, P., 1985. Thermal stability of Whey Proteins- A calorimetric study. *Journal of Dairy Science*, 68(11), pp.2847-2852.

Bhaskar, GV, Havea, and Elston, P, 2006. *Dairy protein process and application*

thereof. United States patent application US 2006/0159804 A1.

Bird, M.R., and Bartlett, M., 1995. CIP OPTIMISATION FOR THE FOOD INDUSTRY: Relationships Between Detergent Concentration, Temperature and Cleaning Time. *Trans IChemE,* 73(C), pp.63-70.

Bird, M.R., and Bartlett, M., 2002. Measuring and modelling flux recovery during the chemical cleaning of MF membranes for the processing of whey protein concentrate. *Journal of Food Engineering,* 53, pp.143-152.

Bird, M.R., 1997, in *Cleaning and Disinfection in the Dairy and Food Processing Industries*. Notes of Continued Education (Auckland University, School of Engineering in Association with ICI Chemical Cleaning).

Bird, M.R., 2009. *pers.comm*. Separation processes lecture course notes taken at the University of Bath.

Blackburn, C.De W., Baylis, C.L., and Petitt, S.B., 1996. Evaluation of Petrifilm methods for enumeration of aerobic flora and coliforms in a wide range of foods. *Letters in Applied Microbiology,* 22, pp.137-140.

Blanpain-Avet, P., Faille, C., and Benezech, T., 2009. Cleaning kinetics and related mechanisms of *Bacillus cereus* spore removal during an alkaline cleaning of a tubular ceramic microfiltration membrane. *Desalination and Water Treatment,* 5, pp.235-251.

Boland, M., 2009. Milk proteins: the future. In: THOMPSON, A., ed., Boland, M., ed., and Singh, H., ed. *Milk Proteins-from Expression to Food.* London: Elsevier. Online version available at: http://knovel.com/web/portal/browse/display?_EXT_KNOVEL_DISPLAY_bookid=3003&VerticalID=0

Bowen, R.W, Doneva, T.A., Stoton, J.A.G., 2002. Protein deposition during cross-flow membrane filtration: AFM studies and flux loss. *Colloids and Surfaces B: Biointerfaces,* 27, pp.103-113.

Bowen, R.W., Fenton, A.S., Lovitt, R.W., and Wright, C.J., 2002. The measurement of *Bacillus mycoides* spore adhesion using atomic force microscopy, simple counting methods and a spinning disk technique. *Biotechnology and bioengineering,* 79(2), pp.170-179.

Bradford, M.M., 1976. A rapid and sensitive method for the quantification of microgram quantities of protein utilising the principle of protein-dye binding. *Analytical biochemistry,* 72. pp.248-254.

Bradley, D. E., and Franklin, J. E., 1958. Electron microscope survey of the surface

configuration of spores of the genus *Bacillus*. *Journal of bacteriology*, 76, pp.618-630.

Bramley, A.J., and McKinnon, C.H., 1990. The microbiology of raw milk. In: Robinson, R.K., ed. *Dairy Microbiology, Volume 1*. London: Elsevier Applied Science.

Brans, G., Schroen, C.G.P.H., Van Der Sman, R.G.M., and Boom, R.M., 2004. Membrane fractionation of milk: state of the art and challenges. *Journal of Membrane Science*, 243, pp.263-272.

Carrera, M., Zandomeni, R.O., Fitzgibbon, J., and Sagripanti, J.-L., 2007. Difference between the spore sizes of *Bacillus anthracis* and other *Bacillus* species. *Journal of Applied Microbiology*, 102, pp.303-312.

Cakl, J., Bauer, I., Doleoek, P., and Mikulasek, P., 2000. Effects of backflushing conditions on permeate flux in membrane crossflow microfiltration of oil emulsion. *Desalination*, 127, pp.189-198.

Chada, V.G.R., Sanstad, E.A., Wang, R., and Driks, A., 2003. Morphogenesis of *Bacillus* Spore Surfaces. *Journal of Bacteriology*, 185 (21), pp.6255-6261.

Cheryan, M., 1998. *Ultrafiltration and Microfiltration handbook.* 2nd ed. Boca Raton: CRC Press.

Cheryan, M., and Alvarez, J.R., 1995. Food and beverage industry application. In: NOBLE, R.D., ed., AND STERN, S.A., ed. *Membrane separations technology principles and application*. Amsterdam: Elsevier, pp.415-445.

Christiansson, A., Ekelund, K., and Ogura, H.M., 1997. Membrane filtration method for enumeration and isolation of spores of *Bacillus cereus* from milk. *International Dairy Journal*, 7, pp.743-748.

Compton, S.J. and Jones, C.G., 1985. Mechanism of dye response and interference in the Bradford protein assay. *Analytical Biochemistry*, 151. pp.369-374.

Coultrate, T.P., 1989. *Food, The chemistry of its components.* 2nd ed. London: The Royal Society of Chemistry.

Cravendale® semi-skimmed [online]. Available from: http://www.arlafoods.co.uk/products/milk/cravendale/cravendale-semi-skimmed/ [Accessed: 15th September 2011].

DairyCo Datum [online]. Available from: http://www.mdcdatum.org.uk/RetailerDataPrices/tnsmilk.html [Accessed: 17th July 2009].

DEFRA (Department for Environment Food and Rural Affairs) [online].

Available from: http://archive.defra.gov.uk/search/ [Accessed: 15th September 2011].

Desmasures, N., Bazin F., and Gueguen, M., 1997. Microbiological composition of raw milk from selected farms in the Camembert region of Normandy. *Journal of Applied Microbiology*, 83, pp.53-58.

De Sousa, G.B., Tamagnini, L.M., Gonzalez, R.D., and Budde, C.E., 2005. Evaluation of Petrifilm™ method for enumerating aerobic bacteria in Crottin goat's cheese. *Revista Argentina de Microbiologia*, 37, pp.214-216

Dequeiroz, G.A., and Day, D.F., 2008. Disinfection of *Bacillus subtilis* spore-contaminated surface materials with a sodium hypochlorite and a hydrogen peroxide-based sanitizer. *Letters in Applied Microbiology*, 46, pp.176-180.

De Wit, J.N., and Klarenbeek, G., 1984. Effects of heat treatments on structure and solubility of whey proteins. *Journal of Dairy Science*, 67, pp.2701-2710.

De Wit, J.N., 1998. Nutritional and Functional Characteristics of Whey Proteins in Food Products. *Journal of Dairy Science*, 81, pp.597-608.

Drake, M.A., Miracle, R.E., and Wright, J.M., 2009. Sensory properties of dairy proteins. In: THOMPSON, A., ed., BOLAND, M., ed., AND SINGH, H., ed. *Milk Proteins-from Expression to Food.* London: Elsevier. Online version available at: http://knovel.com/web/portal/browse/display?_EXT_KNOVEL_DISPLAY_bookid=3003&VerticalID=0

Ellender, R.D. Sharp, S.L. Comar, P.G. and Tettleton, R.P., 1993. Rapid methods to evaluate the bacteriological quality of frozen crabmeat. *Journal of Food Protection*, 47. pp.753-775.

Elwell, M.W., and Barbano, D.M., 2006. Use of microfiltration to improve fluid milk quality. *Journal of Dairy Science*. 89, pp.E20-E30.

Evans, P.J., 2008. *Membrane-Solute-Cleaning agent interaction during the ultrafiltration of black tea liquor.* Thesis (Ph.D). University of Bath. Bath.

Evans, P.J., and Bird, M.R., 2006. Solute-membrane fouling interactions during the ultrafiltration of black tea liquor. *Food and Bioproducts Processing*, 84(C4), pp.292-301.

Fadaei, H., Tabaei, S.R., Roostaazad, R., 2007. Comparative assessment of the efficiencies of gas sparging and back-flushing to improve yeast microfiltration using tubular ceramic membranes. *Desalination*, 217, pp.93-99.

Field, R.W., Wu, D., Howell, J.A., and Gupta, A, B.B., 1995. Critical flux concept for microfiltration fouling. *Journal of Membrane Science*, 100, pp.259-272.

Fox, P.R., 2009. Milk: an overview. In: Thompson, A., ed., Boland, M., ed., and Singh, H., ed. *Milk Proteins-from Expression to Food.* London: Elsevier. Online version available at: http://knovel.com/web/portal/browse/display?_EXT_KNOVEL_DISPLAY_bookid=3003&VerticalID=0

Fox, P.F. and McSweeney, P.L.H., 1998. *Dairy Chemistry and Biochemistry.* New York: Kluwer Academic.

Fritsch, J., and Moraru, C.I., 2008. Development and Optimization of a Carbon Dioxide-Aided Cold Microfiltration Process for the Physical Removal of Microorganisms and Somatic Cells from Skim Milk. *Journal of Dairy Science,* 91, pp.3744-3760.

Glover, F.A., and Brooker, B.E., 1974. The structure of the deposit formed on the membrane during the concentration of milk by reverse osmosis. *Journal of Dairy Research,* 41, pp.89-93.

Goodsell, D.S., and Olson, A.J., 1993. Soluble proteins: size, shape and function. *Trends in Biochemical Sciences,* 18, pp.65-68.

Granum, P.E. and Lund, T., 1997. *Bacillus cereus* and its food poisoning toxins. *FEMS Microbiology Letters*, 157, pp.223-228.

Griffiths, M.W., 1992. *Bacillus cereus* in liquid milk and other milk products. *International Dairy Journal*, Bulletin 275, Brussels, pp. 36-39.

Guerra, A., Jonsson, G., Rasmussen, A., Nielsen, E.W., and Edelsten, D., 1997. Low cross-flow velocity microfiltration of skim milk for removal of bacterial spores. *International Dairy Journal*, 7, pp.849-861

Gunasekaran, S. and Mehmet AK. M., 2003. *Cheese rheology and texture*. Boca Raton: CRC Press.

Havea, P., 2006. Protein interactions in milk protein concentrate powders. *International Dairy Journal,* 16, pp.415-422.

Hayes, M.C., Ralyea, R.D., Murphy, S.C., Carey, N.R., Scarlett, J.M., and Boor, K.J., 2001. Identification and Characterization of Elevated Microbial Counts in Bulk Tank Raw Milk. *Journal of Dairy Science,* 84, pp.292-298.

Handojo, A., Zhai, Y., Frankel, G., and Pascall, M.A., 2009. Measurement of adhesion strengths between various milk products on glass surfaces using contact angle measurement and atomic force microscopy. *Journal of Food Engineering,* 92, pp.305-311.

Hassan, G.M., Al-Ashmawy, M.A.M., Meshref, A.M.S., and Afify, S.J., 2010.

Studies on enterotoxigenic *Bacillus cereus* in raw milk and some dairy products. *Journal of Food Safety*, 30, pp.569-583.

Henyon, D.K., 1999. Extended shelf-life milks in North America: a perspective. *International Journal of Dairy Technology*, 52, pp.91-130.

Hoffmann, W., Kiesner, C., Clawin-Rädecker, I., Martin, D., Einhoff, K., Lorenzen, P. C., Meisel, H., Hammer, P., Suhren, G. and Teufel, P., 2006. Processing of extended shelf life milk using microfiltration. *International Journal of Dairy Technology*, 59(4), pp.229-235.

Holm, S. Malmborg, R. and Svensson, K., 1986. *Method and plant producing milk with low bacterial content.* W0/86/01687.

Hui, Y.H., (ed) 2007. *Handbook of Food Products Manufacturing: Health, Meat, Milk, Poultry, Seafood and Vegetables.* New Jersey: John Wiley & Sons.

Husmark, U., Rönner, U., 1992. The influence of hydrophobic, electrostatic and morphologic properties on the adhesion of *Bacillus* spores. *Biofouling*, 5, pp.335-334

James, B.J., Jing, Y., and Chen, X.D., 2003. Membrane fouling during filtration of milk- a microstructural study. *Journal of Food Engineering*, 60, pp.431-437.

Jimenez-Lopez, A.J.E., Leconte, N., Dehainault, O., Geneste, C., Fromont, L., and Gesan-Guiziou, G., 2007. Role of milk constituents on critical conditions and deposit structure in skimmilk microfiltration (0.1 µm). *Separation and Purification Technology*, 61, pp.33-43.

Jones, S.A., Bird, M.R., and Pihlajamäki, A., 2011. An experimental investigation into the pre-treatment of synthetic membranes using sodium hydroxide solutions. *Journal of Food Engineering*, 105, 128-137.

Jonsson, G., and Wenton, I.G., 1994. Control of concentration polarisation, fouling and protein transmission of microfiltration processes within the agro-based industry. *Proceedings of the ASEAN-EU Workshop on Membrane Technology in Agro Based industry,* Kuala Lumpar, Malaysia, pp.157-166.

Kerry Ingredients. *Ultranor ™ Milk Proteins* [online]. Kerry: Available from: http://www.kerry.com/uploadedFiles/Kerry/Kerry_EMEA/Technologies/Proteins/dairy%20proteins.pdf [Accessed 15th September 2011].

Krstic, D.M., Tekic, M.N., Caric, M.D., and Milanovic, S.D., 2002. The effect of turbulence promoter in cross-flow microfiltration of skim milk. *Journal of Membrane Science*, 208, pp.303-314.

Kuberkar, V.T., and Davis, R.H., 2001. Microfiltration of protein-cell mixtures with

crossflushing or backflushing. *Journal of Membrane Science*, 183, pp.1-14.

Kulozik, U., 1998. Variation of the calcium content in skim milk by diafiltration and ion exchange – Effects on permeation rate and structure of deposited layers in the RO. *Journal of Membrane Science*, 145, pp.91-97.

Kuruzovich, J.N., and Piergiovanni, P.R., 1996. Yeast cell microfiltration: optimization of backwashing for delicate membranes. *Journal of Membrane Science*, 112, pp.241-247.

Lewis, M.J., 2003. Improvements in the pasteurisation and sterilisation of milk. In: Smit, G., ed. *Dairy Processing – Improving Quality*. Cambridge: Woodhead Publishing. Online version available at: http://knovel.com.ezp1.bath.ac.uk/web/portal/browse/display?_EXT_KNOVEL_DISPLAY_bookid=915&VerticalID=0

Lennetech tubular-shaped membranes [online]. Available from: http://www.lenntech.com/tubular-shaped-membranes.htm [Accessed: 15th September 2011].

Liu, M., Xiao, C., and Hu, X., 2012. Fouling characteristics of polyurethane –based hollow fiber membrane in microfiltration process. *Desalination*, 298, pp.59-66.

Ma, H., Hakim, L.F., Bowman, C.N., and Davis, R.H., 2001. Factors affecting membrane fouling reduction by surface modification and backpulsing. *Journal of Membrane Science*, 189, pp.255-270.

Madaeni, S.S., Yasemi, M., and Delpisheh, A., 2011. Milk sterilization using membranes. *Journal of Food Process Engineering*, 34, pp.1071-1085.

Makardij, A., Chen, X.D., and Farid, M.M., 1999. Microfiltration and Ultrafiltration of Milk: Some Aspects Of Fouling and Cleaning. *Trans IChemE*, 77 (C), pp. 107-113.

Malvern. D*ynamic light scattering (DLS)* [online]. Available from: http://www.malvern.com/LabEng/technology/dynamic_light_scattering/dynamic_light_scattering.htm?gclid=CO7V29q6-LECFcxofAodlDUA_g [Accessed 15th September 2011].

McClements, D.J., Decker, E.A., Park, Y., and Weiss, J., 2009. Structural design properties for delivery of bioactive components in nutraceuticals and functional foods. *Critical Reviews in Food Science and Nutrition*, 49(6), pp.577-606.

McKellar, R.C, 1989. *Enzymes of Psychrotrophs in Raw Food.* Boca Raton: CRC Press.

Morr, C.V. and Josephson, R.V., 1968. N-ethylmaleimide and casein upon heat-

induced whey protein aggregation. *Journal of dairy science,* 51(9), pp.1349-1355.

Mourouzidis-Mourouzis, S.A. and Karablas, A.J., 2008. Whey protein fouling of large pore-size ceramic microfiltration membranes at small cross-flow velocity. *Journal of Membrane Science*, 323, pp.17-27.

Muir, D.D., and Banks, J.M., 2003. Factors affecting the shelf-life of milk and milk products. In: SMIT, G., ed. *Dairy Processing – Improving Quality*. Cambridge: Woodhead Publishing. Online version available at: http://knovel.com.ezp1.bath.ac.uk/web/portal/browse/display?_EXT_KNOVEL_DISPLAY_bookid=915&VerticalID=0

Mukhopadhay, S., Tomasula, P.M., Luchansky, J.B., Porto-Fett, A., and Call, J.E., 2010. Removal of Salmonella Enteritidis from commercial unpasteurized liquid egg white using pilot scale cross flow tangential microfiltration. *International Journal of Food Microbiology,* 142(3), pp.309-317.

Mulder, M., 2000. *Basic Principles of Membrane Technology.* 2nd Ed. Netherlands: Kluwer Academic Publishers.

Muthukumaran, S., Kentish, S.E., Ashokkumar, M., and Stevens, G.W., 2005. Mechanisms for the ultrasonic enhancement of dairy whey ultrafiltration. *Journal of Membrane Science*, 258, pp.106-114.

Muthukumaran, S., Kentish, S.E., Stevens, G.W., Ashokkumar, M., and Mawson, R., 2007. The application of ultrasound to dairy ultrafiltration: The influence of operating conditions. *Journal of Food Engineering*, 81, pp.364-373.

Noguchi, N., Nakada, A, Itol, Y., Watanabe, A, Niki, E., 2002. Formation of active oxygen species and lipid peroxidation induced by hypochlorite. *Archives of Biochemistry and Biophysics,* 397(2), pp. 440-447.

Oldfield, D.J., Singh, H., and Taylor, M.W., 1998. Association of β-Lactoglobulin and α- Lactalbumin with the Casein Micelles in Skim Milk Heated in an Ultra-high Temperature Plant. *International Dairy Journal*, 8, pp.765-770.

Olson, B.J.S.C. and Markwell, J., *Assays for determination of protein concentration* [online]. Available from: http://media.wiley.com/CurrentProtocols/0471111848/0471111848-sampleUnit.pdf [Accessed 15th September 2011].

Pafylias, L., Cheryan, M., Mehaia, M.A., and Saglam, N., 1996. Microfiltration of milk with ceramic membranes. *Food Research International*, 29(2), pp.141-146.

Park, C., Lee, Y.H., Lee, S., Hong, S., 2008. Effect of cake layer formation on colloid fouling in reverse osmosis membranes. *Desalination,* 220, pp.335-344.

Petrifilm™ Aerobic Count Plate instruction manual

Pimentel, D, and Pimentel, M., 1979. *Food, Energy and Society.* New York: Wiley.

Pisecky, J., 2007. *Handbook of Milk Powder Manufacture.* Copenhagen: Niro A/S.

Plett, E., 1992. Cleaning and sanitation. *In:* D.R. Heldman and D.B. Lund, ed. Handbook of Food Engineering. New York: Marcel Dekker, pp.719-740.

Popovic, S., Milanovic, S., Llicic, M., Djuric, M., and Tekic, M., 2009. Flux recovery of tubular ceramic membranes fouled with whey proteins. *Desalination*, 249, pp.293-300.

Redkar, S.G., and Davis, R.H., 1995. Enhancement of crossflow microfiltration performance using high-frequency reverse filtration. *American Institute of Chemical Engineers,* 41, pp.501-508.

Riedl, K., Girard, B., and Lencki, R.W., 1998. Influence of membrane structure on fouling layer morphology during apple juice clarification. *Journal of Membrane Science,* 139, pp.155-166.

Romney, A.J.D., 1990. *CIP: Cleaning in place.* 2nd Ed revised and expanded. Huntington: The Society of Dairy Technology.

Rysstad, G. and Kolstad, J., 2006. Extended shelf life milk- advances in technology. *International Journal of Dairy Technology,* 59(2), pp.85-96.

Saboya, L.V., and Maubois, J. -L., 2000. Current developments of microfiltration technology in the dairy industry. *Lait,* 80, pp.541-553.

Sagripanti, J., and Bonifacino, A., 1996. Comparative sporicidal effects of liquid chemical agents. *Applied and Environmental Microbiology,* 62, pp.545-551.

Schuck, P., 2009. Effects of drying on milk proteins. In: Thompson, A., ed.,Boland, M., ed., and Singh, H., ed. *Milk Proteins-from Expression to Food.* London: Elsevier. Online version available at: http://knovel.com/web/portal/browse/display?_EXT_KNOVEL_DISPLAY_bookid=3003&VerticalID=0

Scott, K. and Hughes, R., ed., 1996. *Industrial membrane separation technology.* London: Blackie Academic and Profressional.

Seale, R.B., Flint, S.H., McCQuillan, A.J., and Bremer, P.J., 2008. Recovery of Spores from Thermophilic Dairy *Bacilli* and Effects of Their Surface Characteristics on Attachment to Different Surfaces. *Applied and Environmental Microbiology*, 74(3), pp.731-737.

Shorrock, C.J., and Bird, M.R., 1998. Membrane cleaning: Chemically enhanced

removal of deposits formed during yeast cell harvesting. *Trans IChemE,* 76(C), pp.30-38.

Skrzypek, M., and Burger, M., 2010. Isoflux® ceramic membranes – Practical experiences in dairy industry. *Desalination,* 250, pp.1095-1100.

Smith, K., 2008. Dried dairy ingredients [online]. Available from: http://www.cdr.wisc.edu/programs/dairyingredients/pdf/dried_dairy_ingdients.pdf [Accessed: 15th September 2011].

Sondhi, R., and Bhave, R., 2001. Role of backpulsing in fouling minimization in crossflow filtration with ceramic membranes. *Journal of Membrane Science,* 186, pp.41-52.

Sorhaug, T., and Stepaniak, L., 1997. Psychrotrophs and their enzymes in milk and dairy products: Quality aspects. *Trends in Food Science and Technology, 8,* pp.35-41.

Steffe, J.F., 1996. *Rheological Methods in Food Process Engineering* [online]. 2nd Ed. USA: Freeman Press. Available from: http://www.egr.msu.edu/~steffe/Freebooks/Rheological%20Methods.pdf [Accessed 15th September 2011].

Tarabara, V.V., Koyuncu, I., and Wiesner, M.R., 2004. Effect of hydrodynamics and solution ionic strength on permeate flux in cross-flow filtration: direct experimental observation of filter cake cross-sections. *Journal of Membrane Science,* 241, pp.65-78.

Tavolaro, P., Ferrati, R.A., Destro, M.T., Landgraf, M., and Franco, B.D.G.De M., 2005. Performance of two ready-to-use systems for enumeration of aerobic mesophilic microorganisms in frozen goat milk. *Brazilian Journal of Microbiology,* 36(3), pp.295-300.

Te Giffel, M.C., 2003. Good hygienic practice in milk processing. In: Smit, G., ed. *Dairy Processing – Improving Quality*. Cambridge: Woodhead Publishing. Online version available at: http://knovel.com.ezp1.bath.ac.uk/web/portal/browse/display?_EXT_KNOVEL_DISPLAY_bookid=915&VerticalID=0

Tomasula, P.M., Mukhopadhyay, S., Datta, N., Porto-Fett, A., Call, J.E., Luchansky, J.B., Renye, J., and Tunick, M., 2011. Pilot-scale crossflow-microfiltration and pasteurisation to remove spores of *Bacillus anthracis* (Sterne) from milk. *Journal of Dairy Science*, 94, pp.4277-4291.

Trägardh, G., 1989. Membrane cleaning. *Desalination,* 71, pp.325-335.

Tuinier, R., and De Kruif, C.G., 2002. Stability of casein micelles in milk. *Journal of chemical Physics*, 117, pp.1290-1294.

Van Wazer, J.R., 1963. *Viscosity and Flow Measurement.* New York: Interscience Publishers.

Vela, M.C.V., Blance, S.A., Garcia, J.L., Rodriguez, E.B., 2009. Analysis of membrane pore blocking models adapted to crossflow ultrafiltration in the ultrafiltration of PEG. *Chemical Engineering Journal,* 149, pp.232-241.

Vetier, C., Bennasar, M., and Fuente, B.T.D.L., 1988. Study of fouling of a mineral microfiltration membrane using scanning electron microscopy and physiochemical analyses in the processing of milk. *Journal of Dairy Research,* 55, pp.381-400.

Wakeman, R.J., and Williams, C.J., 2002. Additional techniques to improve microfiltration. *Separation and Purification Technology,* 26, pp.3-18.

Wang, F., and Tarabara, V.V., 2008. Pore blocking mechanisms during early stages of membrane fouling by colloids. *Journal of Colloid Science,* 328, pp.464-469.

Weis, A., 2004. *Fouling and Cleaning synergy in ultrafiltration membrane systems, Chemical cleaning after filtration of spent sulphite liquor.* Thesis (Ph.D). University of Bath, Bath.

Winzeler, H.B., and Belfort, G., 1993. Enhanced performance for pressure-driven membrane processes: the argument for fluid instabilities. *Journal of Membrane Science,* 80, pp.35-47.

Wu, D., and Bird, M.R., 2007. The fouling and cleaning of Ultrafiltration membranes during the filtration of model tea component solutions. *Journal of Food Process Engineering*, 30, 293-323.

Young, S.B., and Setlow, P., 2003. Mechanisms of killing of *Bacillus subtilis* spores by hypochlorite and chlorine dioxide. *Journal of Applied Microbiology*, 95, pp.54-67.

Zandomeni, R.O., Fitzgibbon, J.E., Carrera, M., Stuebing, E., Rogers, J.E., and Sagripanti, J.L., 2005. Spore size comparison between several *Bacillus* species [online]. Available from: http://www.dtic.mil/cgi-bin/GetTRDoc?AD=ADA449686&Location=U2&doc=GetTRDoc.pdf [Accessed 15th September 2011].

Zhou, G., Liu, H., He, J., Yuan, Y., and Yuan, Z., 2008. The occurrence of *Bacillus cereus, B. thuringiensis and B. mycoides* in Chinese pasteurized full fat milk. *International Journal of Food Microbiology,* 121, pp.195-200.

APPENDICES

1. Filtration flux equations

System performance is usually defined in terms of permeate flux (J_v) which can be determined using equation 31. Where V is the volume of permeate collected, in a given time period t, through a known membrane area A_M.

$$J_V = \Delta V \Big/ \Delta t \times A_M \tag{31}$$

Permeate flux can be expressed either as a flow rate having units of litres m^{-2} hr^{-1} (LMH) or as a velocity having units of m s^{-1}.

The first step that needs to be carried out when conducting membrane filtration experiments is the measurement of permeate flux with varying transmembrane pressure using a feed consisting of RO water. This measurement can help determine if the equipment is set up properly by comparing water fluxes with expected values and to calculate the membrane resistance $R_{m.}$

$$R_M = \Delta P \Big/ \mu_p \times J_V \tag{32}$$

Where J_v is the permeate flux (m s^{-1}), μ_p is the permeate fluids viscosity (Pa.s) and ΔP is the transmembrane pressure (Pa).

The membrane resistance can be calculated in one of two ways either from the gradient of a flux data plot or from individual flux data points. Rearranging equation 32 gives: -

$$J_V = \left(1 \Big/ R_M \times \mu_p \right) \Delta P \tag{33}$$

Using equation 33 a plot of J_v against ΔP gives a linear plot with the gradient 1/ R_M μ_p, by knowing the fluid viscosity the resistance of the membrane (R_M) can be calculated using equation 34.

$$R_M = 1 \Big/ \mu_p \times gradient \tag{34}$$

All resistances such as the membrane resistance R_M are calculated with units of m^{-1}.

The total hydraulic resistance R_{TOT} for a filtration experiment was calculated using equation 35. Where J, is the final recorded permeate flux (LMH), ΔP is the transmembrane pressure (bar) at which the experiment was performed and η is the viscosity of the permeate solution collected at the end of the filtration calculated from the total solids transmission measured (as described in section 2.10.1 using equation 15) for the experiment and the equation of the plot shown in Figure 53.

$$R_{TOT} = \frac{\Delta P}{J \times \eta} \tag{35}$$

2. SEM sample preparation protocol

2.1. *Bacillus mycoides* cells

Bacillus mycoides cells were prepared following the method described in section 2.2.1. Two glass coverslips were placed in two wells and covered in 2.5 ml of TS culture this was then placed inside a static incubator at 25 ºC for 6 hours, in order for the bacterial cells to adhere to the coverslip surface.

Prefixation: Each coverslip was then dipped in 0.1 M SCB and then immersed into a solution made up of GDA (2.5 ml, 25%), SCB (12.5 ml, 0.2 M) and distilled water (35 ml) inside a small vial which was then sealed and left inside a fridge overnight.

Rinse 1: Each coverslip was rinsed in buffer- x3 changes left for 5 minutes in each

Postfixation: Both coverslips were left in a solution of Osmium tetroxide (1%) and SCB (0.1 M, pH 7.3) for two hours at room temperature.

Rinse 2: Each coverslip was rinsed in distilled water- x3 changes left for 5 minutes in each

Freeze-drying: One of the coverslips was then frozen and left overnight in the freeze drier

Dehydration: The remaining coverslip was placed in a series of acetone solutions; 30%, 50%, 70%, 80%, 90%, 95% x2 changes in each over 15 minutes, then into 100% dry acetone x4 changes over 30 minutes. The coverslip was transferred into 100% HMDS x2 changes over 20 minutes, after which time as much of the HMDS as possible was pipetted off. The coverslip was then left partially covered inside the fume cupboard in order for the remaining HMDS to evaporate off. Once evaporated the coverslip was placed in silica and left in a sealed container overnight.

2.2. *Bacillus mycoides* spores

Bacillus mycoides spores were prepared following the protocol described in section 2.2.1. During harvesting 10 ml of the solution was left untouched and 10 ml was

removed after each centrifuging and washing step so that 10ml spore culture samples were prepared, one before it had been centrifuged, one after centrifuging and one after each of the three washing steps.

Prefixation: 2.5% (1 ml) glutaraldehyde solution was added to each sample inside a universal bottle which was sealed with paraffin film and left overnight at room temperature.

Rinse 1: Each solution was used to fill two small eppendorf's and centrifuged the supernatant was discarded and replaced with distilled water (cell culture grade) - x3 changes 5 minutes each.

Postfixation: Osmium tetroxide (1%) was added to each solution and left for 1.5 hours at room temperature

Rinse 2: Each eppendorf was centrifuged replacing the supernatant with distilled water (cell culture grade) - x3 changes 5 minutes each

Freeze-drying: All samples were then frozen and left overnight inside the freeze drier.

The accelerating voltage, magnification, spot size and z value used were 15 kV, either x10,000, 30,000 or x45,000, 26 and 15 these values are also shown on the photographs themselves displayed in Figure 21. The sample that had undergone three washing steps had a second set of SEM images taken in order to determine spore size, these were taken using an accelerating voltage of 15 kV, a magnification of x5,000, a spot size of 20 and a z-value of 23.

2.3. Spray dried Ultranor^{TM} 9075 Milk Protein Isolate powder and solution

A 20 wt% MPI solution was prepared following the method described in section 2.1.1.

Freeze-drying: The MPI powder and 20 wt% solution were freeze-dried and left inside a freeze-drier overnight.

The two *Bacillus mycoides* cell samples and the MPI powder and resolubilised solution samples were examined and photographs taken using an accelerating voltage of 15 kV, a spot size of 35 and a z value of 20.

2.4. SEM preparation

All samples during SEM preparation once freeze-dried were stuck onto carbon double sided tape which itself was stuck onto a small circular aluminium disk, known as a specimen stub. They were then placed into a vacuum evaporator to remove any remaining moisture and air from the surface of the samples and finally sputter coated with a thin layer of gold in order to make the samples conductive.

3. Light microscope calibration for spore size measurement

A new calibration had to be carried out for each magnification used for example, using a x40 microscope magnification with a x10 eyepiece magnification = x400 magnification, the following calibration was found:

0.25 mm (on stage micrometer slide) = 98 GU (on eyepiece)
1 GU = 0.00255 mm = 2.55 µm

Using a x100 microscope magnification with a x10 eyepiece magnification = x1000 magnification, the following calibration was found:

99 GU = 0.1 mm
1 GU = 0.00101 mm = 1.01 µm

Once the calibration had been completed the stage micrometer slide was replaced by a specimen slide that has the sample on and the spore size can then be measured in GU and converted to µm using the calibration conversion shown above.

4. Particle size distribution- Correlation against time graphs for MPI solutions prepared using a slow (optimal) stirrer speed.

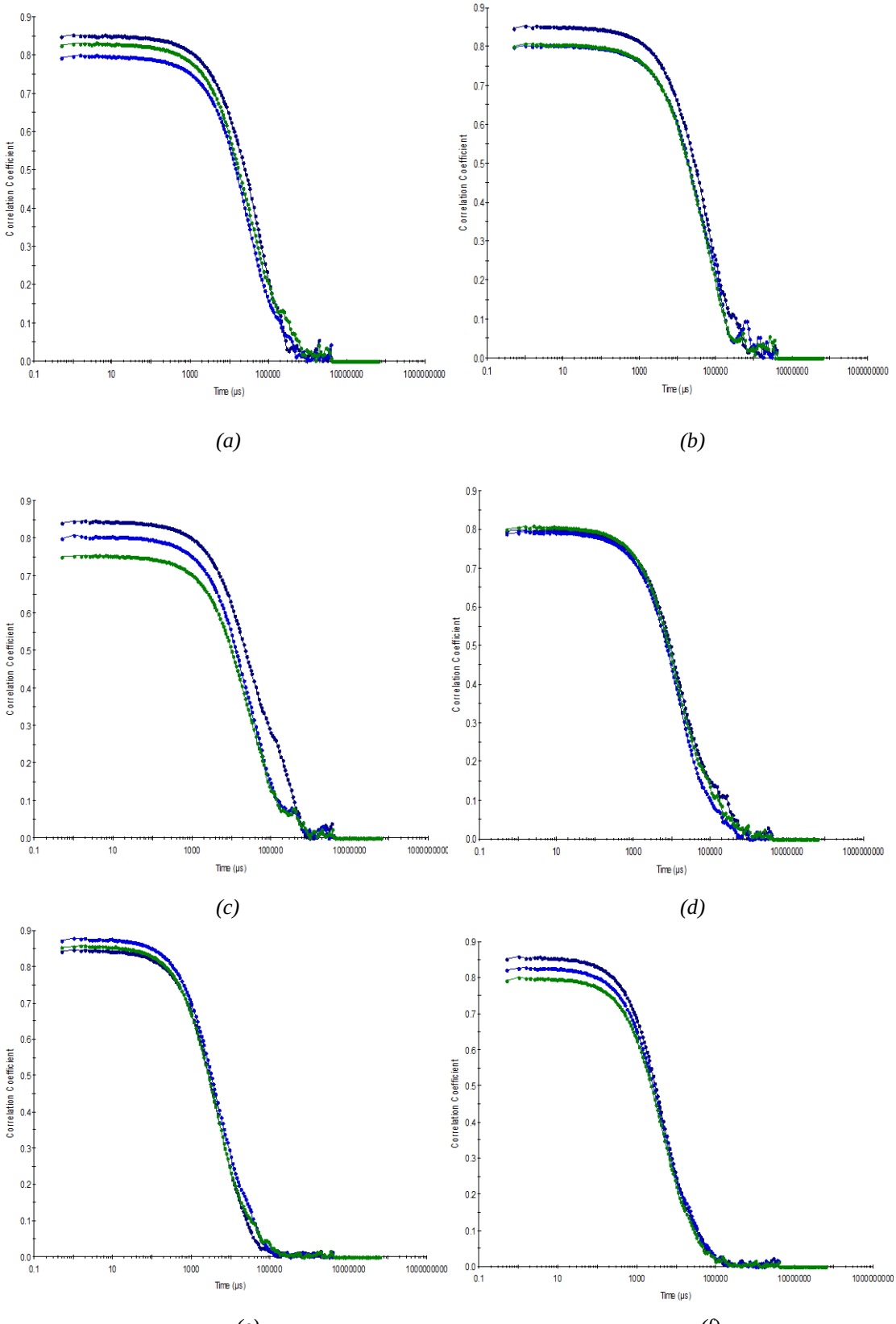

(a) *(b)*

(c) *(d)*

(e) *(f)*

Figure 88. Correlation against time graphs for prepared solutions 1 - 6 (a - f) as described in section 2.4.

5. Correlation against time and volume statistics data tables, for 5, 10 and 15 wt% MPI solutions prepared at 700 rpm.

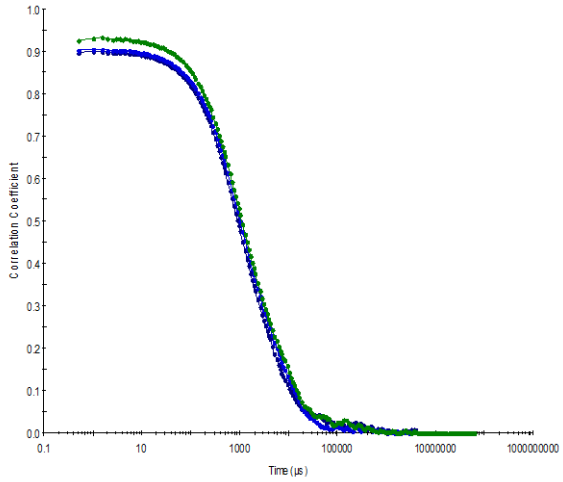

(a)

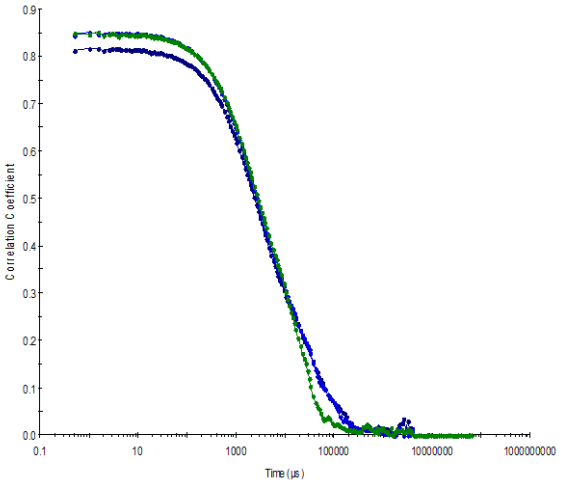

(b)

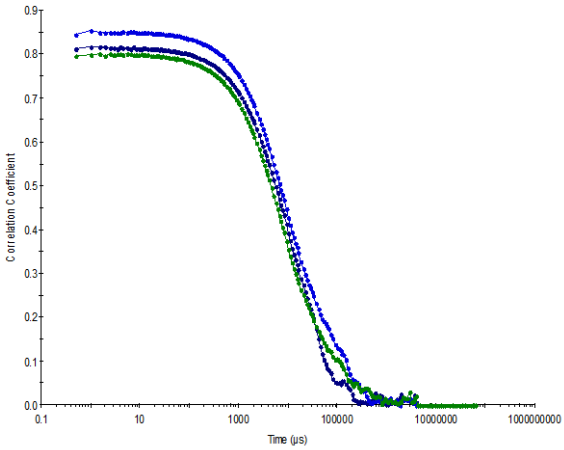

(c)

Figure 89. Correlation against time graphs for 5, 10 and 15 wt% MPI solutions prepared using the faster stirrer speed of 700 rpm.

Table 48. Volume statistics data for 5 wt% MPI resolubilised at 700 rpm.

Size (d. nm)	Mean volume (%)	Standard deviation volume %
37.8	0.2	0.2
43.8	0.8	1.2
50.7	1.3	1.8
58.8	0.9	1.2
68.1	0.1	0.2
142	0.6	0.8
164	1.6	2.3
190	2.8	4.0
220	4.9	3.6
255	11.2	4.6
295	17.0	14.2
342	16.7	17.0
396	9.9	10.8
459	1.9	2.2
615	0.5	0.8
712	1.8	2.6
825	3.5	4.9
955	4.9	6.9
1110	5.5	7.8
1280	5.1	7.2
1480	3.8	5.3
1720	2.0	2.9
1990	0.6	0.8
5560	2.4	3.3

Table 49. Volume statistics data for 10 wt% MPI resolubilised at 700 rpm.

Size (d. nm)	Mean volume (%)	Standard deviation volume %
295	2.6	1.9
342	16.3	4.7
398	35.7	1.9
459	33.1	4.0
531	11.8	3.6
615	0.5	0.9

Table 50. Volume statistics data for 15 wt% MPI resolubilised at 700 rpm.

Size (d. nm)	Mean volume (%)	Standard deviation volume %
220	0.2	0.4
255	5.8	10.1
295	16.2	21.8
342	21.6	18.7
396	17.9	21.2
459	12.0	10.4
531	12.3	21.2
615	10.6	18.3
712	3.3	5.8

6. Mass balance error analysis

The error in the weights given by the mass balance that was used during total solids determination of samples collected during filtration runs was found during the drying protocol development experiment detailed within section 2.10.5. This was achieved simply by placing each of the six containers used within the experiment onto the balance three times. From these weights the standard deviation and error were calculated and found to be no greater than 0.0005 and 0.0003 respectively, as can be seen below in Table 51.

Table 51. Mass balance error data

	0.5 wt%	0.75 wt%	1.0 wt%	1.25 wt%	1.5 wt%	Feed
Weight 1 (g)	51.2288	48.4018	48.4018	48.4018	48.4018	0.6865
Weight 2 (g)	51.2287	48.4021	48.4021	48.4021	48.4021	0.6859
Weight 3 (g)	51.229	48.4019	48.4019	48.4019	48.4019	0.6868
SD	0.00015	0.00015	0.00015	0.00015	0.00015	0.00046
Standard error	8.819×10^{-5}	8.819×10^{-5}	8.819×10^{-5}	8.819×10^{-5}	8.819×10^{-5}	0.00026

7. Osmotic pressure effect calculation

$$\pi = \frac{CRT}{M} \tag{36}$$

Osmotic pressure for a typical 15 wt% feed stream was calculated using equation 36. Where C is the feed concentration (g litre^{-1}), R is the universal gas constant (litre bar K^{-1} mol^{-1}), T is the temperature (K) and M is the molecular weight of the solute (g mol^{-1}). In order to calculate the molecular weight of MPI the assumption was made that it had the molecular weight of glutamic acid, which is the most abundant amino acid in MPI according to Table 7.

$$\pi = \frac{(0.0001552 \times 0.08314 \times 323)}{147.05} = 2.83 \times 10^{-5} bar$$

Osmotic pressure for the respective permeate stream calculated using equation 36.

$$\pi = \frac{(0.000003254 \times 0.08314 \times 323)}{147.05} = 5.94 \times 10^{-7} bar$$

Osmotic pressure difference across the membrane was calculated by subtracting permeate osmotic pressure (bar) from the feed osmotic pressure. For this system this worked out to be a difference of 2.77 x 10^{-5} bar.

During filtration experiments a TMP of either 0.5, 1 or 2 bar has been employed during MPI filtration with the majority of experiments being carried out at 2 bar. As the osmotic pressure difference is so small in comparison to even the lowest TMP of 0.5 bar used it was considered to have a negligible effect during this work.